

Some pages of this thesis may have been removed for copyright restrictions.

If you have discovered material in Aston Research Explorer which is unlawful e.g. breaches copyright, (either yours or that of a third party) or any other law, including but not limited to those relating to patent, trademark, confidentiality, data protection, obscenity, defamation, libel, then please read our [Takedown policy](#) and contact the service immediately (openaccess@aston.ac.uk)

**THE ROLE OF
STABLE NITROXYL RADICAL PRECURSORS
AS ANTIOXIDANTS IN POLYOLEFINS**

BASUKI WIRJOSENTONO

A Thesis submitted for the Degree of Doctor of Philosophy

ASTON UNIVERSITY

August 1991

This copy of the thesis has been supplied on condition that anyone who consults it is understood to recognise that its copyright rests with its author and that no quotation from the thesis and no information derived from it may be published without the author's prior, written consent.

ASTON UNIVERSITY

THE ROLE OF
STABLE NITROXYL RADICAL PRECURSORS
AS ANTIOXIDANTS FOR POLYOLEFINS

BASUKI WIRJOSENTONO

Doctor of Philosophy

August 1991

SUMMARY

Various 2,2,6,6-tetramethyl piperidines and their N-alkyl derivatives of stable nitroxyl radical precursors containing acrylic(s) and methacrylic(s) groups were reactively processed in the presence of a peroxide as bound-antioxidants masterbatches for polyolefin stabilisation. It was found that grafting of the antioxidant monomers onto the polymer backbone was inevitably in competition with homopolymerisation of the monomers as well as melt degradation of the polymer and other side reactions. As previously reported, binding efficiency of bisacrylic nitroxyl precursor was maximum due to formation of unextractable homopolymer of the antioxidant. On the other hand, the binding efficiency of monoacrylic derivatives was low and the homopolymers were found extractable, which suggests that the bound monoacrylic derivatives are entirely grafted onto the polyolefin backbone. Application of bis and tri-functional coagents gave improved binding efficiency of the monoacrylic monomers. This may be due to copolymerisation of the antioxidants with the coagents and grafting of the copolymers onto the polymer backbone.

Comparison of photostabilising activity of the fully extracted bound antioxidants to those of the corresponding unbound analogous showed lower results for the former. However, thermal stabilising activity of the bound antioxidants was higher than that of the unbound analogous due to better substantivity. Analysis using physical techniques and GPC for molecular weight distribution of masterbatches containing the bound monoacrylic antioxidants showed formation of high molecular weight products. Model reaction of a secondary amine derivative in liquid hydrocarbon and analysis of the product using FTIR and NMR spectroscopy indicated a possibility of side reaction, i.e. involvement of the amine active group (>N-H) of the antioxidant in the binding process to form the high molecular weight product. Implementation of various N-alkylated derivatives did not inhibit the side reaction. The photostabilising activity of the bound-antioxidants can be improved when applied in conjunction with small amounts of a benzophenone uv-stabiliser. The synergistic stabilising activity, however, was diminished when the uv-stabiliser was removed from the system during the service time.

Nitroxyl precursors containing methacrylic group(s) gave lower binding efficiency than the corresponding acrylic derivatives. Reversible depolymerisation of the grafted methacrylic antioxidants may be responsible for this. Bis and tris-acrylic coagents improved the binding efficiency, and the presence of methacrylic group improved stabilising activity of the antioxidants. N-methyl derivatives were found to exhibit better stabilising activity than their parent secondary amine derivatives.

Keywords,

nitroxyl-precursors, hindered amines, bound-antioxidants, reactive processing, grafting, stabilisation, polyolefins

ACKNOWLEDGEMENTS

Praise be to The Cherisher and Sustainer, without His mercy this work would not have been possible.

I wish to acknowledge with gratitude the guidance, advice and encouragement given by my supervisors, Dr. S. Al-Malaika and Prof. G. Scott in carrying out this work.

My thanks are also to Dr. H.H. Sheena, especially for his advise and discussion in the preparation of Chapters 1 and 2, and to research fellows of Polymer Processing and Performance Group, Drs. K.B. Chakraborty, M.C. Coker and T. Koenig as well as all research students of the group for their numerous discussions, constructive comments and comradeship during this research work. I am grateful to Dr. M.C. Perry for his discussion and NMR analysis, and to Mr. S. Ludlow and Mr. H.S. Hindle for their technical assistance.

Thanks are extended to The Ministry of Education and Culture of The Republic of Indonesia for providing scholarship and to University of North Sumatra for granting study leave.

Last but by no means least, I gratefully remember my parents, my wife Ramisah, my daughters Retno and Anisa for their love, immense patience and moral support in all these years and my whole-hearted gratitudes to them.

LIST OF CONTENTS

	<u>Page</u>
THESIS TITLE	1
SUMMARY	2
<i>ACKNOWLEDGEMENTS</i>	3
LIST OF CONTENTS	4
LIST OF SCHEMES	9
LIST OF TABLES	10
LIST OF FIGURES	11
ABBREVIATIONS AND SYMBOLS	13
<u>CHAPTER 1</u>	
GENERAL INTRODUCTION AND SCOPE OF THE WORK	15
1.1 INTRODUCTION	15
1.2 DEGRADATION OF POLYOLEFINS	16
1.2.1 Mechanical Degradation of Polyolefins in Melts	17
1.2.2 Thermal Oxidative Degradation	19
1.2.3 Photodegradation of Polyolefins	22
1.3 STABILISATION MECHANISMS OF POLYOLEFINS	23
1.3.1 The Chain-Breaking (CB) Mechanisms	23
1.3.2 The Preventive Mechanisms	24
1.4 SYNERGISM AND ANTAGONISM	25
1.5 STABLE NITROXYL RADICAL PRECURSORS AS ANTIOXIDANTS FOR POLYOLEFINS	28
1.6 ANTIOXIDANT SUBSTANTIVITY IN POLYMER STABILISATION	32
1.6.1 Parameters Influencing Antioxidant Substantivity	32
1.6.2 Approaches to Improve Substantivity of Antioxidants	34

1.7	MODIFICATION OF POLYMER-ANTIOXIDANT SYSTEMS BY REACTIVE PROCESSING	35
1.7.1	Developments in Polymer Modification	35
1.7.2	Reactive Processing of Polymer-Antioxidant Systems	36
1.8	OBJECTIVES AND SCOPE OF THE PRESENT WORK	37

CHAPTER 2

	EXPERIMENTS AND ANALYTICAL TECHNIQUES	40
2.1	MATERIALS	40
2.2	PREPARATION OF ANTIOXIDANTS	40
2.2.1	Synthesis of 1-acryloyl 4-acryloyloxy 2,2,6,6-tetramethyl piperidine (AATP, VI)	41
2.2.2	Synthesis of 4-acryloyloxy 2,2,6,6-tetramethyl piperidine (AOTP, VIII)	45
2.2.3	Synthesis of 1-myristoyl 4-acryloyloxy 2,2,6,6-tetramethyl piperidine (MyATP, IX)	49
2.2.4	Synthesis of 1-acryloyl 4-myristoyloxy 2,2,6,6-tetramethyl- piperidine (AMyTP, X)	53
2.2.5	Synthesis of 4-acryloyloxy 1,2,2,6,6-pentamethyl piperidine (AOPP, XI)	58
2.2.6	Synthesis of 1-ethyl 4-acryloyloxy 2,2,6,6-tetramethyl piperidine (EATP, XII)	62
2.2.7	Synthesis of 1-benzyl 4-acryloyloxy 2,2,6,6-tetramethyl piperidine (BATP, XIII)	66
2.2.8	Synthesis of 4-methacryloyloxy 2,2,6,6-tetramethyl piperidine (MOTP, XIV)	70
2.2.9	Synthesis of 1-methacryloyl 4-methacryloyloxy 2,2,6,6-tetramethyl piperidine (MMTP, XV)	74

2.3	COMPOUNDING	78
2.3.1	Reactive Processing of Polymer-Antioxidant Systems	78
2.3.2	Film Preparation	79
2.4	ANALYSIS OF MASTERBATCHES	79
2.4.1	Assesment of Binding Efficiency of Antioxidants	79
2.4.2	Measurement of Melt Flow Index (MFI)	79
2.4.3	Measurement of Molecular Weight Distribution (MWD)	80
2.5	POLYMER STABILITY TESTS	80
2.5.1	Photostability Test	80
2.5.2	Thermal Ageing Test	81
2.6	FOURIER TRANSFORM INFRARED (FT-IR) SPECTROSCOPY	82
2.7	GEL PERMEATION CHROMATOGRAPHY (GPC)	83
2.8	PROTON AND CARBON-13 NUCLEAR MAGNETIC RESONANCE (NMR) SPECTROSCOPY	85
2.9	ELECTRON SPIN RESONANCE (ESR) SPECTROSCOPY	87

CHAPTER 3

	REACTIVE PROCESSING AND STABILISING ACTIVITY OF ACRYLIC- CONTAINING NITROXYL PRECURSORS IN POLYPROPYLENE	89
3.1	OBJECTS AND METHODOLOGY	89
3.2	RESULTS	93
3.2.1	Optimisation of Binding Efficiency	93
3.2.2	Effect of Reactive Processing on the Photostabilising Activity of Acrylic Nitroxyl Precursors in Polypropylene	101
3.2.3	Reactive Processing of Monoacrylic Secondary Amine (AOTP) in Conjunction with Bisacrylic Nitroxyl Precursor (AATP)	104
3.2.4	Extended Binding of AOTP using Various Binding Agents (Coagents)	108
3.2.5	Thermal Ageing of Diluted Masterbatch (dMB) Films Containing AOTP	116

3.2.6	Effect of A Conventional UV-stabiliser (HOBP) on the Stability of Polypropylene Films Containing AOTP	119
3.3	DISCUSSIONS	124
3.3.1	Binding Efficiency of Acrylic Nitroxyl Precursors using Reactive-Processing Technique	124
3.3.2	Effect of Reactive Processing on Stabilising Activity of Acrylic Nitroxyl Precursors	128
3.3.3	Synergistic Behaviour of AOTP with HOBP	131

CHAPTER 4

ANALYSIS OF MASTERBATCHES CONTAINING ACRYLIC

NITROXYL PRECURSORS AND CHEMISTRY OF MODEL REACTIONS 133

4.1 OBJECTS AND METHODOLOGY 133

4.2 RESULTS 138

4.2.1 Analysis of Masterbatches Containing AATP or AOTP 138

4.2.1.1 Analysis of Insoluble-crosslinked Contents and Antioxidant Concentration in the Masterbatches 138

4.2.1.2 Molecular Weight Distribution (MWD) Data of Masterbatches Containing AATP and AOTP 145

4.2.2 Polymerisation of AOTP in Liquid Hydrocarbon 151

4.2.2.1 FTIR Spectroscopy Measurement 153

4.2.2.2 Proton NMR Measurements 158

4.2.2.3 Carbon-13 NMR Measurements 166

4.2.2.4 "Insitu" Polymerisation of AOTP in NMR Sample Area 176

4.2.2.5 Polymerisation of AOTP in Isooctane 182

4.3 DISCUSSIONS 184

4.3.1 Reactive Processing Mechanism of AATP and AOTP in Polymer Melts 184

4.3.2 Mechanism of AOTP Polymerisation in Solution 190

CHAPTER 5

REACTIVE PROCESSING AND STABILISING ACTIVITY OF N-ALKYLATED ACRYLIC AND METHACRYLIC DERIVATIVES OF STABLE NITROXYL RADICAL PRECURSORS	195
5.1 OBJECTS AND METHODOLOGY	195
5.2 RESULTS	200
5.2.1 Reactive Processing of N-alkylated Nitroxyl Precursors Containing Acrylic Group in Conjunction with TMPTA as Coagent	200
5.2.2 Photo and Thermal Stabilising Activity of N-alkylated Acrylic Nitroxyl Precursors	209
5.2.3 Reactive Processing of Nitroxyl Precursors Containing Methacrylic Group(s)	215
5.2.4 Extended Binding of MOTP and MOPP Using Various Coagents	221
5.2.5 Photostabilising Activity of Extended-Bound Methacrylic Nitroxyl Precursors	231
5.2.6 Binding of Masterbatches During UV-irradiation	235
5.3 DISCUSSION	237
5.3.1 Reactive Processing and Stabilising Activity of N-alkylated Acrylic Nitroxyl Precursors	237
5.3.2 Reactive Processing of Methacrylic(s) Nitroxyl Precursors	242
5.3.3 Stabilising Activity of Methacrylic(s) Nitroxyl Precursors	246

CHAPTER 6

CONCLUSIONS AND RECOMMENDATION FOR FURTHER WORKS	251
6.1 CONCLUSIONS	251
6.2 RECOMMENDATION FOR FURTHER WORKS	257
REFERENCES	261

LIST OF SCHEMES

Scheme	Page
1.1	25
1.2	31
3.1	92
4.1	136
4.2	137
4.3	186
4.4	189
4.5	193
4.6	194
5.1	197
5.2	199
5.3	240
5.4	244
5.5	245

LIST OF TABLES

Table		Table	Page
3.1	91	5.1	196
3.2	96	5.2	198
3.3	99	5.2.a	204
3.4	102	5.3	210
3.5	105	5.4	213
3.6	108	5.6	215
3.7	111	5.7	217
3.8	113	5.8	219
3.9	115	5.9	221
3.10	117	5.10	223
3.11	120	5.11	224
3.12	122	5.12	229
4.1	139	5.13	231
4.2	140	5.14	233
4.3	146	5.15	235
4.4	149		
4.5	183		

LIST OF FIGURES

Figure	Page	Figure	Page
2.1	42	3.4	100
2.2	43	3.5	100
2.3	44	3.6	103
2.4	46	3.7	103
2.5	47	3.8	104
2.6	48	3.9	106
2.7	50	3.10	106
2.8	51	3.11	107
2.9	52	3.12	110
2.10	55	3.13	111
2.11	56	3.14	112
2.12	57	3.15	112
2.13	59	3.16	114
2.14	60	3.17	114
2.15	61	3.18	115
2.16	63	3.19	116
2.17	64	3.20	118
2.18	65	3.21	118
2.19	67	3.22	120
2.20	68	3.23	121
2.21	69	3.24	123
2.22	71	3.25	123
2.23	72	4.1	134
2.24	73	4.2	134
2.25	75	4.3	142
2.26	76	4.4	143
2.27	77	4.5	144
2.28	78	4.6	147
2.29	83	4.7	150
2.30	85	4.8	152
2.31	88	4.9	155
3.1	94	4.10	156
3.2	95	4.11	157
3.3	96	4.12a	159

Figure	Page	Figure	Page
4.12.b	160	5.8	211
4.13.a	162	5.9	212
4.13.b	163	5.10	212
4.13.c	164	5.11	214
4.13.d	165	5.12	214
4.14.a	168	5.13	216
4.14.b	169	5.14	218
4.14.c	170	5.15	218
4.15.a	172	5.16	220
4.15.b	173	5.17	220
4.15.c	174	5.18	222
4.15.d	175	5.19	223
4.16.a	178	5.20	224
4.16.b	179	5.21.a	226
4.16.c	180	5.21.b	227
4.16.d	181	5.21.c	228
5.1	201	5.22	230
5.2	203	5.23	232
5.3	204	5.24	232
5.4	206	5.25	234
5.5	207	5.26	234
5.6	208	5.27	236
5.7	211		

ABBREVIATIONS AND SYMBOLS

A	:	absorbance, antioxidants
AATP	:	1-acryloyl 4-acryloyloxy 2,2,6,6-tetramethyl piperidine
AMyTP	:	1-acryloyl 4-myristoyloxy 2,2,6,6-tetramethyl piperidine
AOTP	:	4-acryloyloxy 2,2,6,6-tetramethyl piperidine
AOPP	:	4-acryloyloxy 1,2,2,6,6-pentamethyl piperidine
B	:	Beer-Lambert constant
(B)	:	bound
BATP	:	1-benzyl 4-acryloyloxy 2,2,6,6-tetramethyl piperidine
BGDM	:	butylene glycol dimethacrylates
CB	:	chain breaking
CB-A	:	chain breaking acceptor
CB-D	:	chain breaking donor
CI	:	carbonyl index
CM	:	closed mixing
C_m, C_i, C_s	:	concentration of antioxidants in masterbatch, insoluble and soluble fractions
D	:	diffusion coefficient, polydispersity index
DCM	:	dichloromethane
DCP	:	dicumylperoxide
D_0	:	exponential factor of diffusion
D_{R-R}	:	dissociation energy of chemical bond
(E)	:	extracted
EATP	:	1-ethyl 4-acryloyloxy 2,2,6,6-tetramethyl piperidine
ESR	:	electron spin resonance
ET	:	embrittlement time
FTIR	:	Fourier transform infrared
GPC	:	gel permeation chromatography
HDA	:	hexane 1,6-diacrylates
HOBP	:	2-hydroxy 4-octyloxy benzophenone
I	:	initiator
Irg.1010	:	Irganox 101 (pentaerythrityl tetrakis-[3,5-ditertiarybutyl 4-hydroxyphenyl] propionate)
Irg.1076	:	Irganox 1076 (octadecyl-[3,5-ditertiarybutyl 4-hydroxyphenyl]-propionate)
IR	:	infra-red
LDPE	:	low density polyethylene
MB	:	masterbatch
MFI	:	melt flow index
MMTP	:	1-methacryloyl 4-methacryloyloxy 2,2,6,6-tetramethyl piperidine
MOPP	:	4-methacryloyloxy 1,2,2,6,6-pentamethyl piperidine
MOTP	:	4-methacryloyloxy 2,2,6,6-tetramethyl piperidine
MWD	:	molecular weight distribution
MWt	:	molecular weight
M_i	:	molecular mass of i-component
M_n	:	number average molecular weight
M_w	:	weight average molecular weight
MyATP	:	1-myristoyl 4-acryloyloxy 2,2,6,6-tetramethyl piperidine
M_z	:	z-property average molecular weight
NMR	:	nuclear magnetic resonance
N_i	:	number of molecules of i-component
P	:	vapour pressure
PD	:	peroxide decomposer
PD-C	:	catalytic peroxide decomposer
PD-S	:	stoichiometric peroxide decomposer
PP	:	polypropylene
PVA	:	polyvinylalcohol
PVC	:	polyvinylchloride

P_i, P_s	: percentages of insoluble and soluble fractions in masterbatch
R	: gas constant
RI	: refractive index
$S.E.$: synergistic efficiency
$S_m, S_1, S_2, S_c, S_{1,2}$: stabilising activity of antioxidant mixture, antioxidant-1, antioxidant-2, control and synergistic system
TMPTA	: trimethylolpropane triacrylates
TMPTM	: trimethylolpropane trimethacrylates
TMS	: tetramethylsilane
Tipox.	: Titanium(IV)isopropoxide
T_m	: melting point
T.101	: Trigonox 101 (2,5-dimethyl 2,5-ditertiarybutylperoxy hexane)
Tin.292	: Tinuvin 292 (bis-[1,2,2,6,6-pentamethyl 4-piperidiny] sebacate)
Tin.770	: Tinuvin 770 (bis-[2,2,6,6-tetramethyl 4-piperidiny] sebacate)
$T_{1,2}$: induction period of degradation of polymer containing antioxidant mixture
(U)	: unextracted
(Ub)	: unbound
UV	: ultra-violet
V_1, V_2	: molar volumes of component-1,2
W_i	: rate of initiation reaction
W_o	: rate of initiation reaction involving participation of impurities
dMB	: diluted masterbatch
g	: proportional constant of electron spin resonance
h ν	: electromagnetic radiation
k_e, k_q	: rate constants of excitation and quenching reactions
l	: thickness
m.r.	: molar ratio of peroxide to antioxidant (additive)
n	: kinetic chain length = number of unit per polymer molecule
ν	: wave number, frequency of precession
ν_i, ν_p	: rates of initiation, propagation
δ	: chemical shift of NMR spectra
ΔCI	: carbonyl index increase
ΔH	: heat of evaporation
Δ	: heat
ΔH_f	: enthalpy of fusion
\hat{E}	: extinction coefficient
\emptyset	: diameter of bore
\emptyset_1, \emptyset_2	: volume fraction of component-1,2
≈ 1	: solvent-solute interaction parameter

CHAPTER 1

GENERAL INTRODUCTION AND SCOPE OF THE WORK

1.1 INTRODUCTION

Although an "olefin based polymer" had been discovered in the eighteenth century, the first commercial polyolefin begins with the discovery of its polymerisation technique by Fawcett and Gibson of Imperial Chemical Industries (ICI) in the early 1930s⁽¹⁾. In polymer science, apparently, the term "polyolefins" has only a restricted meaning to a group of polymers derived from simple hydrocarbons containing one or more unconjugated carbon-carbon double bond(s). This includes only a limited variety of polymers and copolymers of ethylene and propylene derivatives⁽²⁾. However, their commercial applications cover a wide range of properties from hard, glass like, to soft and rubbery materials. In addition, their cheapness, versatility and easy-processability lead to an increasing popularity of these materials both in domestic and industrial applications.

Like other polymeric materials, polyolefins are limited by their chemical instability toward heat, radiation, oxygen and the presence of impurities in the material. A major breakthrough in the stabilisation technology of polyolefins has led to the present increase of world wide annual production of polyolefins from 70 thousand tons in half century ago to over 20 thousand million tons. Not surprisingly, therefore, that polyolefins have consumed more than two-thirds of stabiliser produced for thermoplastics, to fulfill their increasing applications as engineering materials, in the area from domestic and construction to automotive and aerospace industries. Consequently, demand for more effective and efficient stabilisers, which are technically called "antioxidants", has continued unabated.

"Stable Nitroxyl Radical Precursors", i.e. hindered amine derivatives based on the structure of 2,2,6,6-tetramethyl piperidine have been introduced recently as a new

class of effective photo-stabilisers for polyolefins. These antioxidants are capable of forming stable nitroxyl radicals, which are considered to be important intermediates in the photo-stabilisation mechanism. Their uniqueness in stabilisation action and high order of stabilising activity have encouraged continuous investigation of their stabilisation mechanism.

Intrinsic stabilising activity is not the only factor which determines the effectiveness of an antioxidant, since the stabiliser is required to stay in the polymer matrix during the service-life, especially when the material is designed for use at high temperature, in an aggressive and hostile environment. Physical loss of the stabiliser due to evaporation or leaching to the media may not only lead to their absence of effectiveness but also contamination to the environment. This problem is becoming of great attention when the material is used for instance in food and medicinal packaging and clinical appliances. High molecular weight stabilisers have been developed to improve their substantivity and some polymerisable stabilisers have also been incorporated into polymer backbone during polymer synthesis. The effectiveness of the former, however, is not sufficient, whereas the latter is a high cost technique and applied only for a selective polymer. Recently, chemical modification of polymer melts by means of "reactive processing procedure", in an ordinary processing machine as reactor, is gaining momentum in industry to produce a desired modified material from cheap virgin polymer. This method may also be used as the most cost saving and effective technique to attach stabiliser molecules containing polymer-reactive groups onto the polymer backbone to achieve their maximum substantivity.

1.2 DEGRADATION OF POLYOLEFINS

To the polymer chemist, deterioration of polyolefin materials, either when processed to end-product or during outdoor in-service, is a chemical process which involves oxidation chain reactions. This phenomenon has been demonstrated in 1860s, that oxygen was consumed in the degradation of rubber. Modern theory of polymer

oxidation has been found by Farmer and Bolland and their coworkers at the British Rubber Producers Research Association (BRPRA) in 1940s. It was reported that the polymer oxidation is apparently a "chain radical process" and showed the formation of hydroperoxides as the primary products⁽³⁾.

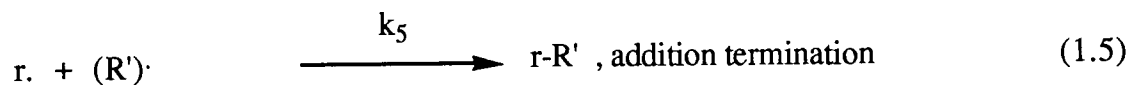
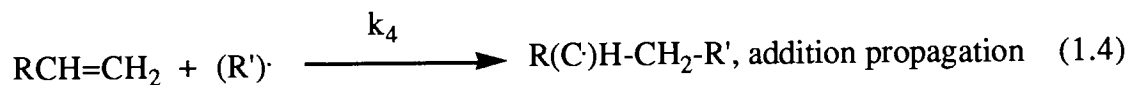
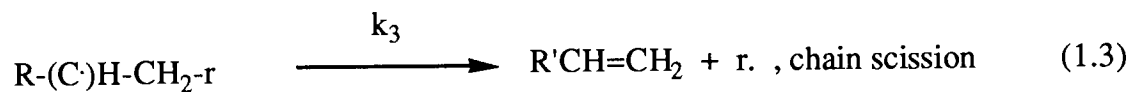
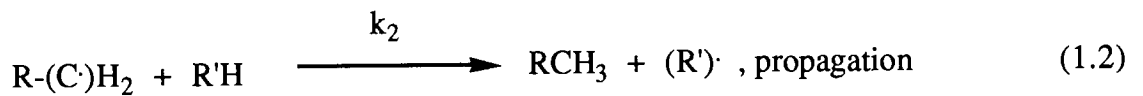
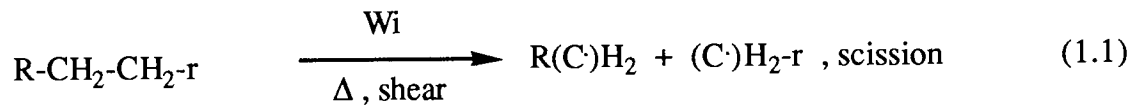
The process of polymer autoxidation is initiated by the formation of reactive macro alkyl radicals in the polymer⁽⁴⁾. External factors which are responsible for the formation of radicals are thermal, mechanical and electromagnetic radiation, which lead to thermal and mechanical degradations during polymer processing and photo-degradation during outdoor service-life. Understanding the mechanisms of these degradation reactions is a prerequisite for prescribing a remedy.

1.2.1 Mechanical Degradation of Polyolefins in Melts

When polyolefin materials are processed under the influence of shear and heat during their commercial exploitation to final products, mechanical degradation of the polymers inevitably occurs. This has been shown by Scott and Chakraborty⁽⁵⁾ that when low density polyethylene (LDPE) was processed at 150°C under air atmosphere, its melt flow index (MFI) increased and the molecular weight distribution (MWD) curve was shifted toward low molecular weight. Mechanical stress and high temperature were reportedly responsible for the formation of the first radicals initiating this degradation. The involvement of oxygen in the processing operation accelerated thermal oxidation and chain scission which in turn brings about the increase of MFI or the decrease of molecular weight.

Gol'dberg and Zaikov⁽⁶⁾ have extensively reviewed kinetics of mechanical degradation of polymer in the melts. It was reported that during mechanical degradation change of molecular weight may be in two directions according to the processing conditions. There are two destructive actions namely, "mechanical degradation" and "thermal oxidation" simultaneously affecting polymer melts during processing. It is well known that the former has a negative temperature effect, whereas the latter occurs

at high temperature in the presence of oxygen. To figure out the kinetics of mechanical degradation in melts it was assumed that during ordinary processing operation, e.g. in an extruder, air access is restricted. It was suggested, therefore, that in the absence of oxygen, mechanical degradation of polyolefins occurs according to the following mechanism (reactions 1.1 - 1.5).



As it was reported that the directions of molecular weight change can be explained from the rate equation of change of number of polymer molecules $[dn/dt]$ derived from the above mechanism, which is inversely related to change of molecular weight :

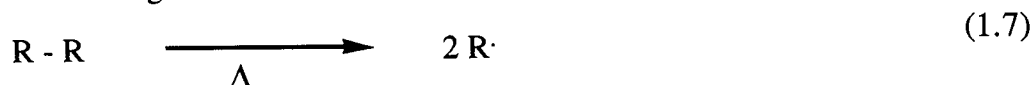
$$[dn/dt] = \{W_i/k_5\}^{1/2}\{k_3 - k_4[>\text{C}=\text{C}<]\} \quad (1.6)$$

Where, $[>\text{C}=\text{C}<]$ is concentration of double bonds in the polymers. It was also reported that the activation energy of chain scission (reaction 1.3) is higher (around 4 times) than that of addition reaction of macroradical to the double bond (reaction 1.4). Therefore, at high temperature, molecular weight tends to decrease (dn/dt positive), since k_3 increases faster than k_4 (in the right hand side of equation 1.6) as temperature of the system increases. High concentration of double bonds in the polymer may increase the molecular weight, because of addition reaction with macro alkyl radical

(reaction 1.4). High molecular weight polymers predominantly undergo chain scission, whereas low molecular weight polymers tend to form more double bonds, which in turn can easily undergo addition reactions. Basedow et.al.⁽⁷⁾ has reported, therefore, that mechanical degradation of polymer melts may cause narrowing of the molecular weight distribution.

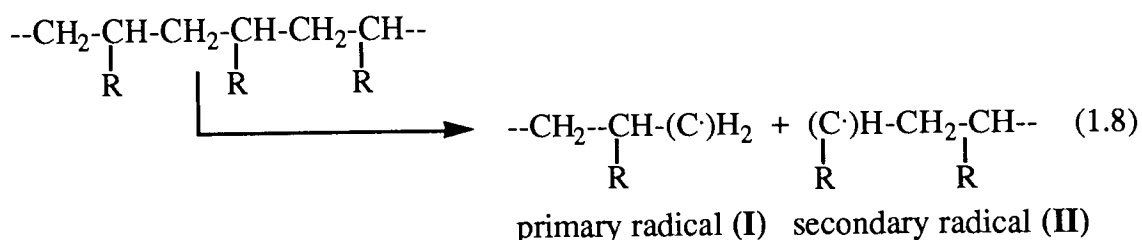
1.2.2 Thermal Oxidative Degradation

The use of polyolefin materials in a high temperature environment, such as in automotive industries for machinery components, is subjected to thermal oxidative degradation. Primary stage of this degradation is a non-oxidative process, which is followed by an oxidative mechanism in the presence of oxidative species. High temperature initiates chain scission of polymer backbone to form radicals, which in turn propagate further degradation.

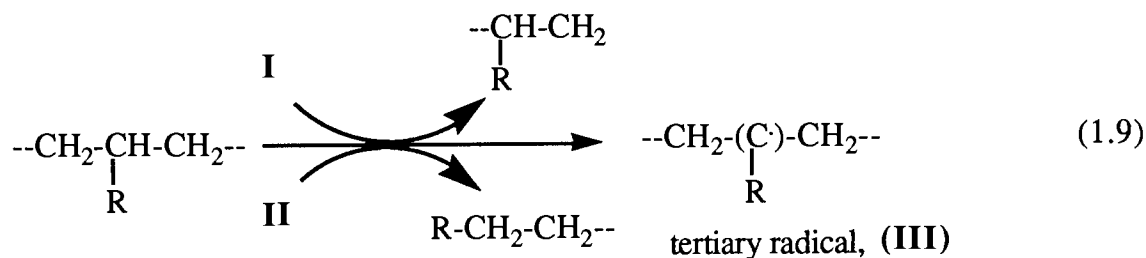


The rate of this initiation process depends on the thermal stability of C-C bonds in the polymer, which is related to the dissociation energy ($D_{\text{R-R}}$) of the bonds⁽⁸⁾.

Detailed mechanism of thermal scission of polypropylene has been reported⁽⁹⁾, which involves the formation of primary (I) and secondary (II) radicals. Moreover, investigation of the thermal degradation of several polyolefins using a pyrolyser⁽¹⁰⁾, suggested that random scission of the polyolefins backbone may take place as follows:



Tertiary radical (III) is also formed from transfer reaction of the radicals I and II with polymers (polypropylene).



In the presence of oxidative species, such as oxygen, thermal scission of polyolefins is followed by secondary stage which involves oxidation process to form hydroperoxides as primary products.



Based on the oxidation of simple hydrocarbon, Stivala et.al.⁽¹¹⁾ have proposed the general mechanism of thermal oxidation of polyolefins in the absence of additives :

Initiation:



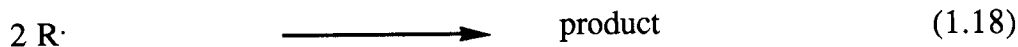
Propagation:



In the presence of double bonds:



Termination:

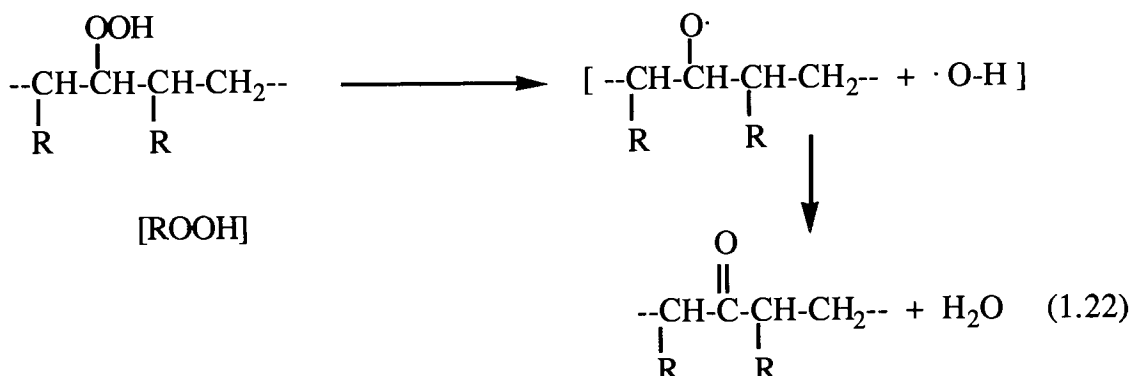


In the presence of high concentration of oxygen, reactions 1.18 and 1.19 may be neglected. Thus the most important termination reaction is reaction 1.20, which involves primary and secondary radicals, whereas tertiary radical may terminate as follows.

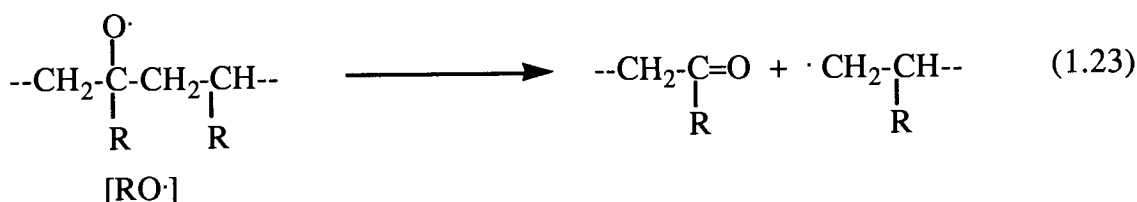


It has been reported that degradation products of thermal oxidation contain carbonyl and hydroxyl groups which may result from decomposition of hydroperoxides⁽¹²⁾. This was also observed by Reich and Stivala⁽¹³⁾ in the infrared spectroscopic investigation of thermal oxidation of polyolefins. They suggested several main paths of carbonyl formation as follows:

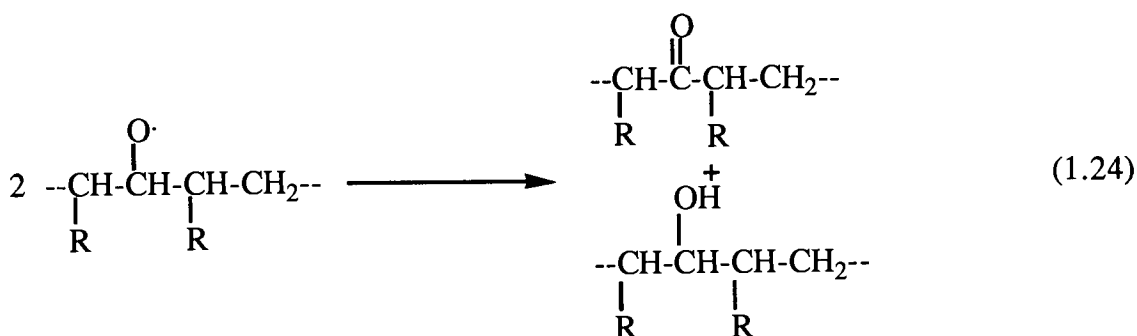
- hydrogen abstraction from hydroperoxide (ROOH),



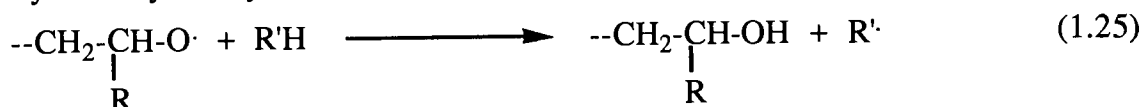
- β-scission process at the end of chain of alkoxy radical (RO·),



- simultaneous reaction from alkoxy radical,



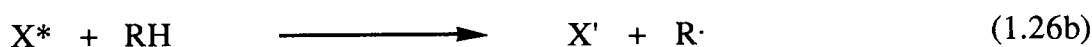
Formation of hydroxyl group may occur as follows; i.e. from hydrogen abstraction of polyolefin by alkoxy radical.



Branched polyolefins, such as polypropylene, oxidises more rapidly than the linear ones, e.g. high density polyethylene.

1.2.3 Photodegradation of Polyolefins

Pure polyolefins, apparently, are quite stable against ultra violet (UV) light, because the polymers do not absorb electro-magnetic radiation energy in the wave length region above 200 nm. Photodegradation of polyolefin materials may occur when initiated by the presence of impurities in the polymers, such as catalyst residues, or oxidation products during processing, e.g. carbonyl or hydroperoxides⁽¹⁴⁾. These act as photoinitiators for chain scission which in turn produce macroalkylradicals.

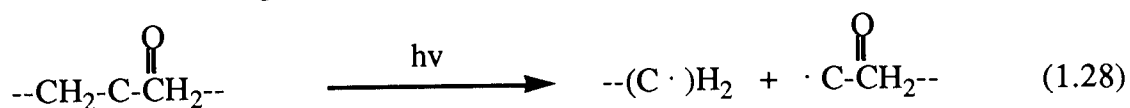


where, X, X* and X' are the photoinitiator, its excited state and transformed product, respectively. Mechanism of photo-oxidation of polyolefins has been briefly reviewed by Vink⁽¹⁵⁾. It was suggested that the photooxidation follows the general mechanism of thermal oxidation shown in Section 1.2.2 (16-18). The difference between the two mechanism lies only in the initiation step, i.e. in the formation of the first radical^(19,20).

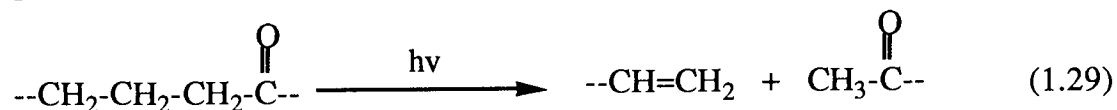
Chakraborty and Scott⁽²¹⁾ have reported that there is no significant carbonyl formation during the early stages of polypropylene degradation. On the other hand the hydroperoxides readily photolyse to give initiating macroalkylradicals⁽²¹⁻²³⁾, and function as important photoinitiators in photodegradation of polyolefins.



In the case of polyethylene the photoinitiation process is slightly different from that for polypropylene. The secondary hydroperoxides of polyethylene are less stable than the corresponding tertiary hydroperoxide of polypropylene. Ginhac et al.⁽²⁴⁾ have observed that the secondary hydroperoxides of polyethylene have no photoinductive effect. In polyethylene, therefore, the carbonyl compound plays the major part in photoinitiation, through a Norrish type I reaction, see reaction 1.28.



Scott et al.⁽²⁵⁾ showed the formation of carbonyls, double bonds and carboxylic acids during oxidation studies of LDPE by infrared spectroscopy. The formation of the unsaturation can be explained from photoreaction of carbonyl compounds through Norrish type II reaction (reaction 1.29).



It is clear, therefore, that photodegradation of polyolefins is initiated by formation of reactive macro radicals and photoinitiators, such as hydroperoxides. Oxidation of the polymers produces various oxidation products, which can be clearly detected using IR and UV-spectroscopy, whereas chain scission and crosslinking also take place during the oxidation. These lead to changes of physical and mechanical properties, such as tensile strength, elongation-at-break and embrittlement properties of the materials, which appear to be good measures to characterise the stability of polyolefin materials⁽²⁶⁾.

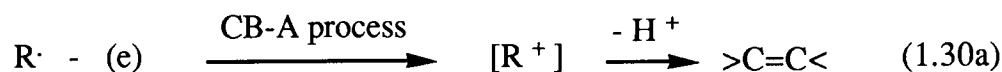
1.3 STABILISATION MECHANISMS OF POLYOLEFINS

The general mechanism of oxidative degradation of polyolefins (Section 1.2), indicates that, (i) degradation of polyolefins is a cyclical chain-oxidative process, and (ii) chain reaction is initiated by formation of macroalkylradicals, or hydroperoxides and excited state molecules, which produce reactive radicals in the presence of heat or light⁽²⁷⁾. Therefore, polyolefins may be protected from the degradative process either by breaking the chain oxidative process, i.e. by chain-breaking (CB) mechanisms, or by preventive actions, such as peroxide decomposition (PD) mechanisms⁽²⁸⁾.

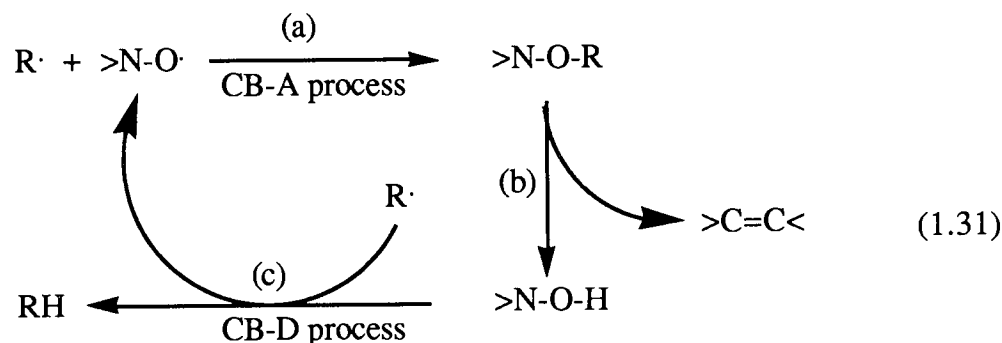
1.3.1 The Chain-Breaking (CB) Mechanisms

The idea of this mechanism is to break the cyclical chain of the degradation process by deactivating its initiating macroradicals. Chain-breaking mechanisms

involve either electron abstraction from macroradicals (chain breaking acceptor "CB-A" process) or electron donation to the macroradicals (chain breaking donor "CB-D" process), see reactions 1.30a and 1.30b.

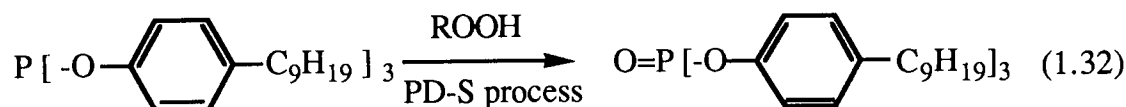


Some CB-antioxidants may behave as both CB-A and CB-D stabilisers⁽²⁹⁾. For instance, nitroxyl radical (>NO \cdot) traps macroalkyl radical via CB-A process, reaction 1.31a, whereas its transformation product, hydroxyl amine (>NOH), donates electron to the radical through CB-D process, reaction 1.31c.



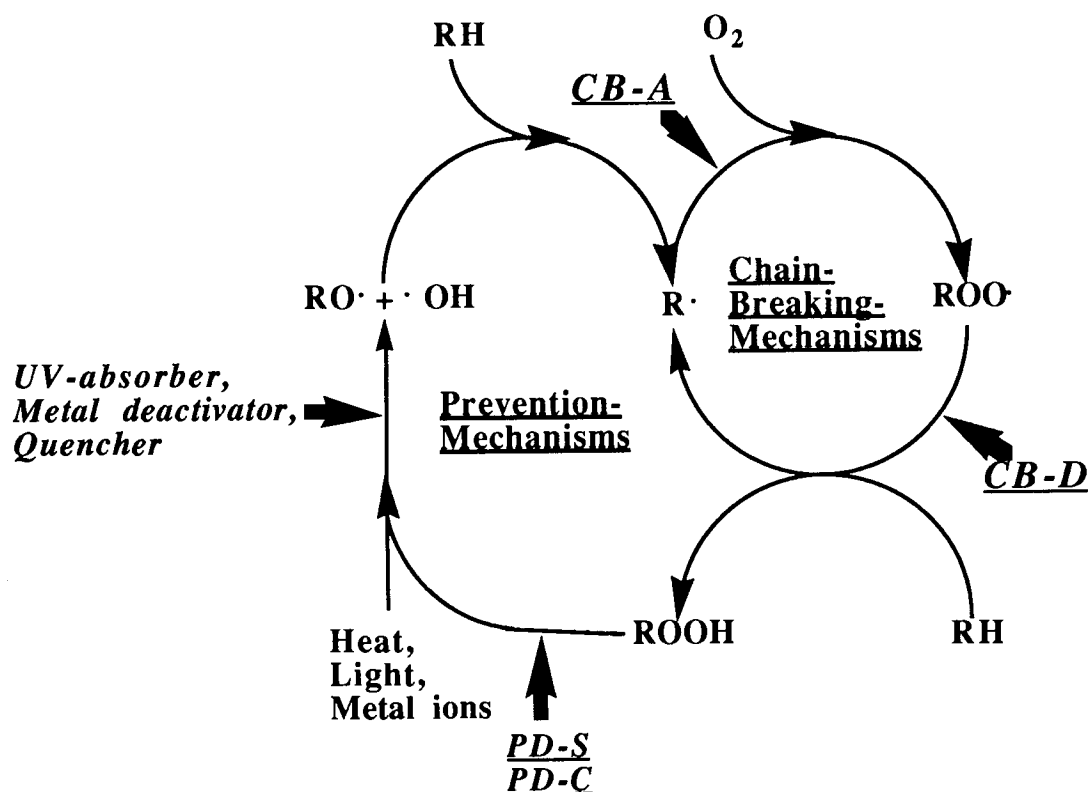
1.3.2 The Preventive Mechanisms

The most effective preventive mechanism is peroxide decomposition (PD), which takes place by either stoichiometric or catalytic reactions. Antioxidants which react stoichiometrically with hydroperoxides, to form alcohols, without free radical formation are called Stoichiometric peroxide decomposers (PD-S), reaction 1.32.



Catalytic peroxide decomposition (PD-C) antioxidants act as catalysts to decompose the hydroperoxides by a non-radical mechanism. These antioxidants possess an enhanced peroxide decomposition activity via a cyclical regenerative mechanism.

Summary of the processes involved in the stabilisation of polyolefins is shown in Scheme 1.1 (30).



Scheme 1.1 Stabilisation mechanisms of polyolefins

1.4 SYNERGISM AND ANTAGONISM

In practice, to enhance activity of a stabilisation system, more than one type of antioxidants which act by different mechanisms are employed. If these stabilisation mechanisms are complementary, a high stabilising activity (higher than the sum of individual activities) can be obtained. This phenomenon is called synergism, which is practically important from an industrial point of view⁽³¹⁾. On the other hand, if these antioxidants interfere antagonistically with each other, lower total activity is observed.

Synergistic Efficiency (S.E., %) of an antioxidant-mixture is defined by the following equation.

$$\text{S.E.} = \frac{[\text{Sm} - \text{Sc}] - \{[\text{S1} - \text{Sc}] + [\text{S2} - \text{Sc}]\}}{[\text{S1} - \text{Sc}] + [\text{S2} - \text{Sc}]} \cdot 100 \% \quad (1.33)$$

Where, Sm, S1, S2 and Sc are stability of polymer samples containing antioxidant mixture, antioxidant 1, antioxidant 2 and without antioxidant (control), respectively.

The mechanism by which the synergistic mixture functions, depends on the original mechanisms of action of each stabiliser or antioxidant. Ivanov and Shlyapintokh (32) have reviewed the general mechanisms of synergism in photostabilisation. They outlined different interactive mode of actions of (usually) two stabilisers or antioxidants which could give rise to strong or medium effects on the stabilising activity of the mixtures.

Protection of light stabiliser (S) with antioxidant (A) during photoreaction. In many polymers, such as polyolefins, it is believed that UV-absorber (S), e.g. a benzophenone, used in the photoreaction (induction period) is destroyed by macroradical formed in the period(33,34). Addition of an antioxidant (A), such as an octadecyl ester, protects the destruction of the UV-absorber through reduction of the concentration of the macroradical. Theoretically, the addition of the antioxidant is equivalent to the increase in UV-absorber concentration (ΔC_S).

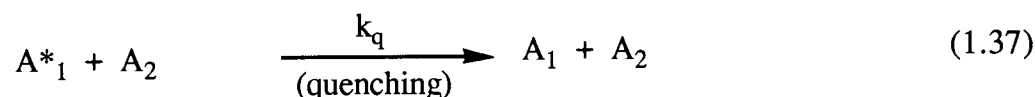
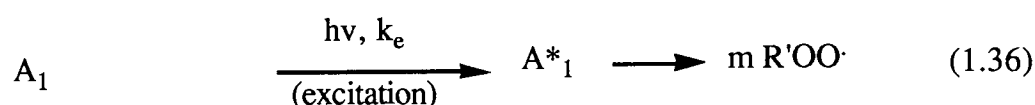
$$\Delta C_S = \frac{[\partial \cdot f_A]}{f_S} \cdot C_A \quad (1.34)$$

Where, f_A and f_S are stoichiometric coefficients of antioxidant and stabiliser, respectively, ∂ is probability of formation of radical in photoreaction and C_A is antioxidant concentration. According to the above equation, synergism is possible when $[\partial \cdot f_A] / f_S > 1$.

Complementary synergism of an antioxidant (A1) during processing and another one (A2) during in service. Severe conditions during polymer processing, e.g. high shear and temperature, may accelerate formation of oxidation products, such as carbonyls and hydroperoxides, which may act as photoinitiators. In addition, some UV-stabilisers may be destroyed during melt processing(35). Based on this evidence, Scott and Chakarborty(36) proposed the use

of a mixture of a benzophenone (as a light stabiliser) and an antioxidant which inhibits polymer oxidation and destruction of the light stabiliser during processing. In addition, antioxidant A2 may also function as photostabiliser during in-service.

Quenching of an antioxidant's (A1) excited state with another quencher antioxidant (A2). Consider a photochemically active antioxidant (A1), which is used in conjunction with another quencher antioxidant (A2). Mechanism of this synergism is based on the ability of quencher A2 to deactivate the excited state species of A1 (A1*)⁽³⁷⁾.

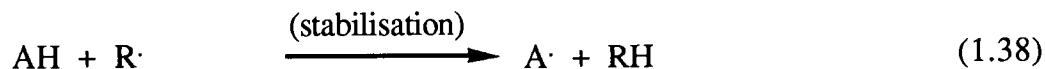


Efficiency of this synergism, therefore, depends on the effectiveness of absorption by the quencher (reaction 1.37) compared to the quantum yield of the excitation (reaction 1.36).

Formation of effective stabilisers from less active or non-stabilising additives. New stabilisers may be formed during thermal processing or photoreaction in polymer matrix. Such stabilisers are possibly more effective than the one used as conventional additive due to possible destruction during processing. This formation, therefore, could give rise to strong synergistic effect in the stabilised polymer. The effectiveness of this synergism is determined by the rate of formation and the reaction yield of the new stabiliser. Allen et al.⁽³⁸⁾ have demonstrated formation of a Nickel complex stabiliser from a weak stabiliser, i.e. 2-hydroxy 4-methoxy acetophenone oxime and Nickel nonanoate, during compression moulding of polypropylene at 200°C. This newly in-situ formed stabiliser was found to be as effective as the one initially added as conventional additive.

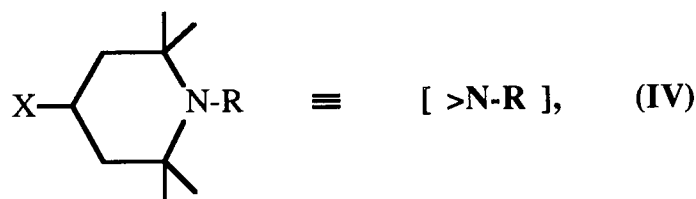
Regeneration of effective stabiliser. Stabilisation action by a stabiliser is apparently an oxidation-reduction process. Addition of a reducing agent (synergist)

may regenerate the stabiliser's conversion products, which again may function as effective stabiliser. Examples of this system are well known in polymer stabilisation, such as mixture of an amine (AH) and a phenolic (PhOH) antioxidants. The synergistic action is based on the following reactions.



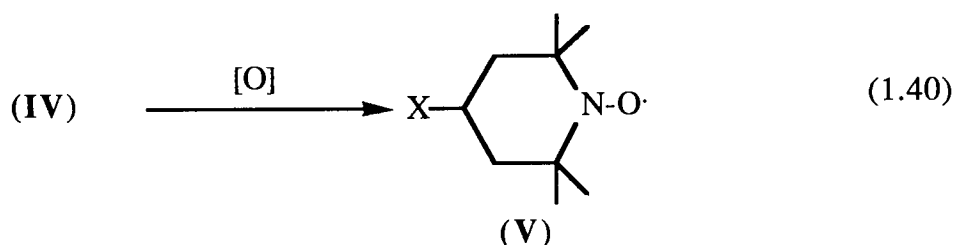
1.5 STABLE NITROXYL RADICAL PRECURSORS AS ANTI-OXIDANTS FOR POLYOLEFINS

Since early 1970s, hindered amine derivatives have been patented as effective photostabilisers for polyolefins⁽³⁹⁻⁴¹⁾. These are mainly secondary and tertiary amines, in which their α -carbon atoms are fully alkylated. Most of them are cyclic aliphatic amines based on the structure of 2,2,6,6-tetramethyl piperidine derivative (IV) (42).



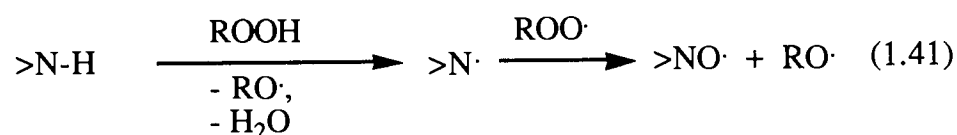
Where X is a group based on nitrogen or oxygen atom, and R is hydrogen, hydroxyl, alkyl, alkoxy or acyl substituents.

The discovery of these antioxidants was inspired by the invention of stable nitroxyl radical (V) by Russian's workers in the late fifties⁽⁴³⁾. These nitroxyl radicals, which are considered to be important intermediates in stabilisation action, can be formed via oxidation of the corresponding hindered amines⁽⁴⁴⁾.

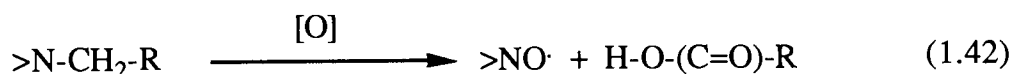


Chemical structure of the nitroxyl radicals is such that the free valence has no possibility to undergo tautomeric transformation, due to the total absence of their α -hydrogen atoms. This brings about localisation of the electron radical only on oxygen or nitrogen atoms, which in turn increase stability of the nitroxyl radicals tremendously^(45,46). No wonder that during stabilisation action the nitroxyl radical easily scavenges degradation-initiating macroalkyl radicals.

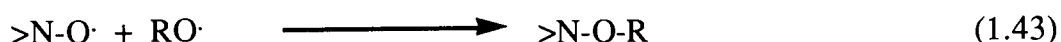
Kurumada et al.⁽⁴⁷⁾ have reported that various N-substituted derivatives of stable nitroxyl radical precursors also act as effective photo-antioxidants for polyolefins, which include secondary amine (>NH), N-hydroxyl (>NOH); N-alkoxyl (>NOR); N-alkyl (>NR); and N-acyl (>N(C=O)R) derivatives. Although the precise route of nitroxyl radical formation from the above nitroxyl precursors is still in dispute, the following oxidation routes have been suggested⁽⁴⁸⁾. The secondary amine is oxidised to nitroxyl radical by radical attack of hydroperoxide reaction.



N-alkylated nitroxyl precursors (>NR) have been reported⁽⁴⁷⁾ to form their parent secondary amine, which is readily oxidised to nitroxyl, and their corresponding carboxylic acids.



The main stabilising action of nitroxyl precursors is based on the high ability of nitroxyl radical to scavenge macroalkyl radicals.

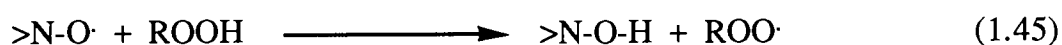
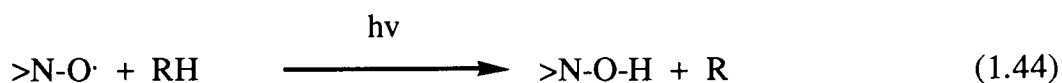


The alkyl radicals, however, are readily oxidised to form alkyl peroxy radicals (reaction

1.10). Therefore, the radical scavenging activity of nitroxyl radical is directly affected by the rate of the reaction.

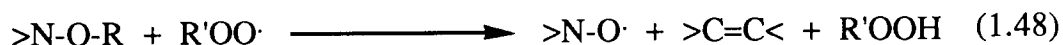
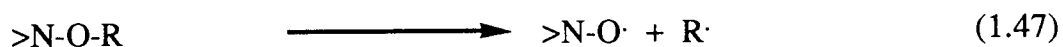
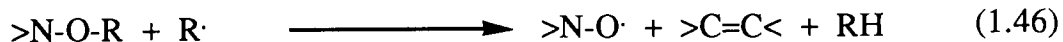


Formation of the hydroxylamines (>NOH) takes place due to the reaction of nitroxyl radicals with polymers or hydroperoxides⁽⁴⁴⁾.

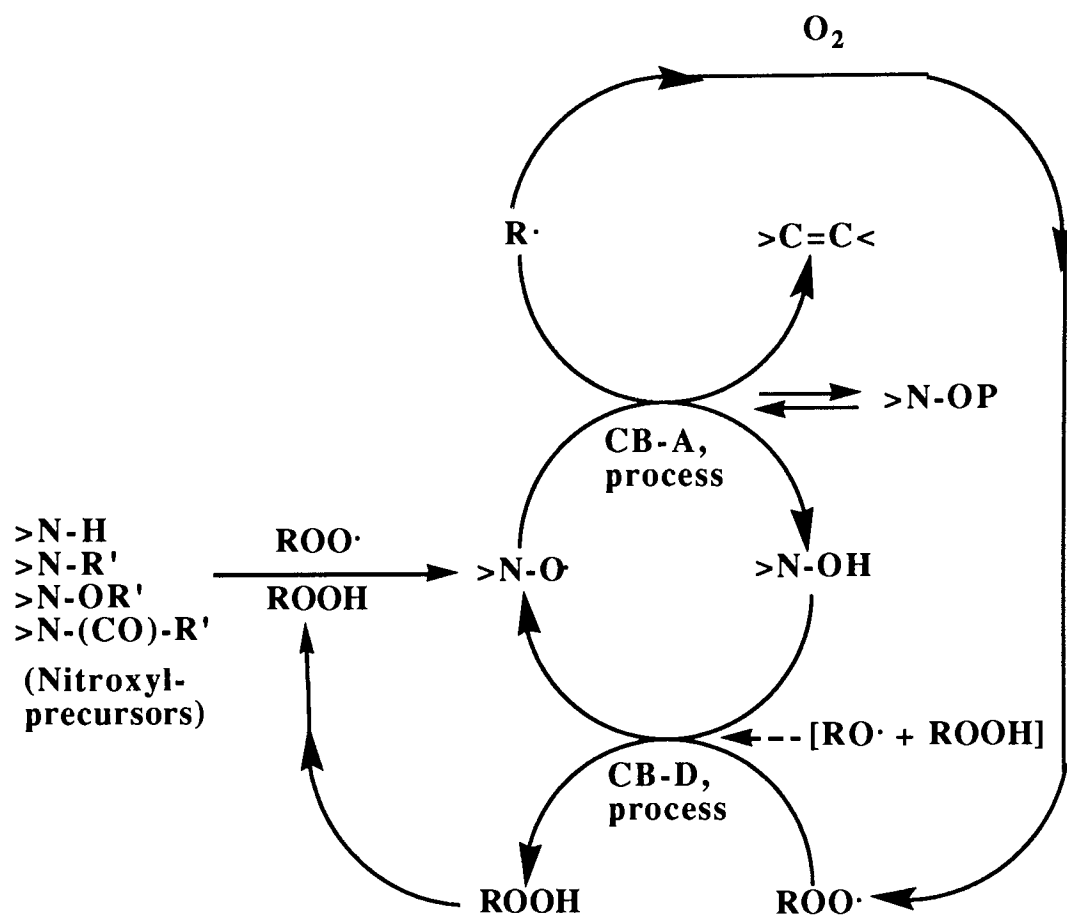


These hydroxylamines are easily oxidised to give nitroxyl radicals in the presence of heat or light.

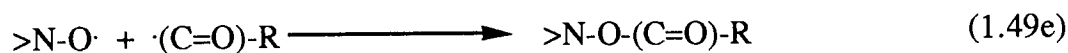
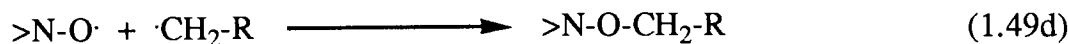
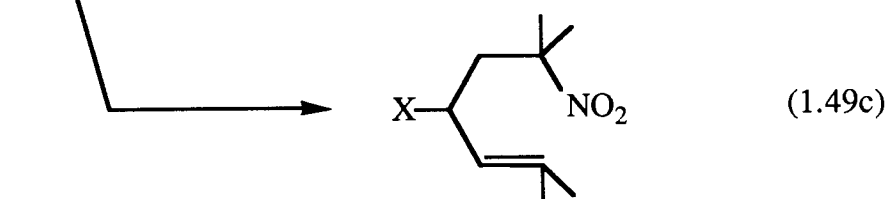
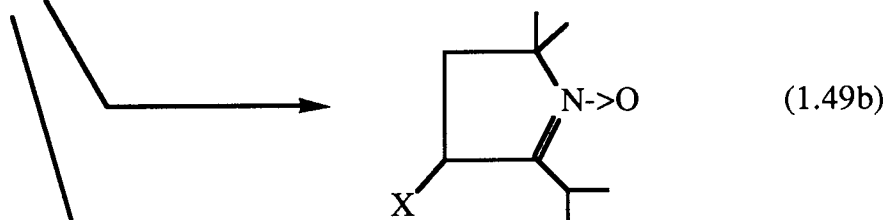
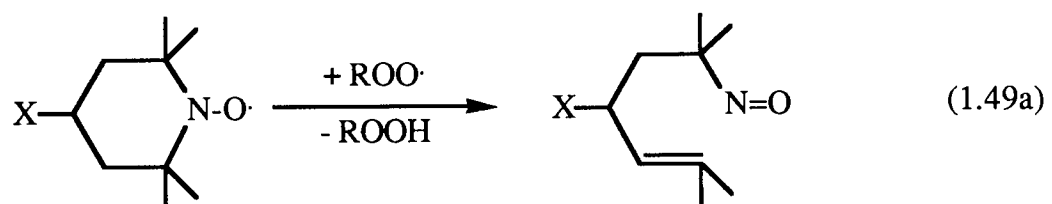
Ethers of the hydroxylamines (>NOR) are formed in trapping the alkyl radicals. These again regenerate nitroxyls on reaction with alkyl or alkyl peroxyradicals^(49,50).



The above reactions can be summarised in Scheme 1.2^(51,52). The Scheme suggests that the stabilisation action of nitroxyl radicals is a "cyclic regenerative process" (52-54). Theoretically, the cyclical radical scavenging mechanism of nitroxyl precursors can stabilise polymer against oxidation indefinitely. Finite stabilising activity of nitroxyl precursors is reported mainly due to destruction of the compounds during stabilisation action. Carlsson and Wiles⁽⁵⁵⁾ observed the reduction of nitroxyl concentration, and it was explained on the basis of the following reactions, see reactions 1.49a - 1.49e.



Scheme 1.2 Stabilisation action of stable nitroxyl radical precursors



1.6 ANTIOXIDANT SUBSTANTIVITY IN POLYMER STABILISATION

The effectiveness of a stabilisation system depends not only on the chemistry of the antioxidant action, but also on physical considerations. The first physical consideration is related to the application of the polymeric materials, such as processing conditions, contact media and environment, where the polymeric material is used, and the nature of the polymeric articles⁽⁵⁶⁾. The second includes all aspects affecting the permanence or substantivity of antioxidants in the polymer matrix. It is well known that low substantivity of antioxidant leads to physical loss of the antioxidant from the polymer, failure in the stabilisation action, and contamination to the media.

1.6.1 Parameters Influencing Antioxidant Substantivity

Mechanism of physical loss of antioxidant is affected by several individual parameters of the antioxidant, such as solubility and compatibility, volatility, and diffusion coefficient of the antioxidant⁽⁵⁷⁾.

Solubility and compatibility of antioxidants in polymers. solubility is associated with an individual parameter of a solute (antioxidant) which affects the homogeneity of the antioxidant in a polymer (solvent). The totality of the parameters which involve interaction between the antioxidant and the polymer and their individual cohesive and adhesive forces is represented by compatibility. During stabilisation, the antioxidants are required to be compatible with the polymers, otherwise they may form aggregates within the polymers and cannot be distributed finely. Degree of solubility of an antioxidant in polymer can be improved by incorporating polar groups into the antioxidant molecules in the case of polar polymers, and non-polar groups for non-polar polymers⁽⁵⁷⁾.

It is well known that solubility of a solute depends on temperature of the solution. Solubility of an antioxidant in polymer, on the other hand, is measured during

hot processing at temperature up to above 200°C. It is not always that the antioxidant remains in the subsaturated state after cooling at room temperature. To predict the solubility of the antioxidant at room temperature, Flory and Huggins⁽⁵⁸⁾ have proposed solubility equation for crystalline solid antioxidant in polymer. Assuming that the volume fraction of a polymer, $\phi_2 \sim 1$ (molar volume = V_2), the solubility of the antioxidant (molar volume = V_1) is measured by the volume fraction of the antioxidant (ϕ_1) in homogenous mixture.

$$-\ln \phi_1 = [\Delta H_f / R][(1/T) - (1/T_m)] + [1 - (V_1 / V_2)] + \approx_1. \quad (1.50)$$

Where, ΔH_f is enthalpy of fusion of the crystalline antioxidant, R is gas constant, T_m is melting point, and \approx_1 is the solvent-solute interaction parameter. Using the above equation, Roe et al.⁽⁵⁹⁾ have measured the solubility of phenolic antioxidants in LDPE. In the polymer melts, the solubility was measured after the disappearance of solid antioxidant, whereas at room temperature the solubility was extrapolated from the high temperature data.

Volatility of antioxidants. Evaporation is the major cause of the loss of antioxidants at elevated temperatures especially from polymer articles with high ratio of surface area to weight. In the first stage, the evaporation takes place only on the surface, then as the concentration of antioxidant on the surface decreases, the antioxidants in the bulk start to diffuse to the surface layer⁽⁵⁶⁾.

Volatility of an antioxidant in polymer, is affected by both intrinsic properties of the antioxidant and external factors. At a given temperature, the effect of internal factor of antioxidant on its solubility is shown by the following Arrhenius equation⁽⁶⁰⁾.

$$\ln P = - [\Delta H / R][1/T] + C. \quad (1.51)$$

According to the above equation, the volatility of antioxidants, which is associated with their vapor pressure (P), decreases as the heat of evaporation $[\Delta H]$ increases. As the $[\Delta H]$ is a function of molecular weight and interaction forces within the polymers, the volatility of antioxidant can be decreased by either incorporating high molecular weight groups or creating interaction bonds between antioxidants and polymers. Schmitt and

Hirt⁽⁶¹⁾ have observed temperature dependence of the vapor pressure of a benzophenone. They found that at temperature above T_m , plot $[\log P]$ versus $[1/T]$ was in good agreement with equation 1.51. However, the slope of the line $[-(\Delta H/R)]$ was deflected at temperature below T_m , which indicates the change of ΔH value in the solid state. Influence of external factors on volatility of antioxidant has been reported by Plant and Scott⁽⁶²⁾ that the change of volatility with time is linear. Free-surface area of the sample is important, whereas the total amount of the antioxidant in the sample does not affect the volatility, provided that this amount is below its solubility.

Diffusion coefficient of antioxidant. As mentioned above, diffusion of antioxidants within the bulk of polymers may affect the rate of evaporation or leaching and stabilisation action of the antioxidant. A diffusive antioxidant migrates easily to the polymer surface, which increases its surface concentration. The diffusion coefficient of antioxidant (D) is expressed as a function of temperature in the following equation⁽⁶³⁾.

$$D = D_0 \exp. [-E_d/R.T]. \quad (1.52)$$

Where, D_0 is a pre-exponential factor and E_d is the energy of activation for the diffusion process, which depends on the chemical structure of the antioxidant and the physical state of the polymer. D is observed from the amount of antioxidant traveling along a certain distance at a certain time. Where both D_0 and E_d are calculated experimentally from diffusion coefficient data at various temperatures.

1.6.2 Approaches to Improve Substantivity of Antioxidants

In general, antioxidant substantivity can be improved either by employing high molecular weight antioxidants or copolymerisation of antioxidant derivatives with monomer during manufacturing (polymer synthesis). The former has been used commercially, but this raises the antioxidant substantivity only to a limited extent^(64,65). whereas the latter can be used only for specific polymers.

Scott⁽⁶⁶⁾ has reviewed the general methods in preparing polymer-bound antioxidants. These methods include: copolymerisation and grafting of monomeric

antioxidants, and binding of non-polymerisable antioxidants onto polymers. Munteanu⁽⁶⁴⁾ has reviewed the same methods, especially in grafting of polymerisable antioxidants into polymers and binding of antioxidants containing reactive groups into grafted polymers.

Consequently, if mobility of antioxidants plays a main role in polymer stabilisation, the polymer-bound antioxidants may have less stabilisation activity. Nevertheless, the effect of the mobility is not that important. In addition, the polymer-bound antioxidants can be employed mostly in the amorphous area of the polymeric materials, in which the degradation most probably takes place. Thus, modification of polymer-antioxidant system during processing can be used effectively to attach antioxidant molecules onto polymer backbone. This technique will be discussed in the following section.

1.7 MODIFICATION OF POLYMER-ANTIOXIDANT SYSTEMS BY REACTIVE PROCESSING

1.7.1 Developments in Polymer Modification

Modification of polymer has been used since 19th century to produce modified materials with desired properties, such as in the vulcanisation of natural rubber⁽⁶⁷⁾ and modification of cellulose in the early 20th century⁽⁶⁸⁾. Basic idea of polymer modification is based on the chemical reaction of a modifying agent with reactive groups in the polymer molecules, e.g. double bond in rubber, and hydroxyl group in cellulose. This reaction has been investigated by Flory⁽⁶⁹⁾, who stated the principles of equal reactivity that "*reactivity of a group in polymer is independent of the chain length and the viscosity (if the mechanism of the reaction does not change)*". Modification of saturated hydrocarbon polymer (polystyrene) had also been reported from the work of Houtz and Adkins⁽⁷⁰⁾ in the radical polymerisation of styrene in the presence of

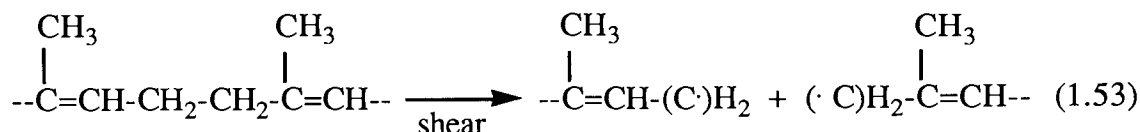
pre-formed polystyrene. It was found that the new polymer product gave higher molecular weight, in which the styrene monomers were attached onto the original polystyrene backbone. In the period after 1960s, modification of polymers experienced a tremendous development. This was mainly due to elegant work of Greber⁽⁷¹⁾, who used a polymeric catalyst to improve catalyst-polymer compatibility. He grafted diethyl aluminum hydride (Ziegler-Natta catalyst) onto polybutadiene to form polyolefin grafts.

The above mentioned polymer modifications were mainly carried out in liquid solution in the presence of a suitable polymer solvent. Chemical reaction of polymer may occur even faster in the melts during processing. Aggressive processing environment, such as high temperature, substantial shear and the presence of oxygen and peroxide, however, create uncontrollable destruction of the polymer. Planned control of chemical changes in the course of polymer processing, on the other hand, can be used to modify the properties of polymer materials by choosing appropriate processing conditions and peroxide or catalyst used as initiator⁽⁷²⁾. This technique, which is well known as "reactive processing" is growing rapidly in industry due to its cost saving and high efficiency. In addition, the process can be carried out from laboratory scale in a batch (internal mixer) to continuous industrial production in extruders or cavity transfer mixers.

1.7.2 Reactive Processing of Polymer-Antioxidant Systems

As has been mentioned in the previous section, section 1.6., the attachment of antioxidant molecules during processing may provide solution to the problem of physical loss of the antioxidant. It also has been reported^(73,74) that several antioxidants can be bound using the polymer modification technique during vulcanisation of rubber. Workers at the Malaysian Rubber Producers Research Association^(75,76) have reported that various N-substituted 4-nitroso aniline derivatives became chemically bonded to the rubber during vulcanisation. The modified antioxidant-rubber was found could not be removed from the rubber matrix even after

exhaustive solvent extraction. During processing of polymers, mechano-scission process has reportedly taken place to form free macro radicals, which can initiate further radical reactions⁽⁷⁷⁾.

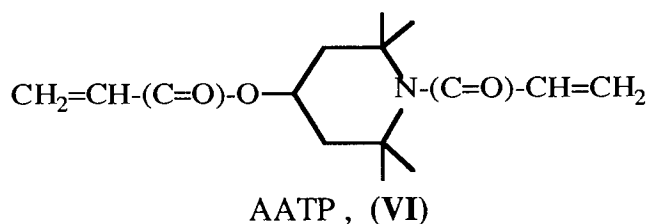


Using the same process Sumida and Vogl⁽⁷⁸⁾ have successfully grafted vinyl antioxidants onto elastomer backbone during processing. Recently, using saturated hydrocarbon polymers, such as polyolefins, various modification of polymer-antioxidant systems have been carried out⁽⁷⁹⁻⁸¹⁾. Al-Malaika et al⁽⁸²⁾ has successfully bound a bis-acrylic antioxidant in polypropylene during reactive processing in a batch hot mixer (torque-rheometer), in the presence of small amount of peroxide. Masterbatches (concentrates) of polymer-bound antioxidants, with concentration up to 20%, have been prepared and more consequently diluted down in fresh polymer to the normal antioxidant concentration level.

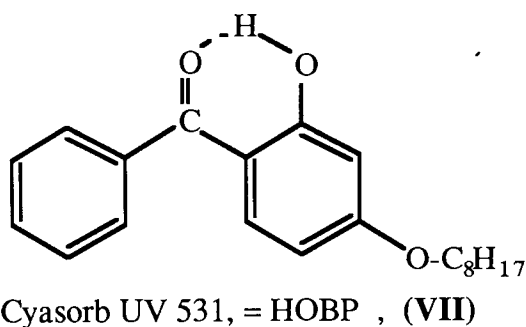
1.8 OBJECTIVES AND SCOPE OF THE PRESENT WORK

N-substituted derivatives of stable nitroxyl radical precursors based on the structure 2,2,6,6-tetramethylpiperidine have been reported to be effective antioxidants for polyolefins^(47,53,54). These derivatives may react with hydroperoxides to produce secondary amines which are further oxidised to stable nitroxyl radicals. Furthermore, these derivatives have been synthesised from a starting compound : 2,2,6,6-tetramethyl 4-piperidinol ^(39,83). Acrylic and methacrylic derivatives of these compounds have also been synthesised successfully⁽⁸⁴⁻⁸⁶⁾.

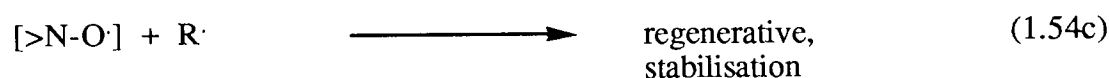
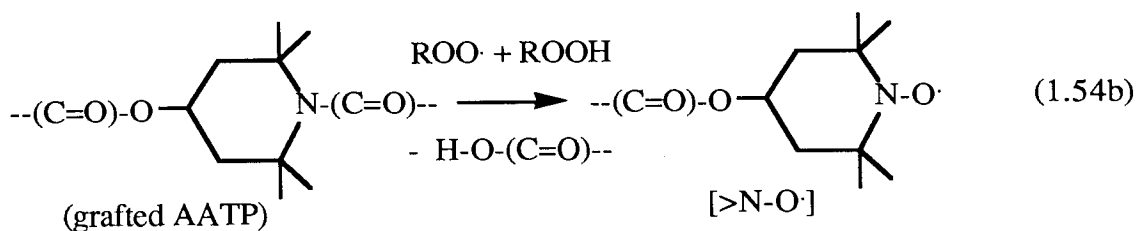
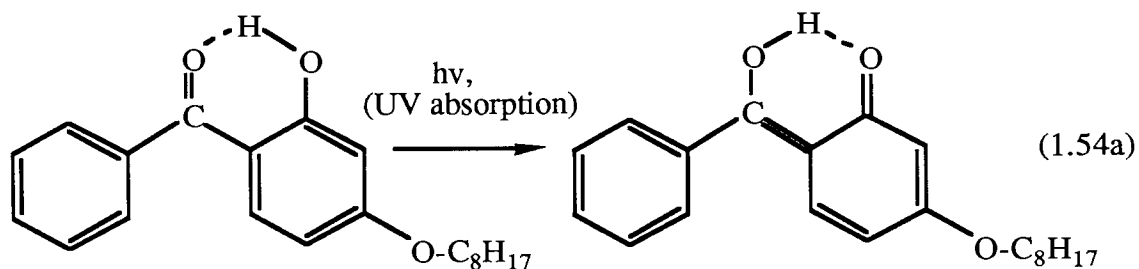
Recently⁽⁸²⁾, it has been reported that 1-acryloyl 4-acryloyloxy 2,2,6,6-tetramethyl piperidine (AATP, VI) showed an effective photoantioxidant activity in polypropylene.



Although it can be 100%-mechano-chemically bound into the polymer, the bound-antioxidant is ineffective stabiliser. Surprisingly, when the grafted antioxidant was employed in conjunction with a small amount of a conventional UV-stabiliser, such as 2-hydroxy 4-octyloxy benzophenone (HOBP) or Cyasorb UV 531 (VII), it became exceptionally effective photostabiliser.



The reason for this behaviour is not very clear. It was suggested that the UV-stabiliser protects the bound-antioxidant during the early stage of photoreaction. This period allows the bound nitroxyl precursor to build-up sufficient nitroxyl radical concentration necessary for further regenerative stabilisation by the nitroxyl, see reactions 1.54a - 1.54c.



The object and scope of the present work is to carry out mechanistic investigations of grafting reactions of reactive nitroxyl precursors as antioxidants (hindered amine derivatives containing polymer reactive function) in polymer melts and in hydrocarbon model compounds under conditions closely related to polymer processing. Another important object of the work is to maximise the grafting efficiency of reactive nitroxyl precursors during the processing operations using a new approach whereby other compounds containing at least two polymer reactive functions (referred here to as 'coagents') will be used as co-reactants. Reactions of these antioxidants with the polymer in presence or absence of coagents will be carried out during polymer processing (using the processing equipment as a chemical reactor) and the operation is referred to as 'reactive processing'. The stabilising effectiveness of the highly grafted (bound) antioxidant systems will be examined and compared with commercial antioxidants containing similar antioxidant function. The following approaches, therefore, will be investigated.

- (1). To study the behaviour of acrylic and methacrylic (polymer reactive function) derivatives of nitroxyl precursors during the grafting process in the polymer melt.
- (2). To optimise the efficiency of the reactive processing operation using various processing conditions in the presence of different concentrations of peroxides and coagents.
- (3). To investigate mechanisms of the grafting reaction of the above antioxidants during processing operation in polymer melt as well as in hydrocarbon model compounds under similar conditions to the processing.
- (4). To study the antioxidant effectiveness of bound nitroxyl precursors in polyolefins against thermal and photodegradation.
- (5). To investigate the effect of low concentrations of commercial UV-stabilisers on the antioxidant activity of these hindered amine antioxidants containing acrylic or methacrylic groups in polyolefins.

CHAPTER 2

EXPERIMENTS AND ANALYTICAL TECHNIQUES

2.1 MATERIALS

Polypropylene (Propathene ICI, HF-26) was supplied by I.C.I. (Plastic Division) Ltd. 2,2,6,6-tetramethyl 4-piperidinol was supplied by Ciba-Geigy, Switzerland. Methyl acrylate, myristoyl chloride, methyl myristate, acryloyl chloride, methyl methacrylate, titanium (IV) isopropoxide (Tipox), anhydrous potassium carbonate, methyl bromide, ethyl bromide and benzyl bromide are all ex-Aldrich Chemical and were used directly without further purification. Dicumylperoxide, DCP (recrystallised from methanol) and 2,5-dimethyl 2,5-di-tertiarybutylperoxy hexane (Trigonox 101) were supplied by Akzo Chemical. Trimethylol propane triacrylates (TMPTA), hexane diacrylates-1,2 (HDA), trimethylol propane trimethacrylates (TMPTM), butylene glycol dimethacrylates (BGDM) and 4-methacryloyloxy 1,2,2,6,6-pentamethyl piperidine (MOPP) were supplied by Ancomer Ltd., England.

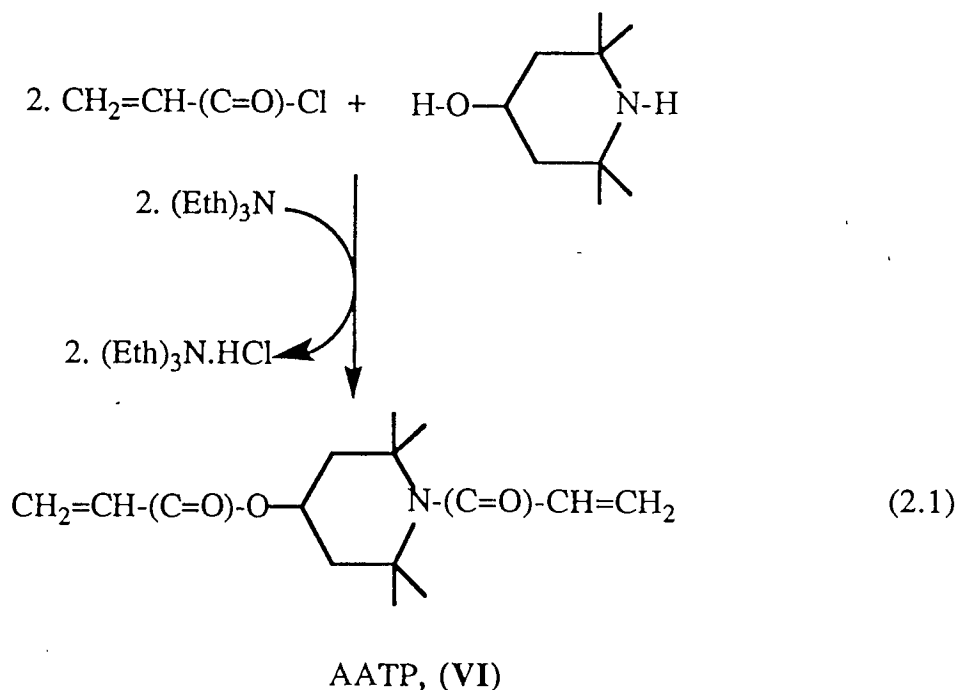
2.2 PREPARATION OF ANTIOXIDANTS

Various stable nitroxyl radical precursors based on hindered piperidine derivatives were synthesised as reported in the patents by Murayama et al⁽³⁹⁻⁴¹⁾. High yields were obtained by ester interchange reaction in the presence of titanium(IV) isopropoxide (Tipox) as catalyst. Detailed synthetic methods are shown below.

2.2.1 Synthesis of 1-acryloyl 4-acryloyloxy 2,2,6,6-tetramethyl piperidine (AATP, VI)(39-41).

15.7 gram (0.1 mol) of 2,2,6,6-tetramethyl 4-piperidinol, 29.2 ml (0.2 mol) triethylamine were dissolved in dry benzene, and then cooled down below 10°C in an ice bath. A solution of 18.6 ml (0.2 mol) of acryloyl chloride in dry benzene was added dropwise with constant stirring. The stirring was continued at that temperature for another hour and at room temperature for 12 hours, reaction 2.1. Solid triethyl amine hydrochloride formed was filtered out, the filtrate was washed with aqueous potassium hydrogen carbonate and dried over anhydrous sodium carbonate. After vacuum evaporation an oily crude product was obtained. This was then washed with hexane to get a slightly yellow product, yield = 60%.

Elemental analysis: N = 5.3 % ; C = 68.0 % ; H = 8.7 % , (Calculated). N = 4.5 % ; C = 68.8 % ; H = 8.1 % , (Found). FTIR-analysis, (liquid film), Figure 2.1 : ester >C=O, 1728 cm⁻¹(s); amide >C=O , 1651 cm⁻¹(s); unsaturation >C=C<, 1608 cm⁻¹(m). Proton and Carbon-13 NMR spectra (in CDCl₃) are shown in Figures 2.2 and 2.3.



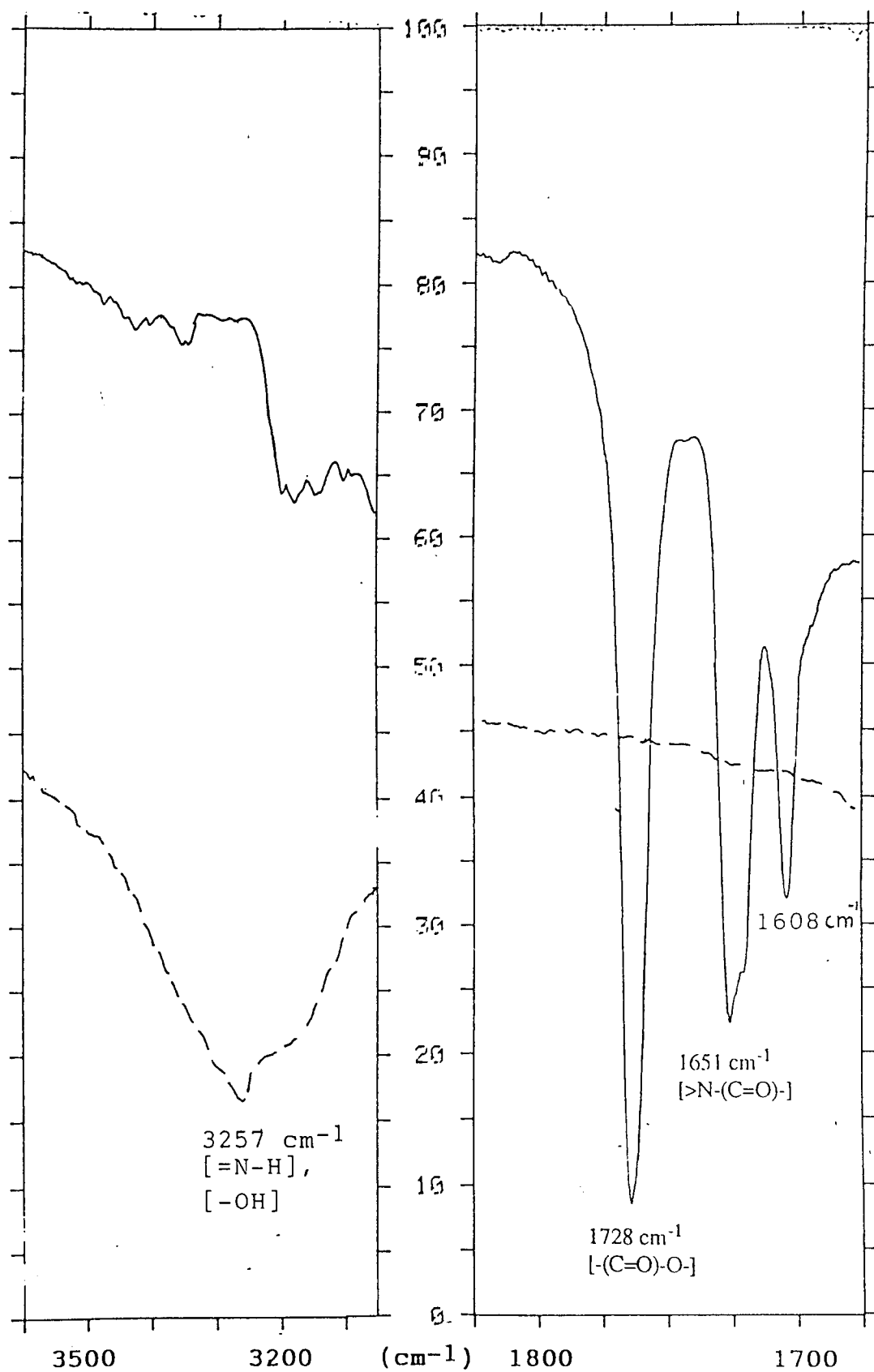


Figure 2.1 FT-IR spectra of 1-acryloyl 4-acryloyloxy 2,2,6,6-tetramethyl piperidine (AATP, VI), as liquid film (—), compared to that of 2,2,6,6-tetramethyl 4-piperidinol (- - - -)

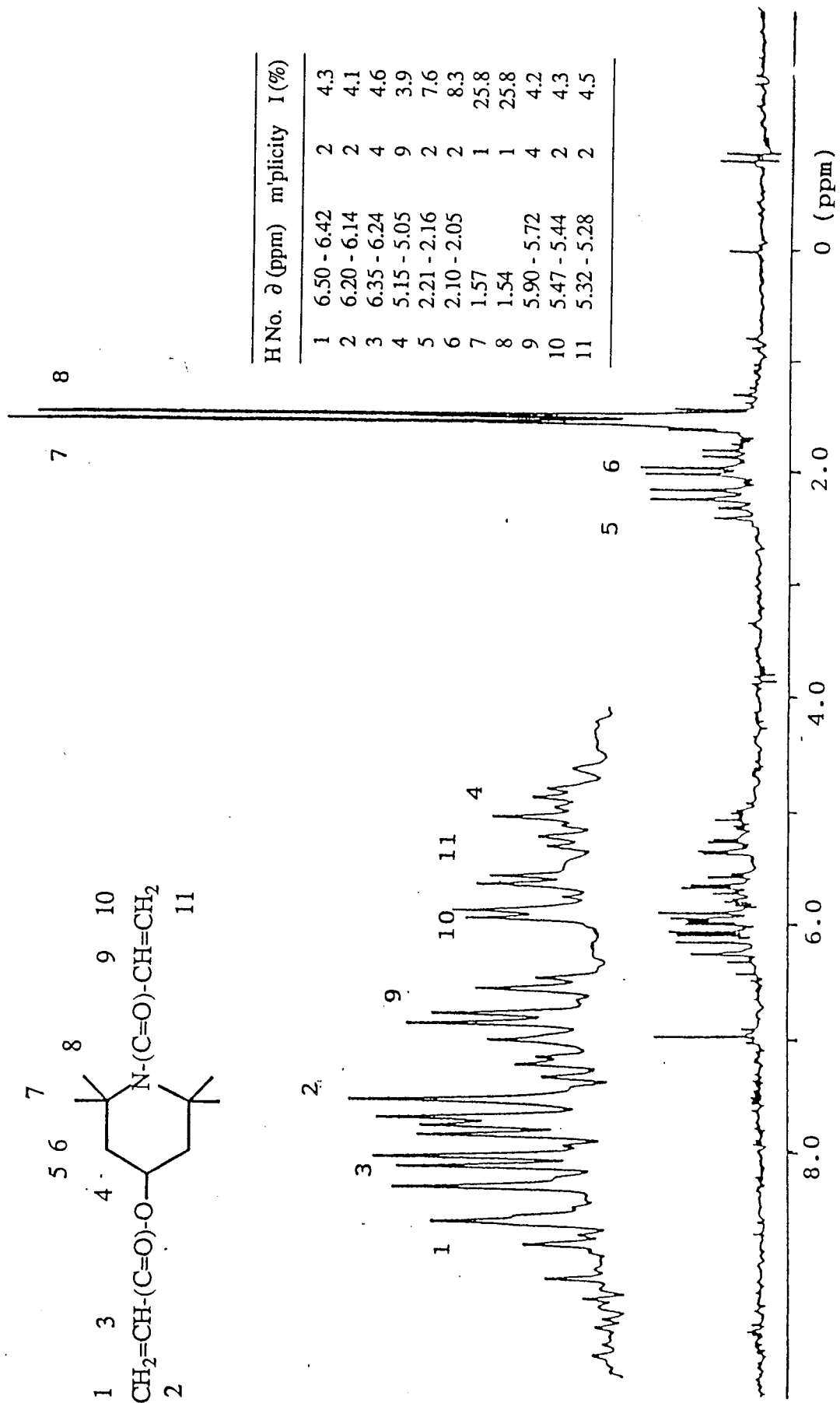


Figure 2.2. Proton NMR spectra of 1-acryloyl 4-(2,2,6,6-tetramethyl piperidino)oxybutane (AATP, VI) in deuterated chloroform

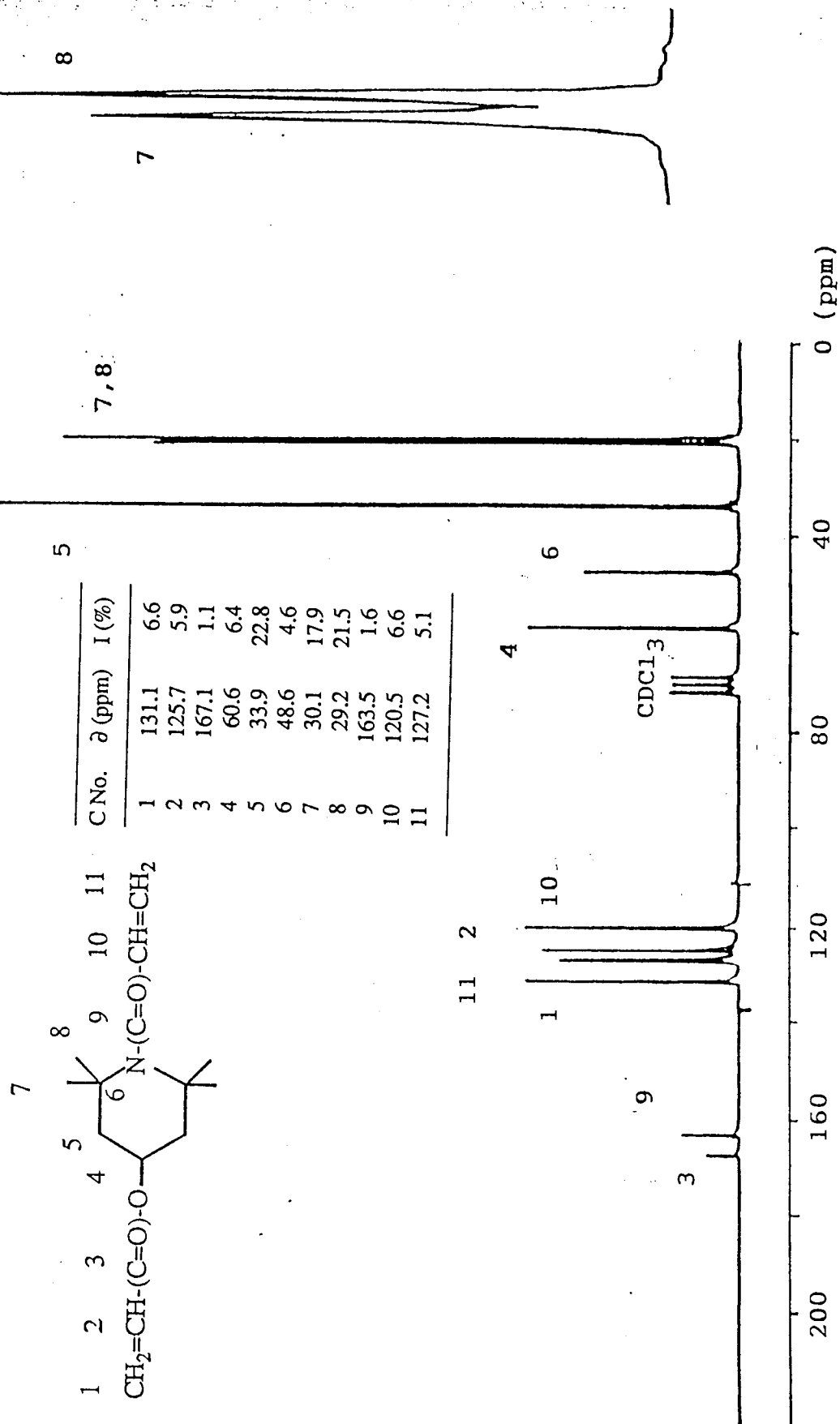
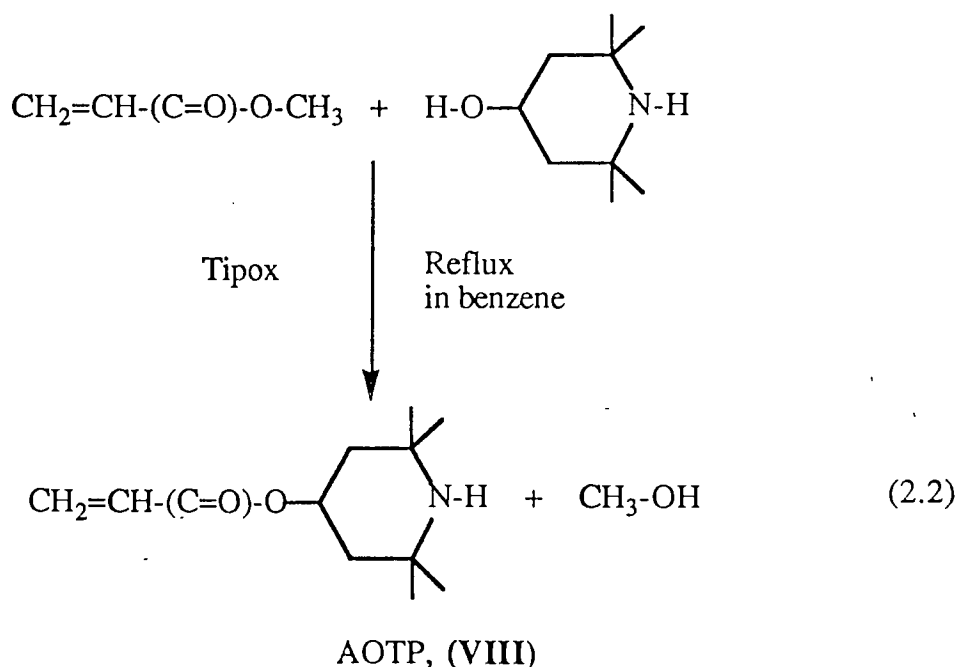


Figure 2.3. Carbon-13 NMR spectra of 1-acryloyl 4-(2,2,6,6-tetramethylpiperidin-1-yl)oxybutane (VI) in deuterated chloroform

2.2.2 Synthesis of 4-acryloyloxy 2,2,6,6-tetramethyl piperidine (AOTP, VIII)(39-41).

15.7 gram (0.1 mol) of 2,2,6,6-tetramethyl 4-piperidinol and 8.4 ml (0.1 mol) of methyl acrylate were dissolved in dry benzene. The solution was then boiled in an oil bath under nitrogen atmosphere. 3 ml (0.01 mol) of titanium isopropoxide (Tipox) was then added, and the solution was refluxed continuously for 24 hours (reaction 2.2). The reaction product was treated with 50 ml aqueous sodium bicarbonate, filtered and vacuum evaporated. A white solid was obtained. This was then recrystallised from hexane, yield 70%.

Melting point : 50-52°C. Elemental analysis: N = 6.6 %; C = 68.3 %; H = 9.9 % (Calculated). N = 6.1 % ; C = 70.8 % ; H = 11.0 % (Found). FTIR-analysis (KBr disc), Figure 2.4. : secondary >N-H, 3317 cm⁻¹(w); ester >C=O , 1704 cm⁻¹(s); unsaturation >C=C<, 1617 cm⁻¹(m). Proton and Carbon-13 NMR spectra (in CDCl₃) are shown in Figures 2.5 and 2.6.



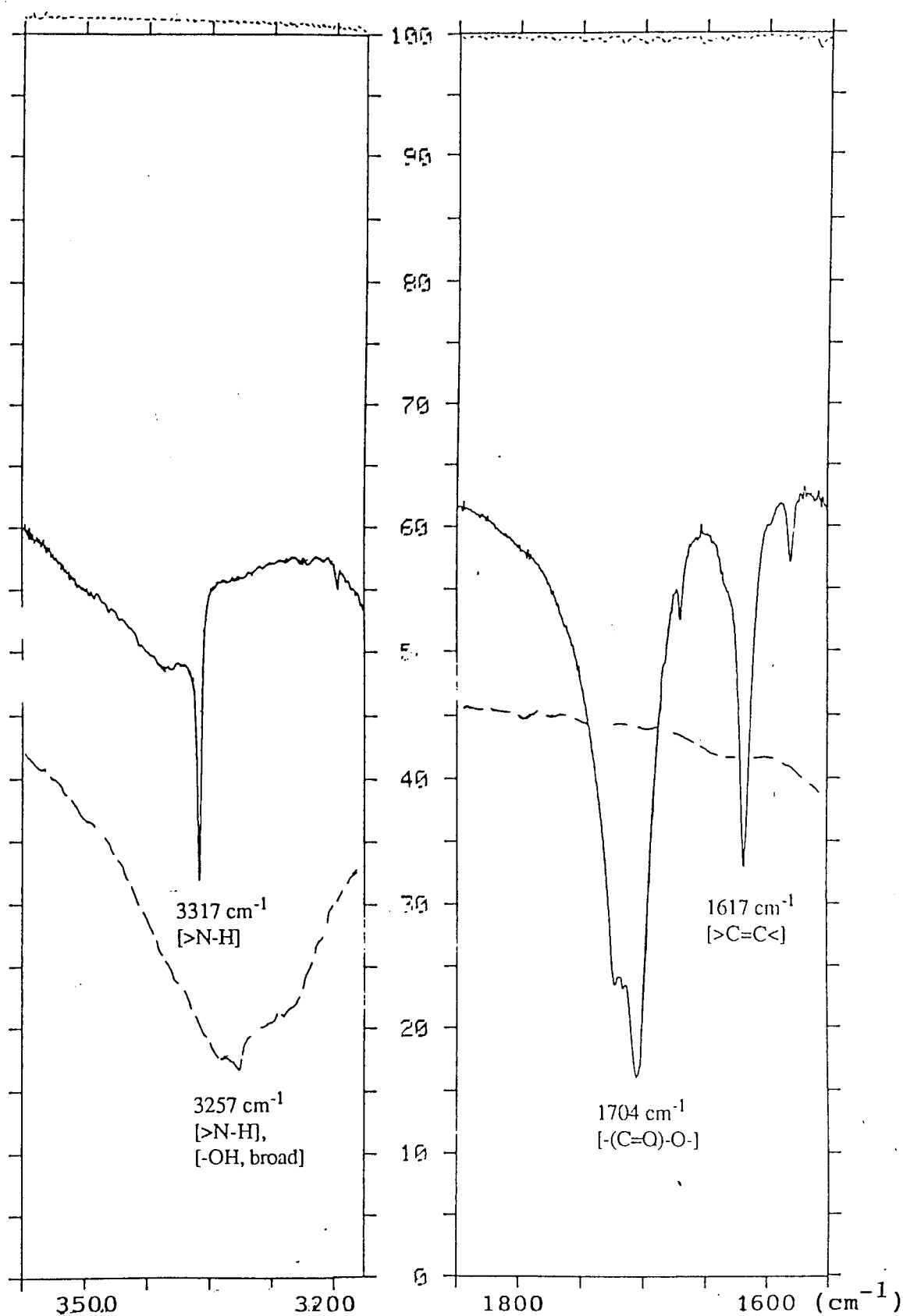


Figure 2.4 FT-IR spectra of 4-acryloyloxy 2,2,6,6-tetramethyl piperidine (AOTP, VIII), in KBr disc (—), compared to that of 2,2,6,6-tetramethyl 4-piperidinol (-----)

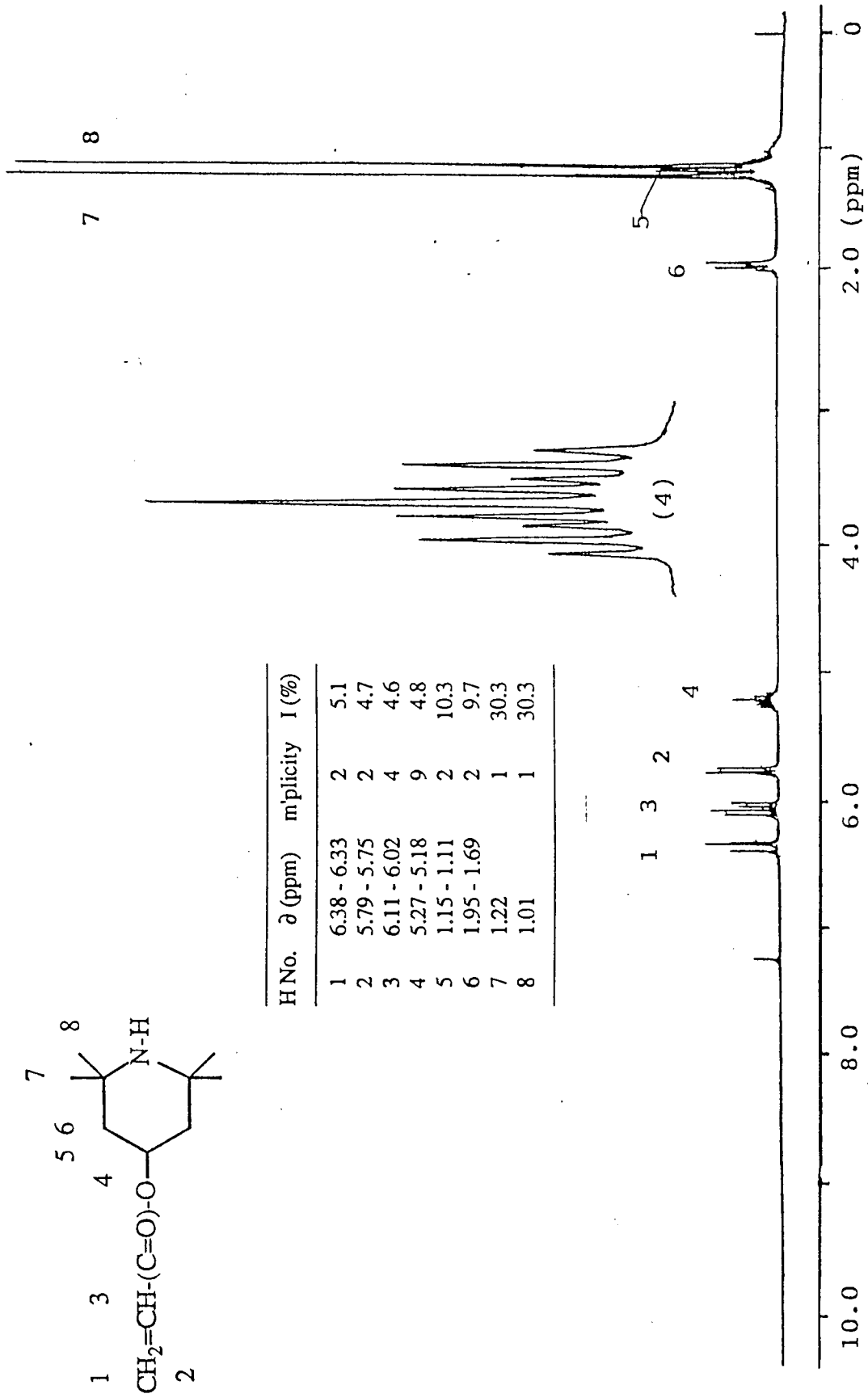


Figure 2.5. Proton NMR spectra of 4-acryloyloxy 2,2,6,6-tetramethyl piperidine (AOTP, VIII) in deuterated chloroform

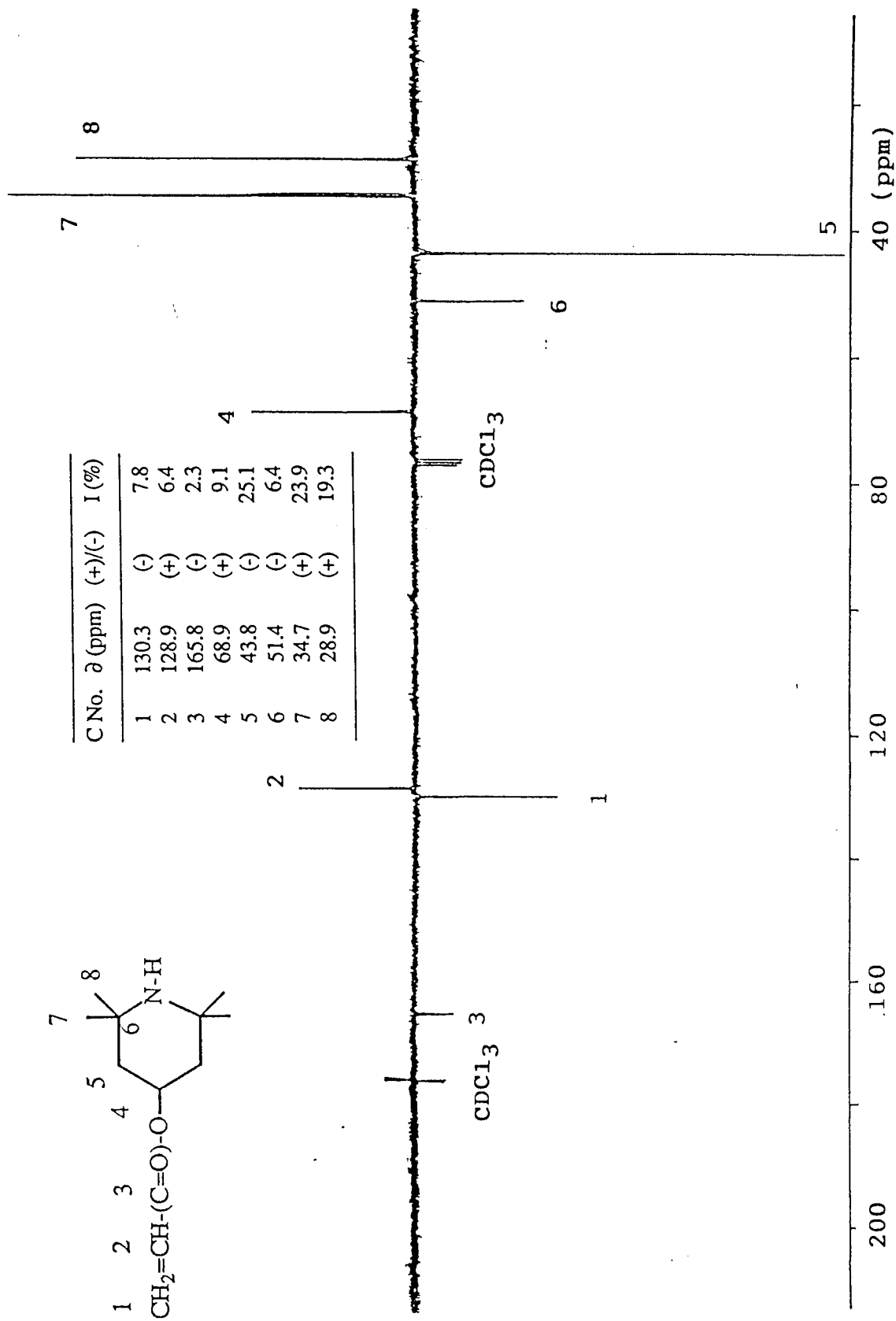


Figure 2.6. Carbon-13 NMR spectra of 4-acryloyloxy 2,2,6,6-tetramethyl piperidine (AOTP, VIII) in deuterated chloroform

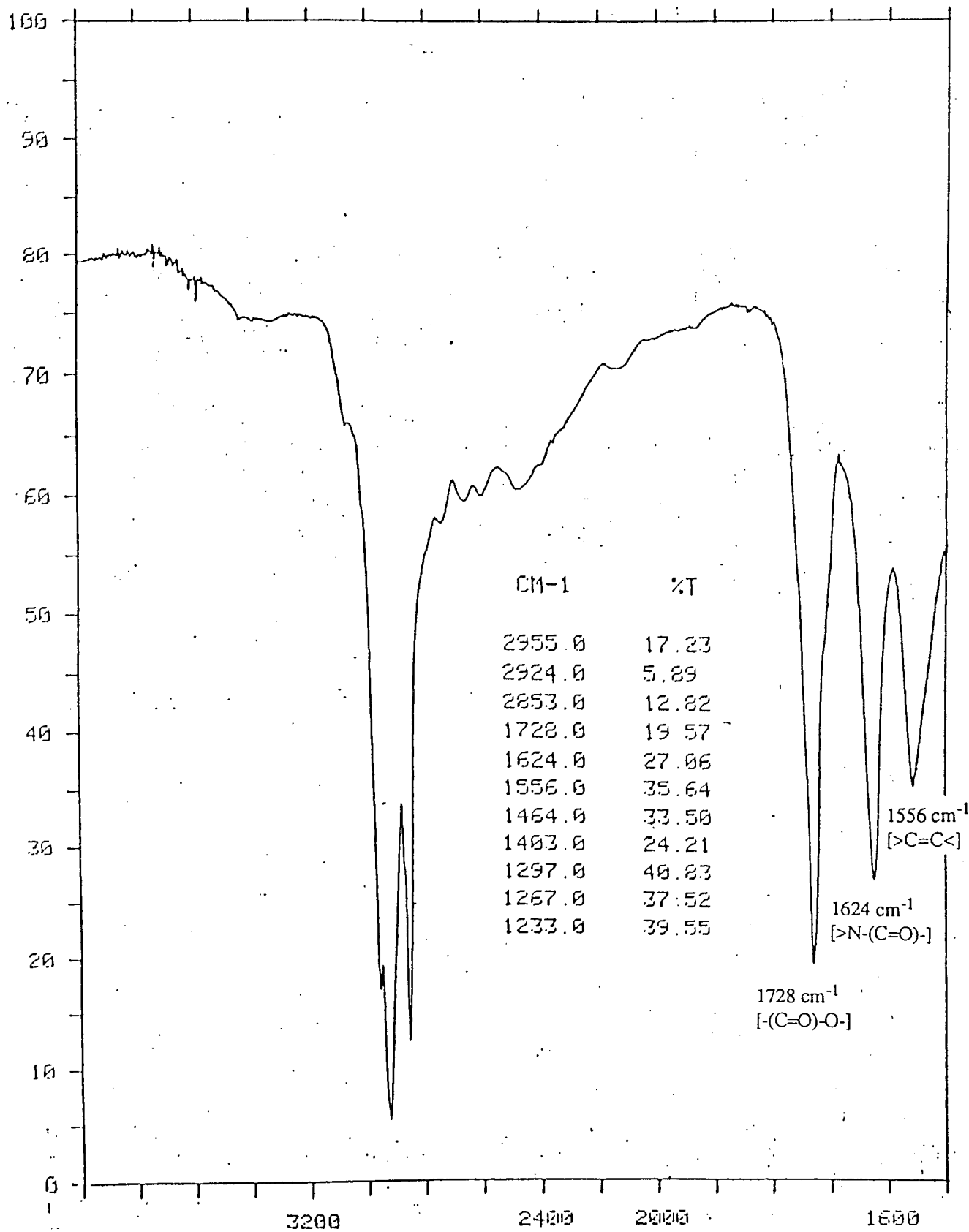
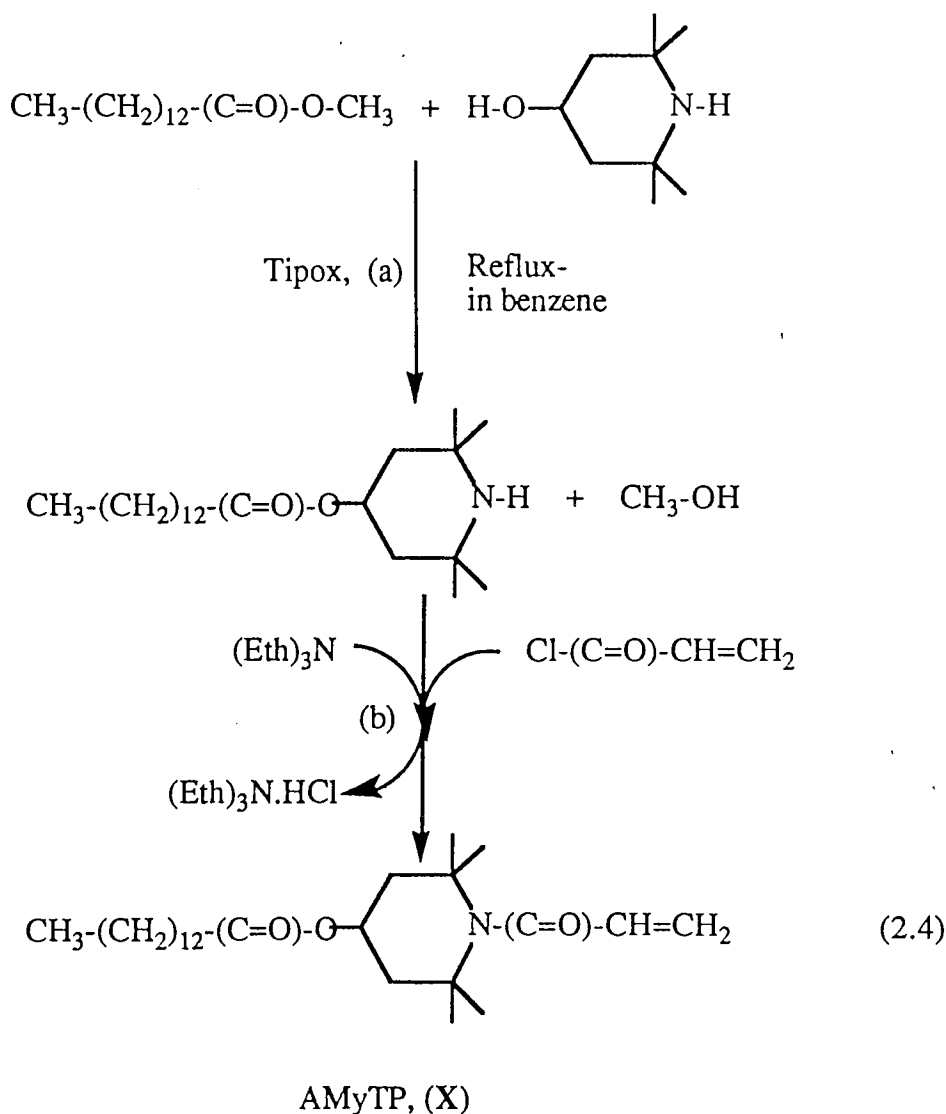


Figure 2.7 FT-IR spectra of 1-myristoyl 4-acryloyloxy 2,2,6,6-tetramethyl piperidine (MyATP, IX), as liquid film

2.2.4 Synthesis of 1-acryloyl 4-myristoyloxy 2,2,6,6-tetra methyl piperidine (AMyTP, X)(39-41).

15.7 gram (0.1 mol) of 2,2,6,6-tetramethyl 4-piperidinol, 20.9 ml of methyl myristate (0.1 mol), and 3 ml (0.01 mol) of Tipox were refluxed in dry benzene as in procedure 2.2.2., see reaction 2.4.a. After washing in hexane, 36.7 gram (0.1 mol) of the oily product obtained and 14.6 ml (0.1 mol) of triethylamine were dissolved in dry benzene. Solution of 9.05 gram (0.1 mol) of acryloyl chloride in benzene was then added with stirring at temperature below 10°C as in procedure 2.2.1 (reaction 2.4.b).



A yellowish oily liquid was obtained after washing in hexane, yield = 50%.

Elemental analysis: N = 3.3 %; C = 74.3%; H = 11.2 %, (Calculated). N = 3.5 %; C = 74.1 %; H = 10.2 %, (Found). FTIR-analysis (liquid film), Figure 2.10.: ester $>C=O$, 1734 cm^{-1} (s); amide $>C=O$, 1651 cm^{-1} (s); unsaturation $>C=C<$, 1608 cm^{-1} (m). Proton and Carbon-13 NMR spectra (in $CDCl_3$) are shown in Figure 2.11 and 2.12.

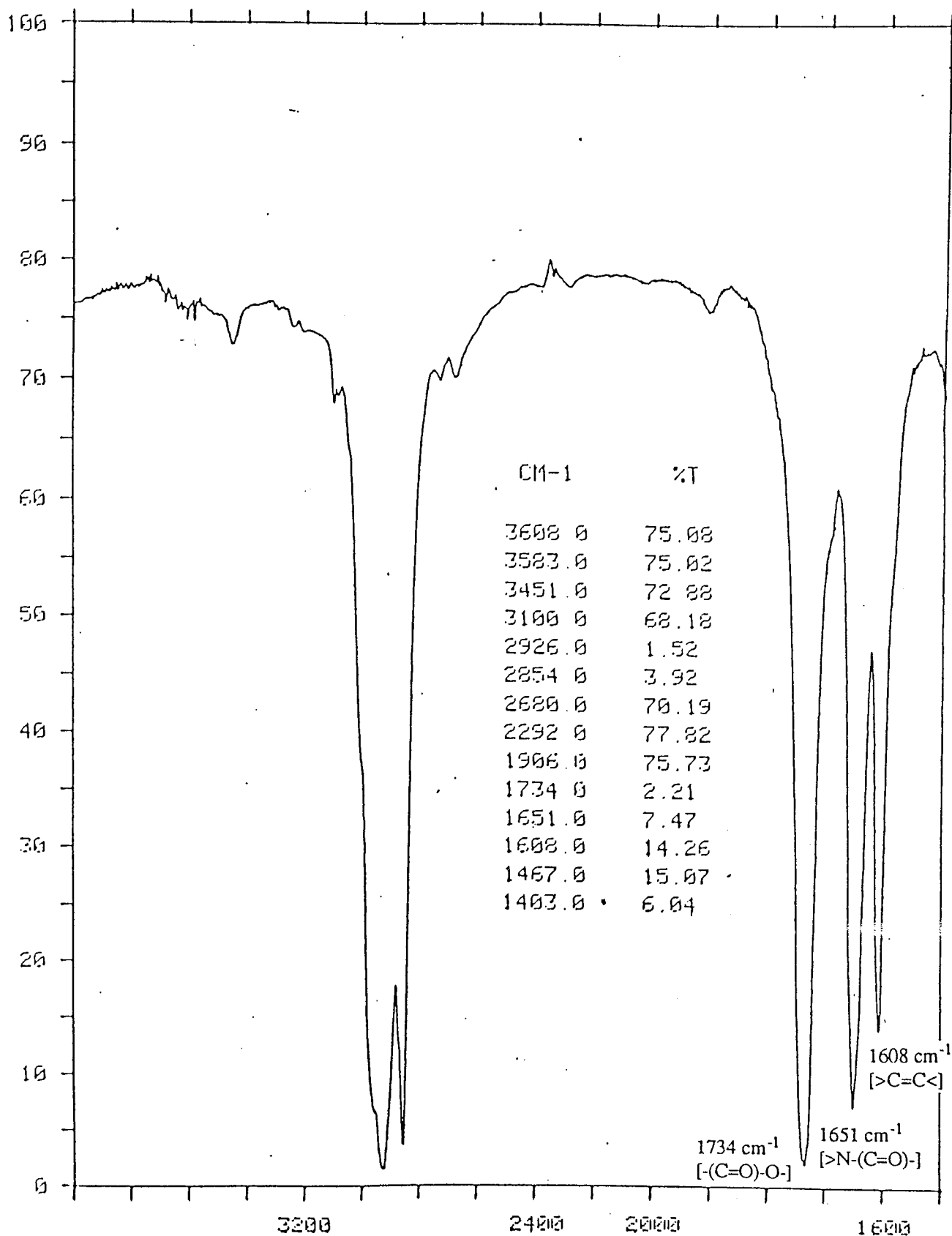


Figure 2.10 FT-IR spectra of 1-acryloyl 4-myristoyloxy 2,2,6,6-tetramethyl piperidine (AMyTP, X), as liquid film

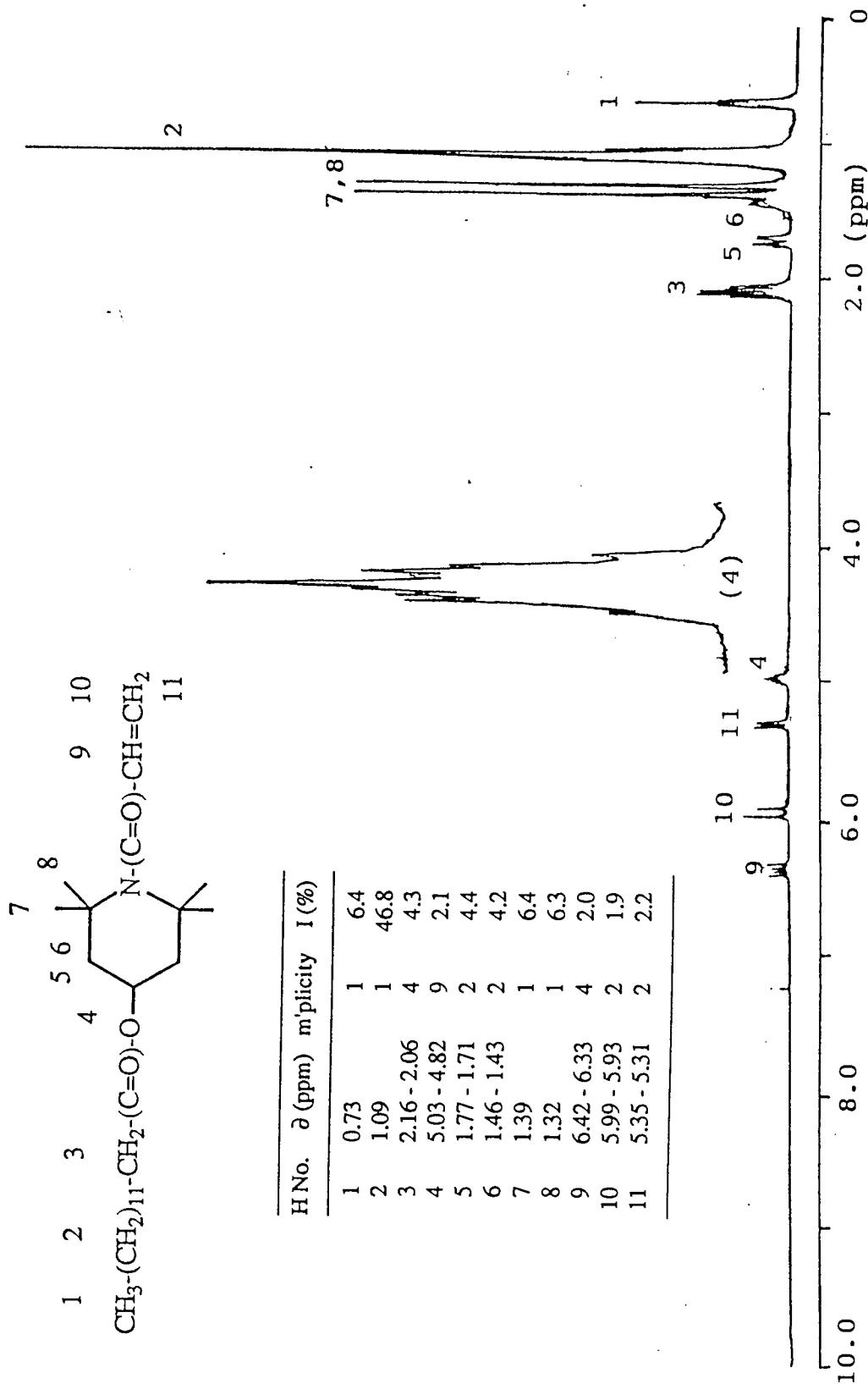


Figure 2.11. Proton NMR spectra of 1-acryloyl 4-myristoyloxy 2,2,6,6-tetramethyl piperidine (AMyTP, X) in deuterated chloroform

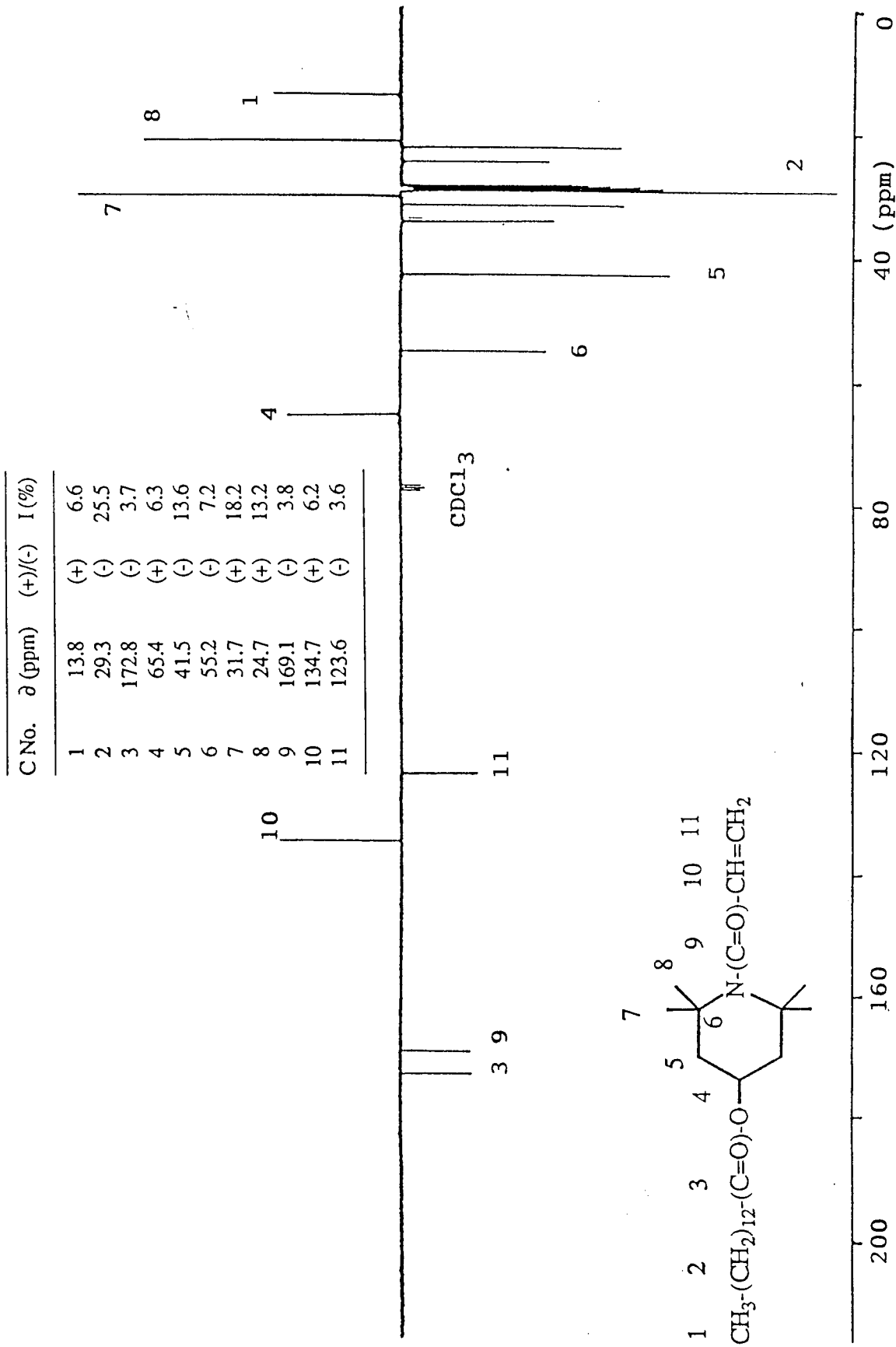
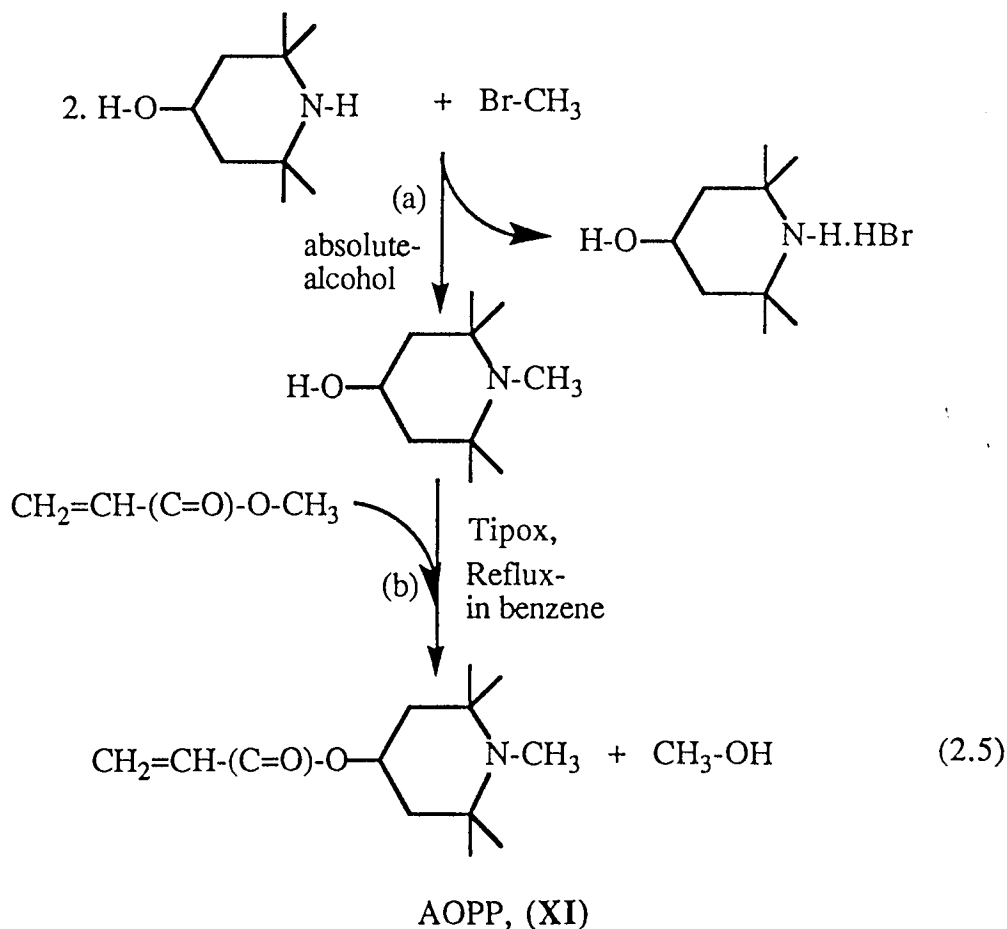


Figure 2.12. Carbon-13 NMR spectra of 1-acryloyl 4-myristoyloxy 2,2,6,6-tetramethyl piperidine (AMyTP, X) in deuterated chloroform

2.2.5 Synthesis of 4-acryloyloxy 1,2,2,6,6-pentamethyl piperidine (AOPP, XI)(47,53).

31.4 gram (0.2 mol) of 2,2,6,6-tetramethyl 4-piperidinol and 9.4 gram (0.1 mol) of methyl bromide were refluxed in absolute alcohol overnight under nitrogen atmosphere, reaction 2.5.a. The precipitated compound was filtered, and after vacuum evaporation, the residue was recrystallised in hexane. 17.1 gram (0.1 mol) of the purified residue, 8.4 gram (0.1 mol) of methyl acrylate and 3 ml (0.01 mol) of Tipox were then refluxed in dry benzene for 24 hours under nitrogen as described in procedure 2.2.2, reaction 2.5.b. After purification a yellowish oily liquid was obtained and was washed in hexane, yield = 30%.

Elemental analysis: N = 6.2 %; C = 69.3 %; H = 10.2 %, (Calculated). N = 5.4 %; C = 71.2 %; H = 10.2 %, (Found). FTIR-analysis (liquid film), Figure 2.13.: ester $>C=O$, 1724 cm^{-1} (s); unsaturation $>C=C<$, $1619 - 1637\text{ cm}^{-1}$ (m). Proton and Carbon-13 NMR spectra (in $CDCl_3$) are shown in Figure 2.14 and 2.15.



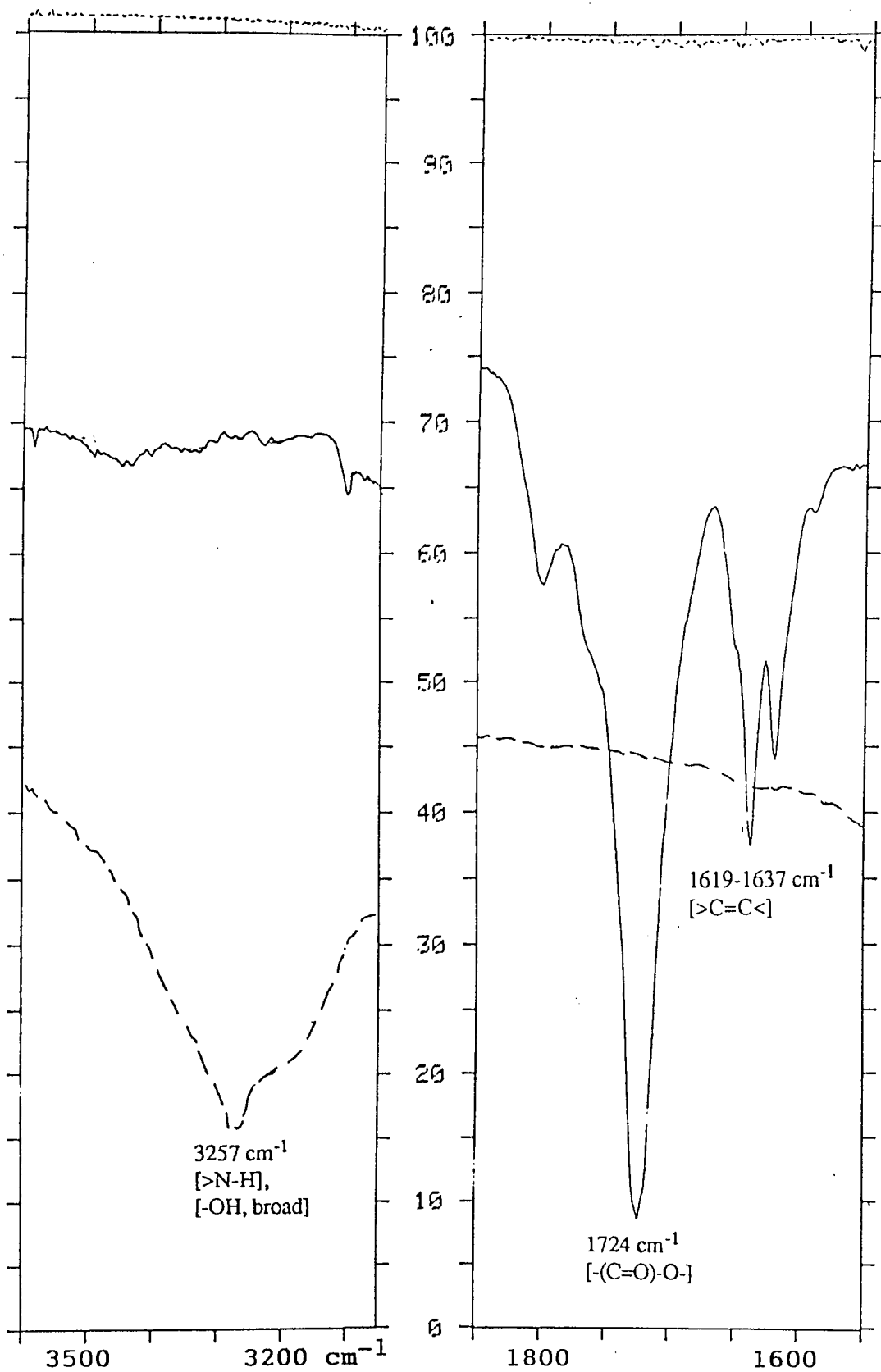


Figure 2.13 FT-IR spectra of 4-acryloyloxy 1,2,2,6,6-pentamethyl piperidine (AOPP, XI), as liquid film (-----), compared to that of 2,2,6,6-tetramethyl 4-piperidinol (.....)

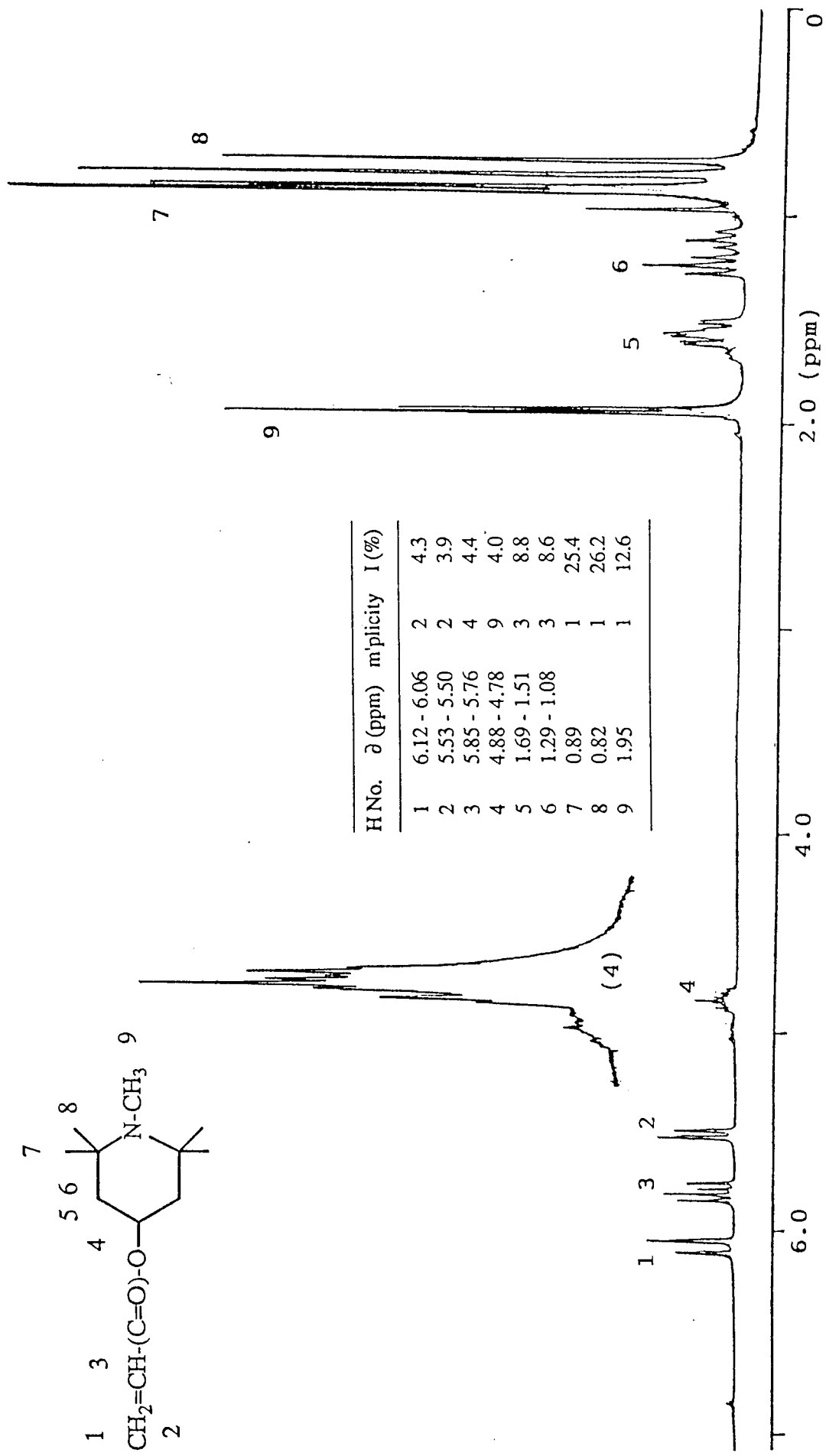


Figure 2.14. Proton NMR spectra of 4-acryloyloxy 1,2,2,6,6-pentamethyl piperidine (AOPP, XI) in deuterated chloroform

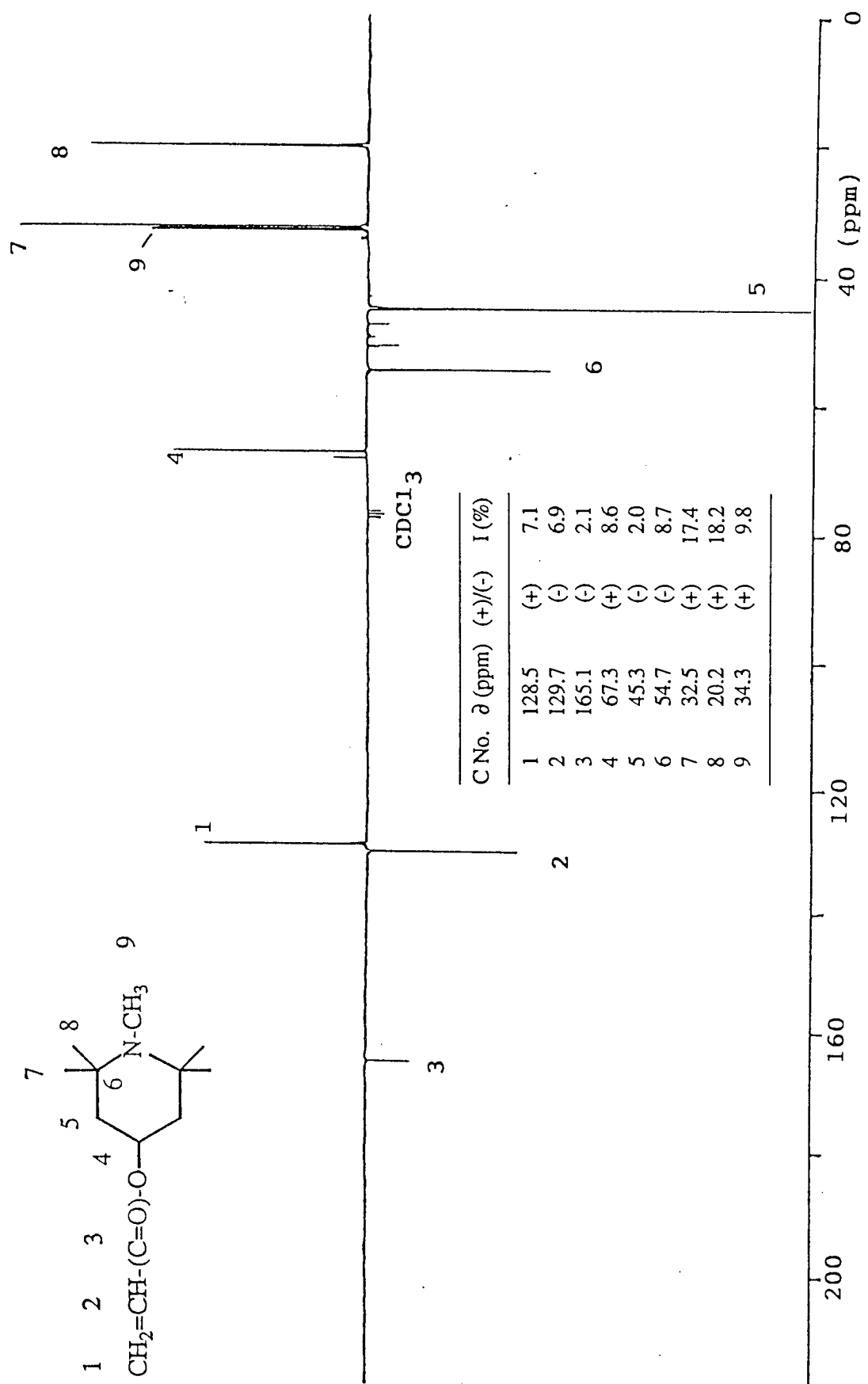
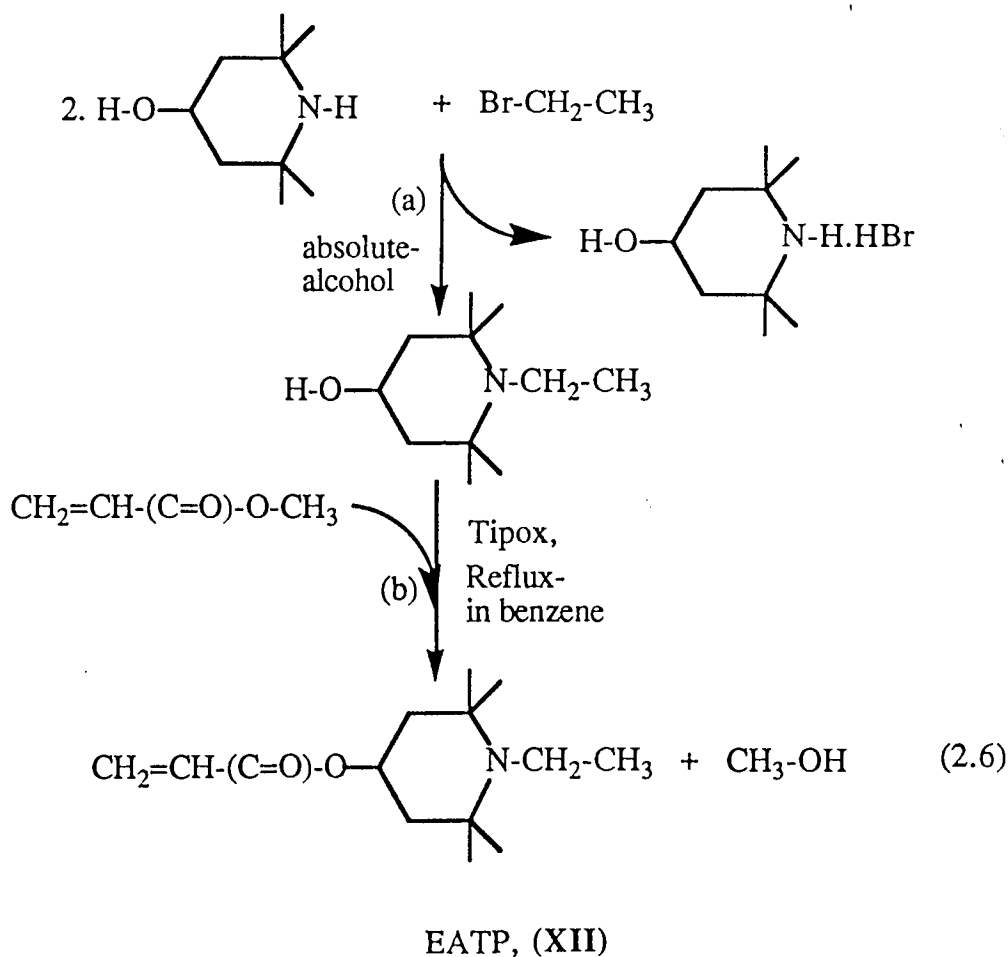


Figure 2.15. Carbon-13 NMR spectra of 4-acryloyloxy 1,2,2,6,6-pentamethyl piperidine (AOPP, XI) in deuterated chloroform

2.2.6 Synthesis of 1-ethyl 4-acryloyloxy 2,2,6,6-tetramethyl piperidine (EATP, XII)^(47,53).

31.4 gram (0.2 mol) of 2,2,6,6-tetramethyl 4-piperidinol and 10.8 gram (0.1 mol) of ethyl bromide were refluxed in absolute alcohol overnight under nitrogen atmosphere, reaction 2.6.a. The precipitate was filtered off, and after vacuum evaporation, the residue was recrystallised in hexane. 18.5 gram (0.1 mol) of the purified white solid, 8.4 gram (0.1 mol) of methyl acrylate and 3 ml (0.01 mol) of Tipox were then refluxed in dry benzene for 24 hours under nitrogen as in procedure 2.2.2., reaction 60b. After exhaustive washing in hexane a slightly yellow oily liquid was obtained, yield = 30%. Elemental analysis: N = 5.9 %; C = 70.3 %; H = 10.5 %, (Calculated). N = 6.5 %; C = 69.8 %; H = 11.5 %, (Found). FTIR-analysis (liquid film), Figure 2.16.: ester $>C=O$, 1734 cm^{-1} (s); unsaturation $>C=C<$, $1608 - 1638\text{ cm}^{-1}$ (m). Proton and Carbon-13 NMR spectra (in CDCl_3) are shown in Figures 2.17 and 2.18.



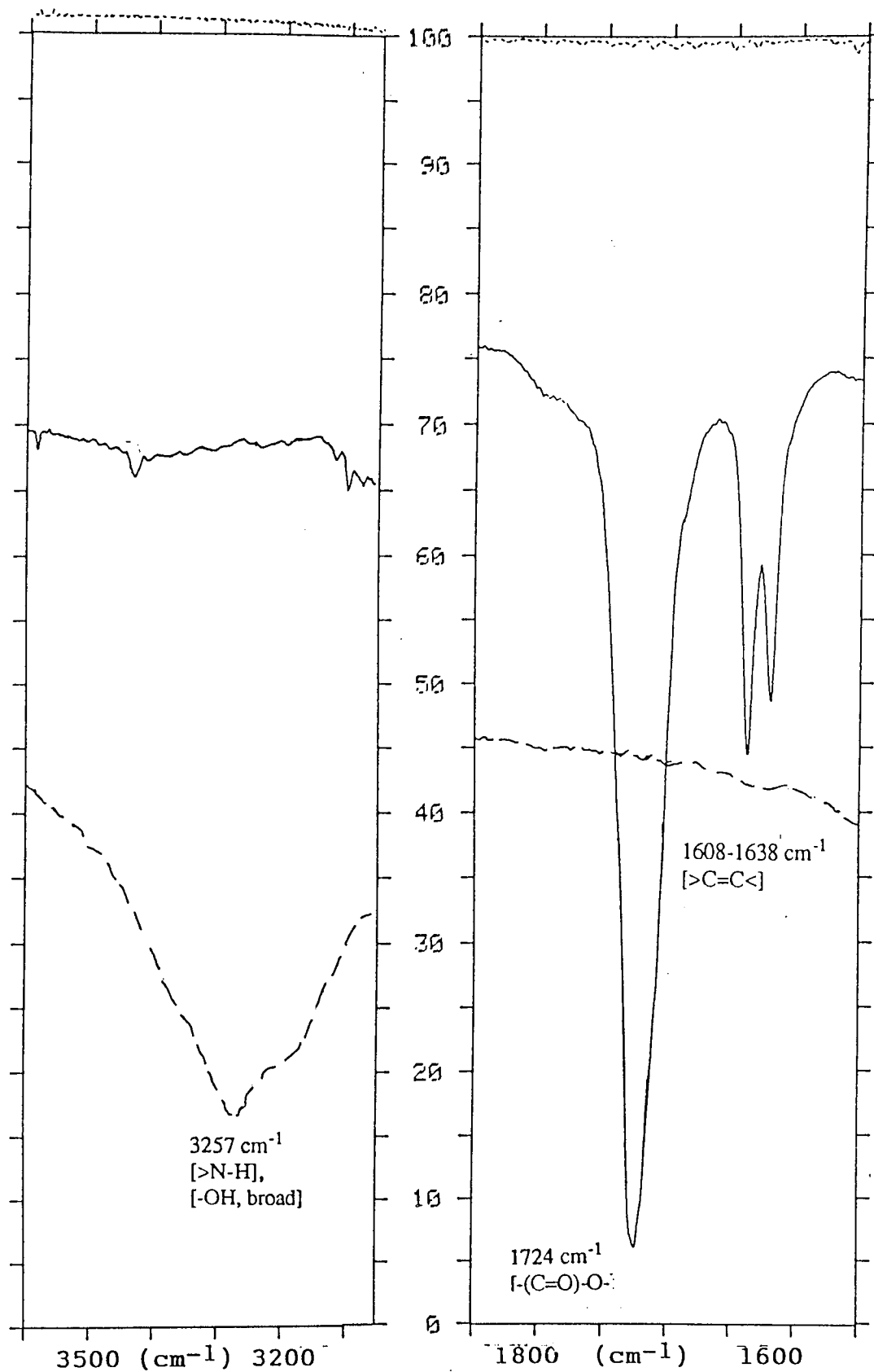


Figure 2.16 FT-IR spectra of 1-ethyl 4-acryloyloxy 2,2,6,6-tetramethyl piperidine (EATP, XII), as liquid film (-----), compared to that of 2,2,6,6-tetramethyl 4-piperidinol (- - - -)

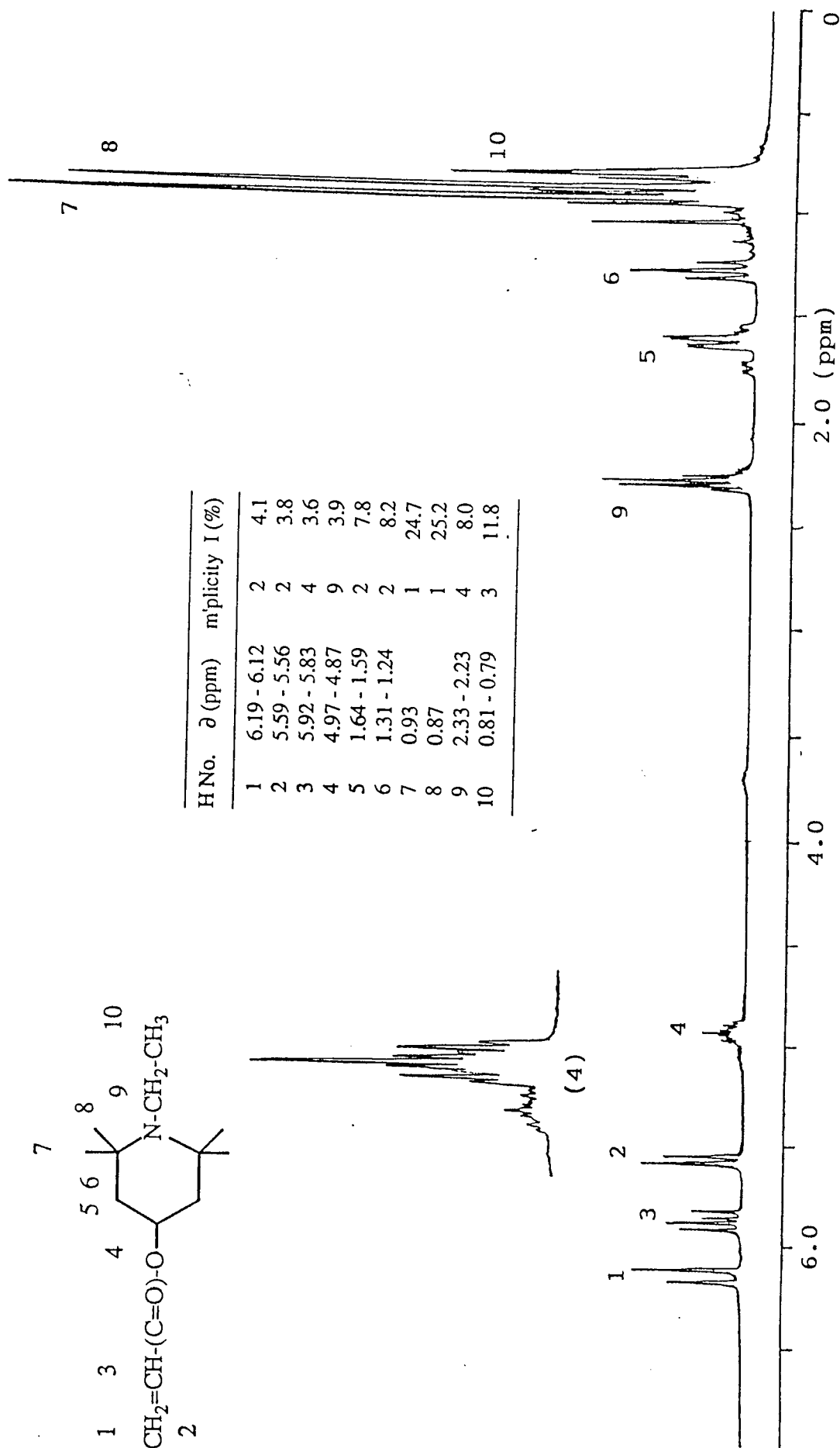


Figure 2.17. Proton NMR spectra of 1-ethyl 4-acryloyloxy 2,2,6,6-tetramethyl piperidine (EATP, XII) in deuterated chloroform

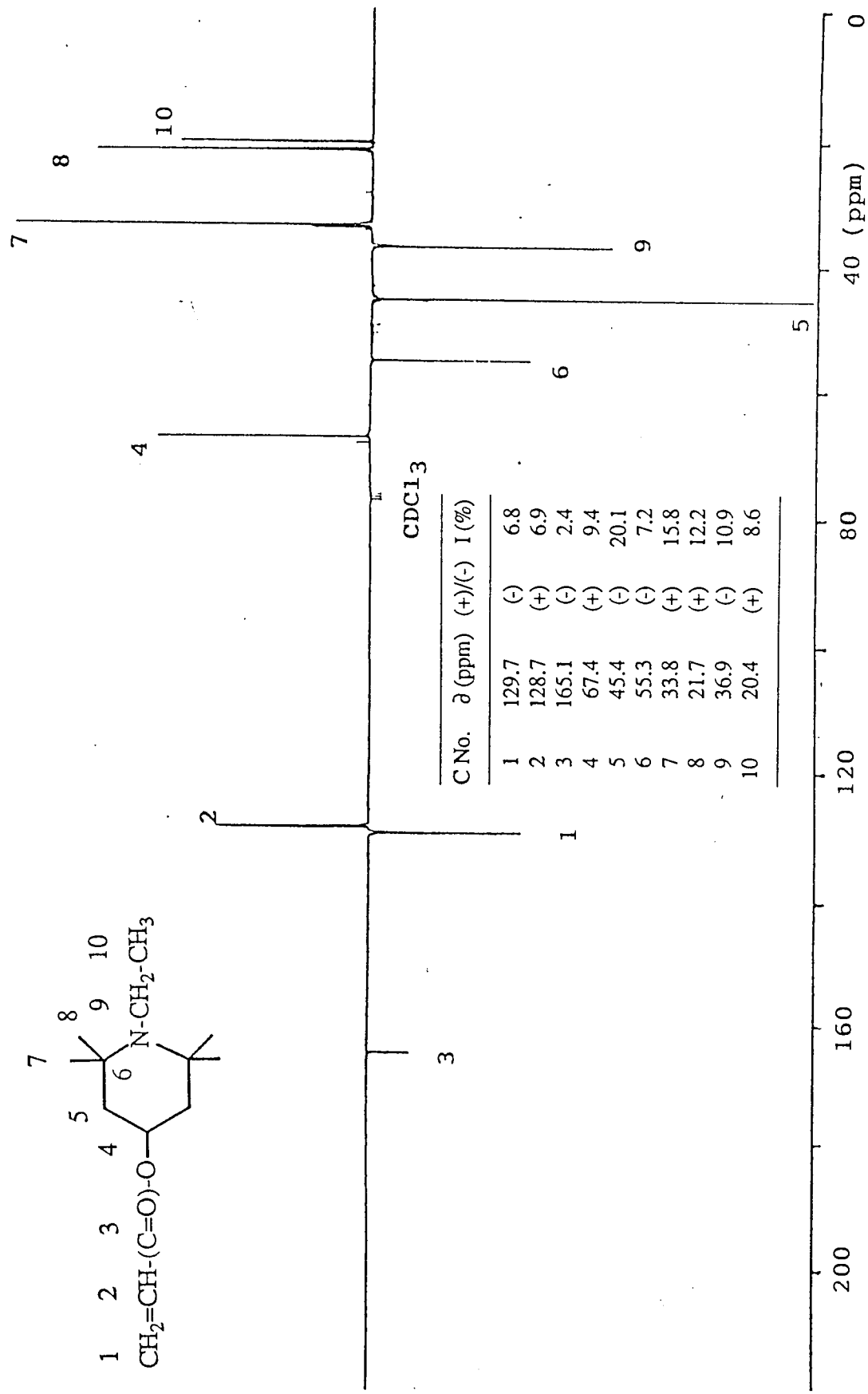
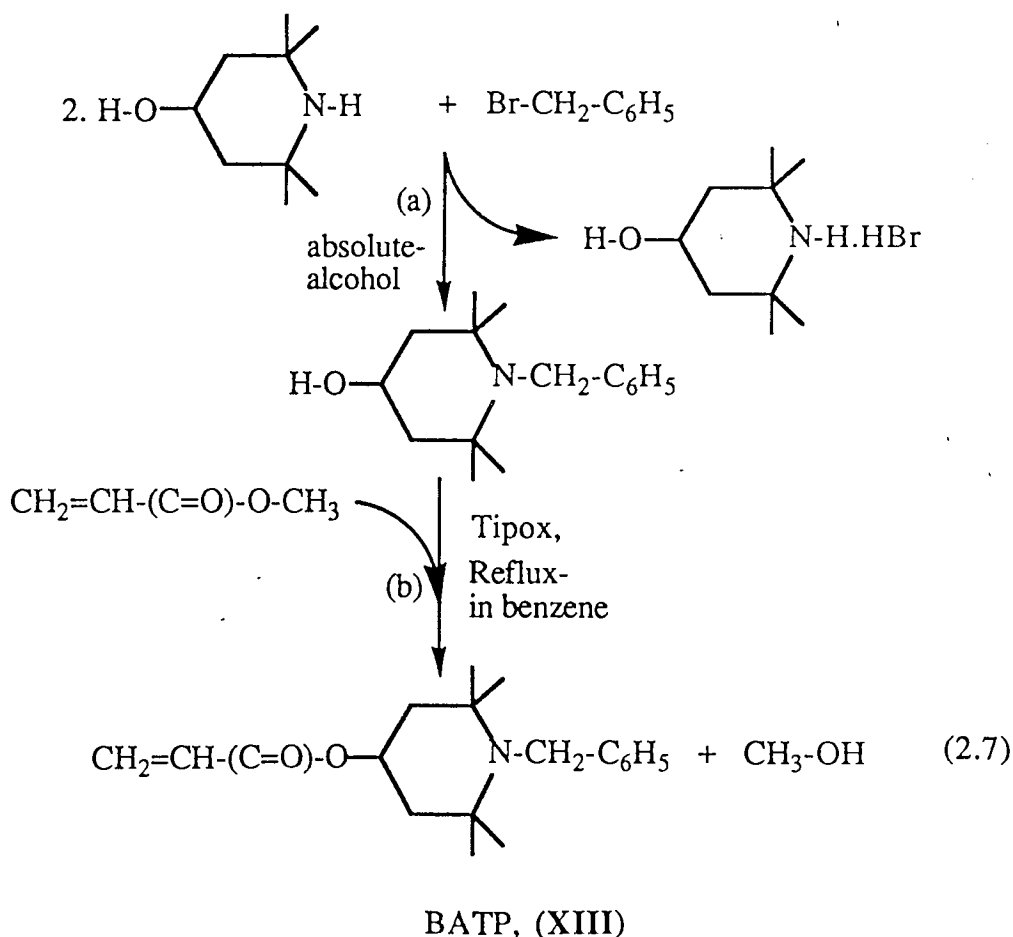


Figure 2.18. Carbon-13 NMR spectra of 1-ethyl 4-acryloyloxy 2,2,6,6-tetramethyl piperidine (EATP, XII) in deuterated chloroform

2.2.7 Synthesis of 1-benzyl 4-acryloyloxy 2,2,6,6-tetramethyl piperidine (BATP, XIII)(37,53).

31.4 gram (0.2 mol) of 2,2,6,6-tetramethyl piperidine and 17.0 gram (0.1 mol) of benzyl bromide were refluxed in absolute alcohol overnight under nitrogen atmosphere, reaction 2.7.a. The precipitate was filtered off, and after vacuum evaporation, the residue was recrystallised in hexane. 24.7 gram (0.1 mol) of the purified white crystals, 8.4 gram (0.1 mol) of methyl acrylate and 3 ml (0.01 mol) of Tipox were then refluxed in dry benzene for 24 hours under nitrogen as in procedure 2.2.2., reaction 2.7.b. After purification, i.e exhaustive washing in hexane, a yellowish oily product was obtained, yield = 30%. Elemental analysis: N = 4.7 %; C = 75.7 %; H = 9.0 %, (Calculated). N = 4.2 %; C = 75.5 %; H = 10.2 %, (Found). FTIR-analysis (liquid film), Figure 2.19. ester $>C=O$, 1734 cm^{-1} (s); unsaturation $>C=C<$, 1636 cm^{-1} (m), benzene ring $>C=C<$, $1604 - 1619\text{ cm}^{-1}$ (m). Proton and Carbon-13 NMR spectra (in CDCl_3) are shown in Figures 2.20 and 2.21.



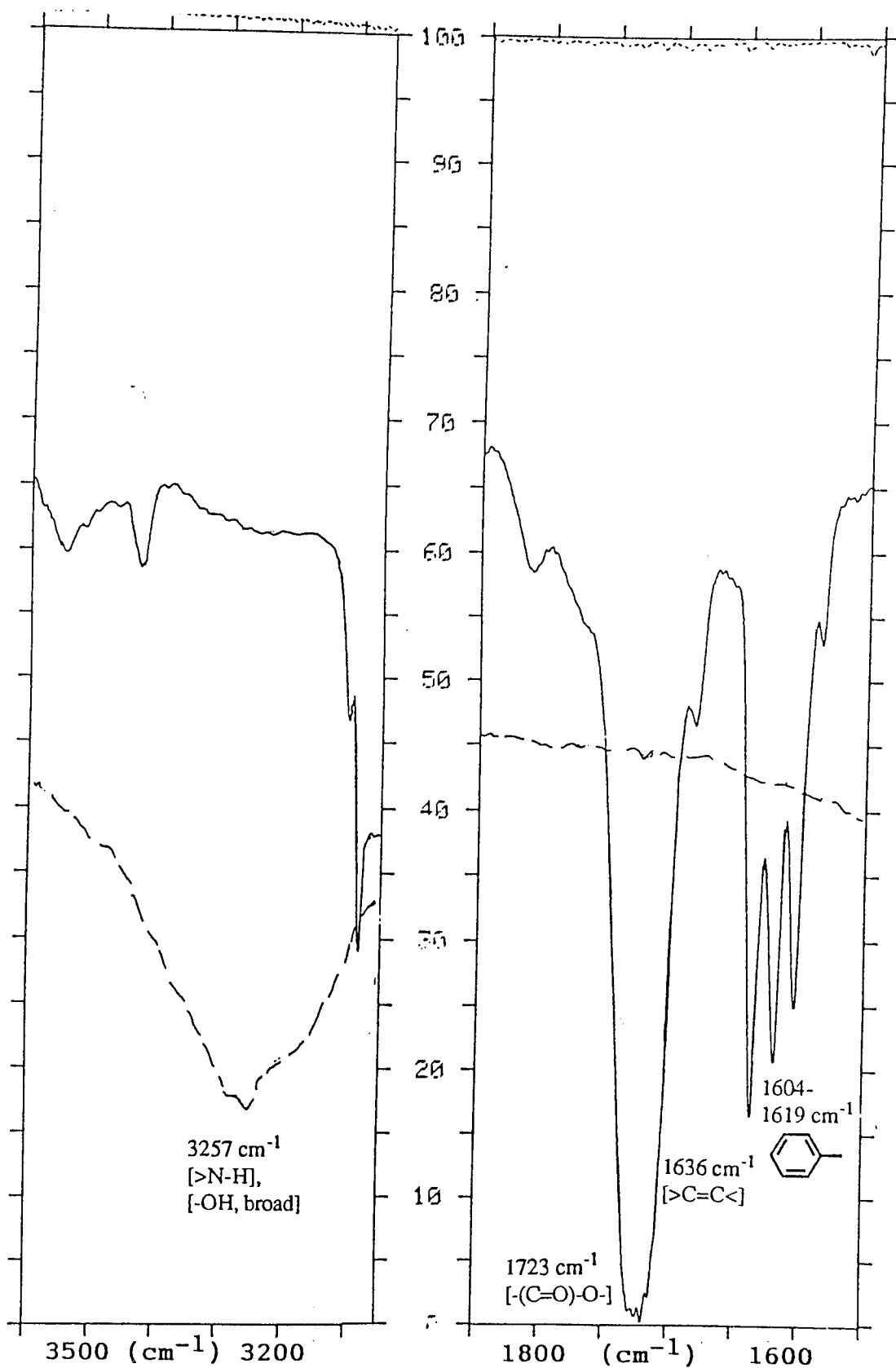
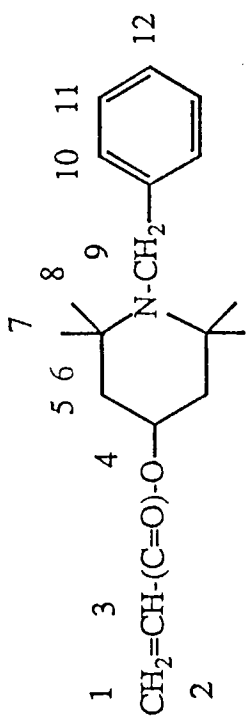


Figure 2.19 FT-IR spectra of 1-benzyl 4-acryloyloxy 2,2,6,6-tetramethyl piperidine (BATP, XIII), as liquid film (-----), compared to that of 2,2,6,6-tetramethyl 4-piperidinol (- - - -)



HNo.	δ (ppm)	multiplicity	I (%)
1	6.50 - 6.45	2	3.5
2	5.84 - 5.80	2	3.6
3	6.23 - 6.14	4	3.3
4	5.39 - 5.29	9	3.2
5	2.05 - 2.01	2	7.1
6	1.78 - 1.70	3	6.8
7	1.26	1	9.9
8	1.08	1	11.1
9	3.90	1	6.2
10	7.52 - 7.49	2	7.1
11	7.41 - 7.33	3	6.7
12	7.23 - 7.20	2	6.4

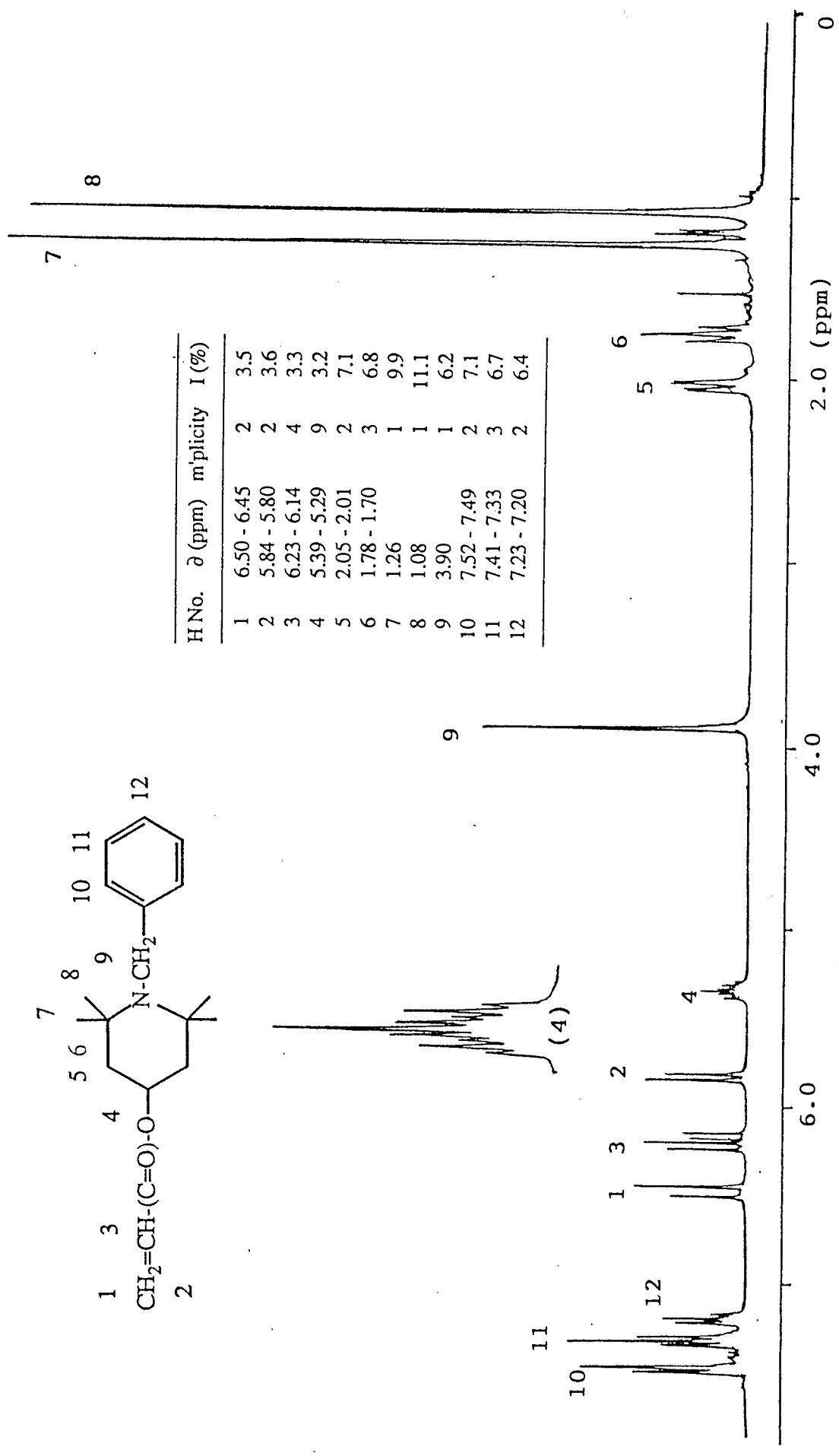


Figure 2.20. Proton NMR spectra of 1-benzyl 4-acryloyloxy 2,2,6,6-tetramethyl piperidine (BATP, XIII) in deuterated chloroform

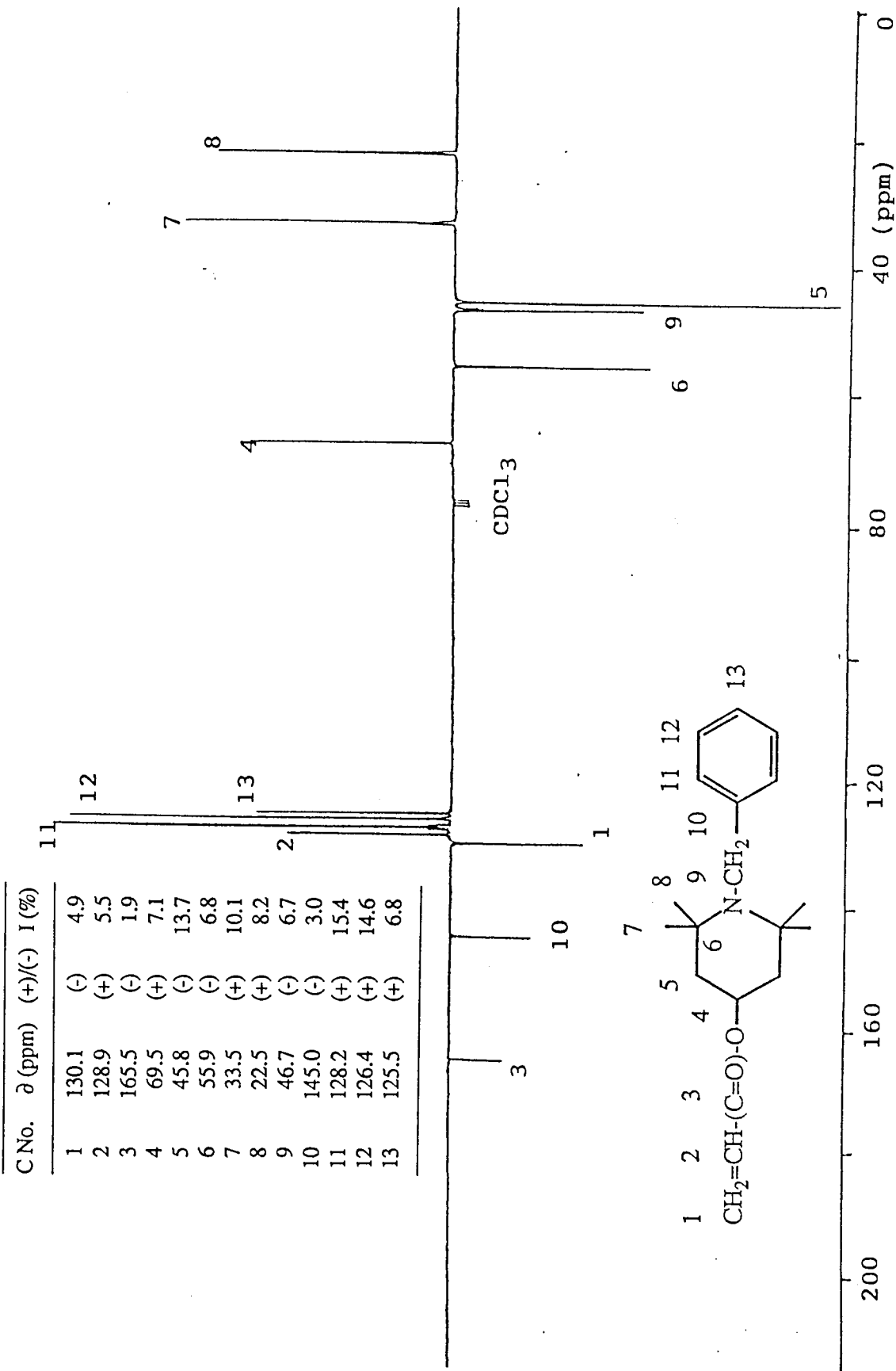
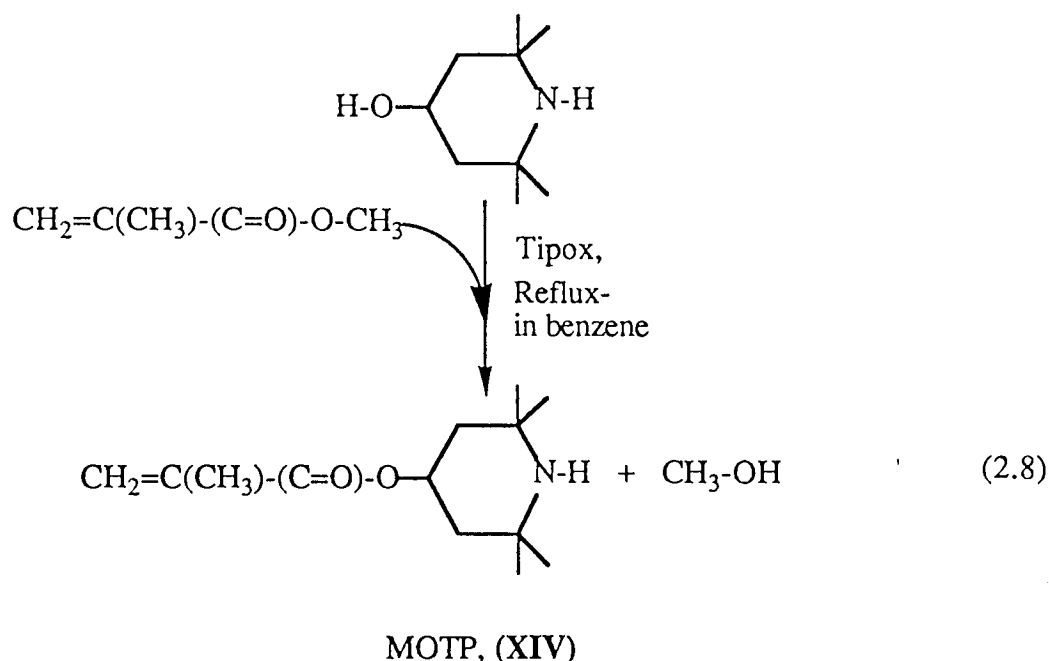


Figure 2.21. Carbon-13 NMR spectra of 1-benzyl 4-acryloyloxy 2,2,6,6-tetramethyl piperidine (BATT, XIII) in deuterated chloroform

2.2.8 Synthesis of 4-methacryloyloxy 2,2,6,6-tetramethyl piperidine (MOTP, XIV)(39-41).

The procedure of this synthesis is similar to that of procedure 2.2.1, synthesised using: 15.7 gram (0.1 mol) of 2,2,6,6-tetramethyl 4-piperidinol, 9.4 ml (0.1 mol) of methyl methacrylate, and 3 ml (0.01 mol) of Tipox, reaction 2.8.



After recrystallisation in hexane, white crystals were obtained, yield = 70%. This was identified as follows, melting point 55-57°C, elemental analysis: N = 6.2 %, C = 69.3 %, H = 10.2 %, (Calculated). N = 7.1 %, C = 69.2 %, H = 11.5 %, (Found). FTIR-analysis (KBr-disc) Figure 2.22: secondary >N-H, 3313 cm⁻¹ (w); ester >C=O, 1703 cm⁻¹ (s); unsaturation >C=C<, 1635 cm⁻¹ (m). Proton and Carbon-13 NMR spectra (in CDCl₃) are shown in Figures 2.23. and 2.24.

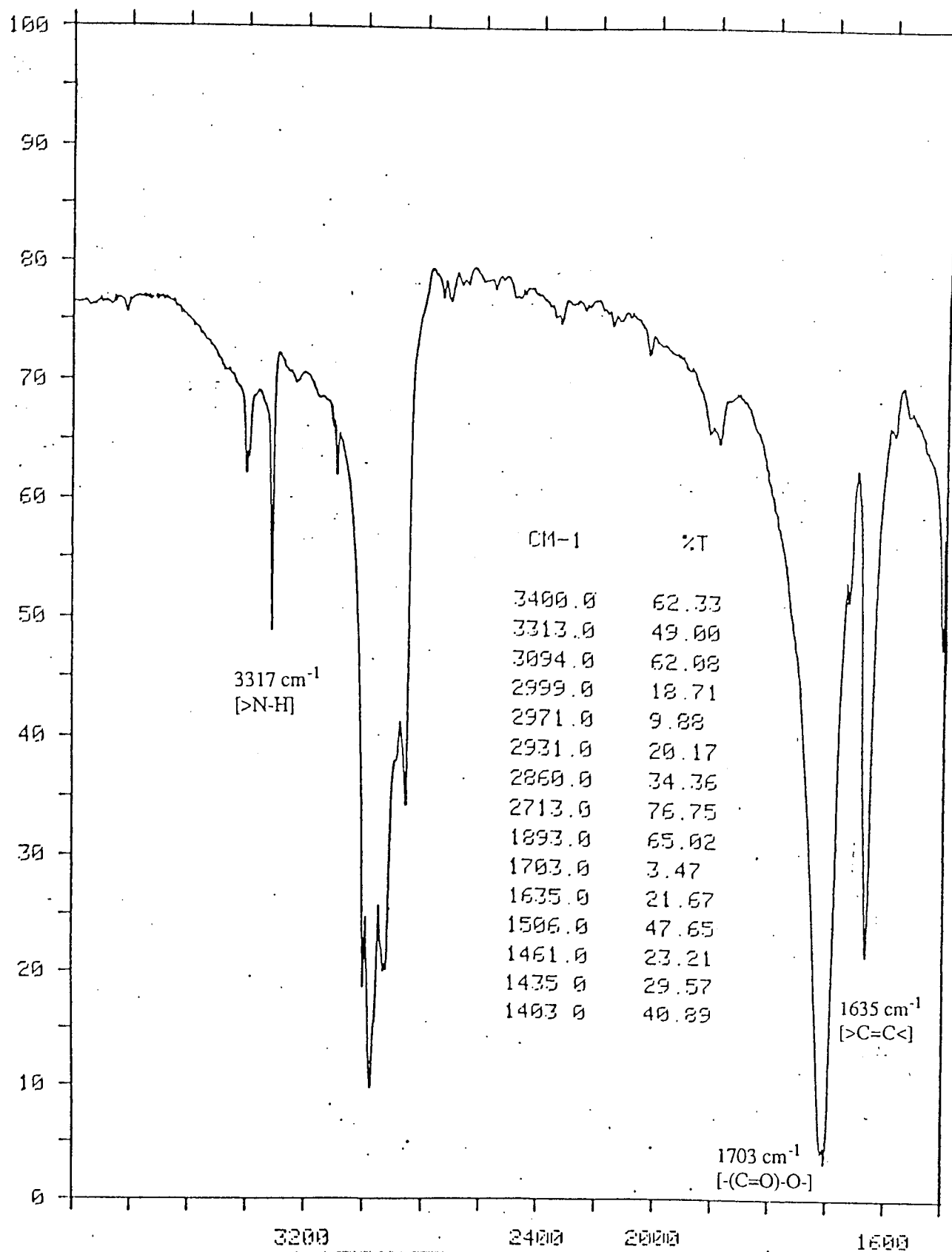


Figure 2.22 FT-IR spectra of 4-methacryloyloxy 2,2,6,6-tetramethyl piperidine (MOTP, XIV), in KBr disc

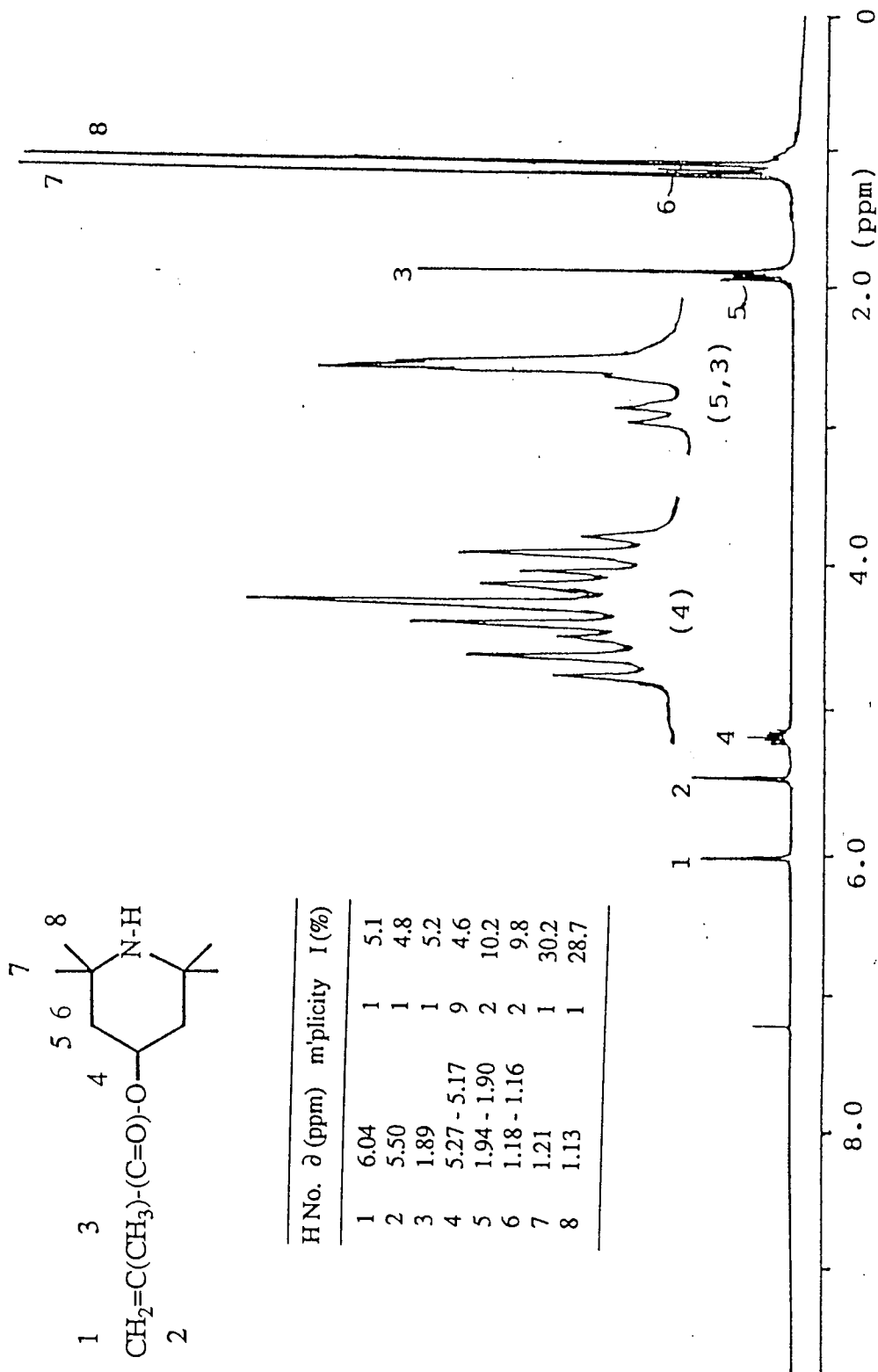
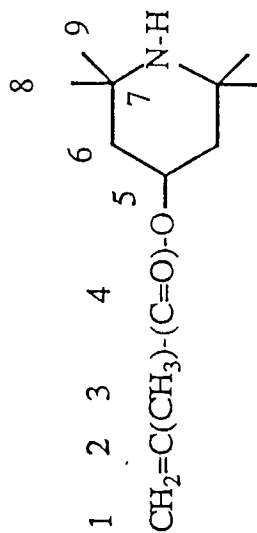


Figure 2.23. Proton NMR spectra of 4-methacryloyloxy 2,2,6,6-tetramethyl piperidine (MOTP, XIV) in deuterated chloroform



C No.	δ (ppm)	(+)/(−)	I (%)
1	125.1	(−)	8.5
2	136.7	(−)	1.7
3	18.3	(+)	6.9
4	167.0	(−)	1.3
5	69.1	(+)	10.2
6	51.5	(−)	6.7
7	43.8	(−)	23.7
8	34.7	(+)	21.8
9	29.0	(+)	20.9

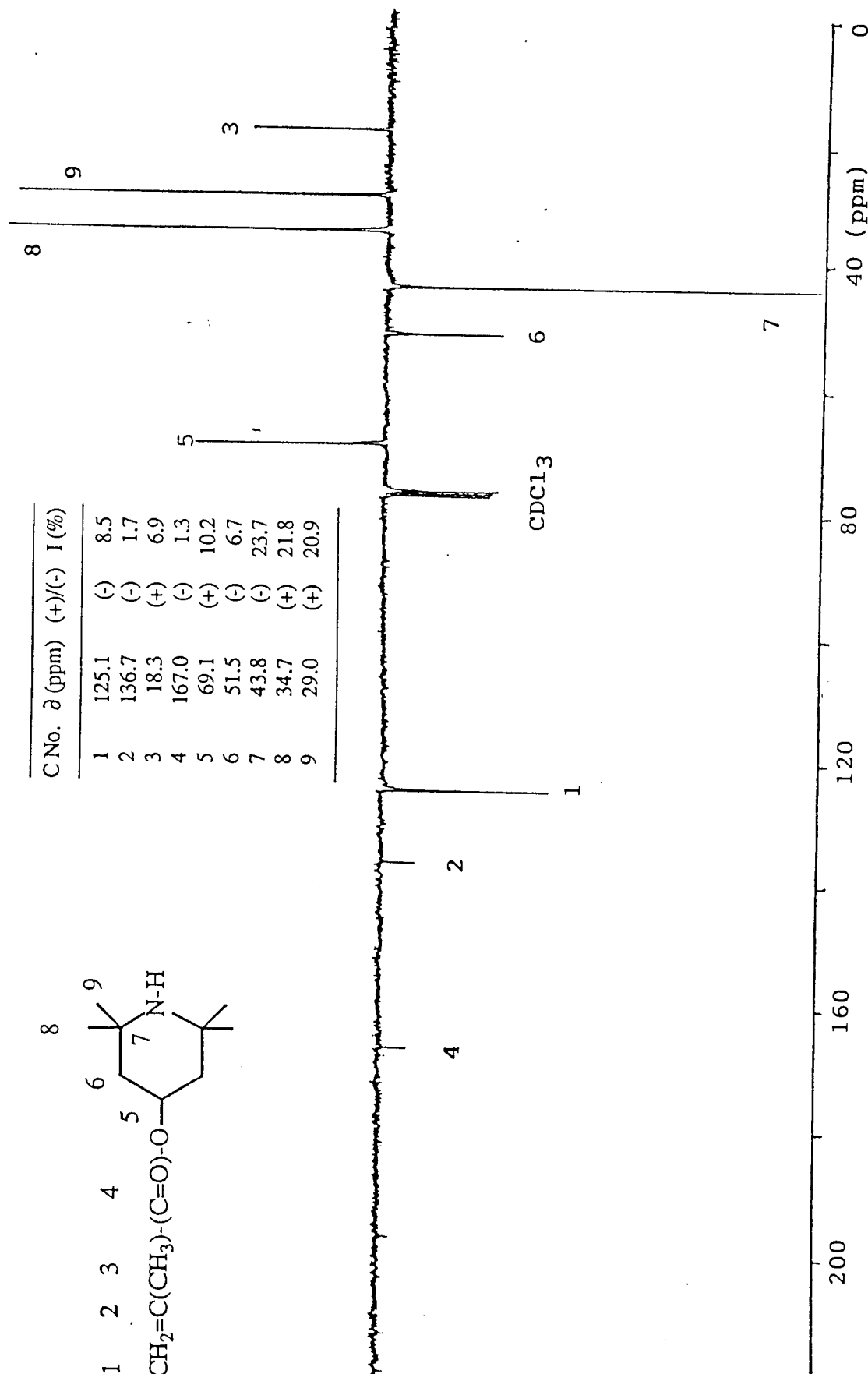


Figure 2.24. Carbon-13 NMR spectra of 4-methacryloyloxy 2,2,6,6-tetramethyl piperidine (MOTP, XIV) in deuterated chloroform

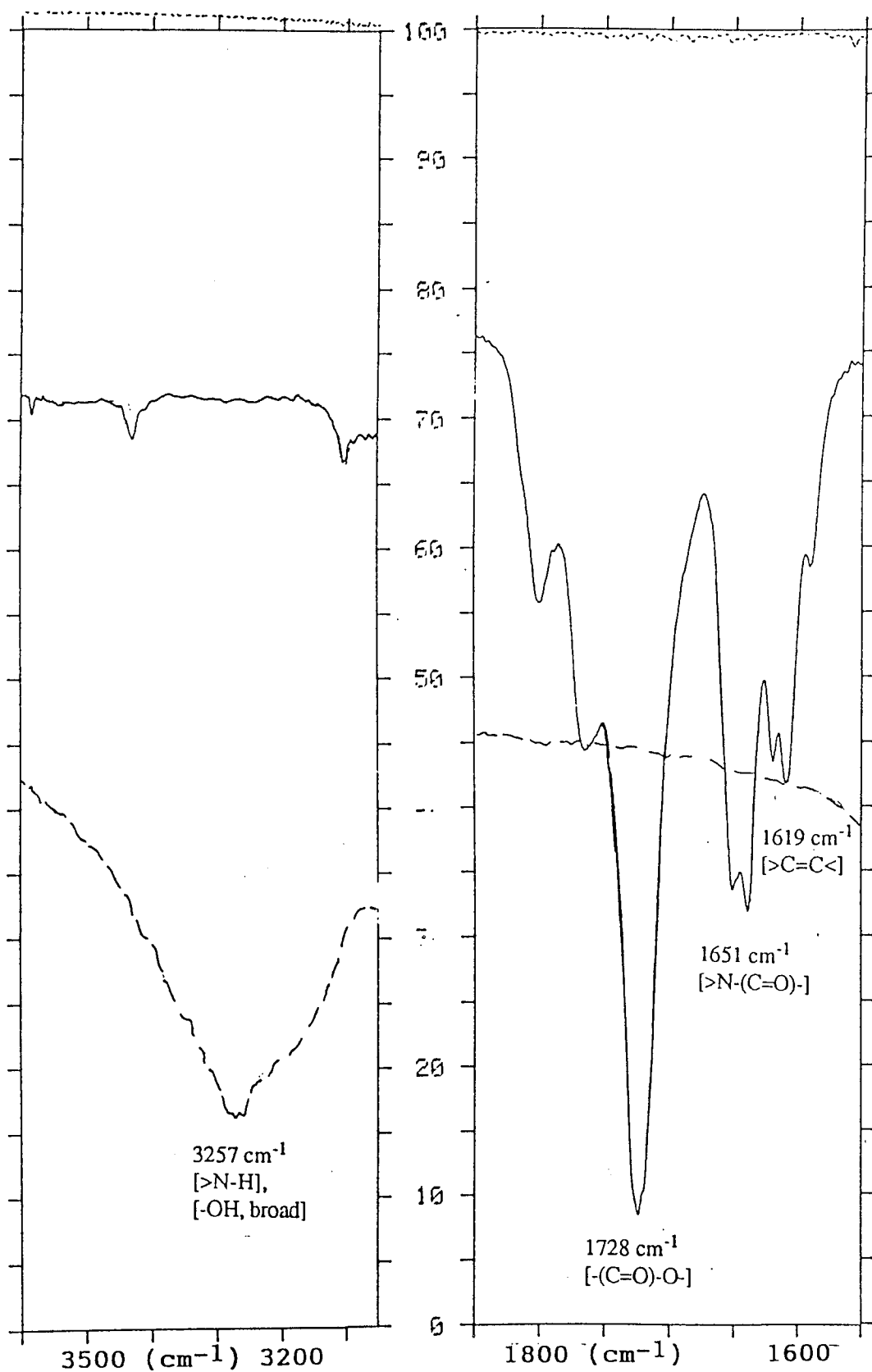
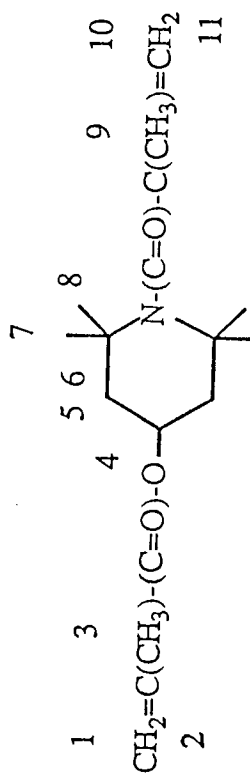


Figure 2.25 FT-IR spectra of 1-methacryloyl 4-methacryloyloxy 2,2,6,6-tetramethyl piperidine (MMTP, XV), as liquid film (—), compared to that of 2,2,6,6-tetramethyl 4-piperidinol (-----)



HNo.	δ (ppm)	m'plicity	I (%)
1	6.34	1	4.1
2	5.85	1	3.8
3	2.08	1	4.0
4	5.39 - 5.29	9	4.1
5	1.80 - 1.79	2	8.2
6	1.20 - 1.19	2	7.8
7	1.29	1	24.2
8	1.08	1	23.9
9	2.02	1	12.1
10	6.26	1	4.2
11	5.69	1	4.3

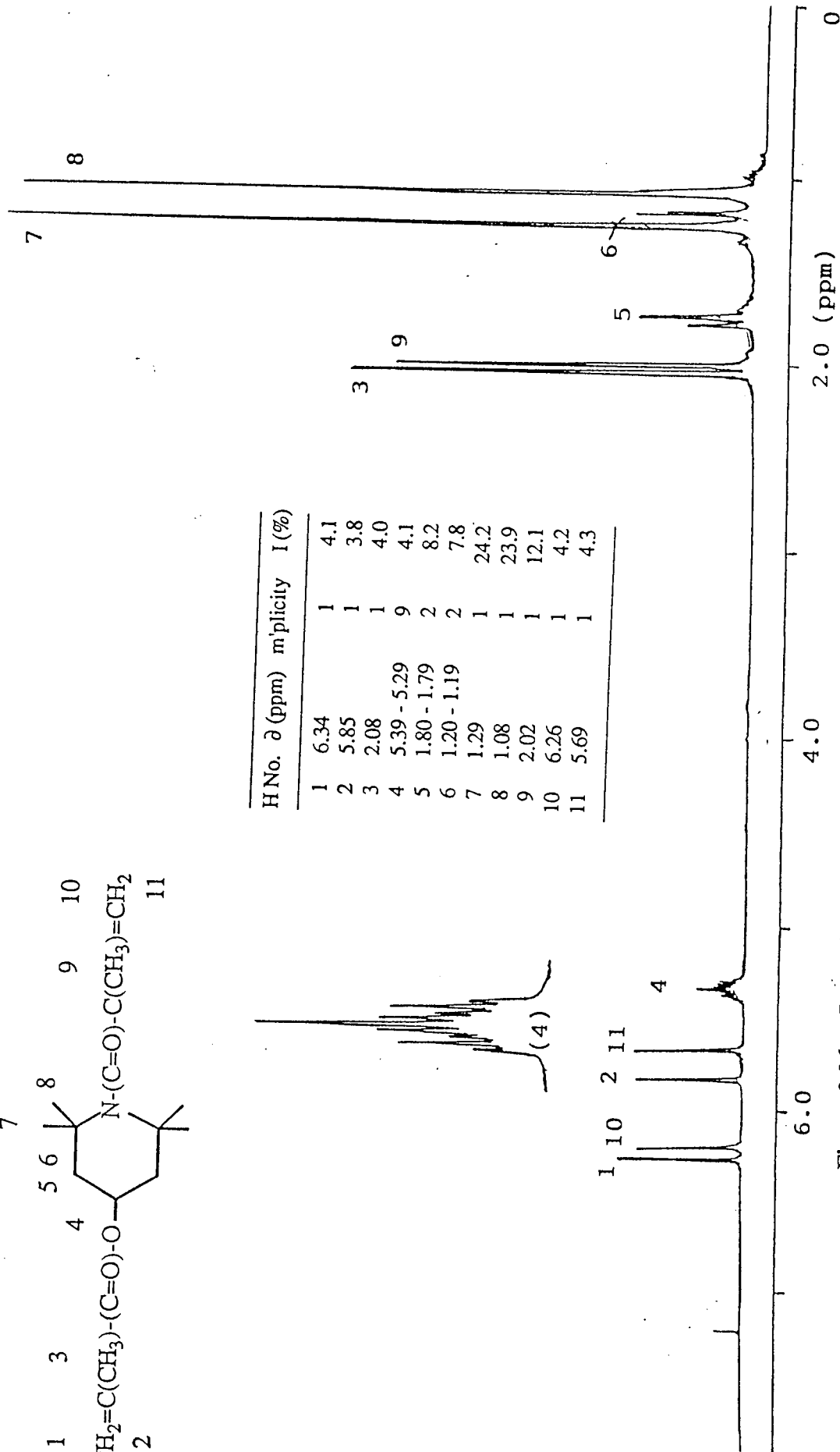


Figure 2.26. Proton NMR spectra of 1-methacryloyl 4-methacryloyloxy 2,2,6,6-tetramethyl piperidine (MMTP, XV) in deuterated chloroform

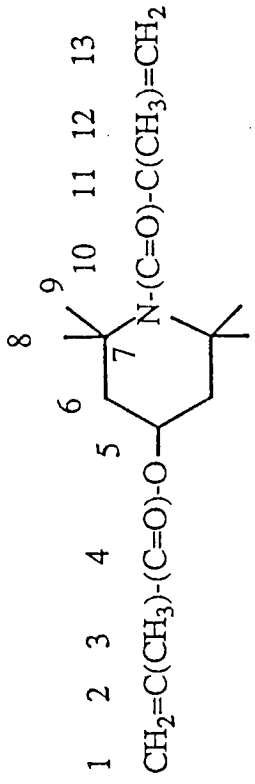
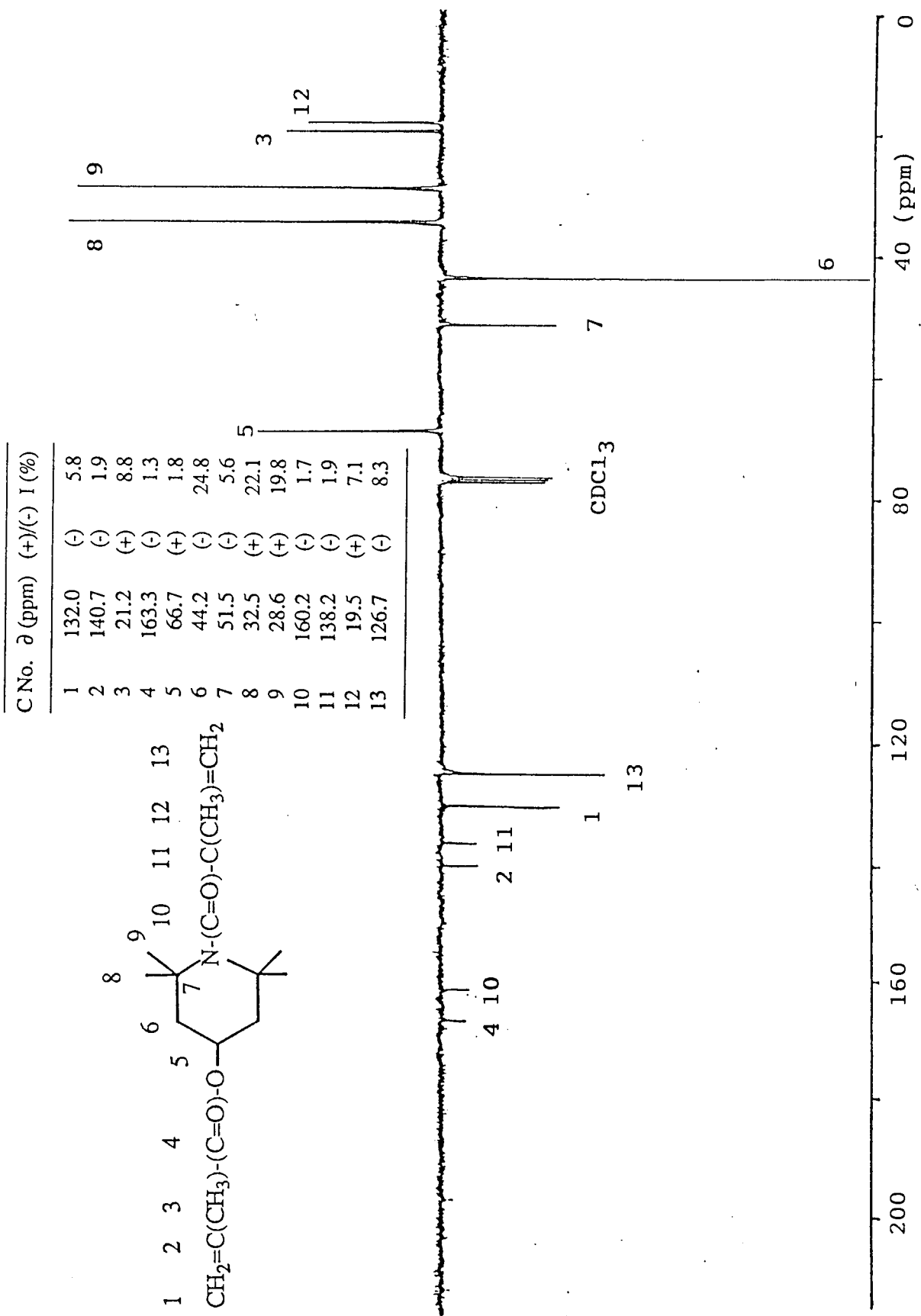


Figure 2.27. Carbon-13 NMR spectra of 1-methacryloyl 4-methacryloyloxy 2,2,6,6-tetramethyl piperidine (MMTP, XV) in deuterated chloroform

2.3 COMPOUNDING

2.3.1 Reactive Processing of Polymer-Antioxidant Systems

Unstabilised polypropylene (Propathene ICI, HF-26), freshly prepared antioxidant, coagent, and peroxide (as radical generator), were tumble mixed at room temperature in 50 ml of dichloromethane solution. The antioxidant, coagent and initiator concentrations were varied, keeping the total weight of the polymer sample constant (35 gram) to charge the full capacity of the processing chamber. After exhaustive vacuum evaporation at room temperature, the polymer sample was then processed in a HAMPDEN-RAPRA Torquerheometer coupled to motor drive of a BRABENDER plasticorder (Figure 2.28), under closed mixer condition (CM), with the ram down (i.e. under restricted oxygen access) for 10 minutes at 180°C and rotating speed 60 rotation per minute. These processing parameters are the "standard processing condition" and will be used throughout the work unless otherwise stated. The torque reading was recorded every 15 seconds during the processing operation. Finally, the processed polymer was removed instantly from the processing chamber and chilled in cold water.

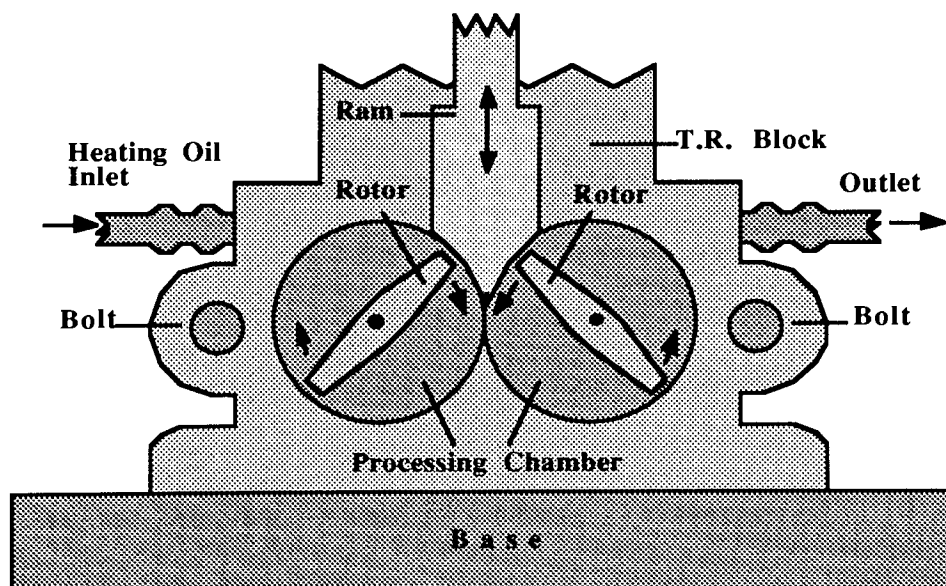


Figure 2.28 Processing chamber of a Brabender torquerheometer (internal mixer)

2.3.2 Film Preparation

7 gram of the polymer sample (masterbatch) was placed between two polished stainless steel plates, which were laminated with heat resistant cellophane films. This was preheated at 180°C in an electric compression moulding machine (DANIELS) for 1 minute without pressure. The pressure of 85 kg/cm² was then applied at that temperature for 1.5 minutes before the platens were cooled down to below 100°C, using running cold water, while maintaining the full pressure.

2.4 ANALYSIS OF MASTERBATCHES

2.4.1 Assessment of Binding Efficiency of Antioxidants

Sample films were selected to have the same thickness (0.1 - 0.2 mm) and cut in three pieces of 2 x 3 cm² in size. These films were exhaustively Soxhlet extracted in dichloromethane (DCM) for 48 hours, under nitrogen atmosphere. It was found that 48 hours extraction was sufficient to remove all unbound additive. The extracted films were dried under vacuum at room temperature for 12 hours.

Carbonyl absorption of antioxidants (all contain ester or amide functionals) was used to calculate the amount of the antioxidants in polymer samples by using a PERKIN-ELMER Fourier Transform Infrared (FTIR) Spectrophotometer model 1710. The carbonyl area index of the ester group, i.e. ratio of carbonyl absorption area (at 1811 - 1668 cm⁻¹) over that of >CH- group of polypropylene (at 2752 - 2697 cm⁻¹), before and after extraction was compared, for the three film samples of each antioxidant and an average was taken.

2.4.2 Measurement of Melt Flow Index (MFI)

5 grams of finely cut masterbatches was used in this measurement using a

Davenport Melt Flow Indexer. The masterbatch was preheated for 4 minutes before applying a weight of 2.16 kg to extrude the polymer masterbatch through a die with a standard diameter ($\varnothing = 0.1181$ or 0.2362 cm). The first 1 gram of the extrudate was discarded, after that three pieces (about 0.5 gram each) of the extrudate were collected at a certain interval of time and the correct weight of the extrudates were measured. The MFI was calculated in gram of the molten polymer passed through the die in 10 minutes

2.4.3 Measurement of Molecular Weight Distribution (MWD)

Measurement of molecular weight distribution of the masterbatches was carried out by using Gel Permeation Chromatography (GPC) at RAPRA Technology Ltd. Around 0.1 gram of polymer sample was dissolved in a gently boiled 1,2-dichloro benzene. The solution was then filtered and injected into a GPC columns (P.L. gel 2x Mixed gel, 20 Micron packing, 30 cm columns) at 140°C with flow rate of 1.0 ml/minute. The molecular weight distribution (MWD) data of the sample was calibrated by third order polynomial using polystyrene standard.

2.5 POLYMER STABILITY TESTS

2.5.1 Photostability Test

Three pieces of polymer film sample (0.1 -0.2 mm in thickness and $2 \times 3 \text{ cm}^2$ in size) were irradiated in a UV-cabinet, which is composed of 1 : 3 combination of 20 watts fluorescent sunlamps and black lamps, mounted vertically around the UV-cabinet's periphery. The samples were placed around a rotating drum fixed inside the cabinet. in which the light beam fell perpendicularly on the film surface. The distance of the samples from the light source was 10 cm, and the temperature inside the cabinet was $30 \pm 1^{\circ}\text{C}$. The intensity of radiation falling on the surface of the samples was calculated⁽⁸⁷⁾ to be 5.5 W.h.m^{-2} . UV-stability of the exposed film samples were

tested by measuring embrittlement time (ET), which is the time needed for the polymer film to break, when bended at an angle of 180°. For such films which do not show a sharp embrittlement time, the time to failure was measured when they can be torn after bending to both sides at 180°. Carbonyl area index of the irradiated films was also measured from the ratio of their carbonyl area (at 1811 - 1668 cm^{-1}) to the >CH- area of the polymer (at 2752 - 2697 cm^{-1}).

2.5.2 Thermal Ageing Test

The thermal ageing test of polymer film was carried out in a single cell Wallace oven at 140°C under a constant airflow of 85 liter/hour. Three films (0.1 - 0.2 mm in thickness and 4 x 6 cm^2 in size) were used for each sample. Carbonyl area index as well as embrittlement time were measured to estimate thermal stability of the films, as in the photostability test (Section 2.5.1).

2.6 FOURIER TRANSFORM INFRARED (FT-IR) SPECTROSCOPY

Application of a numerical calculation known as Fourier transform method in infrared spectroscopy has provided a high resolution and more sensitive instrumentation called *Fourier Transform Infrared (FT-IR) Spectroscopy*. This development was first demonstrated in 1965 in the work of Cooley and Tukey⁽⁸⁸⁾, in which they used a Michelson interferometer to observe "interferogram", instead of direct intensity, of the transmitted light from sampling area. The main advantage of this technique is that the interferogram, $I(\delta)$, which is a sinusoidal function of wave number (ν) of the infrared light, can be more accurately measured using a computer calculation.

The relation between absorbance (A) and concentration (C) also follows the Beer-Lambert law.

$$A = \log.(I_0 / I) = \hat{\epsilon} C l. \quad (2.10)$$

Where, I_0 and I are radiation intensities before and after passing the sample, $\hat{\epsilon}$ is extinction coefficient and l is the thickness of the sample. Sensitivity in IR spectroscopy, however, is not as high as that of electronic spectroscopy, due to that the molar extinction coefficient in infrared spectroscopy is in the range of $1 - 10^2 \text{ cm}^3 \cdot \text{mmole}^{-1} \cdot \text{cm}^{-1}$, which is about $10 - 10^2$ times lower than that for electronic spectroscopy⁽⁸⁹⁾.

In quantitative measurement of infrared spectra of polymer films, one can eliminate experimental error due to thickness variation of the films, using a known non-variable peak (reference) of the polymer, for instance in the case of polypropylene the reference peak is the absorption peak of $>\text{CH}-$ group at $2752 - 2697 \text{ cm}^{-1}$. This allows the measurement of an absorption index of the sample (A_S / A_R), i.e. ratio of absorbance of the sample peak with the absorbance of the reference peak, which is thickness independent. The Beer-Lambert law then can be written in the form,

$$(A_S / A_R) = B C_S. \quad (2.11)$$

where, subscript s refers to the sample, r represents the reference and B is a new

gel-forming-compound, which can crosslink to form a certain pore size in the column⁽⁹¹⁾.

In the measurement of molecular weight distribution of polymers, the sample solution is injected into the GPC column. Lower MWt fractions diffuse more easily into the interstices of the gel column and will be retained longer in the column. After continuous elution by a suitable solvent, the eluent fractions containing the distributed sample are detected in a sensor detector to measure the amount of polymer sample in the eluent fractions. Molecular weight of each eluent is calibrated against a reference eluent, which is usually a polystyrene standard. Plot of the amount of polymer versus log molecular weight follows normal distribution, and is called molecular weight distribution (MWD) curve, see figure 2.30. In practice, the amount of polymer sample can be measured using any physical or chemical techniques based on the properties of the polymer sample, such as refractive index, uv-absorption, infrared absorption, polarisability etc. The first two methods or their combination are generally used, which are referred as refractive index (RI) and ultra-violet (UV) detectors.

Molecular weight of a polymeric material is determined from the averages of range of its molecular weights, since polymer materials are polydisperse compounds which contain molecules of different sizes and molecular weights. By definition, there are several methods of calculating average molecular weight of polymers⁽⁹²⁾.

- **Number average molecular weight (Mn)**, is calculated from the total weight of polymer ($\sum N_i M_i$) divided by its total molecule ($\sum N_i$).

$$M_n = \frac{\sum N_i M_i}{\sum N_i} \quad (2.12)$$

- **Weight average molecular weight (Mw)** is based on the average of total weight of the polymer ($\sum N_i M_i$).

$$M_w = \frac{\sum N_i M_i^2}{\sum N_i M_i} \quad (2.13)$$

- **Z-property average molecular weight (Mz)**. This is a theoretical average

molecular weight, which is defined as :

$$M_z = \frac{\sum N_i M_i^3}{\sum N_i M_i^2} \quad (2.14)$$

It is evident that for polydisperse polymer the M_w is always greater than the M_n . This is due to the fact that the M_w is higher in the presence of high molecular weight molecules, whereas the M_n is affected by the presence of low molecular weight polymer, see figure 2.30. The M_w is equal to M_n when the polymer is monodispers, i.e. when the polymer contains identical size of molecules. The ratio of M_w / M_n is known as *polydispersity index* (D) of the polymer, which represents the degree of molecular weight differences.

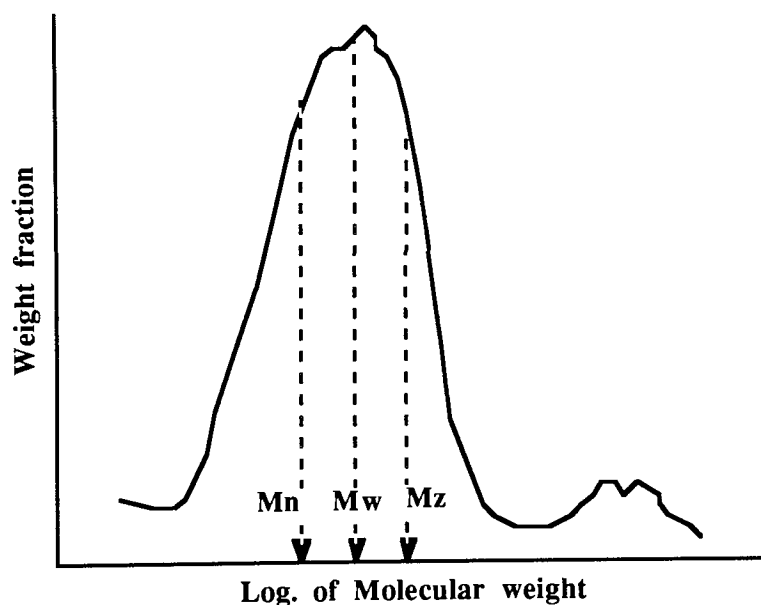


Figure 2.30 Molecular weight distribution curve of a polydisperse polymer, $M_z > M_w > M_n$

2.8 PROTON AND CARBON-13 NUCLEAR MAGNETIC-RESONANCE (NMR) SPECTROSCOPY

It is generally known⁽⁹³⁾ that each proton in a molecule possesses its own magnetic field due to different neighbouring atomic environment. The higher the

electron density of the proton the greater the magnetic field, and hence higher external magnetic field is required to promote to its excited state (high level energy), this nuclei is referred as "shielded". For instance, protons of tetramethyl silane (TMS) contain high electron density due to positive inductive effect (+I) from the silicon atom, which in turn appear on the NMR spectra with "chemical shift" on the high magnetic field area (right hand side). On the other hand, proton adjacent to a quaternary ammonium ion (R_4N^+) which contains low electron density (deshielded) appears on the low chemical shift (low field). In practice, the chemical shifts is expressed in δ -unit which is defined as the difference of the applied magnetic field (in ppm) from that of TMS (δ of TMS = 0). Another factor affecting the shape of proton NMR signals is due to interaction with their neighbouring proton(s), spin-spin coupling, which splits NMR signal a proton into (n+1) signals with intensities ratio follows Pascal's triangle formula (n = number of neighbouring protons).

NMR signal of ^{13}C , on the other hand, is weaker than that of 1H due to its lower electron negativity and lower natural abundance of ^{13}C in every carbon atom (only 1.1 %), in addition to its lower magnetic moment. Presentation of ^{13}C NMR spectra also uses TMS as standard ($\delta = 0$ ppm), whereas position of particular carbon signal is affected by its electronic charge, in which hybridisation state of the carbon atom determine their signal positions, i.e. sp^2 carbon appear on the lowest field ($\delta = 100 - 150$ ppm), followed by sp carbon ($\delta = 70 - 80$ ppm) and sp^3 carbon at highest field ($\delta = 0 - 60$ ppm)⁽⁹⁴⁾.

Spin-spin couplings between ^{13}C - ^{13}C atoms are not observed in ^{13}C NMR, due to their low probability. On the other hand, coupling constant between ^{13}C - 1H in a protonated Carbon is wider than that for 1H - 1H due to high magnetic moment of 1H . This causes the ^{13}C spectra of original NMR experiment suffered from long-range C - H couplings with ^{13}C -multiplet signal for every protonated Carbon. To eliminate this confusion, modern NMR procedure utilises 1H -decoupling method by excitation of all protons to their saturated state, which results in the equalisation of energy-level population of the protons. However, this technique also eliminates coupling

information of the NMR spectra since all Carbon resonance appears as a singlet signal. Other NMR technique use partial (off-resonance) decoupling method by reducing C-H coupling constant to distinguish various protonated and unprotonated carbon. A computer software has also been used to record spectral data of different carbon modes and to process in such a way that signals of primary (-CH₃, with 4-splits) and tertiary (>CH-, with 2-splits) Carbons will appear as positive (+) peaks, whereas signals of secondary (>CH₂, 3-splits) and quaternary (>C<, singlet) carbons appear as negative (-) peaks.

2.9 ELECTRON SPIN RESONANCE (ESR) SPECTROSCOPY

ESR method can be used for identifications of radicals both qualitatively and quantitatively, provided that the radical is stable enough and in the molar concentration above the sensitivity limit of the ESR measurement⁽⁹⁵⁾. To measure the radical concentration, the sample is recorded simultaneously with a reference of different g-value and known concentration. For measurement of nitroxyl radical (>N-O.), for instance, copper sulphate solution is used as the reference. A known weight and concentration of the reference is sealed in a capillary tube and fastened to the outer surface of the sample tube. As the ESR signal is generally broad the concentration of radical is represented by the area, instead of only by the height of the signal. The following formula, therefore, is generally used to measure the area of ESR signal quantitatively⁽⁵¹⁾.

$$\frac{Y_{m_s} (\Delta H_{pp_s})^2}{Y_{m_r} (\Delta H_{pp_r})^2} = \frac{C_s}{C_r} \quad (2.15)$$

Where, Y_m (in cm) and ΔH_{pp} (in Gauss) are the height and the width of the signal, as shown in figure 2.40., subscripts s and r represent sample and reference.

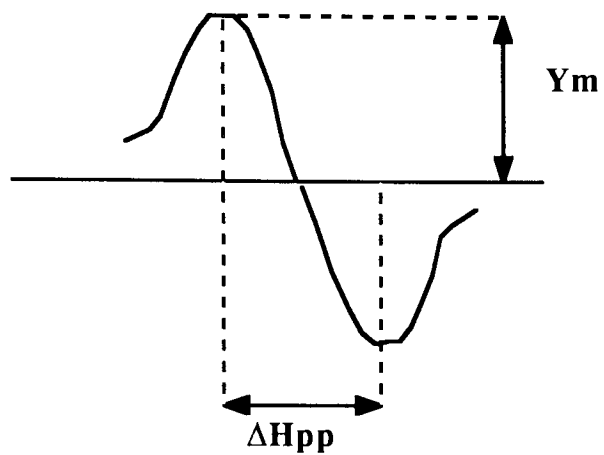


Figure 2.31 Measurement of ESR signal area

CHAPTER 3

REACTIVE PROCESSING AND STABILISING ACTIVITY OF ACRYLIC-CONTAINING NITROXYL PRECURSORS IN POLYPROPYLENE

3.1 OBJECTS AND METHODOLOGY

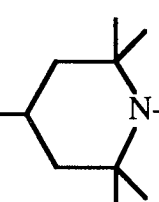
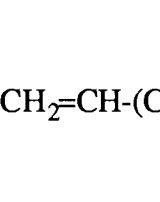
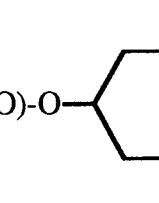
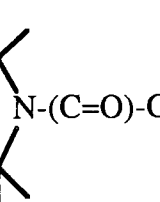
Recently it was reported⁽⁸²⁾ that a stable nitroxyl radical precursor containing two acrylic groups ; 1-acryloyl 4-acryloyloxy 2,2,6,6-tetramethyl piperidine, abbreviated as AATP (VI), can become chemically bound onto the polypropylene backbone to very high extent during a reactive processing procedure. However, it was shown that when polypropylene film samples containing this bound-antioxidant were exposed to uv-light, their photo-stability was lower than that of the corresponding analogues containing the unbound-antioxidant, i.e. when the AATP was used as a conventional additive. Surprisingly, when the bound-AATP was used with a very small amount of a conventional uv-stabiliser, e.g. 2-hydroxy 4-octyloxy benzophenone (HOBP), its photostabilising activity increased synergistically.

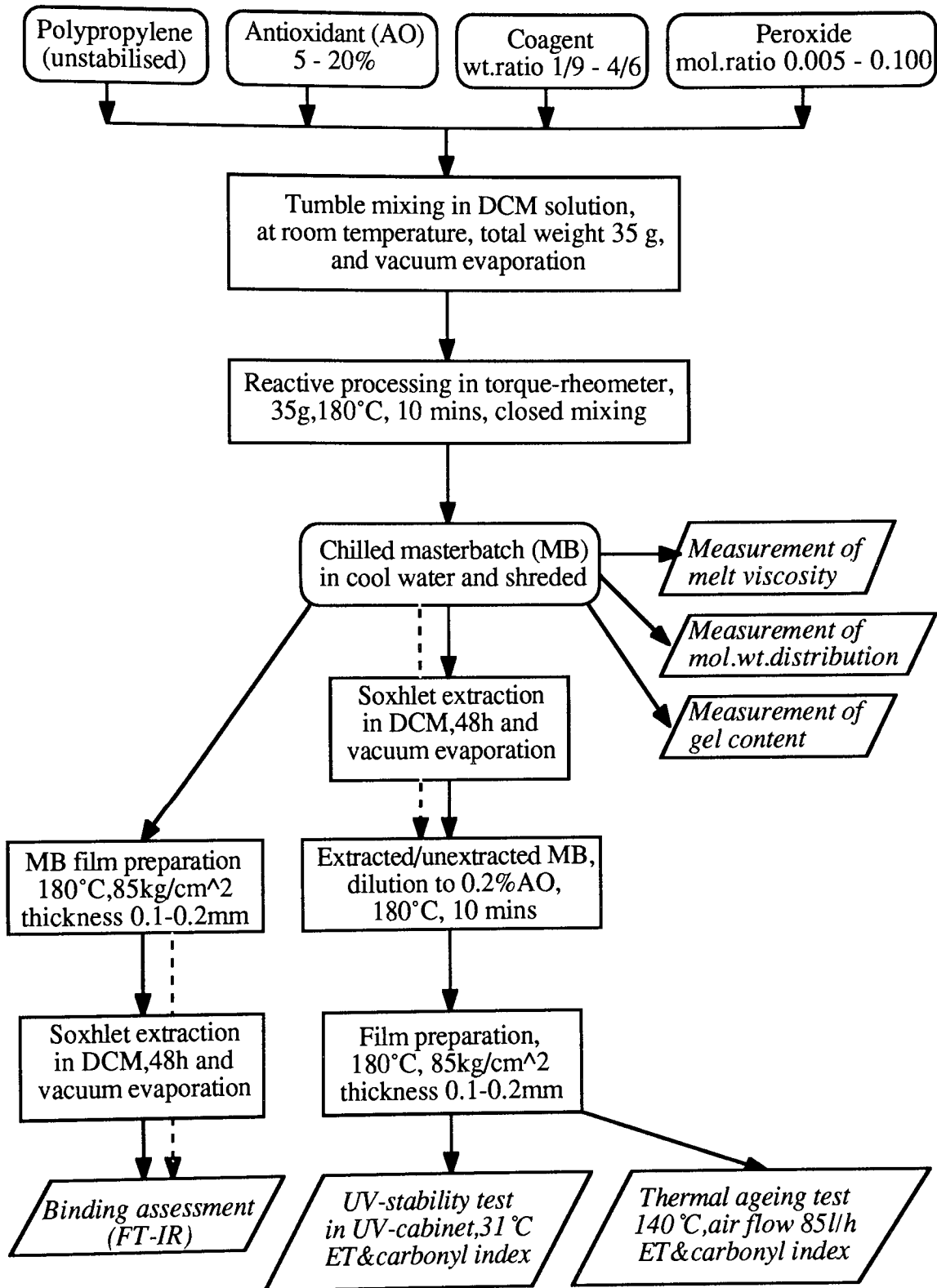
In this chapter the above behaviour was investigated further with the aim of developing new bound stable nitroxyl radical precursors as effective antioxidants for polyolefins. Work described here, therefore, is three fold, firstly to investigate the effect of reactive processing on antioxidant activity of various acrylic nitroxyl precursors in polypropylene. Secondly, to establish the site of binding of AATP, the approach here was to prepare analogues containing various saturated and unsaturated ester or amide derivatives of the nitroxyl precursors, see Table 3.1 (for preparative methods see Section 2.2). Thirdly, to develop more effective bound antioxidant systems, masterbatches containing highly bound antioxidant were prepared, and moreover the most effective derivatives of the nitroxyl precursors were chosen and their

binding efficiencies were examined at various processing conditions, peroxide contents and in the presence of various coagents. The photo and thermal stabilising activity of the bound antioxidants as well as synergistic mixtures with a conventional uv-screen (HOBP) in diluted masterbatch (d-MB) films were also tested.

The general experimental procedure of the work was as follows: Polypropylene (Propathene ICI HF26) was tumble mixed in dichloromethane with different antioxidants (concentration 5 - 20%), in the presence of peroxide at different molar-ratios (0.005 - 0.1) to the antioxidant, at room temperature and were subsequently vacuum evaporated. 35 grams of each mixture were then reactively processed in a Brabender torque-rheometer at 180°C for 10 minutes, under closed mixing condition (i.e. at standard condition, as has been mentioned in Section 2.3.1, Chapter 2). These masterbatches were then compression moulded into films of identical thickness (0.1 - 0.2 mm). The schematic diagram describing the procedure of reactive processing used is shown in Scheme 3.1.

Table 3.1 Various acrylic ester and amide derivatives of nitroxyl precursors.

Structure number	Chemical structure, name and molecular weight (MWt)	Abreviation
VI	$\text{CH}_2=\text{CH}-(\text{C}=\text{O})-\text{O}-\text{C}_6\text{H}_9\text{N}(\text{C}=\text{O})-\text{CH}=\text{CH}_2$  <p>1-acryloyl 4-acryloyloxy 2,2,6,6-tetramethyl piperidine (MWt=265)</p>	AATP
VIII	$\text{CH}_2=\text{CH}-(\text{C}=\text{O})-\text{O}-\text{C}_6\text{H}_9\text{N}-\text{H}$  <p>4-acryloyloxy 2,2,6,6-tetramethyl piperidine (MWt=211)</p>	AOTP
IX	$\text{CH}_2=\text{CH}-(\text{C}=\text{O})-\text{O}-\text{C}_6\text{H}_9\text{N}-(\text{C}=\text{O})-(\text{CH}_2)_{12}\text{CH}_3$  <p>1-myristoyl 4-acryloyloxy 2,2,6,6-tetramethyl piperidine (MWt=421)</p>	MyATP
X	$\text{CH}_3-(\text{CH}_2)_{12}(\text{C}=\text{O})-\text{O}-\text{C}_6\text{H}_9\text{N}-(\text{C}=\text{O})-\text{CH}=\text{CH}_2$  <p>1-acryloyl 4-myristoyloxy 2,2,6,6-tetramethyl piperidine (MWt=421)</p>	AMyTP



Scheme 3.1 A schematic diagram of reactive processing procedure and stabilisation tests of polymer-antioxidant systems

3.2 RESULTS

3.2.1 Optimisation of binding efficiency

Effect of antioxidant concentration on binding efficiency was investigated using various saturated and unsaturated ester or amide derivatives of nitroxyl precursors, such as AATP, AOTP, MyATP and AMyTP, see Table 3.1. These antioxidants were reactively processed at different concentrations with polypropylene in the presence of various molar ratios of DCP (see Section 3.1 and Scheme 3.1 for procedure). When compared to that before processing, concentration of the antioxidant in the polymer after processing, for example shown by the infrared spectra of polymer film containing AOTP prepared by casting in xylene compared to that of compression moulded polymer film after processing without peroxide, was fairly similar (see Figure 3.1). This indicates that during reactive processing of the antioxidant in closed mixing condition for 10 minutes there was no considerable evaporation of the antioxidant.

Binding efficiency of antioxidants in each film was calculated by measuring the antioxidant concentration in the masterbatch films using Fourier Transform Infrared (FTIR) spectroscopy before and after exhaustive soxhlet extraction in dichloromethane (DCM). The reproducibility of the binding results of these (minimum three) masterbatches, which were based on the amount remaining in the polymer after processing, was found to be better than 5%. Typical infrared spectra of the polymer film samples before and after extraction used for binding efficiency purposes are shown in Figure 3.2.

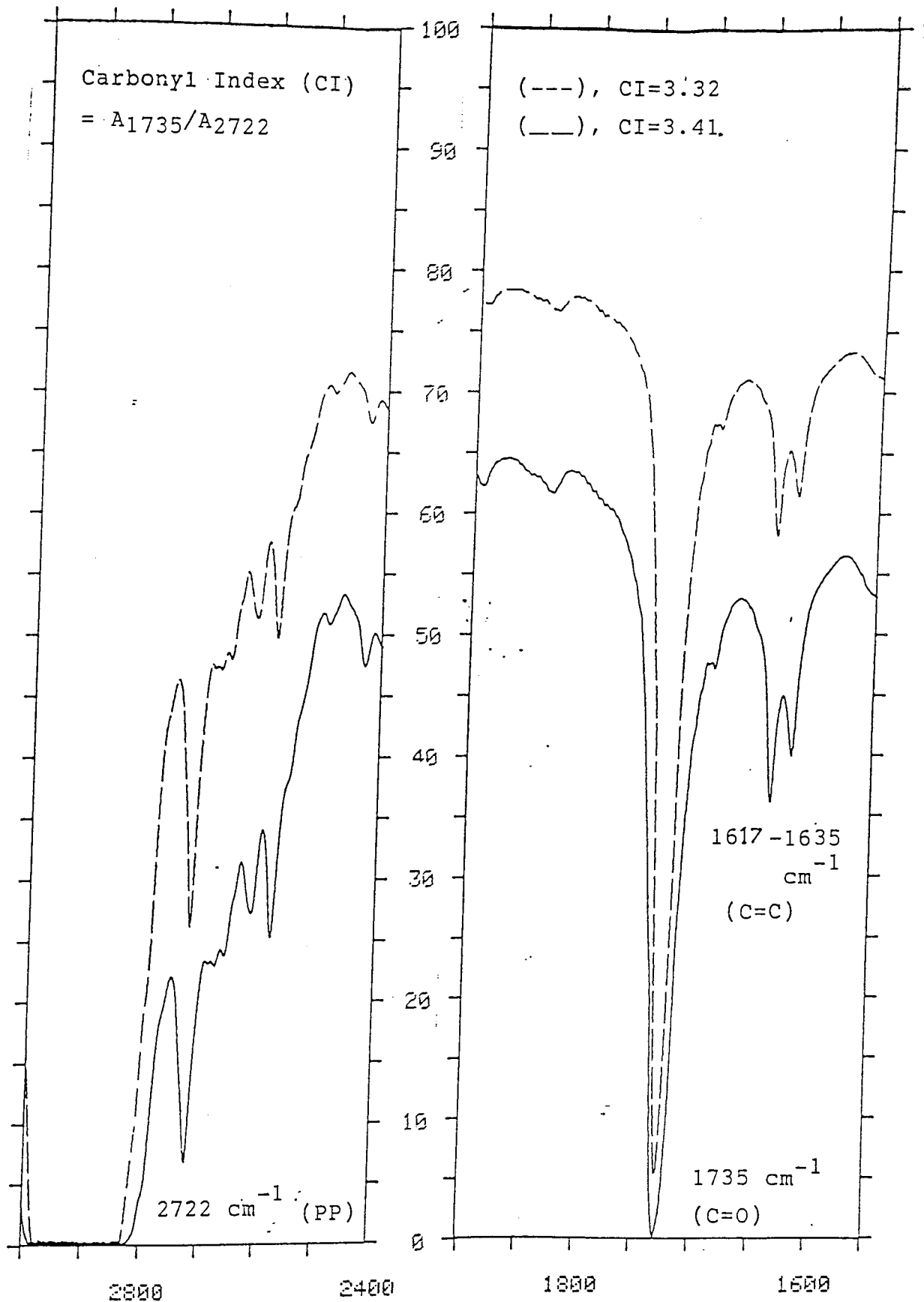


Figure 3.1 Infrared spectra of compression moulded PP films containing 10% of AOTP processed without peroxide in closed mixing condition at 180°C for 10 minutes (---) compared to that containing similar amount of AOTP prepared by casting in xylene (—)

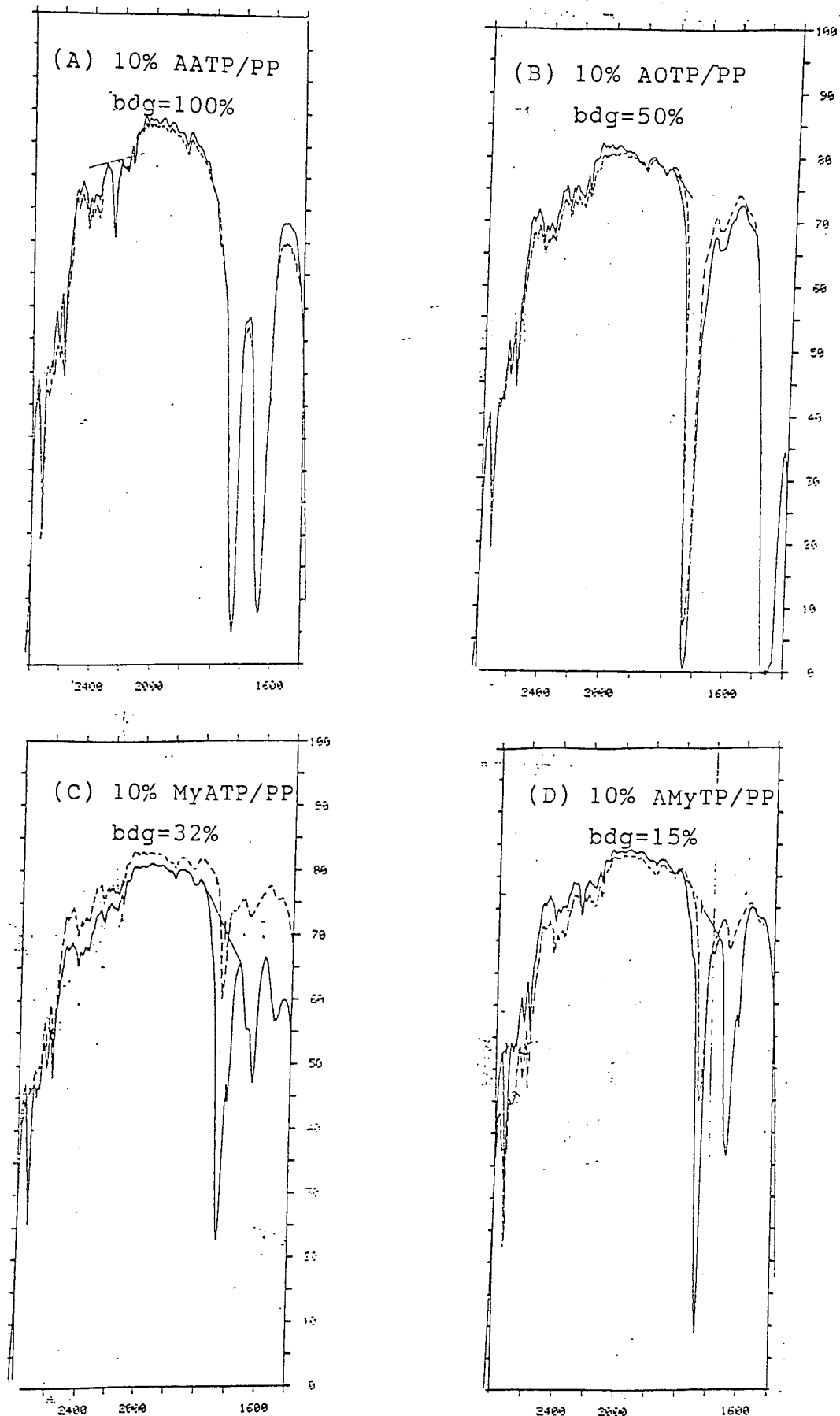


Figure 3.2 Infrared spectra of PP films containing 10% of : (A) AATP, (B) AOTP, (C) MyATP and (D) AMyTP processed in the presence of DCP 0.005 molar ratio at 180°C in standard condition, before (—) and after exhaustive soxhlet extraction in dichloromethane (- - -)

As shown in Table 3.2 and Figure 3.3, the binding efficiency of all antioxidants generally increase only slightly as antioxidant concentration in the masterbatch increases upto 20%.

Table 3.2 Effect of antioxidant concentration on the binding efficiency of acrylic nitroxyl precursors, processed at 180°C for 10 minutes, in the presence of DCP 0.01 molar ratio

Antioxidant-conc. (% w/w)	Binding of masterbatches containing 10 % of			
	AATP	AOTP	MyATP	AMyTP
5	95	35	28	10
10	100	50	32	15
15	100	50	35	15
20	100	52	35	15

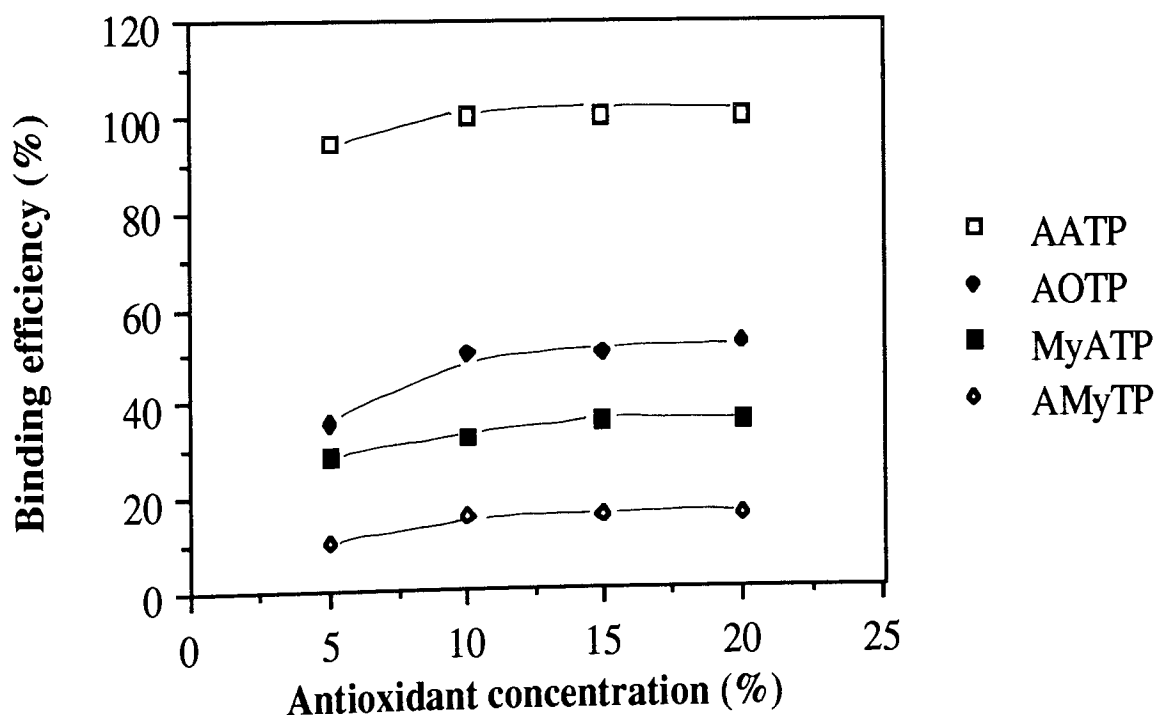


Figure 3.3 Binding level of various concentrations (5 - 20%) of acrylic nitroxyl precursors in polypropylene, processed at 180°C in standard condition, in the presence of DCP 0.010 molar ratio

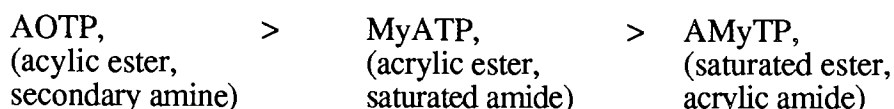
The antioxidant concentration can not be increased above 20% due to the incompatibility of some antioxidants in the polymer at these higher concentrations. At concentration of 30% AOTP, for instance, a powdery material was found to separate out from the masterbatch (concentrate). In the case of AATP (bisacrylate), when masterbatch containing 30% of the AATP was processed in a torque-rheometer in the presence of DCP 0.005 molar ratio at standard condition, the mixture generated very high torque after 3 minutes processing and for safety reason the processing was stopped.

Effect of peroxide concentration on binding efficiency was investigated by preparing 10% masterbatches of different antioxidants in polypropylene at standard processing condition, but with various peroxide concentrations (i.e. using different molar ratios of peroxide to the corresponding antioxidant). Their binding efficiency as well as melt viscosity (observed as melt flow index, MFI in g/10 minutes) were measured to estimate the degree of polymer destruction by the peroxide, see general procedure in Scheme 3.1.

Table 3.3 and Figure 3.4 show that, in general, the higher the peroxide concentration, the higher the binding efficiency. At high peroxide concentration, however, the polymer showed signs of destruction, which was observed by a large increase in MFI values, see Figure 3.5. The presence of peroxide may lead to chain scission which in-turn decreases the molecular weight of the polymer, (molecular weight is inversely related to the MFI). It was also found that masterbatches containing 10% of AATP (bisacrylic) do not show high MFI increase with increasing peroxide content (MFI increased from 0.6 - 16.5 g/10 mins as peroxide content increased from 0 - 0.08 molar ratio). Whereas other masterbatches containing similar concentration of monoacrylic nitroxyl precursors (AOTP, MyATP and AMyTP) exhibit much higher MFI increase (0.7 - 47.4 to 0.9 - 73.9 g/10 mins). When polypropylene was reactively processed without any antioxidant but in the presence of various DCP contents equivalent to those of AOTP-masterbatches, the MFI increase was much higher (0.8 - 87.7 g/10minutes), see Table 3.3. This indicates that the presence of

nitroxyl-precursors in the masterbatches may reduce the polymer destruction by the peroxide during processing. Optimum binding with high polymer-antioxidant compatibility and minimum destruction by the peroxide, was therefore achieved by 10% masterbatches using peroxide molar ratio of 0.005 - 0.010.

Under various peroxide contents, see Table 3.3 and Figure 3.4, the binding efficiency of monoacrylic nitroxyl precursors were always found to be in the order of,



whereas, their MFI increase follows an opposite order, see Figure 3.5. It seems likely that when the nitroxyl precursors bind at higher efficiency their MFI exhibits a lower value. When the total binding efficiency of MyATP (binding = 32%) and AMyTP (binding = 15%) masterbatches is compared to that of AATP masterbatch (binding = 100%), it was found that the total binding of both types of monoacrylic nitroxyl precursors is much lower than that of AATP alone, see Table 3.2. This evidence suggests that when both acrylic ester and acrylic amide groups are present in the same molecule (such as in AATP), their total binding efficiency may be increased.

Table 3.3 Effect of peroxide (DCP) content on the binding efficiency of 10% masterbatches containing acrylic nitroxyl precursors, processed at standard condition. *MFI was measured using small die ($\varnothing = 0.1181$ cm. **Polypropylene controls were processed using DCP molar ratio equivalent to those of AOTP-masterbatches

10% concentrate-containing:	Peroxide (DCP)-molar ratio	Binding (%)	MFI* (g/10mins.)
AATP	0.000	20	0.6
	0.005	100	0.5
	0.010	100	0.7
	0.040	100	5.7
	0.080	100	16.5
AOTP	0.000	8	0.7
	0.005	50	1.6
	0.010	50	2.8
	0.014	53	3.8
	0.020	53	12.7
	0.030	60	19.1
	0.080	63	47.4
MyATP	0.000	0	0.8
	0.005	32	2.0
	0.010	32	4.1
	0.018	35	15.6
	0.046	41	28.2
	0.080	43	56.2
AMyTP	0.000	0	0.9
	0.005	14	1.9
	0.010	15	4.3
	0.019	15	12.2
	0.050	20	37.3
	0.100	28	73.9
PP, unprocessed	----	--	0.4
PP, processed**	0.000	--	0.8
	0.005	--	4.1
	0.010	--	9.0
	0.020	--	19.5
	0.040	--	43.9
	0.080	--	87.7

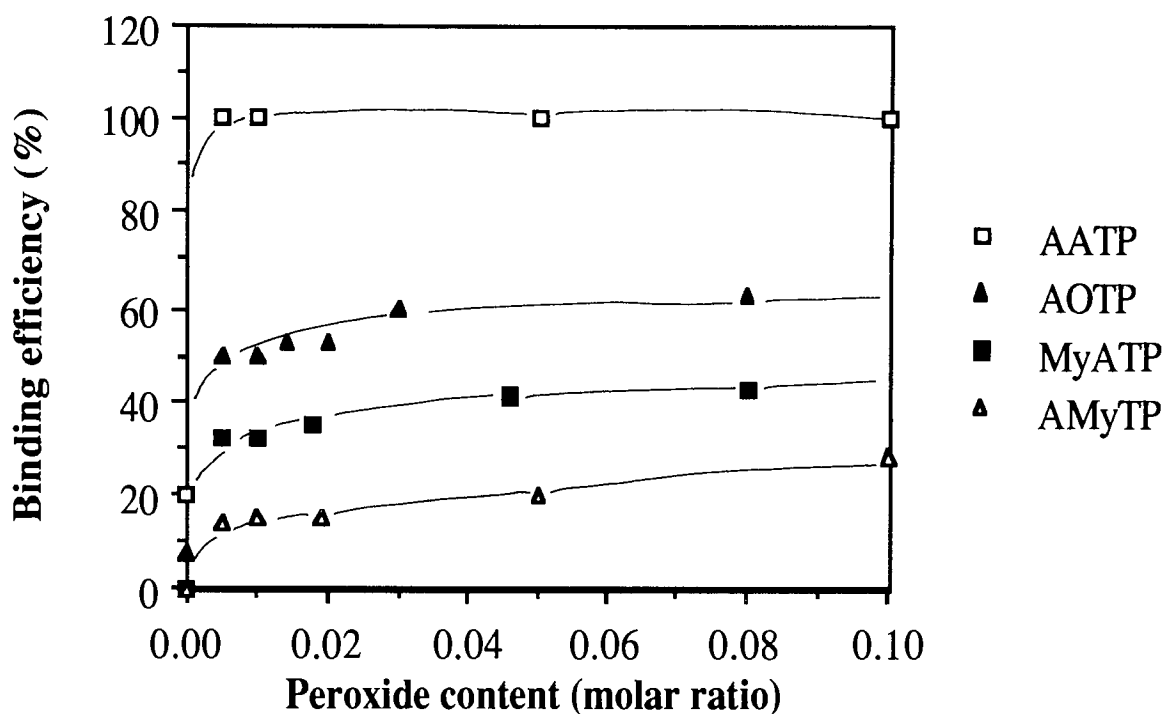


Figure 3.4 Binding level of acrylic nitroxyl precursors in 10% masterbatches processed in the presence of various concentrations of DCP at 180°C under standard condition

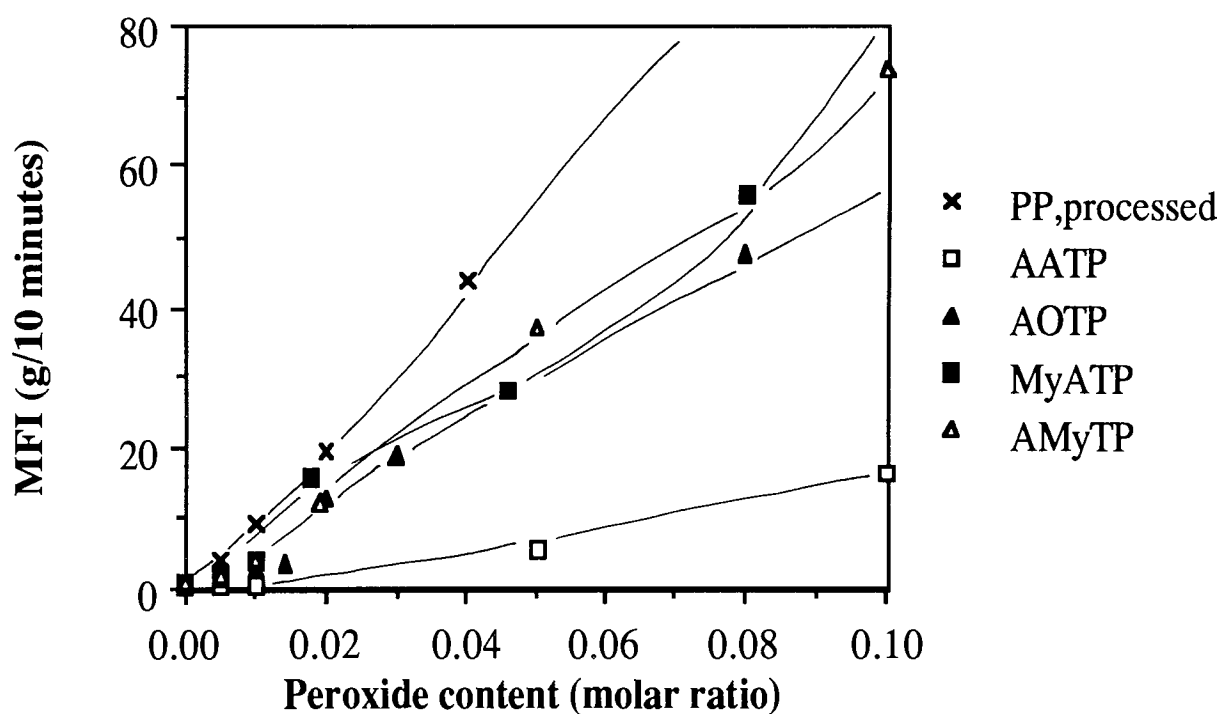


Figure 3.5 MFI of masterbatches containing 10% of different nitroxyl precursors processed in the presence of various concentrations of DCP at 180°C under standard condition

3.2.2 Effect of reactive processing on the photostabilising activity of acrylic nitroxyl precursors in polypropylene

Masterbatches containing 10% of various antioxidants processed in the presence of dicumylperoxide (DCP) 0.005 molar ratio to the antioxidant as mentioned in Section 3.1 were shredded and exhaustively extracted in DCM. The masterbatches were then diluted down to 0.2% (w/w), based on the amount of bound-antioxidant retained in the masterbatches, and compression moulded in a "Daniels" press at 180°C to form polymer-film 0.1 - 0.2 mm in thickness, see Section 2.3.2 for detail of film preparation. Photostability of these extracted PP films containing bound-antioxidant (B,E) were tested in a UV-cabinet and compared to those of PP-films containing 0.2% (w/w) of unbound-antioxidant (Ub), i.e. diluted from 10% masterbatches processed without peroxide as conventional additive, see Scheme 3.1 (see Section 2.5.1 for the uv-irradiation procedure). Controls for the photostabilising test were processed polypropylene film and those containing 0.2% (w/w) of commercial antioxidants, such as Tinuvin 770 (bis-[2,2,6,6-tetramethyl 4-piperidiny] sebacate), Irganox 1076 (octadecyl-[3,5-ditertiarybutyl 4-hydroxyphenyl] propionate) and Cyasorb UV-531 (2-hydroxy 4-octyloxy benzophenone = HOBP).

As shown in Table 3.4 and Figures 3.7 - 3.8, photostabilising activity of bound extracted antioxidants, shown by embrittlement time (ET) and carbonyl index increase (Δ CI) of the PP films during irradiation, are much lower than those of their corresponding unbound analogues (i.e. higher stabilising activity of the unbound antioxidants is indicated by longer embrittlement time and lower carbonyl index increase of the corresponding PP films). The decrease of uv-stabilising activity of bound extracted bisacrylics (AATP, ET decrease from 1350 to 220 h) is lower than those of bound monoacrylics (AOTP, MyATP and AMyTP, ET decrease from 1500 - 1350 h to 500 - 420 h). This may be due to inhibition of nitroxyl radical formation in the case of bound-AATP, since the AATP may be grafted through both its acrylic ester and amide groups. On the other hand, the acrylic amide derivative (AMyTP, ET = 420

h), which can only bind through the amide side, does not seem to show much lower uv-stabilising activity when compared to that of acrylic ester derivative (MyATP, ET = 480 h).

Table 3.4 Binding and uv-stability of various Acrylic Nitroxyl Precursors in PP-films containing 0.2 % of bound antioxidants, diluted from 10% extracted masterbatches. *Films containing unbound antioxidant were diluted from 10% masterbatches processed without peroxide as conventional additive.

Film sample (0.2 % AO)	Binding (%)	<u>Embrittlement Time (ET, hours).</u>	
		(bound,E)	(unbound)*
PP-processed	--	--	70
Tinuvin 770	--	--	1600
Irganox 1076	--	--	140
HOBP	--	--	730
AATP	100	220	1350
AOTP	50	500	1500
MyATP	32	480	1500
AMyTP	14	420	1350

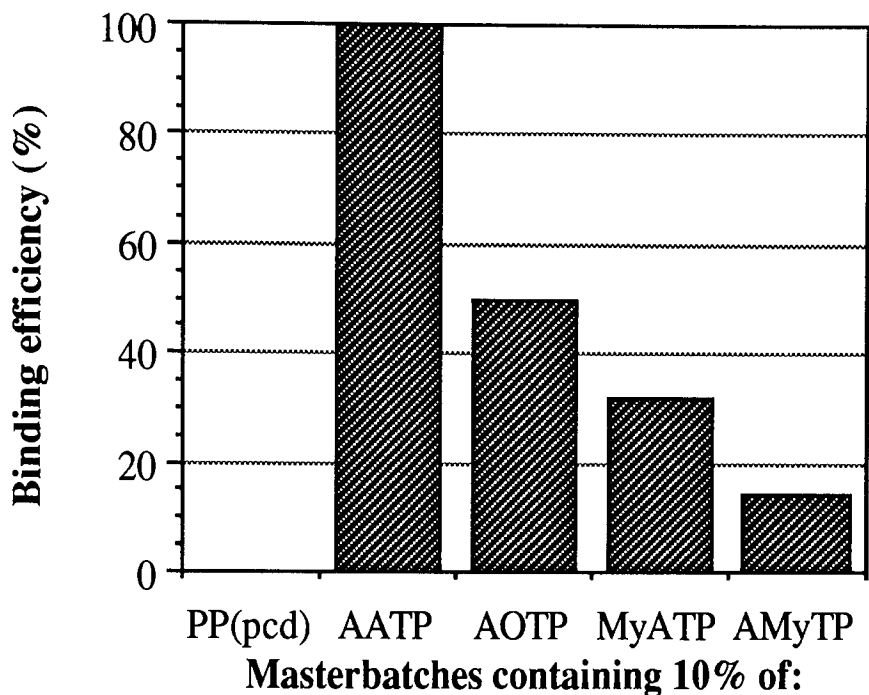


Figure 3.6 Binding of various acrylic nitroxyl precursors in 10% masterbatches processed at standard condition with DCP 0.01 molar ratio

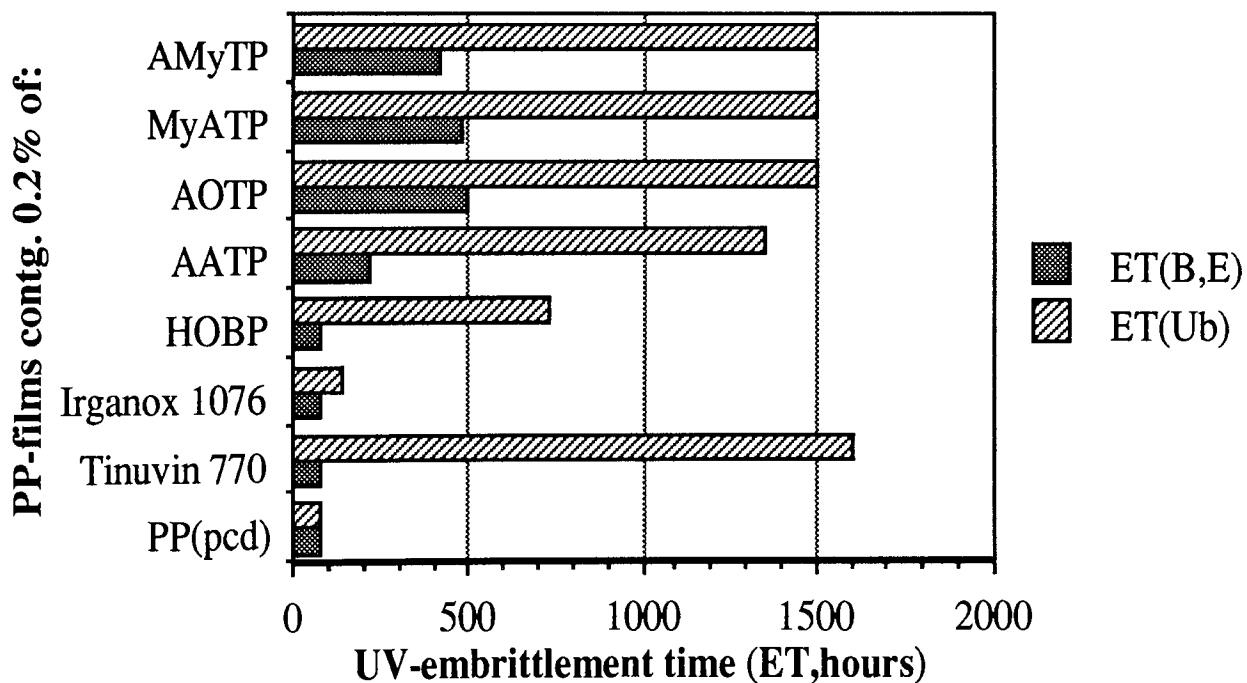


Figure 3.7 Embrittlement time of diluted concentrate-films containing 0.2% of various unbound (Ub) and bound-extracted (BE) acrylic nitroxyl precursors

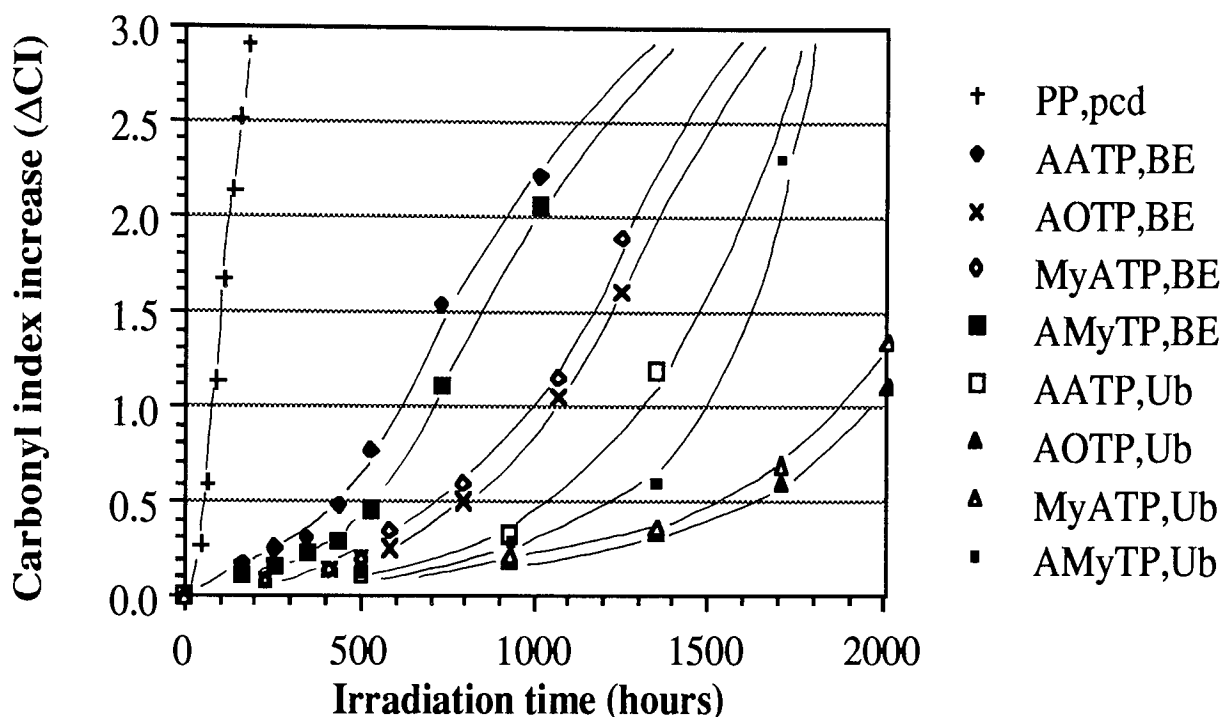


Figure 3.8 Carbonyl index increase (ΔCI) during uv-irradiation of diluted masterbatch films containing 0.2% of Ub and BE nitroxyl precursors

3.2.3 Reactive processing of monoacrylic secondary amine (AOTP) in conjunction with bisacrylic nitroxyl precursors (AATP)

Nitroxyl precursors containing monoacrylic group (such as AOTP) have been reported in the previous sections to exhibit low binding efficiency (upto 50%) after reactive processing at various concentrations and peroxide contents under standard condition. On the other hand, the bisacrylic derivative (AATP) exhibited high binding efficiency in polypropylene. To improve the binding efficiency of the AOTP, reactive processings of the antioxidant in conjunction with the bifunctional (AATP) were carried out at various weight ratios of AATP to AOTP.

Masterbatches containing 10 % mixture of various compositions of AATP and AOTP were prepared by reactive processing procedure in the presence of DCP 0.005 molar ratio to total antioxidants. The binding efficiency of AOTP (calculated after subtraction of carbonyl index due to AATP before and after extraction) as well as

photostability of the extracted diluted masterbatch films containing 0.2% bound AOTP (BE) compared to those of PP films containing similar concentration of unbound AOTP are shown in Table 3.5.

Table 3.5 Extended binding of AOTP processed in PP in conjunction with AATP (total concentration = 10%) in the presence of DCP 0.005 molar ratio under standard condition and its effect on uv-stability of their diluted masterbatch (d-MB) films containing 0.2% of antioxidant mixtures compared to *films containing unbound antioxidant were diluted to similar concentration from 10% masterbatches processed without peroxide as conventional additive

Masterbatch containing 10% of :	Binding (%) of AOTP	Embrittlement Time (hour) of PP-film contg.	
		(0.2% of bound,E)	(0.2% of unbound)*
PP-processed (control)	-	--	70
AATP,only	100	220	1350
AOTP, only	50	500	1500
AATP/AOTP (2:8)	70	440	1500
AATP/AOTP (4:6)	87	330	1500

Results from Table 3.5 and Figure 3.9 show that total binding of the antioxidants were improved (from 50 - 87%) as AATP ratio was increased to 4 : 6. The uv-stabilising activity of bound extracted antioxidant mixtures, however, seemed to decrease with increasing AATP content, (see Figures 3.10 and 3.11 for embrittlement time and carbonyl index increase), which indicate that low stabilising activity of bound AATP may contribute to the total stabilising activity of the mixtures. Their unbound antioxidant mixtures (diluted from 10% masterbatches processed without peroxide), on the other hand, showed good stabilising activity.

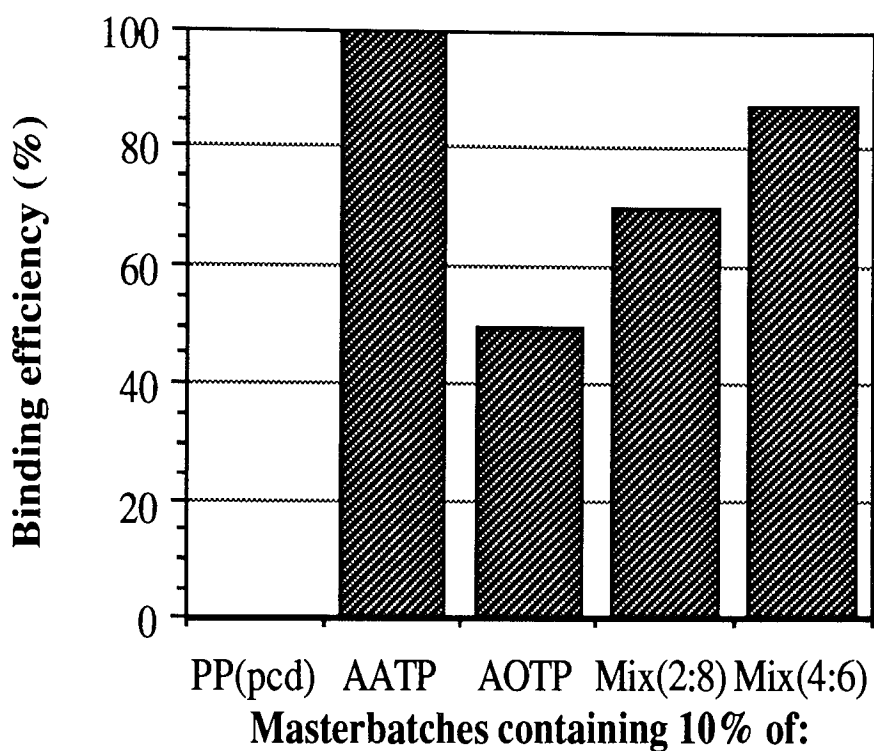


Figure 3.9 Binding of masterbatches containing 10% of AATP and AOTP mixtures at various composition

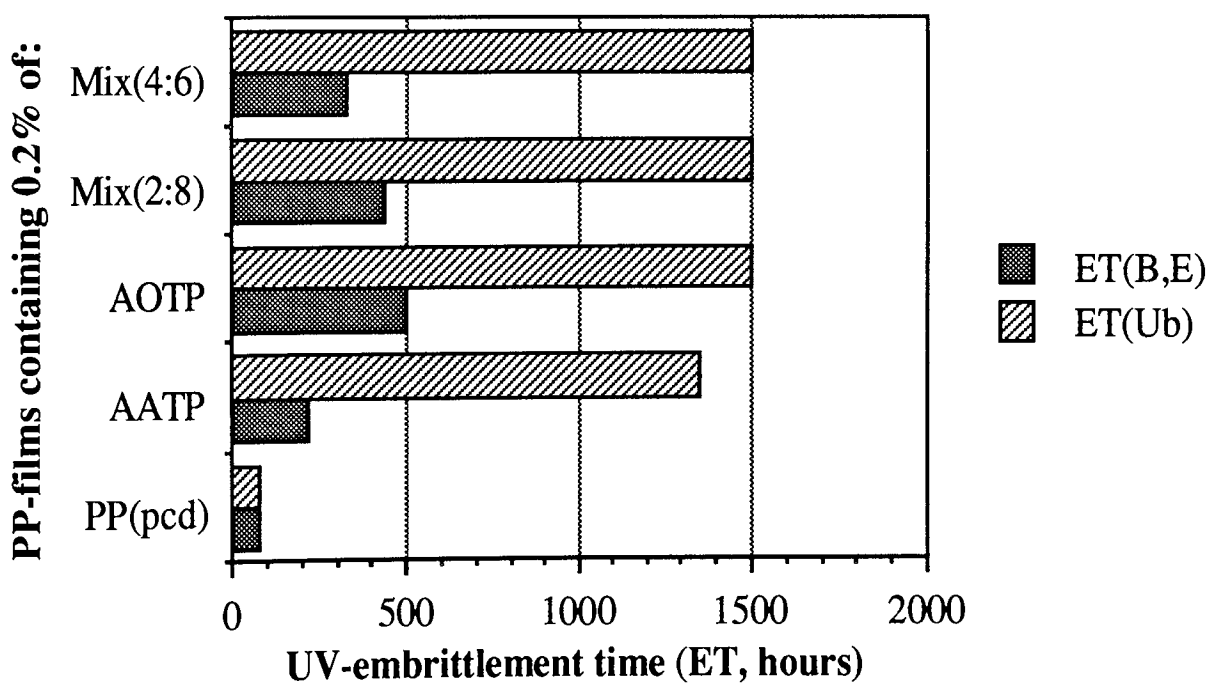


Figure 3.10 ET of diluted masterbatch films containing 0.2% of Ub and BE AATP/AOTP mixtures at various composition

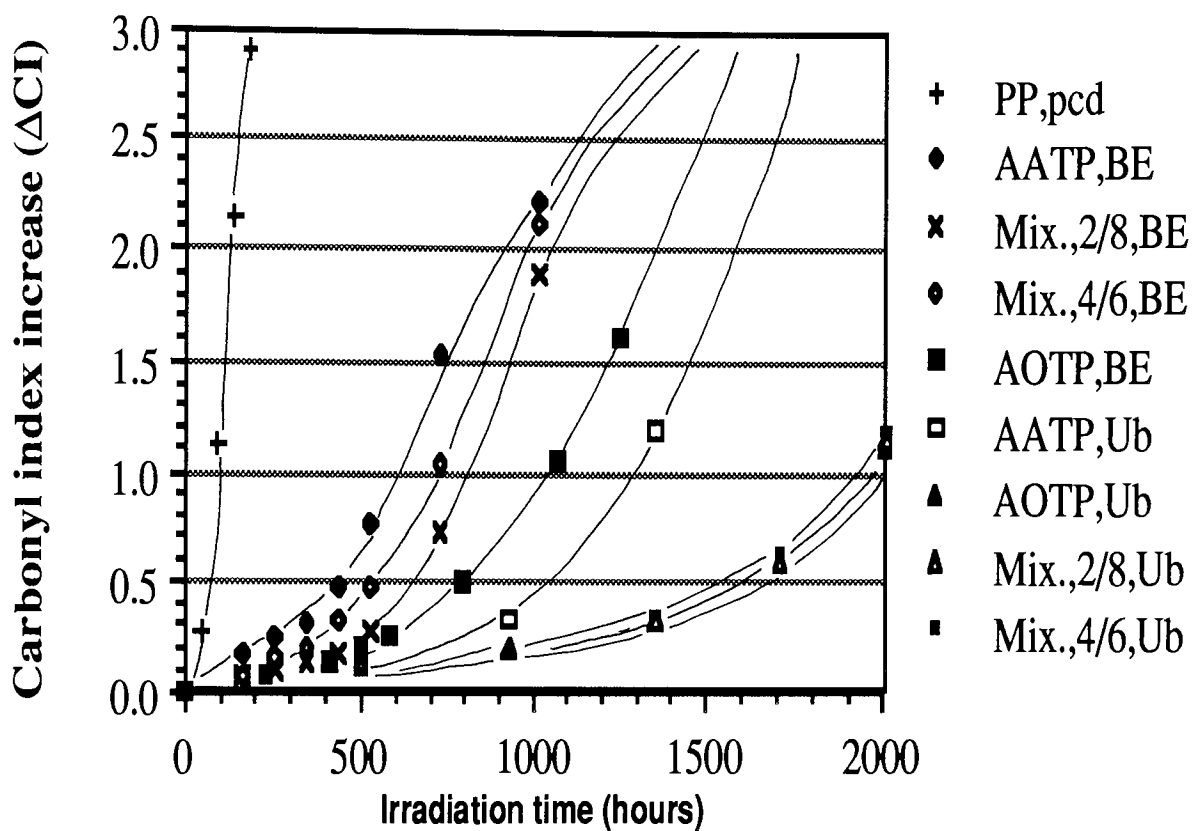


Figure 3.11 Carbonyl index increase during uv-irradiation of diluted masterbatch films containing 0.2% of Ub and BE AATP/AOTP mixtures at various composition

3.2.4 Extended binding of AOTP using various binding agents (coagents)

Reactive processing of AOTP in conjunction with AATP (a bifunctional), increased the binding efficiency (from 50 to 87%) only after using high ratio of AATP to AOTP (4/6 ratio, see Table 3.5). This composition is not a desired system, since high ratio of AATP may lead to the decrease of stabilising activity of the system (Table 3.5 and Figure 3.10). In this section, binding of AOTP was extended using various binding agents (coagents) containing di- or tri-acrylates or methacrylates groups, see Table 3.6 for their chemical structures. These coagents have been used in polymers mainly as crosslinking agents^(72,92,96).

Table 3.6 Various coagents used to extend the binding of antioxidants

Structure number	Chemical structure, name and molecular weight (MWt)	Abreviation
XVI	$[\text{CH}_2=\text{CH}-(\text{C}=\text{O})-\text{O}-\text{CH}_2-]_3 \text{C}-\text{C}_2\text{H}_5$ trimethylolpropane triacrylates (MWt=296)	TMPTA
XVII	$[\text{CH}_2=\text{CH}-(\text{C}=\text{O})-\text{O}-\text{CH}_2-\text{CH}_2-\text{CH}_2-]_2$ hexane 1,6-diacrylates (MWt=226)	HDA
XVIII	$[\text{CH}_2=\text{C}(\text{CH}_3)-(\text{C}=\text{O})-\text{O}-\text{CH}_2-]_3 \text{C}-\text{C}_2\text{H}_5$ trimethylolpropane trimethacrylates (MWt=348)	TMPTM
XIX	$[\text{CH}_2=\text{C}(\text{CH}_3)-(\text{C}=\text{O})-\text{O}-\text{CH}_2-\text{CH}_2-]_2 \text{O}$ butylene glycol dimethacrylates (MWt=270)	BGDM

Masterbatches containing 10% of mixtures of various coagents and AOTP (coagent ratio to AOTP = 2 : 8) were reactively processed in the presence of DCP (molar ratio = 0.005 to total additives) under standard condition. Their binding efficiency as well as stabilising activity were tested as in the previous procedure shown in Scheme 3.1. However, it should be noted that carbonyl absorption of AOTP and those of coagents overlap (at 1811 - 1668 cm^{-1}), therefore the level of binding of AOTP in the mixture with coagent was calculated after subtraction of carbonyl index due to coagent before and after extraction, see Figure 3.12 for their FTIR spectra.

Binding of AOTP masterbatches containing tri-acrylates and methacrylates coagents (TMPTA and TMPTM), as shown in Table 3.7. and Figure 3.13, are slightly higher than those containing bis-acrylates and methacrylates coagents (HDA and BGDM). On the other hand, when AOTP was bound using methacrylate coagents (TMPTM and BGDM) it exhibited higher uv-stabilising activity as shown in Figures 3.14 and 3.15 This may be due to the fact that methacrylate group of the coagents, which is better radical scavenger than the corresponding acrylate group, is also involved in the stabilisation action.

High binding of AOTP as a 20% masterbatch in the presence of triacrylate (TMPTA) coagent, ratio 2:8, has been cross examined. A correct amount of 7.94 g of masterbatch containing 20% of AOTP and TMPTA (ratio 2:8 to AOTP) processed with DCP 0.005 molar ratio to total additives was exhaustively soxhlet extracted in DCM. The amount of extractable AOTP in the DCM-extract was measured by means of FTIR-spectroscopy using the calibration curve for an AOTP solution in DCM. It was found that 0.21 g of AOTP can be recovered from the DCM-extract, which is equivalent to 16 % of AOTP from the original masterbatch and indicates that the binding efficiency of the AOTP is 84%.

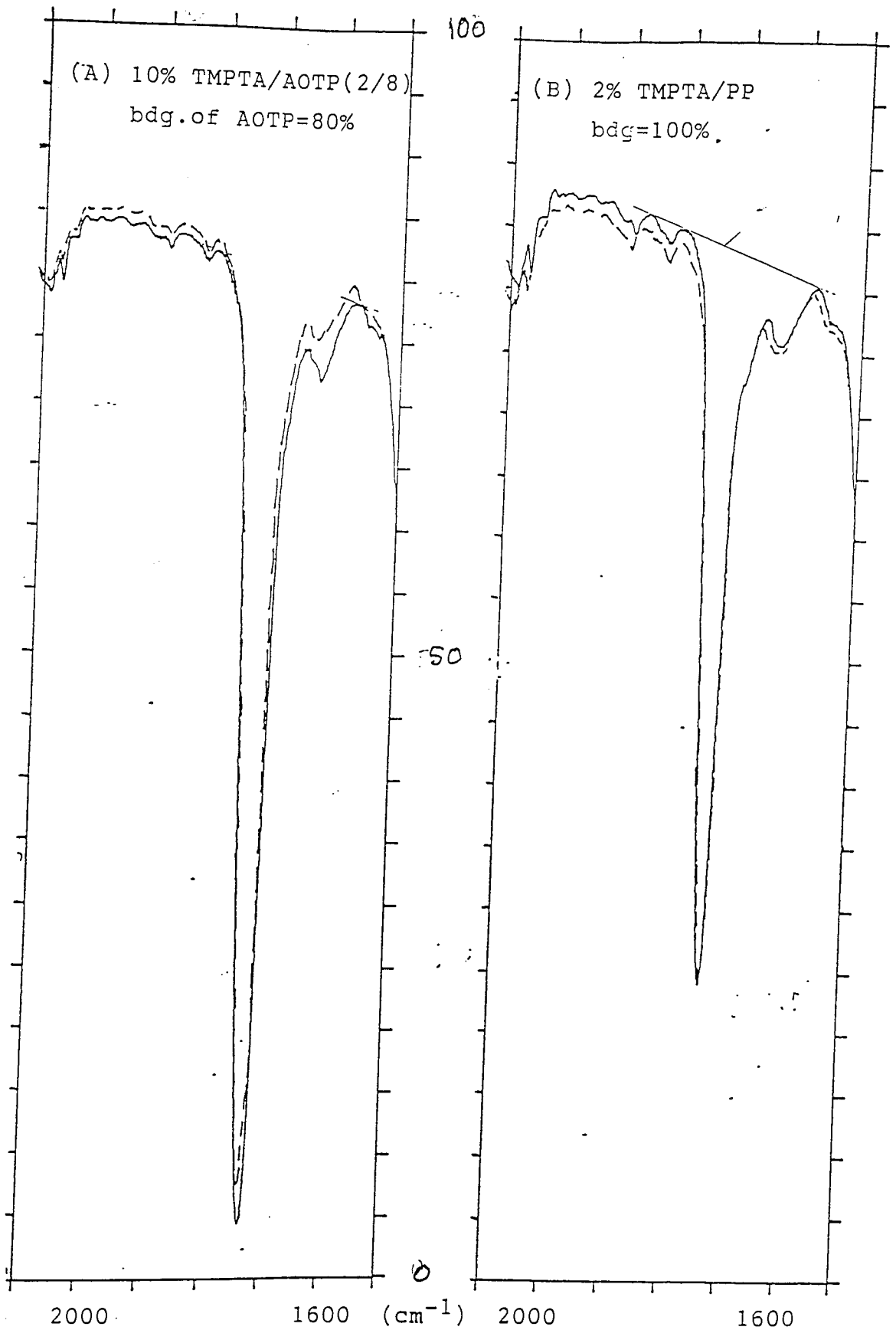


Figure 3.12 FTIR spectra, before (—) and after extraction (---), of PP films containing : (A) 10% of TMPTA/AOTP (2 : 8) processed in the presence of DCP 0.005 molar ratio, compared to those of containing 2% of TMPTA (B) processed at similar condition

Table 3.7 Extended binding of AOTP masterbatches containing various coagents, coagent-ratio = 20:80, DCP = 0.005 molar ratio Embrittlement time (ET) was measured using diluted bound extracted (B,E) masterbatch films containing 0.2% bound AOTP, *binding level of AOTP was calculated after subtraction of carbonyl index due to coagent before and after extraction

Masterbatch-mixtures(2:8)	Binding(%) of Coagent-alone	Binding(%) of AOTP in the mixture*	ET of extracted and diluted (B,E)-masterbatch films (h)
TMPTA/AOTP	100	80	450
HDA/AOTP	82	77	400
TMPTM/AOTP	97	81	510
BGDM/AOTP	20	64	500
AATP/AOTP	100	70	440
AOTP, alone	--	50	500

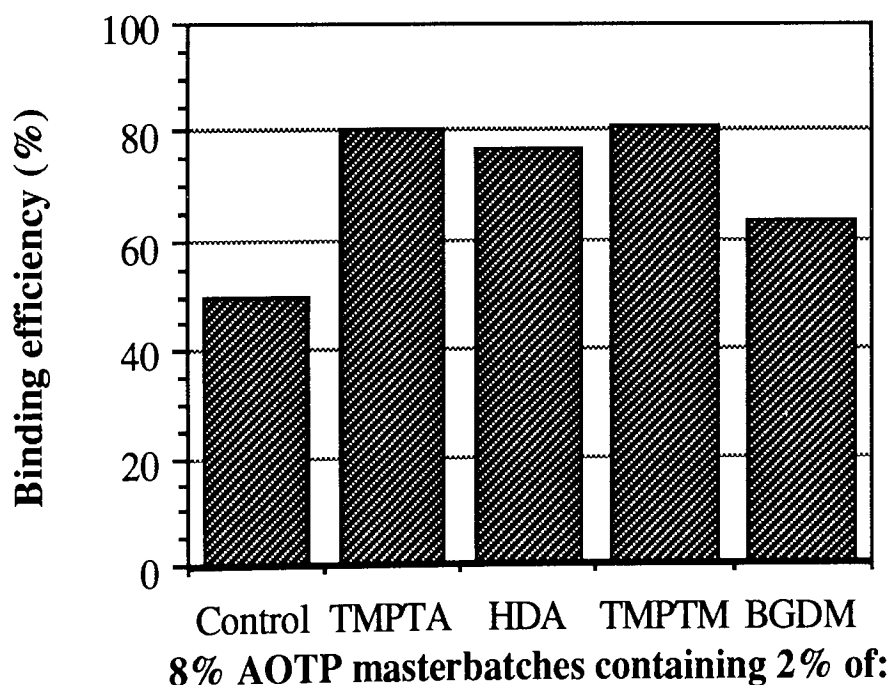


Figure 3.13 Binding of 10% AOTP masterbatches processed with various coagents at standard processing condition

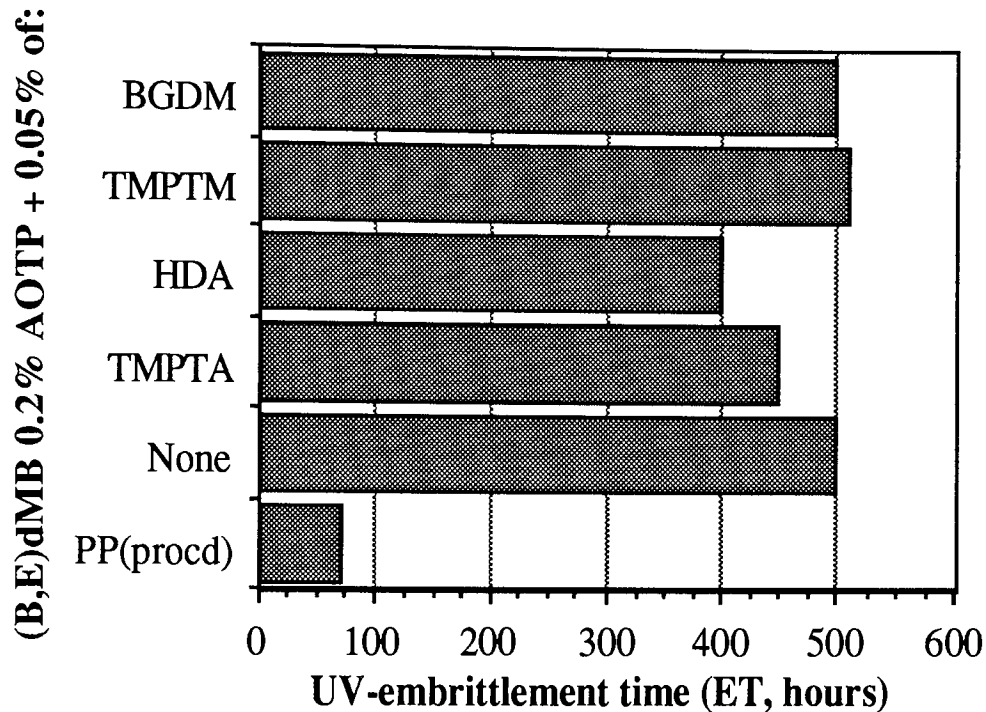


Figure 3.14 ET of diluted masterbatch films containing 0.2% of AOTP(BE), processed at standard condition with various coagents

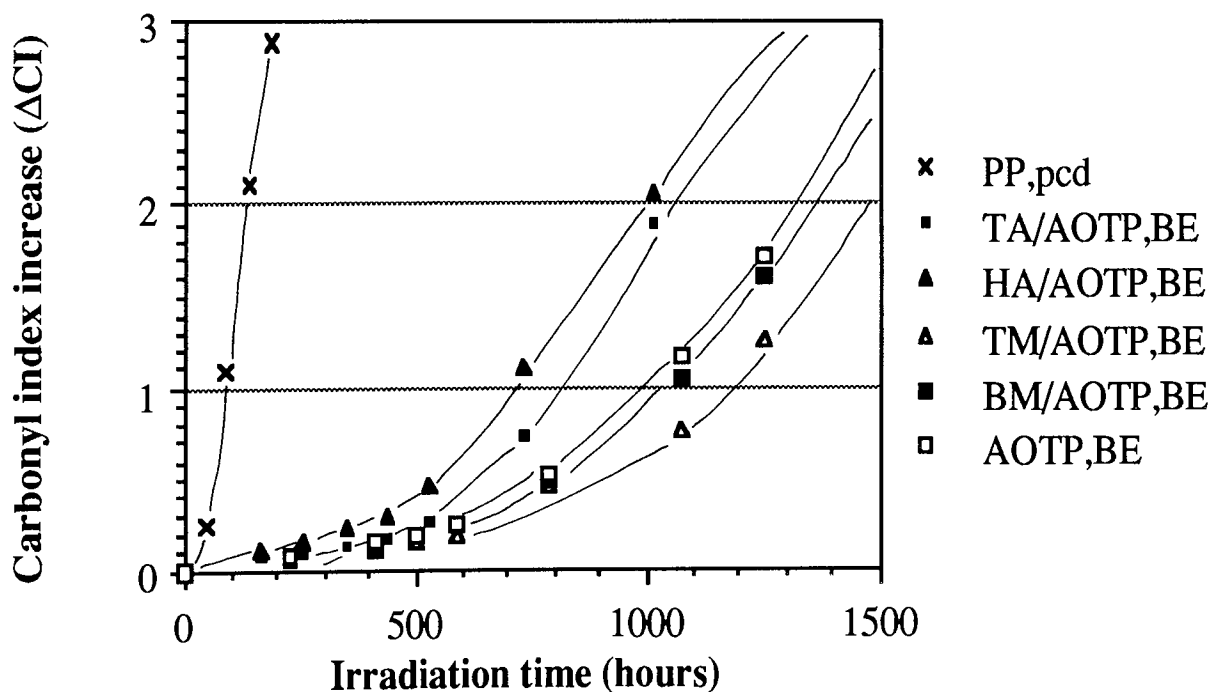


Figure 3.15 Carbonyl index increase during uv-irradiation of diluted masterbatch-films containing 0.2% of AOTP(BE), with various coagents

To investigate the effect of coagent (TMPTA) concentration on the binding efficiency of TMPTA/AOTP systems, masterbatches containing 10% of TMPTA and AOTP mixtures at various composition were prepared in the presence of DCP 0.005 molar ratio to total additives at standard processing condition. Binding level of AOTP as well as MFI (g/10 minutes) of these masterbatches were measured and their extracted diluted masterbatch films containing 0.2% of bound AOTP were tested for uv-stability, see Scheme 3.1 for general procedure. Results of binding level, MFI and photostabilising activity are shown in Table 3.8.

As shown in Figure 3.16, binding of AOTP containing TMPTA increased considerably as TMPTA concentration increased. Their MFIs, however, increase slightly as the TMPTA content increases to 4/6 ratio. This may be due to the decrease in AOTP concentration in the masterbatches, which functions as a melt stabiliser. On the other hand, uv-embrittlement time of the extracted diluted masterbatch films containing 0.2% of bound AOTP, processed in the presence of TMPTA, do not show any significant decrease when compared to that containing bound AOTP processed without TMPTA, see Figures 3.17 and 3.18.

Table 3.8 Extended binding of AOTP using TMPTA, in the presence of DCP (mr = 0.005 to total additives), at various coagent ratio, *MFI was measured using small die ($\varnothing = 0.1181$ cm). **Binding level of AOTP was calculated after subtraction of carbonyl index due to TMPTA

TMPTA/AOTP Weight Ratio	Binding(%) of AOTP**	MFI(g/10min)* (hours)	uv-embrittlemet time of (B,E)-films, (hours)
0/10	50	0.63	500
1/9	64	0.77	480
2/8	80	1.68	450
3/7	86	1.79	420
4/6	90	2.02	420

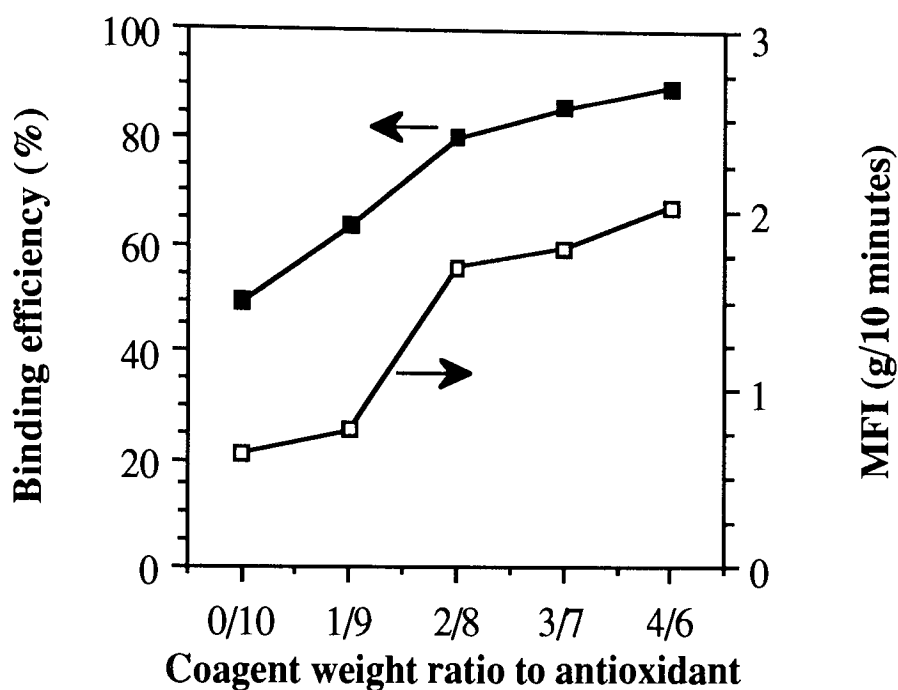


Figure 3.16 Binding and MFI of AOTP in 10% masterbatches processed with various composition of TMPTA

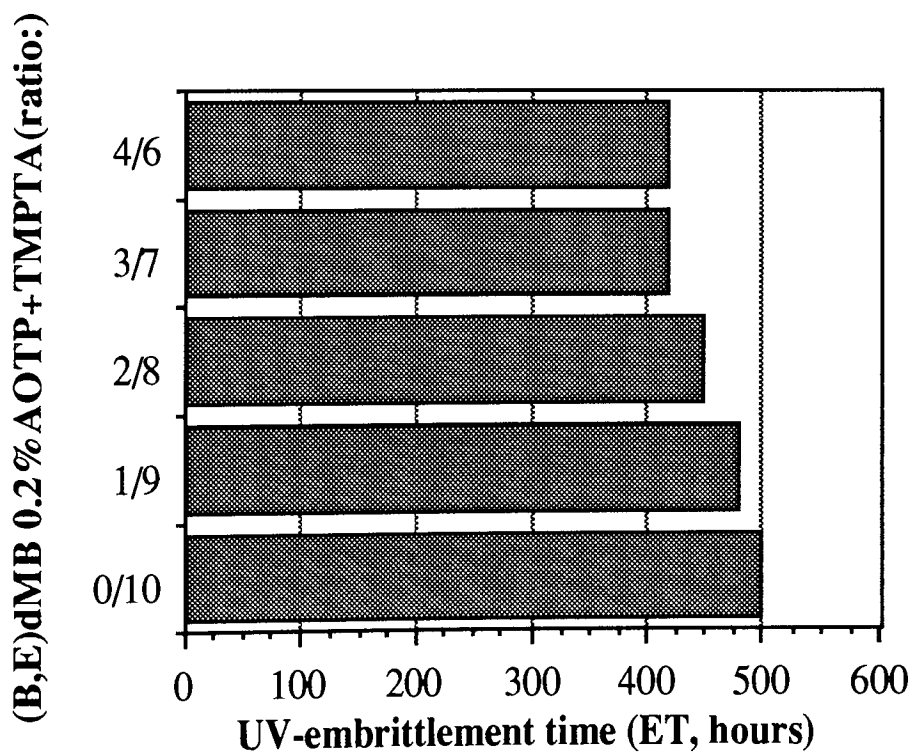


Figure 3.17 ET during irradiation of diluted masterbatch-films containing 0.2% AOTP(BE) processed with TMPTA at various compositions (TMPTA/AOTP weight ratio from 0/10 to 4/6)

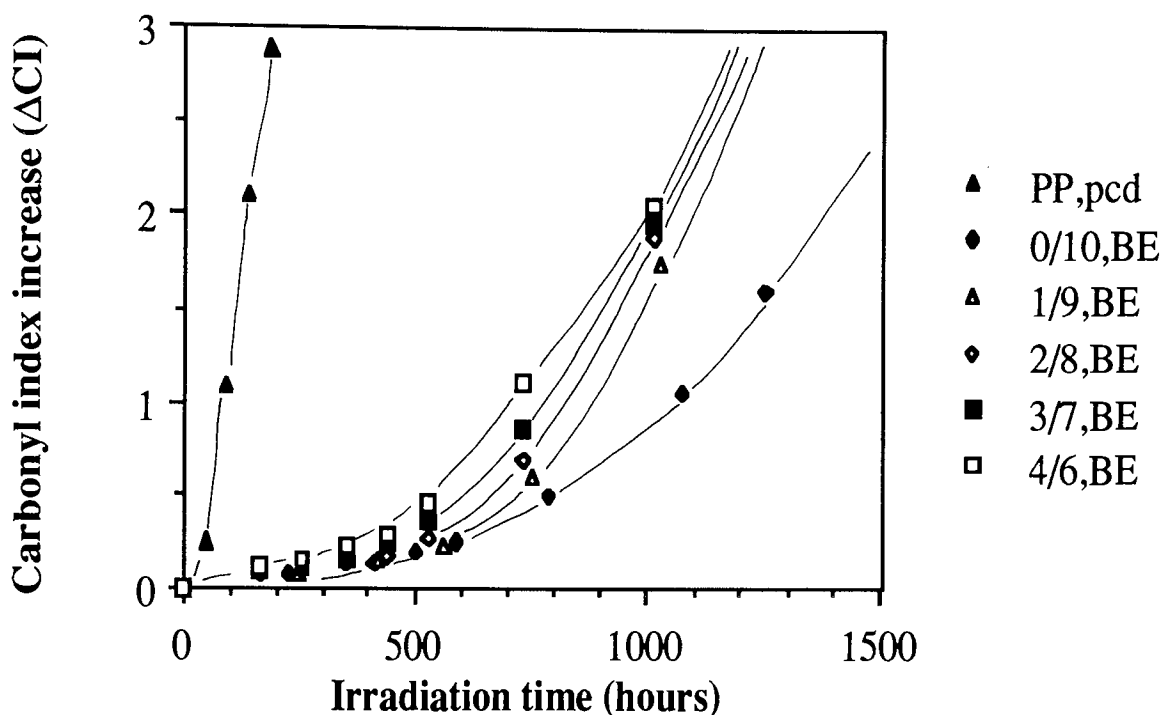


Figure 3.18 Carbonyl index increase during irradiation of diluted masterbatch- films containing 0.2% AOTP(BE) processed with TMPTA at various composition

Effect of peroxide content was investigated by preparing 10 % masterbatches of TMPTA and AOTP mixtures (ratio 2 : 8) at various DCP contents. Change on the physical properties of the masterbatches was observed by measuring their MFI using a melt flow indexer with small die ($\varnothing = 0.1181$ cm).

Table 3.9 Extended binding of AOTP using TMPTA, with coagent-ratio = 20:80, at various DCP content. * MFI was measured using small die (diameter 0.1181 cm). **Binding level of AOTP was calculated without interference of TMPTA as in Section 3.2.4

DCP molar ratio	Binding of AOTP(%)**	MFI (g/10 min)*
0.000	45	1.1
0.005	80	1.7
0.010	80	4.8
0.020	87	10.9

Results in Table 3.9 and Figure 3.19 show a slight increase in binding as the peroxide content increases. Unfortunately, their MFI values also increase sharply, which indicates severe destruction of polymer in the masterbatches. Reactive processing of AOTP, in the presence of TMPTA (ratio 2 : 8), using lower peroxide contents of 0.005 - 0.010 molar ratio, therefore, is recommended to avoid further destruction by the peroxide.

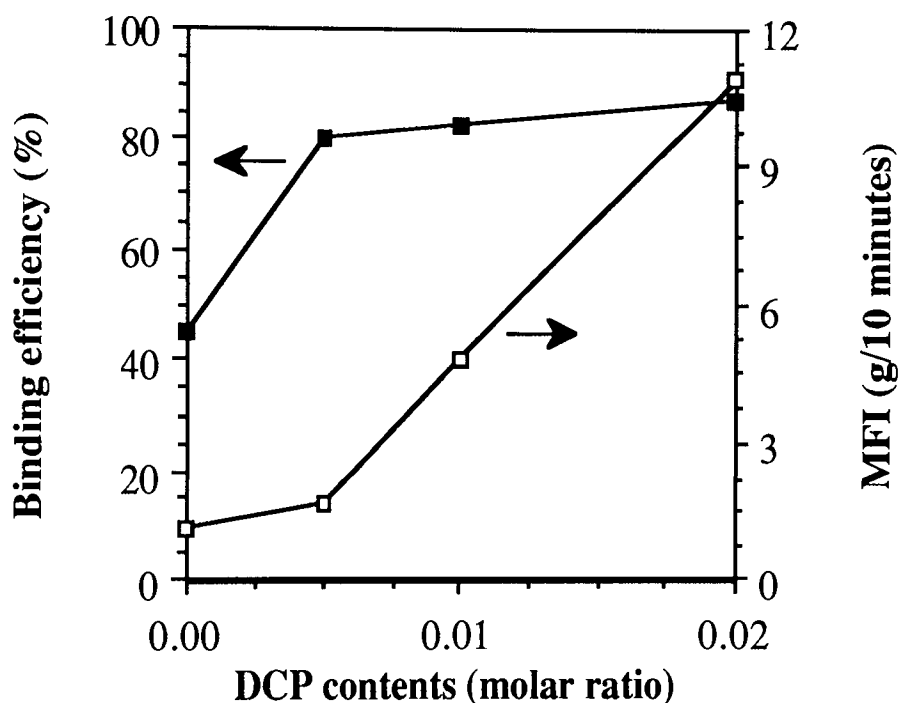


Figure 3.19 Binding and MFI of 10% TMPTA/AOTP(2:8) masterbatches processed at various peroxide contents

3.2.5 Thermal ageing of diluted masterbatch (dMB) films containing AOTP

Hindered piperidine compounds have been used commercially as one of the most effective uv-stabiliser systems for polyolefins. In the area of thermal stabilisation, however, these compounds are not widely used due to their volatility and ineffectiveness at elevated temperature. Various unextracted diluted masterbatch films

containing 0.2% of bound but unextracted (B,Ue) and unbound (Ub) AOTP were heated in a thermal oven at constant temperature (140°C) and air flow 85 l/h. Thermal stability of these films and controls (i.e. films containing 0.2% of Tinuvin 770 and Irganox 1076) were observed by measuring their embrittlement time as well as increase in carbonyl area index.

Results in Table 3.10 and Figures 3.20 and 3.21 clearly show that thermal stabilising activity of unbound AOTP, like commercial hindered amine (Tinuvin 770), is much lower than that of its corresponding bound analogue. This is mainly due to its poor substantivity in the films, notably at high temperature. Intrinsic antioxidant activity is not the only factor which determines the effectiveness of an antioxidant as thermal stabiliser, substantivity and solubility of the antioxidant in the polymer is also important(73).

Table 3.10 Thermal stability of PP-films (thickness = 0.1 - 0.2 mm) containing 0.2 % of bound-(B) and unbound-AOTP (Ub) at 140°C, air flow 85 l/h

PP-films containing 0.2% of,	Thermal-embrittlement Time (hours)
PP (unprocessed)	2
Tinuvin 770	15
Irganox 1076	275
AOTP(Ub)	22
TMPTA/AOTP(2:8)(B,Ue)	123
AOTP(B,Ue)	145

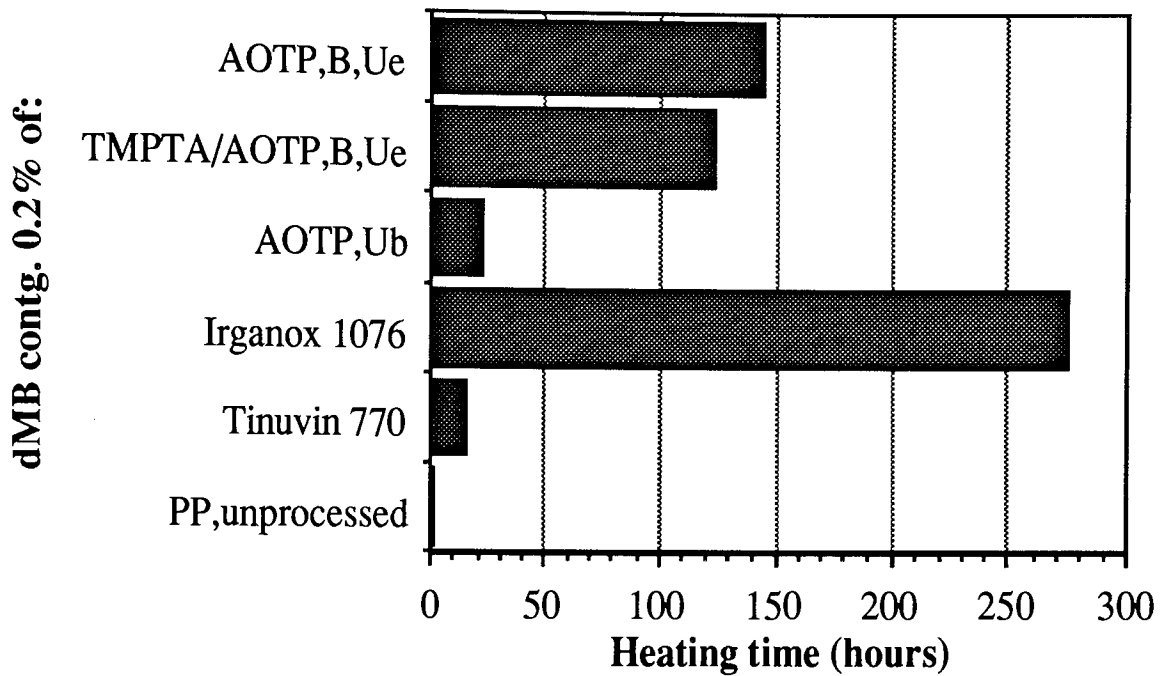


Figure 3.20 Thermal embrittlement time of diluted masterbatch films containing 0.2% of AOTP processed at various conditions with and without TMPTA

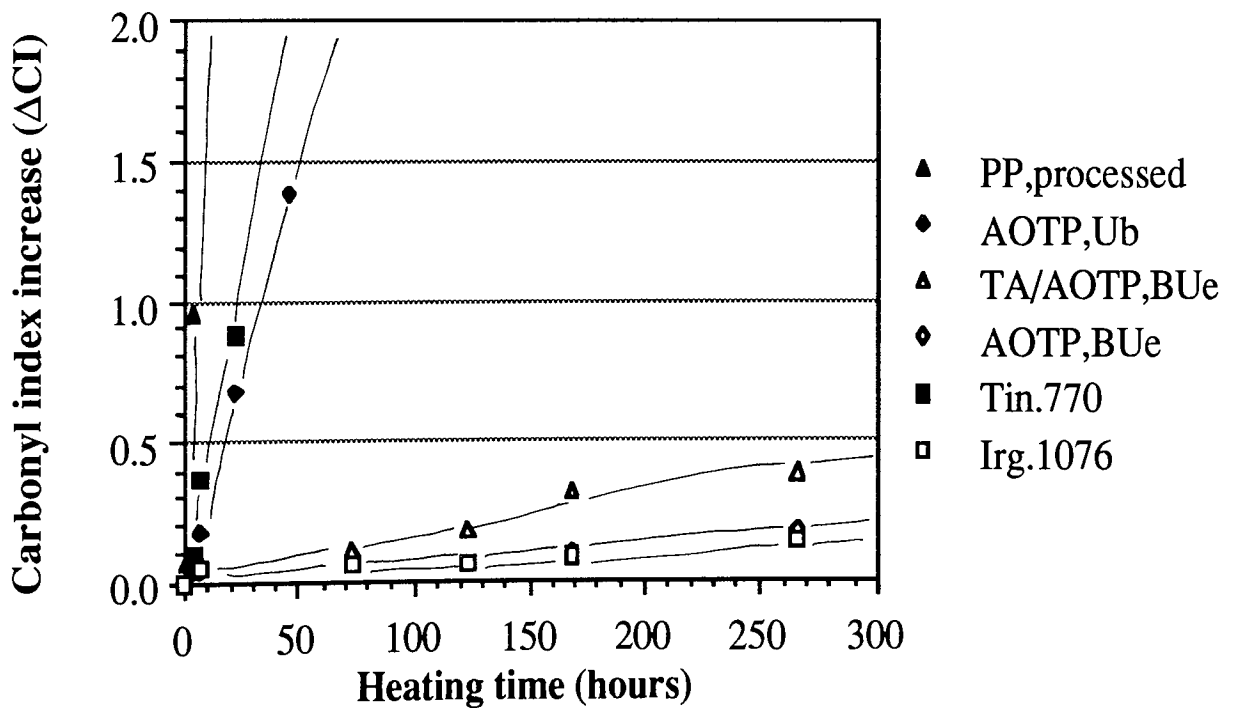


Figure 3.21 Carbonyl index increase during thermal ageing of diluted masterbatch-films containing 0.2% of AOTP processed at various conditions with and without TMPTA

When thermal-stability of diluted masterbatch films containing bound AOTP processed without and with TMPTA were compared, the former exhibited a slightly higher thermal stability (ETs = 145h and 123h, respectively). Two factors may affect the thermal stabilising activity of bound AOTP, i.e. the ease of nitroxyl formation and its substantivity.

3.2.6 Effect of a conventional UV-stabiliser (HOBP) on the stability of polypropylene films containing AOTP

2-Hydroxy 4-octyloxy benzophenone, abbreviated as HOBP, has been used for years as commercial photostabiliser (photo-screen) for polypropylene. This antioxidant has also been reported as a powerful synergist for bound AOTP⁽⁸²⁾. However, the mechanism of the synergistic action is still not clear. To study the synergistic action, effects of HOBP on stabilising activity of polypropylene films containing bound unextracted and extracted AOTP were investigated.

Masterbatches containing 10% AOTP processed without and with TMPTA (ratio 2:8) using Trigonox-101 (2,5-dimethyl 2,5-ditert.butylperoxy hexane) as peroxide (0.005 molar ratio), were diluted down to 0.2%, without extraction, with addition of 0.2% HOBP. Trigonox-101 was used instead of DCP in further processing, since high concentration of DCP may function as photosensitiser for uv-light^(21,23). It was found that the binding level and stabilising activity (Table 3.11 and Figures 3.22 and 3.23) of AOTP processed in the presence of Trigonox-101 0.005 molar ratio without TMPTA (binding = 50%) and with TMPTA (binding = 82%) show no considerable difference when compared to those processed with similar molar ratio of DCP (see Table 3.8). HOBP exhibited a good synergistic action with AOTP processed in the presence and in the absence of TMPTA. Embrittlement times of the unextracted synergistic mixtures (ET=2450h-2720h) were much higher than the total embrittlement times of bound-unextracted AOTP (ET=660h) and HOBP (ET=730h).

Table 3.11 Photostability of diluted masterbatches containing 0.2% of bound unextracted (B,Ue)* AOTP with addition of 0.2% of HOBP.

PP-films containing:	Binding (%)	Embrittlement Time (hours)
AOTP(B,Ue)* + HOBP	--	2450
TMPTA/AOTP(2:8)(B,Ue)* + HOBP	--	2720
AOTP(B,Ue)*	50	630
TMPTA/AOTP(2:8)(B,Ue)*	82	660
HOBP	--	730

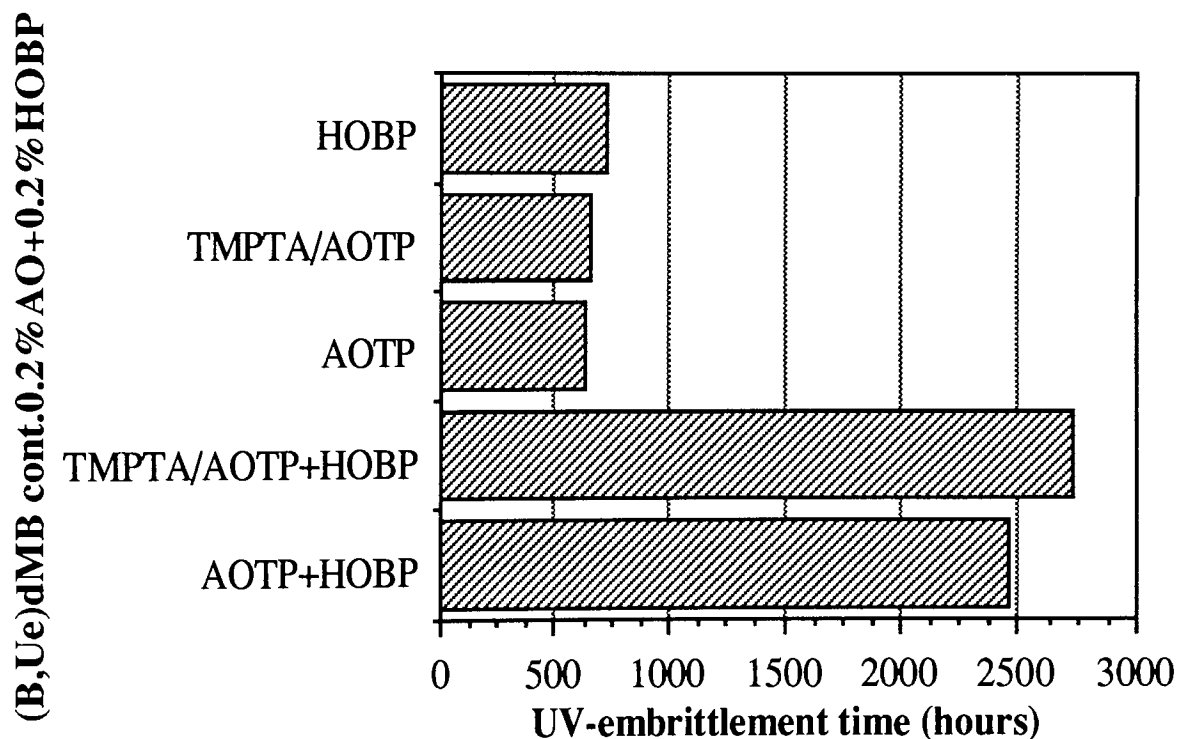


Figure 3.22 ET of uv-irradiated diluted masterbatch-films containing 0.2% AOTP(BUe) with addition of 0.2% HOBP(Ue)

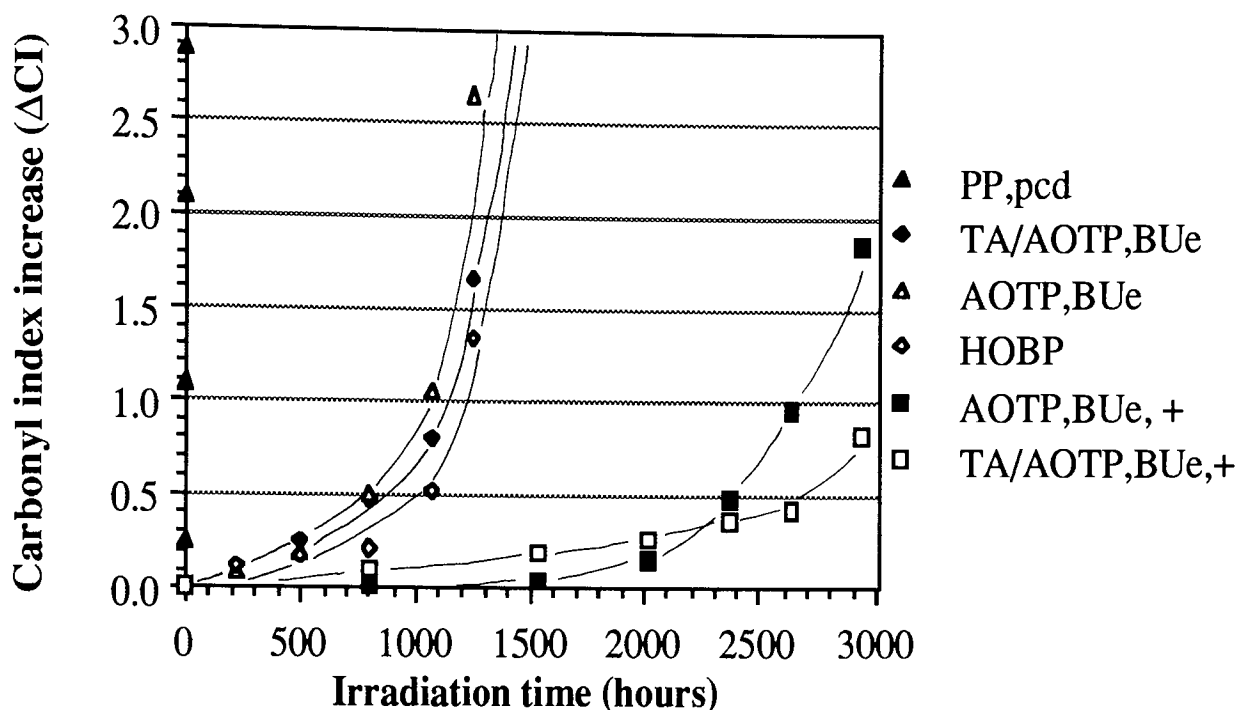


Figure 3.23 Carbonyl index increase of uv-irradiated diluted masterbatch films containing 0.2% AOTP(BUe) with addition of 0.2% HOBP

Effect of HOBP on uv-stabilising activity of diluted and extracted masterbatch films containing 0.2% bound AOTP was further investigated to examine whether there is any effect of the unbound AOTP on the synergistic action. 10% masterbatches of AOTP and TMPTA (ratio 2:8 to AOTP) processed using Trigonox-101 0.005 molar ratio to total additives under standard processing condition, were shredded, exhaustively soxhlet extracted in DCM, vacuum evaporated at room temperature and finally were diluted down to 0.2% AOTP (B,E) with addition of 0.2% of HOBP. Films of these diluted masterbatches were then irradiated in uv-cabinet for uv-stability test. After various irradiation times, the films were again extracted to remove the remaining HOBP and were further uv-irradiated.

Results in Table 3.12 and Figures 3.24 and 3.25 show that embrittlement time of PP film containing bound extracted (B,E) AOTP processed in the presence of Trigonox 101 is similar to that of processed in the presence of DCP, which indicated that after extraction there was no effect of the type of peroxide used on the stability of

the PP films. It was also shown that HOBP also synergises effectively with bound and extracted AOTP (B,E) processed with TMPTA (ET = 1710 h). However, when the HOBP was extracted from the synergistic mixture after various irradiation time, the uv-stabilising activity of the remaining bound AOTP does not exhibit any considerable increase when compared to that of without HOBP. It is clear therefore, that the presence of HOBP throughout the course of stabilisation is necessary for the synergistic action between the AOTP and HOBP.

Table 3.12 Embrittlement time of diluted and extracted masterbatch films containing 0.2% bound AOTP (B,E)*, processed using Trigonox-101 0.005 molar ratio, with addition of 0.2 % HOBP. ** = film extracted after irradiation for 150, 300 and 500 hours following by further irradiation until embrittlement

PP-films containing:	Embrittlement Time (hours)
TMPTA/AOTP(2:8)(B,E)* + HOBP(Ue)	1710
TMPTA/AOTP(2:8)(B,E)* + HOBP(E,150h)**	560
TMPTA/AOTP(2:8)(B,E)* + HOBP(E,300h)**	690
TMPTA/AOTP(2:8)(B,E)* + HOBP(E,500h)**	810
TMPTA/AOTP(2:8)(B,E)*	450
HOBP	730

(BE)dMB cont.0.2%AO+0.2%HOBP

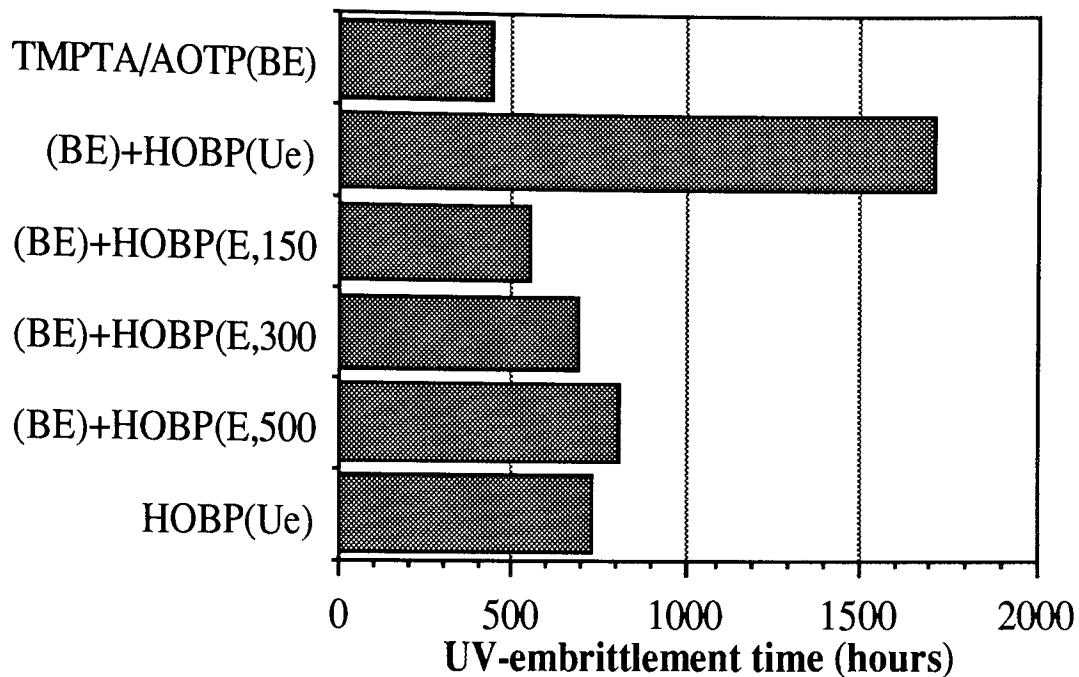


Figure 3.24 ET of uv-irradiated diluted masterbatch-films containing 0.2% of AOTP(BE) with addition of 0.2% HOBP extracted after various irradiation time

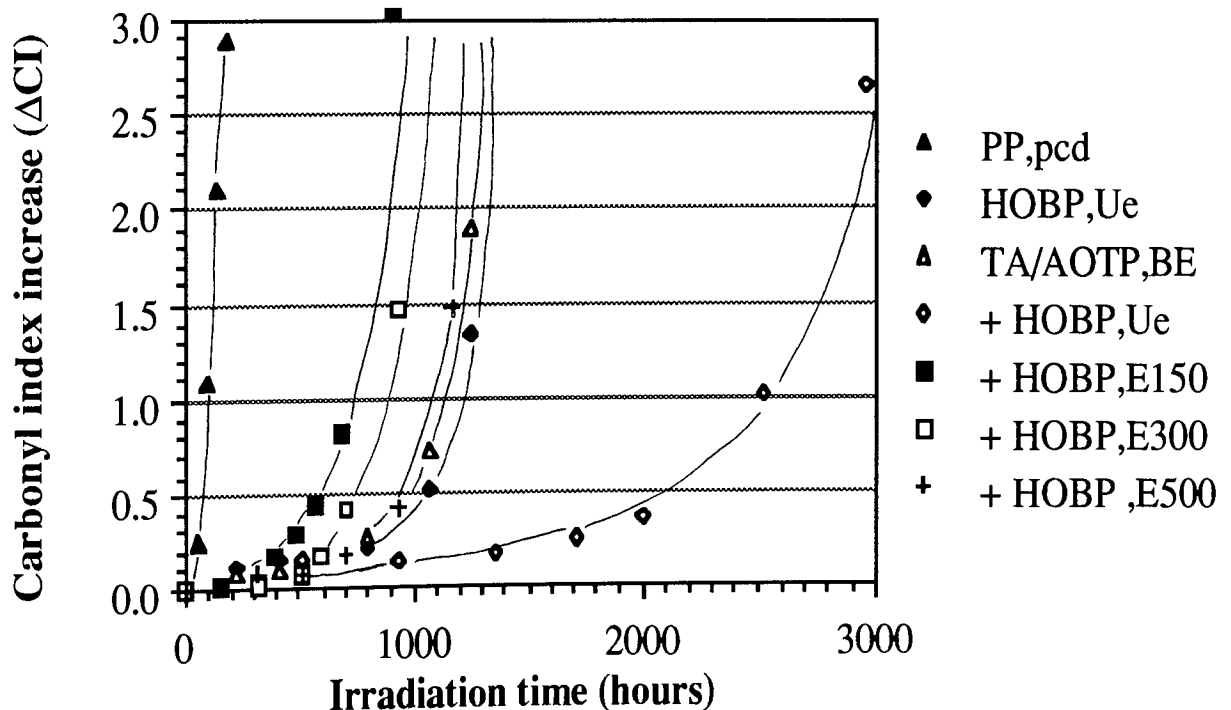


Figure 3.25 Carbonyl index increase of uv-irradiated diluted masterbatch-films containing 0.2% AOTP(BE) with addition of 0.2% HOBP extracted after various irradiation times (150, 300 and 500 hours) and further irradiated to embrittlement

3.3 DISCUSSIONS

3.3.1 Binding efficiency of acrylic nitroxyl precursors using reactive processing technique

Reactive processing of polymer-antioxidant systems involves a competitive reaction between grafting of the antioxidant onto polymer backbone (desired reaction) and homopolymerisation (undesired reaction) of the antioxidant^(97,98). The degree of binding of the antioxidant on the polymer backbone is determined by the ratio of rate of the grafting reaction and the antioxidant homopolymerisation. On the other hand, formation of high molecular weight homopolymer may also decrease solubility of the antioxidant, especially in the case of polyfunctional antioxidant monomers. As the binding of the antioxidant after reactive processing is measured by comparing both antioxidant concentration in the polymer films before and after exhaustive soxhlet extraction in dichloromethane (DCM), the grafted as well as the highly homopolymerised antioxidants, may be unextractable and will be retained in the polymer.

At high antioxidant concentration, more antioxidant molecules will attach onto both grafted and homopolymer backbones. The antioxidant attached onto the backbone became chemically bound, whereas the ones homopolymerised may lower the solubility of the homopolymer (due to greater MWt). Not surprisingly, therefore, that at higher antioxidant concentration, in general, the binding efficiency increases. However, at very high antioxidant concentration (above its solubility) possibility of the homopolymerisation process is higher due to poor distribution of the antioxidant in polymer matrix. Therefore binding efficiency does not increase considerably at higher concentration.

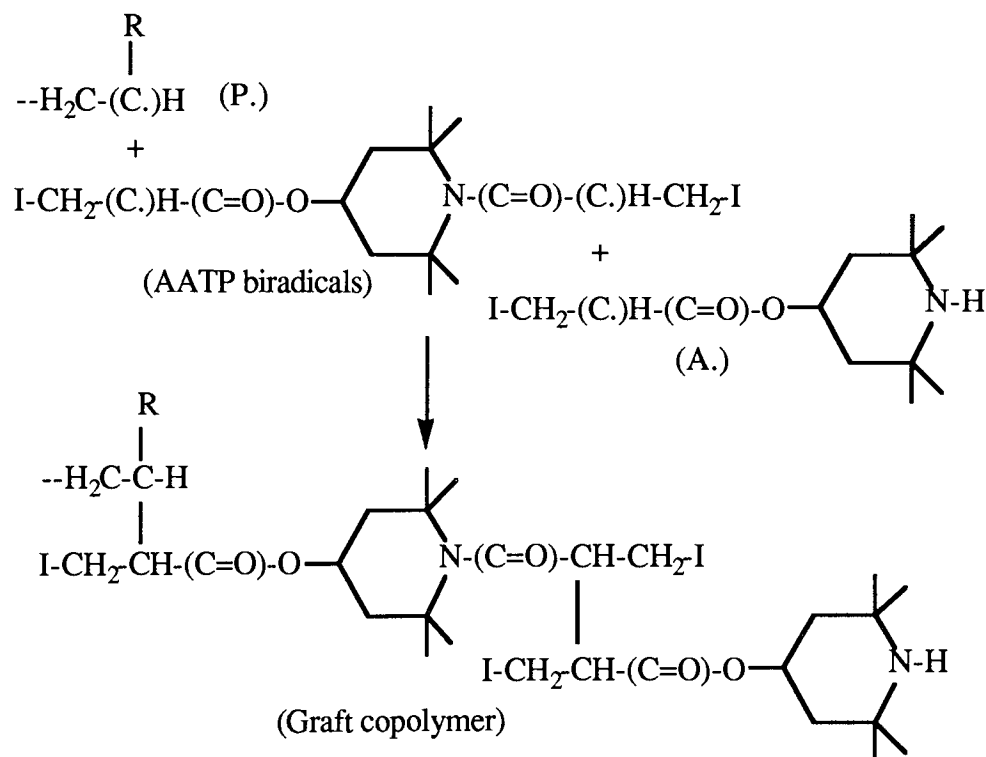
It is clear that the rates of grafting as well as homopolymerisation processes depend on the concentration of the active radicals [R.] along with the antioxidant concentration [A]. It is also well known that formation of these active radicals in the

initiation process is directly affected by the concentration of peroxide as initiator. Thus, higher concentration of peroxide may also increase the antioxidant's binding efficiency. However, reactive processing of masterbatches containing high peroxide concentration may lead to severe degradation of the polymer. This destruction may be in competition with peroxide consumption for grafting and homopolymerisation processes. Antioxidants with high grafting and homopolymerisation activity will consume more peroxide content leaving less peroxide which may destroy the polymer backbone. This may be one of the reasons why the order of the binding efficiency of nitroxyl-precursors are in opposite direction to the order of changes in their MFI. In addition, formation of highly crosslinked bound antioxidant in the polymer may also decrease the MFI.

Acrylic ester nitroxyl-precursors (e.g. MyATP, binding=32%) exhibit higher binding efficiency than the corresponding acrylic amide derivatives (e.g. AMyTP, binding=14%). This result may be explained on the basis of higher reactivity towards radical polymerisation of acrylic ester than the acrylic amide^(84,99). Therefore, in the case of AATP, it is possible that the binding process takes place more favorably on the ester compared to the amide side. MyATP, however, binds to a lesser extent when compared to AOTP, in spite of the fact that both antioxidants have identical acrylic ester groups. This may be due to lower mobility of MyATP (higher molecular weight, because of its myristic amide group) in the polymer matrix. The fact that AOTP has free >N-H but MyATP has >N-(C=O)-R group, which may affect the level of binding of both antioxidants will be investigated in Chapter 4. When both acrylic ester and amide are present in the same compound (such as AATP), the compound shows much higher binding efficiency than the total binding efficiency of monoacrylic ester (MyATP, binding=32%) and the monoacrylic amide (AMyTP, binding=14%) derivatives. Assuming that both acrylic groups of AATP have similar reactivity, reaction probability of acrylic polymerisation not only doubles, but is $N^2 = 4$ times, where N is number of polymerisable (acrylic) groups in the antioxidant. Formation of soluble homopolymer (oligomer) may contribute to the low binding efficiency of monoacrylic,

whereas, the homopolymerised AATP is completely insoluble in the extracting solvent (DCM)(82).

In the presence of acrylics and methacrylic bi- and tri-functional coagents, the binding efficiency of the monoacrylic nitroxyl-precursor, AOTP, can be improved considerably (to more than 80%). The improved binding efficiency can be explained by copolymerisation of the antioxidant and coagent and grafting of the resulting copolymer on the polymer backbone. For instance, the following copolymerisation reaction (reaction 3.1) may take place during a typical reactive processing procedure of AOTP and AATP in the presence of DCP as initiator (I)(100).



3.1

Based on the above assumption (reaction 3.1) at least one AOTP molecule can be grafted per-unit AATP molecule. Therefore, when 8 g of AOTP (=0.0379 mol) was reactively processed in the presence of 2 g of AATP(= 0.0075 mol), mol-ratio of AOTP/AATP is 5 : 1, the percentage of AOTP grafted onto AATP unit is 20% of its total amount in the polymer. This means that the presence of AATP (weight ratio of AATP/AOTP = 2 : 8) may increase the binding efficiency of AOTP up to 20%

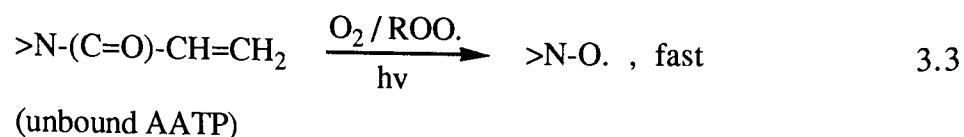
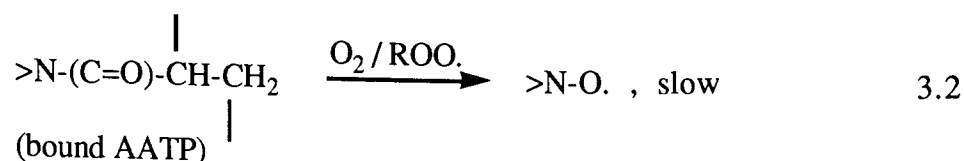
compared to that of without AATP. The fact that the presence of AATP has increased the binding level of AOTP from 50 to 80% (30% increase, see Table 3.5) indicated that more than one AOTP molecule may be grafted per molecule of AATP. On the other hand, the copolymerisation process does not completely eliminate the possibility of formation of soluble AOTP homopolymers. Therefore, 100% binding efficiency of AOTP processed with AATP could not be achieved at low AATP weight ratio to the AOTP, see Table 3.5.

Reactive processing of AOTP using tri-functional coagents, e.g. TMPTA or TMPTM, rather than the bi-functionals, e.g. HDA or BGDM, showed higher binding efficiency, see Table 3.7. It is well known that the possibility of grafting of AOTP onto a tri-functional coagent is greater than onto a bi-functional molecule. Similarly, when 8 g of AOTP (= 0.0379 mol) was reactively processed in the presence of 2 g of TMPTA (= 0.0068 mol), molar ratio of AOTP/TMPTA = 5.6 : 1, the calculated % of AOTP grafted onto TMPTA (assuming that 2 mol of AOTP may grafted per mol TMPTA) is 35%, which means that the presence of TMPTA (weight ratio to AOTP = 2 : 8) may increase binding efficiency of AOTP upto 35%. However, results from Table 3.8 showed increase of binding level of AOTP from 50% (without TMPTA) to 80% (30% increase), which indicated that less than two AOTP molecule may be grafted per unit molecule of TMPTA. Theoretically, maximum (100%) binding efficiency using reactive processing method of monoacrylic derivatives is impossible, unless the homopolymerised antioxidant monomer is unextractable (insoluble).

3.3.2 Effect of reactive processing on stabilising activity of acrylic nitroxyl precursors

Reactive processing procedures have been used extensively for binding of polymerisable antioxidant in saturated hydrocarbon polymer (101,102). The presence of peroxides is intended to initiate chemical reactions between the generated alkyl polymer radicals and the polymerisable antioxidant. However, the peroxide may also initiate thermal and melt degradation of the polymer as well as homopolymerisation of the antioxidant. Consequently, during reactive processing, the antioxidant has been consumed to protect the thermal and melt degradation. Reactive processing of antioxidant in polymer melt, therefore, may sacrifice to some extent of the antioxidant's stabilising capacity. Allen et al.⁽¹⁰³⁾ reported the decrease of uv-stabilising activity of Tinuvin 770 in polypropylene film after reprocessing, compared to that in single processed film.

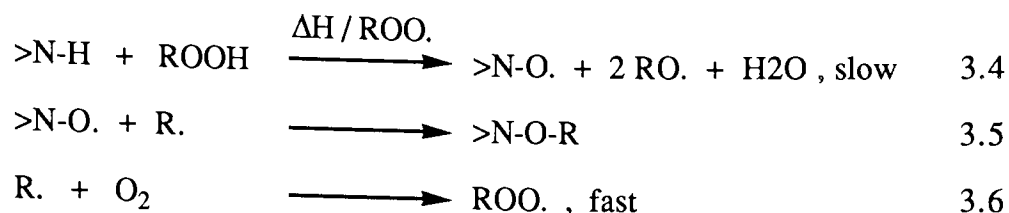
Lower stabilising activity of bound antioxidants when compared to their corresponding unbound antioxidants, see Tables 3.4, 3.5 and 3.7, is presumably due to stabilising action during the reactive processing operation. It has been frequently reported (84,104) that polypropylene films containing polymerised antioxidants exhibit lower uv-embrittlement time than those containing the corresponding unpolymerised antioxidant monomers. The bound and extracted bisacrylic containing antioxidant (AATP, BE) showed larger decrease in its photostabilising activity, compared to the bound and extracted monoacrylic derivative, e.g. AOTP, BE, (ET from 1500 to 500 h). Al-Malaika et al.⁽⁸²⁾ reported that AATP binds effectively through both acrylic ester and acrylic amide sides. It was found from ESR study that nitroxyl generation from the bound and extracted AATP was much slower than from the unbound analogue. Formation of nitroxyl radical from the bound AATP requires a breakage of the saturated amide bond ($>N-CO-R$), whereas the acrylic amide group ($>N-CO-CH=CH_2$) of the unbound AATP may function as photosensitiser, which lowers the activation energy for the photocleavage.



Surprisingly, the bound monoacrylic ester derivative (AOTP) also underwent lower photostabilising activity, in spite of the fact that the bound AOTP is supposed to have free secondary amine (>N-H) group, which could generate the corresponding nitroxyl radical (>N-O.) more easily. Structural changes of stable nitroxyl radical precursors during reactive processing and their possible effect on uv-stabilising activity will be further discussed in Chapter 4.

Reactive processing of AOTP in conjunction with various acrylate and methacrylate coagents had improved its binding efficiency. The photostabilising activity of the improved bound AOTP, however, was also lower than that of the corresponding unbound analogue. When AOTP was bound using bis- or tri-methacrylates coagents, it exhibited higher uv-stabilising activity compared to that of the corresponding analogous processed with acrylic coagents, see Tables 3.7 & 3.8 and Figures 3.12 & 3.15. This may be due to the fact that methacrylate coagents are better radical scavengers than the acrylate coagents^(84,105). Like methacrylates polymers, when the methacrylates coagents bind with antioxidant in a polymer, the bound polymerised coagents may depolymerise during further processing or irradiation⁽¹⁴⁾.

Stable nitroxyl radical precursors have been widely used as photo-antioxidants for polyolefins. However, these compounds have been shown to be ineffective melt and heat stabilisers for the polymers^(51,106). This is attributed to the slow reaction of the nitroxyl precursors (>N-H) with hydroperoxide, which gives rise to the corresponding nitroxyl radicals (>N-O.). Consequently, the antioxidants cannot compete effectively with oxygen for the macroalkyl radicals

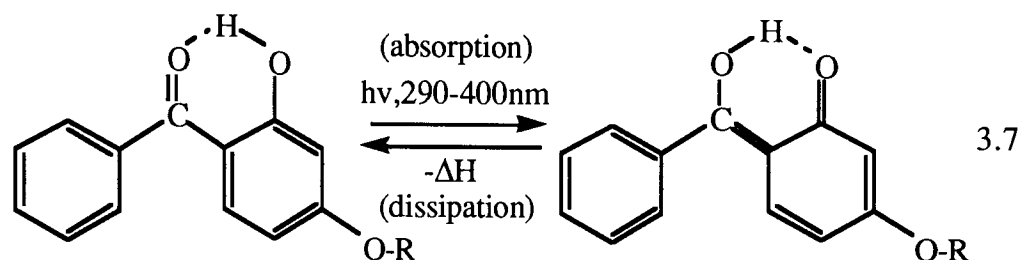


On the other hand, it has been reported⁽¹⁰⁷⁾ that commercial monomeric and polymeric hindered amines do inhibit to some extent the thermal degradation of polyolefins. Pre-heated polymer films containing the hindered amines were shown to even exhibit an improved photostabilising activity.

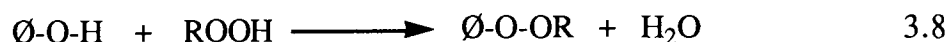
There are two factors affecting the thermal stabilising behaviour of the nitroxyl precursors, firstly, the ease of nitroxyl formation. In this case, the monomeric and unbound nitroxyl precursors oxidise faster to form the corresponding nitroxyl radicals^(82,107) than the polymeric or bound analogues. The second factor is the permanence (substantivity) of the nitroxyl precursors in the polymer, especially at high temperature up to 140°C, in which the polymerised and bound antioxidants are more substantive. As shown in Table 3.10, therefore, the unbound AOTP, like the commercial antioxidant (e.g. Tinuvin 770) showed lower thermal stabilising activity than the bound AOTP. Whereas, the bound unextracted AOTP processed without TMPTA (binding efficiency = 50%) exhibited slightly higher thermal stabilising activity than the one processed with TMPTA (binding = 80%).

3.3.3 Synergistic behaviour of AOTP with HOBP

2-Hydroxy 4-octyloxy benzophenone (HOBP = Cyasorb UV531) is one of the earliest uv-screen used for stabilisation of polyolefins. The uv-screening action is reported^(30,108) due to keto-enol tautomerism of the hydroxy benzophenone, which absorbs uv-light from 290 - 400 nm and dissipates the radiation into thermal energy, as has been shown in Section 1.8.

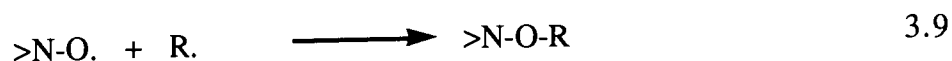
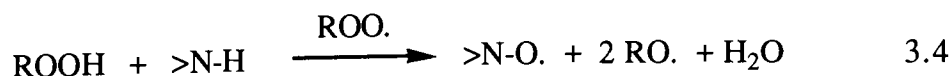


Moreover, Chakraborty and Scott^(33,109) reported that HOBP may function as a radical scavenger for alkoxy radicals and this, in turn, is responsible for the destruction of the HOBP. The nature of this process is still unclear, but it was suggested⁽¹¹⁰⁾ that this involves hydrogen abstraction from the HOBP.



(HOBP)

When the HOBP is applied in conjunction with nitroxyl precursors as radical scavengers, the latter may inhibit the destruction of the uv-screen, which in turn increases the stabilising activity of the system synergistically.



This type of synergistic mechanism is well known, as has been reviewed in Section 1.4. Work by Al-Malaika et.al⁽⁸²⁾ showed that HOBP synergised effectively with bound AATP. It was suggested that in the presence of HOBP, the uv-stabiliser would be able to protect the early stage of polymer degradation until enough nitroxyl radical

concentration is produced from the bound AOTP, which can regeneratively protect the further degradation.

In this work, HOBP was also found to synergise with bound unextracted and extracted AOTP to high extent, see Tables 3.11 and 3.12. However, when the HOBP was removed from the polymer films after various irradiation times, the remaining bound AOTP could not protect the polymer degradation any further. It is known that uv-light is the main factor which triggers the formation of alkyl radicals during photodegradation of polymer. In the presence of a uv-screen, dissipation of the radiation energy may lower the alkyl radical concentration. Therefore, low concentration of nitroxyl radical is sufficient to perform as the alkyl radical scavenger. When the HOBP was removed from the polymer film, the rate of photoreaction to form the alkyl radical becomes faster. Thus, slow production of nitroxyl radical from the bound antioxidant cannot inhibit the oxidation of alkyl radical to form alkyl peroxy radicals and other oxidation products.

As it has been reported, HOBP is a well known uv-screen, whereas AOTP like any other nitroxyl precursors, is mainly chain breaking antioxidant⁽¹¹¹⁾. This results suggests that the effective synergistic action between bound AOTP and HOBP may be due to the complementary action of AOTP as chain breaking antioxidant and HOBP as uv-screen. When the HOBP was removed from the synergistic mixture, therefore, the system may lose its complementary synergistic action. Synergistic mixture of bound-AOTP and bound-HOBP, which improves its resistivity in the polymer, is recommended for further work.

CHAPTER 4

ANALYSIS OF MASTERBATCHES CONTAINING ACRYLIC NITROXYL PRECURSORS AND CHEMISTRY OF MODEL REACTIONS

4.1 OBJECTS AND METHODOLOGY

It was shown in Chapter-3 that acrylic containing nitroxyl precursors are good photo-antioxidants in polypropylene when used as conventional additives, i.e. processed in the absence of peroxide, see Table 3.4. However, when they were bound (processed in the presence of peroxide) and extracted, their antioxidant activities decreased. Moreover, inspite of the very high binding efficiency of the bisacrylic antioxidant (AATP), its photostabilising activity was even lower than the corresponding bound monoacrylic analogues.

When polypropylene was processed at 180°C in a torque-rheometer under closed mixing condition for 10 minutes, the torque (which represents the change in melt viscosity) decreased sharply in the first few seconds due to melting of the solid polymer. The torque continued to decrease steadily and finally levels off at a constant value at the end of processing. In the presence of a peroxide the decrease in torque was even lower, which may be due to chain scission initiated by the peroxide^(5,6). In the reactive processing of polypropylene containing 10% AATP in the presence of DCP 0.005 molar ratio, it was found that the torque increased to a maximum value after around 3 minutes processing before leveling down to a constant value, see Figure 4.1, which was also observed by previous workers⁽⁸²⁾. This maximum, which indicates crosslinking, was even higher in the case of masterbatch containing higher AATP concentration (20%). Torque records of masterbatches containing AOTP, on the other hand (see Figure 4.2) showed only a small maximum after 3 minutes processing.

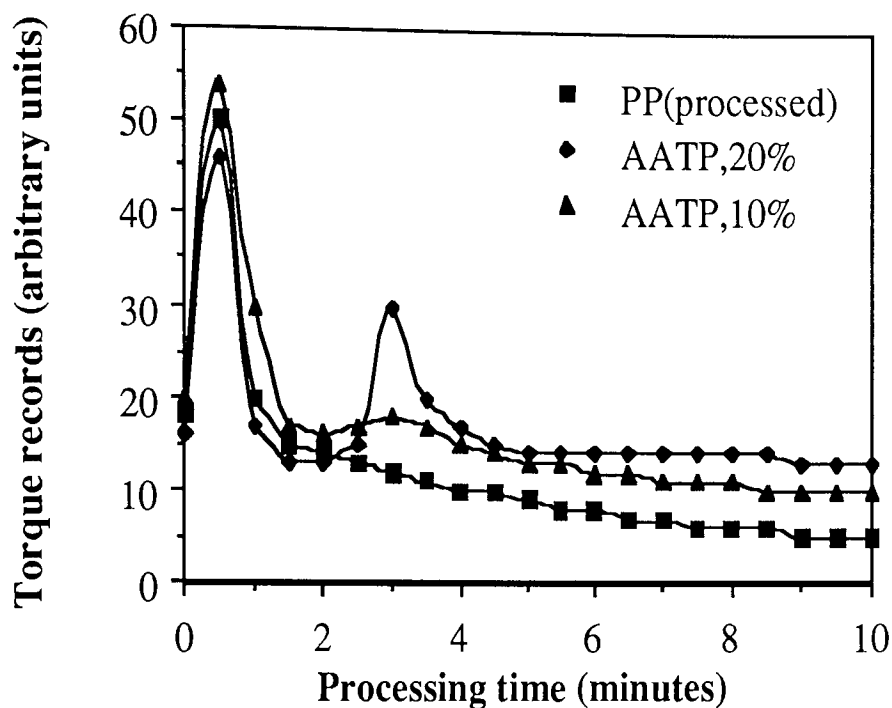


Figure 4.1 Torque records of masterbatches containing 10 and 20% of AATP during reactive processing at standard condition, in the presence of DCP 0.005 molar ratio

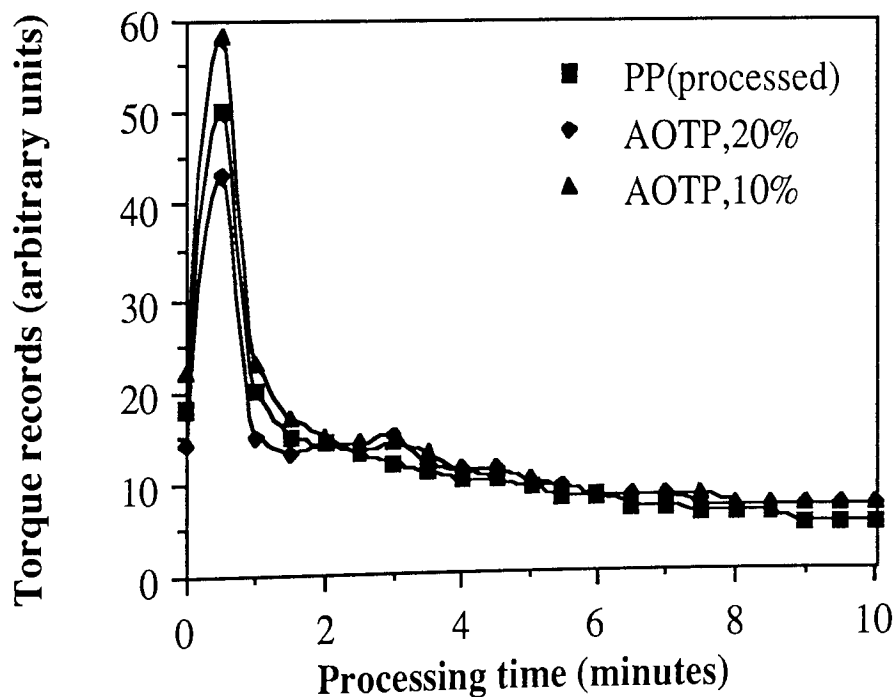
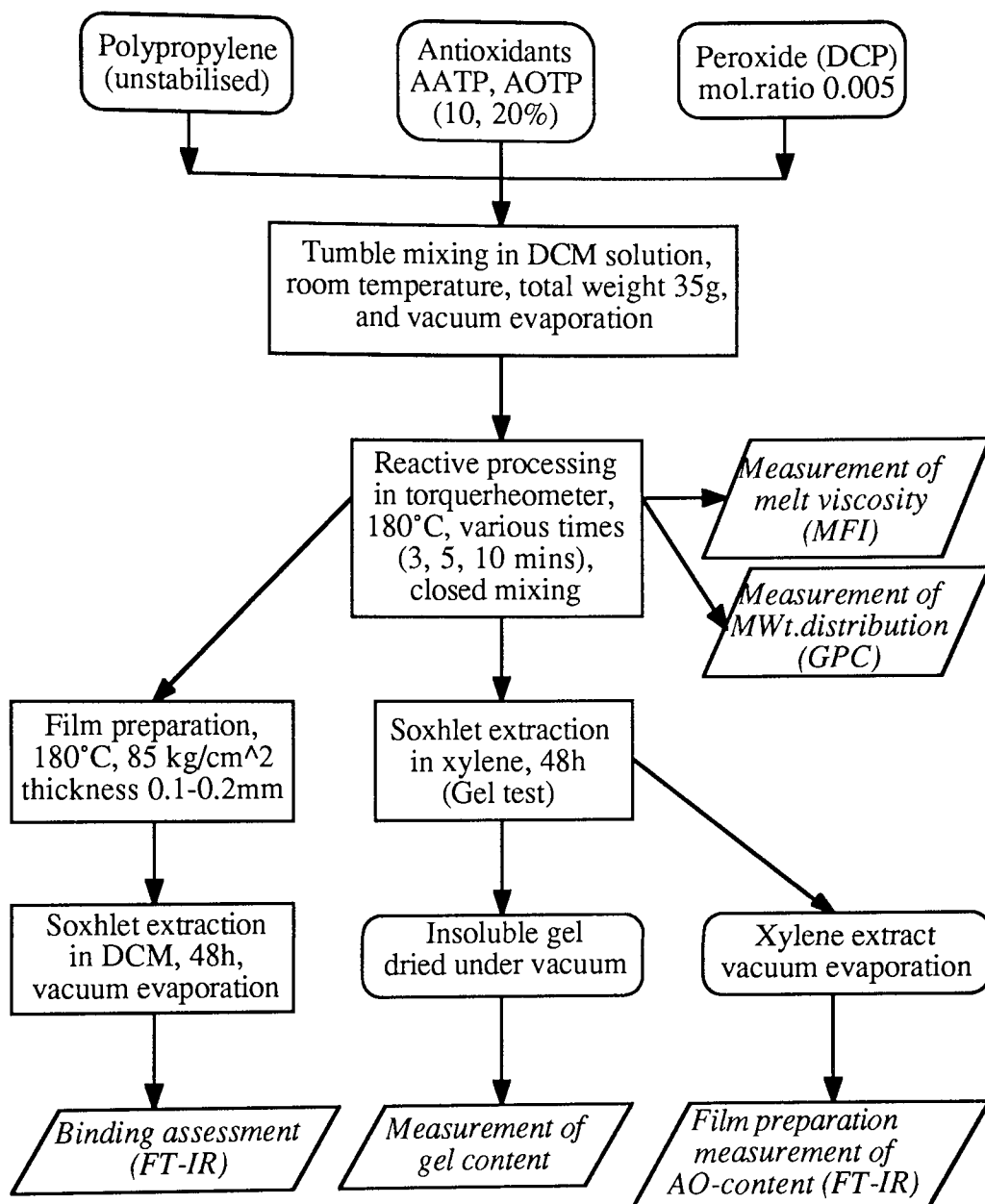


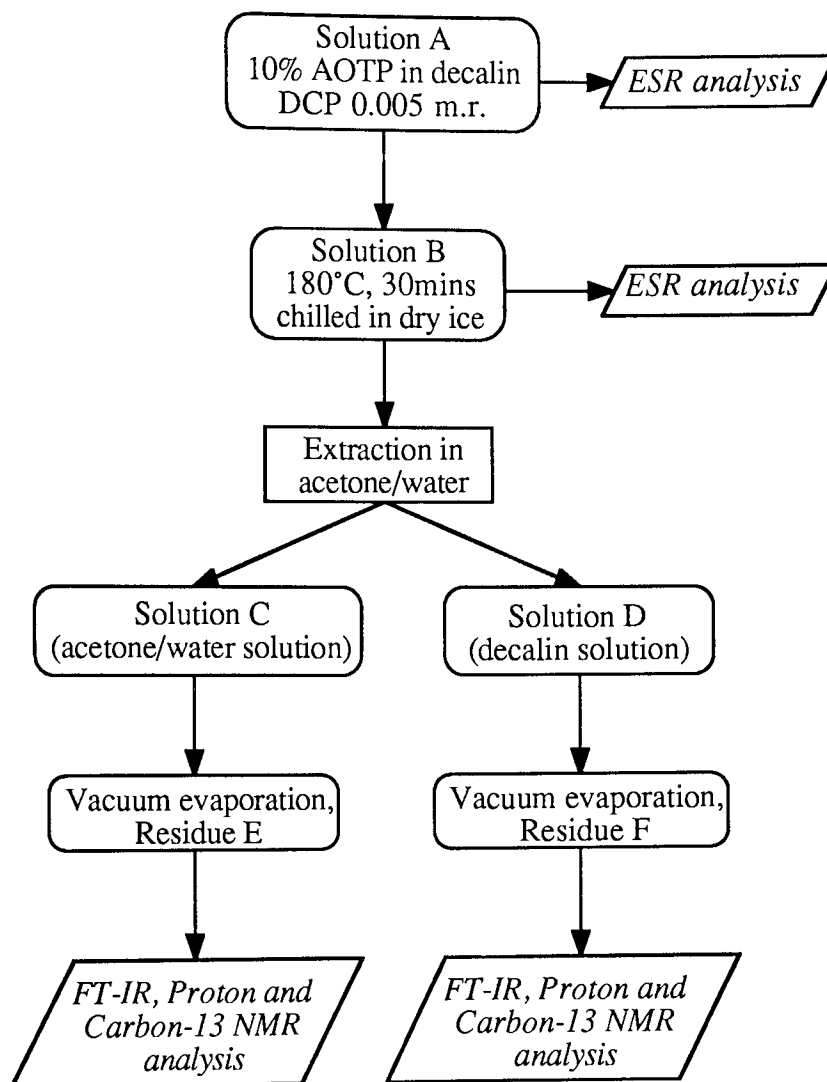
Figure 4.2 Torque records of masterbatches containing 10 and 20% of AOTP during reactive processing at standard condition, in the presence of DCP 0.005 molar ratio

In the first part of the work described in this chapter, masterbatches containing various concentrations of bisacrylic (AATP) and monoacrylic (AOTP) nitroxyl precursors were analysed using physical and spectroscopic methods. To examine the degree of crosslinking in the AATP and AOTP masterbatches, various samples were reactively processed for different times (3, 5 and 10 minutes) in the presence of DCP 0.005 molar ratio at 180°C in closed mixing condition. Melt flow index (MFI) and molecular weight distribution (MWD) of the masterbatches as well as the binding level of the antioxidants were measured. A correct amount of around 5 g of the shredded masterbatches were then separately Soxhlet extracted in xylene (b.p. 135°C) for 48 hours under argon atmosphere. Residues and the extracts were dried under vacuum at 40°C for constant weight for gel content measurement and their films were further analysed using FTIR for antioxidant contents, see Scheme 4.1 for schematic procedure of the analysis. Possibility of physical and chemical changes of the bound antioxidant during processing both in the gel and soluble fractions of the masterbatches, which may affect their stabilising activity was investigated.

The second part deals with simulation of the reactive processing procedure of the nitroxyl precursors in liquid hydrocarbons as model compounds for polyolefins. Solution of 10% AOTP in decalin (decahydronaphthalene, b.p. 190°C), i.e. Solution-A, was polymerised at 180°C in a constant temperature oil bath under argon atmosphere in the presence of DCP 0.005 molar ratio. After 30 minutes, the reaction mixture in decalin (Solution B) was chilled instantly in dry ice-acetone, the unreacted AOTP was then washed in acetone-water (1:1). Both acetone-water extract (Solution C) and extracted decalin solution (Solution D) were vacuum evaporated to constant weight at room temperature and 40°C, respectively. Residues from acetone-water extract (Residue E) and from extracted decalin solution (Residue F) were analysed using FTIR and Proton & Carbon-13 NMR spectroscopy and their spectra were compared to that of fresh AOTP. The schematic diagram of the polymerisation procedure is shown in Scheme 4.2. Controls for the AOTP polymerisation in the presence or in the absence of peroxide without liquid hydrocarbon were also carried out.



Scheme 4.1 Schematic procedure of analysis of masterbatches containing 10 and 20% of AATP or AOTP processed in the presence of DCP 0.005 molar ratio at standard condition



Scheme 4.2 Schematic procedure of AOTP polymerisation in decalin in the presence of DCP 0.005 molar ratio at 180°C for 30 minutes under argon atmosphere

4.2 RESULTS

4.2.1 Analysis of masterbatches containing AATP or AOTP

4.2.1.1 Analysis of insoluble-crosslinked contents and antioxidant concentrations in the masterbatches

Results of insoluble content (measured after exhaustive Soxhlet extraction in xylene) as well as melt flow index (MFI, measured in a melt flow indexer using large die, $\varnothing = 0.2096$ cm, due to some of the sample's low MFI) of masterbatches containing different concentrations of AATP or AOTP processed at various times are shown in Table 4.1, see Scheme 4.1 for experimental procedure. It is clearly shown that masterbatches containing AOTP do not show any xylene insoluble content even at higher antioxidant concentration (20%). Supports this evidence whereby the torque only exhibits a very small maximum after 3 minutes processing. Furthermore, the melt flow index of these masterbatches give much higher values when compared to analogues AATP masterbatches.

The white insoluble crosslinked material produced from AATP masterbatches were hard, an attempt to compression mould it to form polymer films was unsuccessful. Unfortunately, therefore AATP content in the insoluble masterbatches cannot be measured directly using FTIR spectroscopy. Evaporated residues of the xylene extract of the masterbatches, see Scheme 4.1, on the other hand, were entirely polymeric material, and the corresponding films can be easily prepared. Using calibration curve of AATP masterbatches obtained empirically, which follows a linear equation :

$$C = 2.47 CI - 0.11 \quad 4.1$$

where, C is antioxidant concentration (%w/w) and CI is carbonyl area index, concentration of AATP in the soluble masterbatches can be measured. AATP content in the insoluble masterbatches was then calculated by subtraction of AATP content in

soluble fraction from total AATP concentration in fresh masterbatches (10% or 20%). Compositions of AATP and PP both in insoluble and soluble fractions of the AATP masterbatches are shown in Table 4.2.

Table 4.1 Insoluble content (%) and MFI (g/10 mins, *measured using large die $\varnothing = 0.2096$ cm) of masterbatches containing different concentrations of AATP or AOTP, processed at 180°C and various processing times in the presence of DCP 0.005 molar ratio, **DCP content in PP equivalent to DCP 0.005 molar ratio of 10% AATP masterbatch

Masterbatch containing :	Processing time (minutes)	Insoluble content (%)	M.F.I.* (g/10min)
AATP, 20%	3	27	0.0
	5	22	0.5
	10	3	3.2
AATP, 10%	3	25	0.1
	5	20	2.8
	10	2	8.0
AOTP, 20%	2.5	0	5.4
	5	0	32.1
	10	0	57.1
AOTP, 10%	2.5	0	39.8
	5	0	38.0
	10	0	51.7
PP (processed)	10	0	29.1
PP + DCP**	10	0	87.7

Table 4.2 Composition of AATP (%) and PP (%) both in the soluble and insoluble fractions of masterbatches containing 10 or 20% of AATP processed in the presence of DCP 0.005 molar ratio at various times at standard condition

Masterbatch containing :	Processing Time (mins)	Insoluble fraction		Soluble fraction	
		AATP (%)	PP (%)	AATP (%)	PP (%)
AATP, 20%	3	19.7	7.3	0.4	72.6
	5	17	5	3	75
	10	2	1	18	79
AATP, 10%	3	9.3	15.7	0.8	74.2
	5	6	14	4	76
	10	0.9	1.1	8.8	89.2

As shown in Table 4.2, for both masterbatches containing 10% and 20% AATP processed at 3 minutes, after extraction in xylene the AATP concentration in the soluble fractions are very low (less than 1%). This means that at the beginning of the reactive processing, almost the entire AATP had been crosslinked to form xylene insoluble residue. The crosslinking formation is also clearly shown by the high maximum torque during 3 minute processing time, see Figure 4.1. In addition, FTIR spectra of masterbatch films containing 10% AATP, Figure 4.3, indicates total disappearance of unsaturation peak at 1617 cm^{-1} , suggesting that even within 3 minute processing both acrylic groups of AATP had completely reacted.

When the reactive processing went on to 10 minutes, the AATP content in the soluble parts of both masterbatches containing 10% and 20% AATP become higher (upto 9% and 18.5%, respectively), approaching the original AATP concentrations in the fresh masterbatches. The fact that even the xylene-soluble bound AATP is unextractable in DCM (binding efficiency 100%, see Table 3.2, Chapter 3), suggests that the AATP molecules may be still partially crosslinked or grafted onto the polymer

matrix.

As shown in Figure 4.4, FTIR spectrum of masterbatch-film containing 10% of AOTP processed with peroxide exhibited low absorption of unsaturation at 1608 cm^{-1} , which indicates that during reactive processing the majority of AOTP has been polymerised or grafted. When the reactively processed masterbatch was Soxhlet-extracted in DCM, however, it was found that the FTIR spectra of evaporated DCM-extract (Figure 4.5) clearly indicates the decrease of the unsaturation peak at 1610 cm^{-1} when compared to that of fresh AOTP. Spectra of Figure 4.5 also shows that the carbonyl peak of extracted AOTP (---, dashed line) has shifted to higher wave number (absorption maximum from 1704 to 1735 cm^{-1}), which is almost certainly due to formation of saturated acrylic group of the polymerised or grafted AOTP.

AOTP monomer was then polymerised without solvent at 180°C under Argon gas atmosphere for 30 minutes in the presence of DCP 0.005 molar ratio. The solubility of the AOTP polymer was tested in DCM as well as in hexane. It was found that even at room temperature the entire homopolymer product of AOTP was soluble in DCM, but only partially soluble in hexane. This suggests that the DCM-extract of AOTP-masterbatches contains both fresh unreacted as well as homopolymerised AOTP.

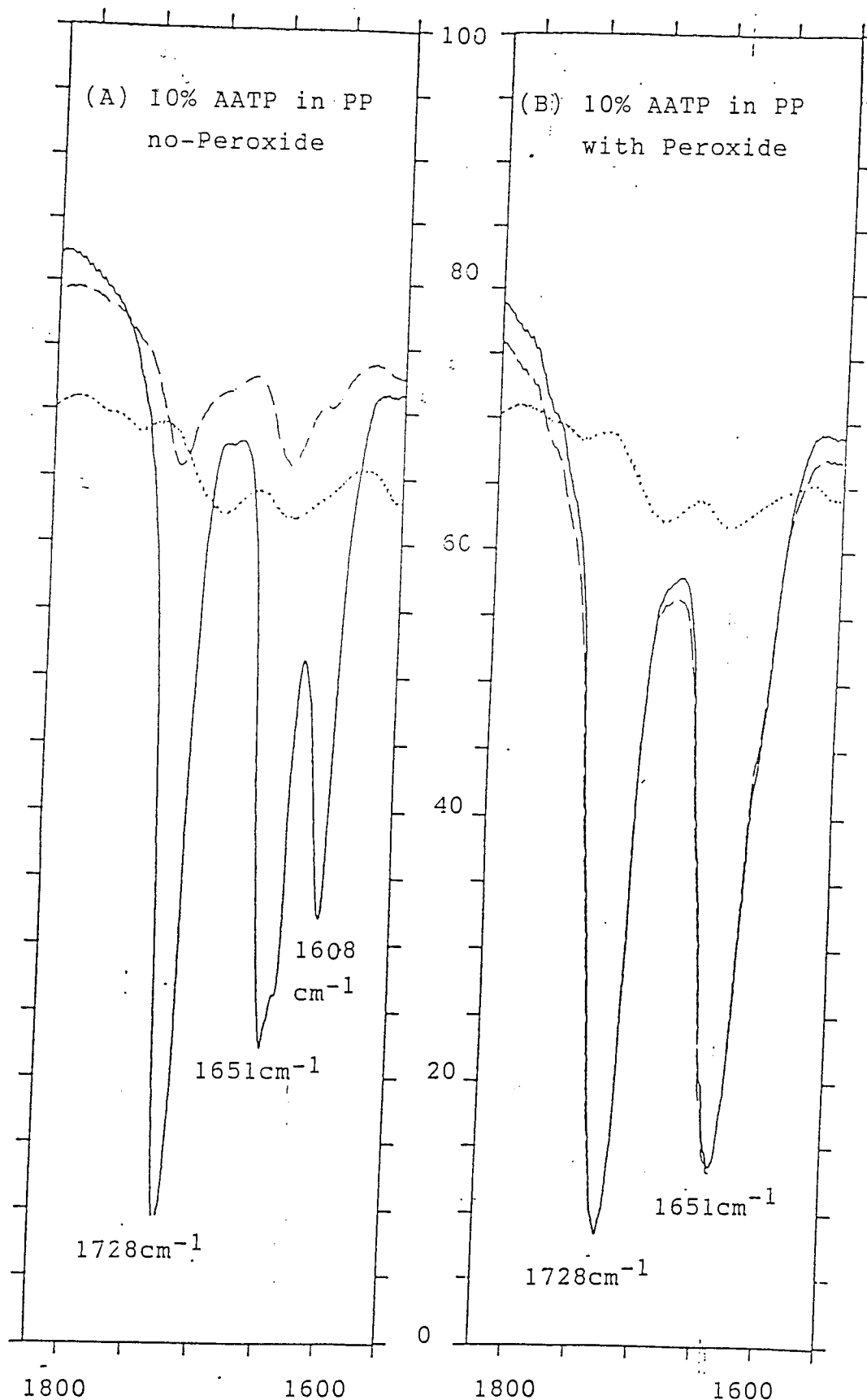


Figure 4.3 FTIR spectra (absorption window at 1850 to 1550 cm^{-1}) of masterbatch films containing 10% AATP processed for 10 minutes without peroxide (A) and processed for 3 minutes with DCP 0.005 molar ratio at standard condition (B), before (—) and after exhaustive Soxhlet extraction in DCM (- - - -), compared to that of polypropylene film (· · · ·)

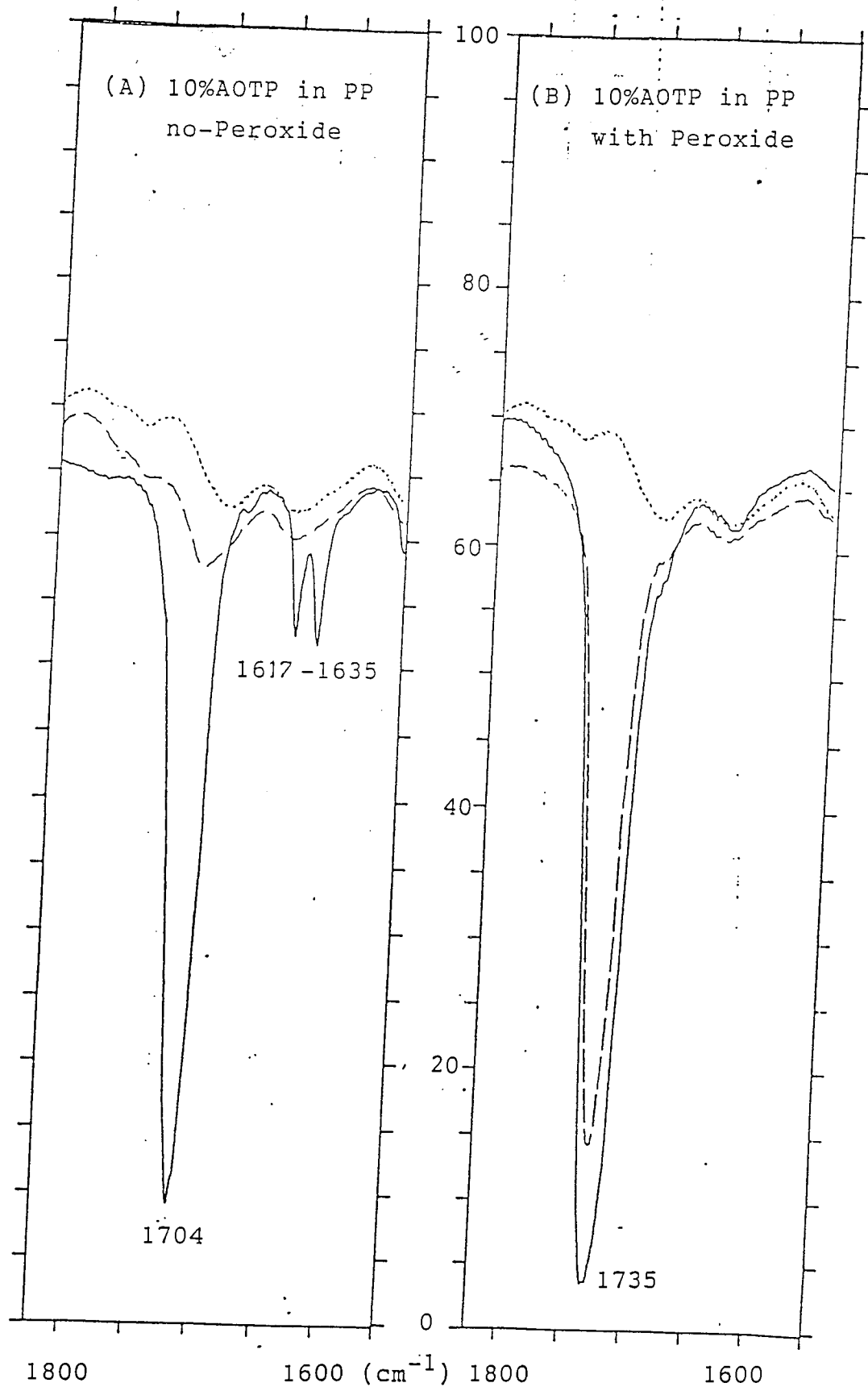


Figure 4.4 FTIR spectra (window in region $1900 - 1550 \text{ cm}^{-1}$) of masterbatch films containing 10% of AOTP processed at 180°C in closed mixing condition without peroxide for 10 minutes (A) and with peroxide (DCP 0.005 molar ratio) for 3 minutes (B), before extraction (—) and after exhaustive Soxhlet extraction in DCM (----) compared to that of PP film (.....)

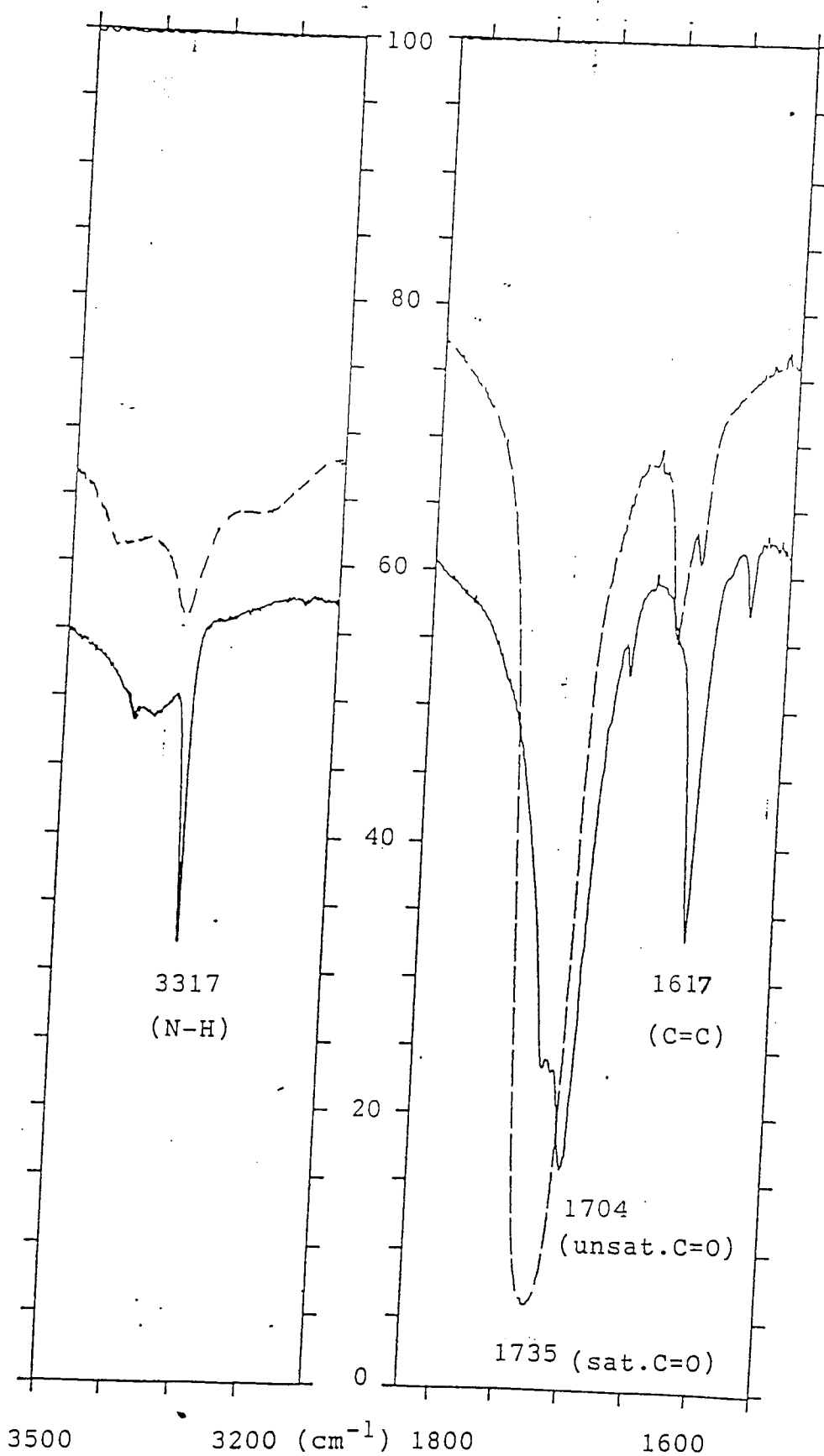


Figure 4.5 FTIR spectra (in KBr disc, 3650 - 3050 cm^{-1} and 1900 - 1550 cm^{-1}) of evaporated DCM extract of masterbatch film containing 10% of AOTP processed at 180°C in closed mixing condition in the presence of DCP 0.005 molar ratio (-----) compared to that of fresh AOTP (—)

4.2.1.2 Molecular weight distribution (MWD) data of masterbatches containing AATP or AOTP

Measurement of molecular weight distribution of reactively processed masterbatches containing AATP and AOTP was carried out by RAPRA Technology Ltd. Around 0.1 g of polymer samples were dissolved in 10 ml of gently boiled o-dichlorobenzene. The hot solution was then filtered and injected into GPC-column at 150 - 170°C (see Section 2.4.4 for full experimental procedure). Table 4.3 shows MWD data of AATP and AOTP masterbatches processed at various times. Repetition of the measurement showed good reproducibility of the results. It is clearly shown that the MWD curves of masterbatches containing 10% of AATP and AOTP processed at 10 minutes are shifted towards lower MWt-values from that of fresh (unprocessed) polypropylene (see Figure 4.6). Number average molecular weights (M_n) of these masterbatches shown in Table 4.3 are also lower than that of fresh-PP (but not as low as PP processed with DCP) in the order of :

Fresh-PP > AATP masterbatches > AOTP masterbatches > (PP + DCP)

This may be due to chain scission of the polypropylene when processed in the presence of peroxide, whereas the presence of AOTP and AATP may reduce the extent of chain scission by consuming some of the peroxide for the grafting reaction. In addition, formation of grafted (bound) antioxidant onto the PP backbone especially in the case of AATP may also contribute to the higher M_n of the AATP masterbatches.

Table 4.3 Molecular weight distribution (MWD) data of masterbatches containing different concentrations of AATP or AOTP, processed without and with TMPTA in the presence of DCP (molar ratio = 0.005) at 180°C in closed mixing condition at various times

Polymer sample (masterbatches)	Processing time (mins)	Binding (%)	\overline{Mn} (10^4) of,		% of high MWt component
			low MWt	high MWt	
PP-unprocessed	10	--	3.28	--	--
PP + DCP	10	--	1.95	--	--
AATP,20%	3	98	2.83	--	--
	5	100	2.75	--	--
	10	100	2.82	--	--
AATP,10%	3	96	2.77	--	--
	5	98	2.67	--	--
	10	97	2.76	--	--
AOTP,20%	2.5	53	2.50	584	5.8
	5	55	2.00	671	10.9
	10	59	1.98	853	16.0
AOTP,10%	2.5	37	3.62	--	--
	5	49	2.70	110	6.5
	10	50	2.02	521	13.4
AATP/AOTP,10%(2:8)	10	70	2.95	698	4.9
AATP/AOTP,10%(4:6)	10	90	2.14	--	--
TMPTA/AOTP,10%(1:9)	10	64	1.86	740	10.7
TMPTA/AOTP,10%(2:8)	10	80	2.85	773	9.2
TMPTA/AOTP,10%(3:7)	10	86	2.60	707	4.8
TMPTA/AOTP,10%(4:6)	10	90	2.97	446	3.6
TMPTA,4%	10	100	1.94	--	--

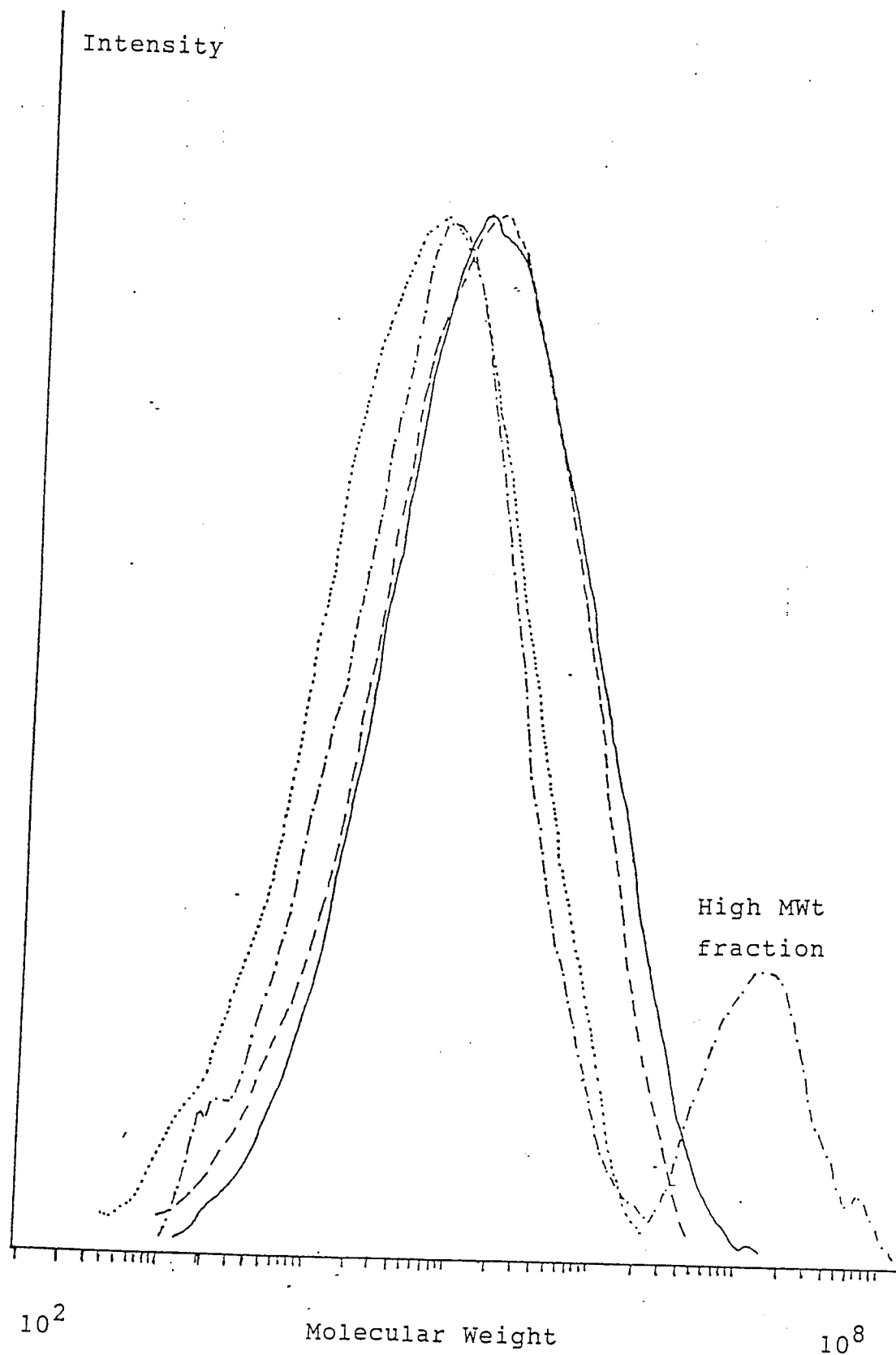


Figure 4.6 Molecular weight distribution curves of masterbatches containing 10% of AATP (- - - -) and AOTP (- · - · - ·) processed with DCP 0.005 molar ratio, compared to those of PP processed with similar amount of DCP (· · · · ·) and fresh (unprocessed) PP (—)

Interestingly, it is clear from Table 4.3 and Figure 4.6, that all masterbatches containing AOTP showed an additional peak exhibiting high MWt. Both low and high MWt peaks were then separately calibrated using polystyrene standard for MWD data. It was found that the Mn of the high MWt peaks is around 50 - 200 times higher than that of the corresponding low MWt peaks. This evidence indicates that the high MWt component of AOTP masterbatches may contain grafted and crosslinked structures, which are still soluble in polymer solvents (e.g. o-dichlorobenzene and xylene). When the percentages of the high MWt components were calculated, from the ratio of peak areas, the values varied from 5 - 16% at various processing time and becomes higher as the processing time increases to 10 minutes, see Table 4.3.

An attempt has been carried out to separate the high MWt component from the masterbatches. 5 g of masterbatches containing 10% AOTP was exhaustively soxhlet extracted in DCM to remove the remaining unbound antioxidant. The masterbatches was further extracted in toluene (b.p. 110°C) for 40 hours (Toluene-extract). Finally, the remaining residue was extracted in xylene (b.p. 135°C), which was completely soluble in the xylene (Xylene-extract). Both extract fractions were vacuum evaporated at room temperature to constant weight, and were then analysed using GPC for MWD data and FTIR for the concentration of bound AOTP in each extracts and compared to that of original AOTP masterbatch.

As shown in Table 4.4 and Figure 4.7, the Toluene-extract contains only less than 1.5% of high MWt component. Whilst the Xylene-extract has both low and high MWt components. Percentage of the high MWt component in Xylene-extract (18%), on the other hand, is higher than that of fresh AOTP masterbatch (13%). From FTIR analysis, it was found that AOTP concentration in Xylene-extract (2.1%) is less than those of fresh AOTP masterbatch (5%) and Toluene-extract (6.8%), see Table 4.4. This suggests that in the original fresh AOTP masterbatch, more bound AOTP is present in the low MWt component, which may be grafted onto the PP backbone.

Table 4.4 Concentration of bound-AOTP and MWD data of fractions obtained by extraction in toluene and in xylene from original masterbatch containing 10% of AOTP

Extract fractions of AOTP-MB.	Conc.(%) of bound-AOTP	Mn(10^4) of,		% of High-MW component
		Low-MW	High-MW	
Toluene-extract	6.8	1.37	631	1.5
Xylene-extract	2.1	2.54	1130	18.2
Original AOTP-MB	5.0	2.02	521	13.4

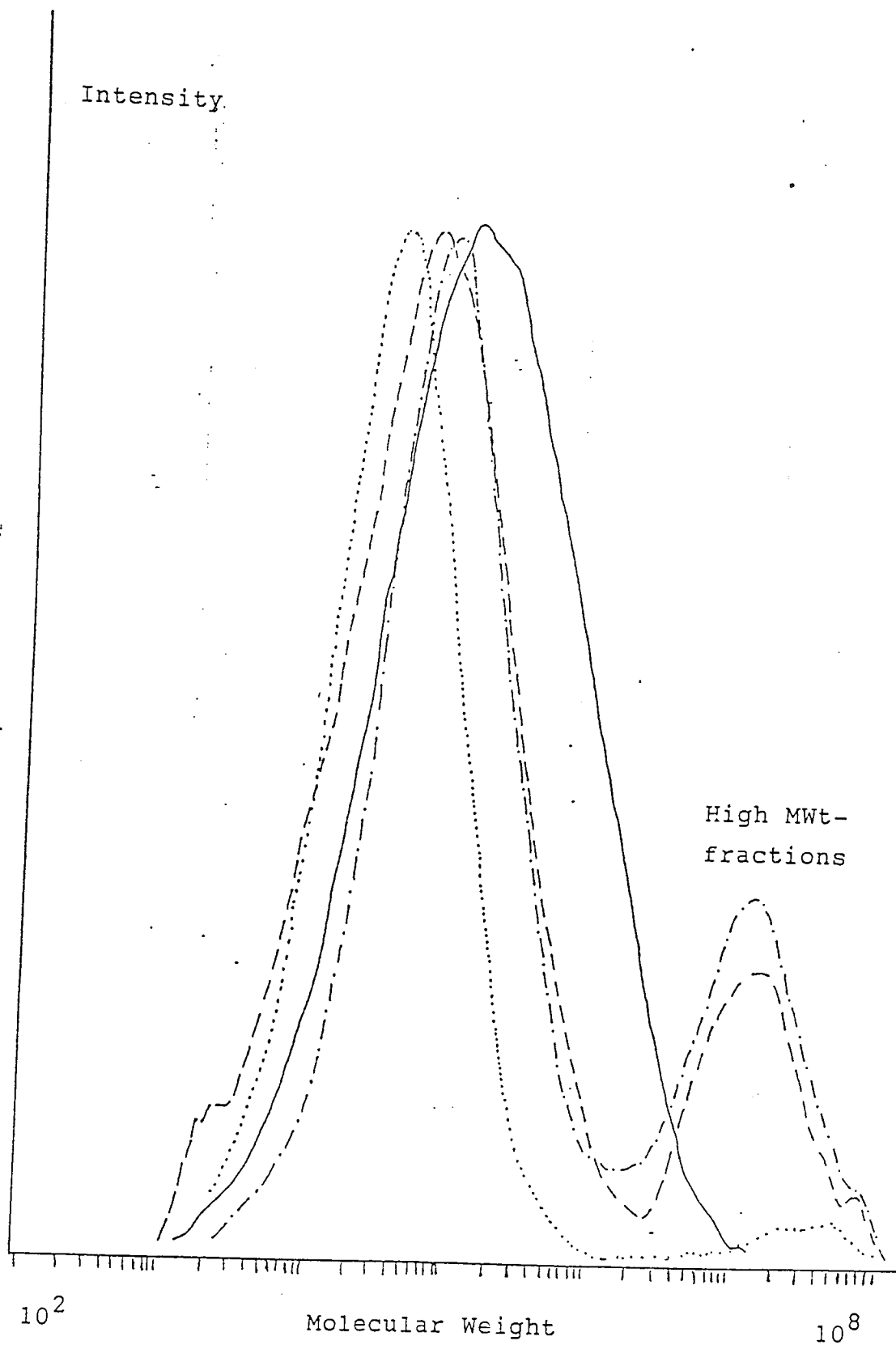


Figure 4.7 Molecular weight distribution curves of fractions obtained by exhaustive Soxhlet extraction in toluene (Toluene-extract, ·····) and in xylene (Xylene-extract, - · - · - ·) of masterbatch containing 10% of AOTP, compared to those of fresh PP (—) and the fresh masterbatch (- - - -)

4.2.2 Polymerisation of AOTP in liquid hydrocarbon

In order to simulate reaction conditions of antioxidant in polyolefins during reactive processing at 180°C, decalin (decahydronaphthalene), which is a high boiling (b.p. 190°C) hydrocarbon liquid, was used as a substrate in the polymerisation of AOTP in the presence of peroxide. Effect of shear, however, cannot be simulated in the model compound studies. Detail of the polymerisation procedure has been mentioned in Section 4.1 and Scheme 4.2.

Solution A and B (solution of 10% of AOTP in decalin before and after 30 minutes polymerisation at 180°C, see Scheme 4.2) were preliminarily analysed using ESR spectroscopy for their nitroxyl radical contents, along with CuSO₄ solution as reference. It was found that, AOTP solution before polymerisation (Solution A) shows trace concentration of nitroxyl radical, presumably due to oxidation during synthesis. However, after polymerisation (Solution B) the nitroxyl concentration diminishes to almost zero, see the ESR spectra in Figure 4.8. This may be due to reaction of the nitroxyl radical with any other radicals formed during polymerisation.

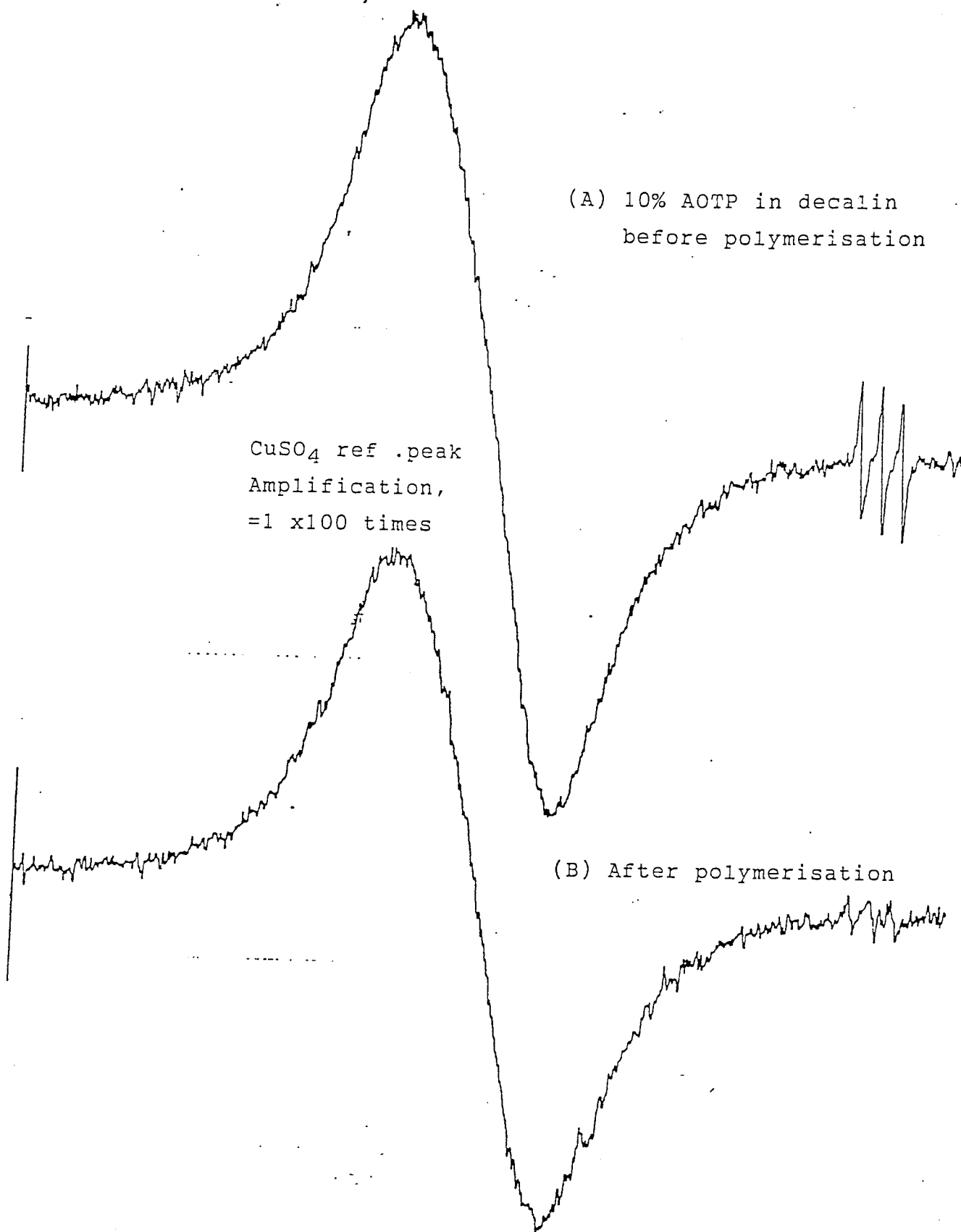


Figure 4.8 ESR spectra (amplification = 1 x 100) of 10% AOTP solution in decalin before (A) and after (B) polymerisation at 180°C for 30 minutes under Argon atmosphere measured using reference solution containing 2×10^{-6} mol of CuSO₄

4.2.2.1 FTIR spectroscopy measurement

From the FTIR spectra of fresh AOTP in Figure 4.9 (————), the particular peaks of interest are, carbonyl (1704 cm^{-1} , s), unsaturation (1617 cm^{-1} , m), and secondary amine (3317 cm^{-1} , m), s and m refer for sharp and medium intensity. Spectrum (- - - -) of acetone-water extractable product (Residue E, extracted in acetone-water from polymerised AOTP solution in decalin and evaporated) is similar to that of fresh AOTP, except its carbonyl band has broadened and shifted slightly to higher wave number (maximum shifted from 1704 to 1728 cm^{-1}), which may be due to some extent of polymerisation of the antioxidant. This indicates that the acetone-water extractable product not only contains the unreacted but also some homopolymerised AOTP. Spectrum (· · · · ·) of polymerised-AOTP in decalin (Residue F, obtained after vacuum evaporation of extracted polymerised AOTP solution in decalin), on the other hand, does not show any unsaturation peak, indicating that the polymerised AOTP in the extracted decalin solution (Solution D) contains only polymerised AOTP. Its carbonyl band also has further shifted towards higher wave number with a maximum of 1735 cm^{-1} as a result of saturation of the acrylic-ester group through polymerisation. Surprisingly, however, the intense peak of secondary amine at 3317 cm^{-1} has also disappeared, suggesting that the $>\text{NH}$ group of the polymerised AOTP may also be susceptible to radical attack which in turn promotes branch polymerisation to form crosslinking as exhibited by the presence of high MWt component shown in MWD-curve, see Table 4.3 and Figure 4.6.

For comparison, two control experiments using similar procedures were carried out. Firstly, AOTP was polymerised without decalin in the presence of DCP 0.005 molar ratio at 180°C for 30 minutes under Argon atmosphere. FTIR spectra (in KBr disc) of the polymerised AOTP compared to that of fresh AOTP, see Figure 4.10 (————), again shows disappearance of unsaturation peak (1617 cm^{-1}) as well as the $>\text{N-H}$ peak (3317 cm^{-1}). This evidence supports the above and indicates that the reaction of $>\text{N-H}$ during polymerisation does not necessarily involve decalin substrate.

In the second control experiment, Tinuvin 770 (bis-[2,2,6,6-tetra methyl 4-piperidiny]-sebacate), a secondary amine nitroxyl precursor without acrylic group was polymerised for 30 minutes with 2 molar ratio of 2-ethylhexylacrylate (EHA), a high boiling acrylate ester (b.p. 214 - 219°C), in the presence of DCP 0.005 molar ratio to total reagent under similar conditions. From the FTIR spectra (run in nujol) of the mixture before and after polymerisation (Figure 4.11), it is clear that the EHA has polymerised, which was indicated by the decrease of the unsaturation band (1621 cm^{-1}). However, unlike in the case of the first control experiment (polymerised AOTP without decalin), it was found that FTIR spectra of both fresh and polymerised EHA with Tinuvin 770 still exhibited >N-H peak at 3321 cm^{-1} . Calculation of the >N-H peak area index (relative to their corresponding >C=O peak at 1733 cm^{-1}) showed no considerable difference between both >N-H index before and after polymerisation. Repetition of this control experiment with longer reaction times (for 60 and 120 minutes) showed similar FTIR spectra, suggesting that even after 30 minutes the reaction has completed and there was no indication of reaction involving the >N-H group of the Tinuvin 770 during polymerisation with the EHA.

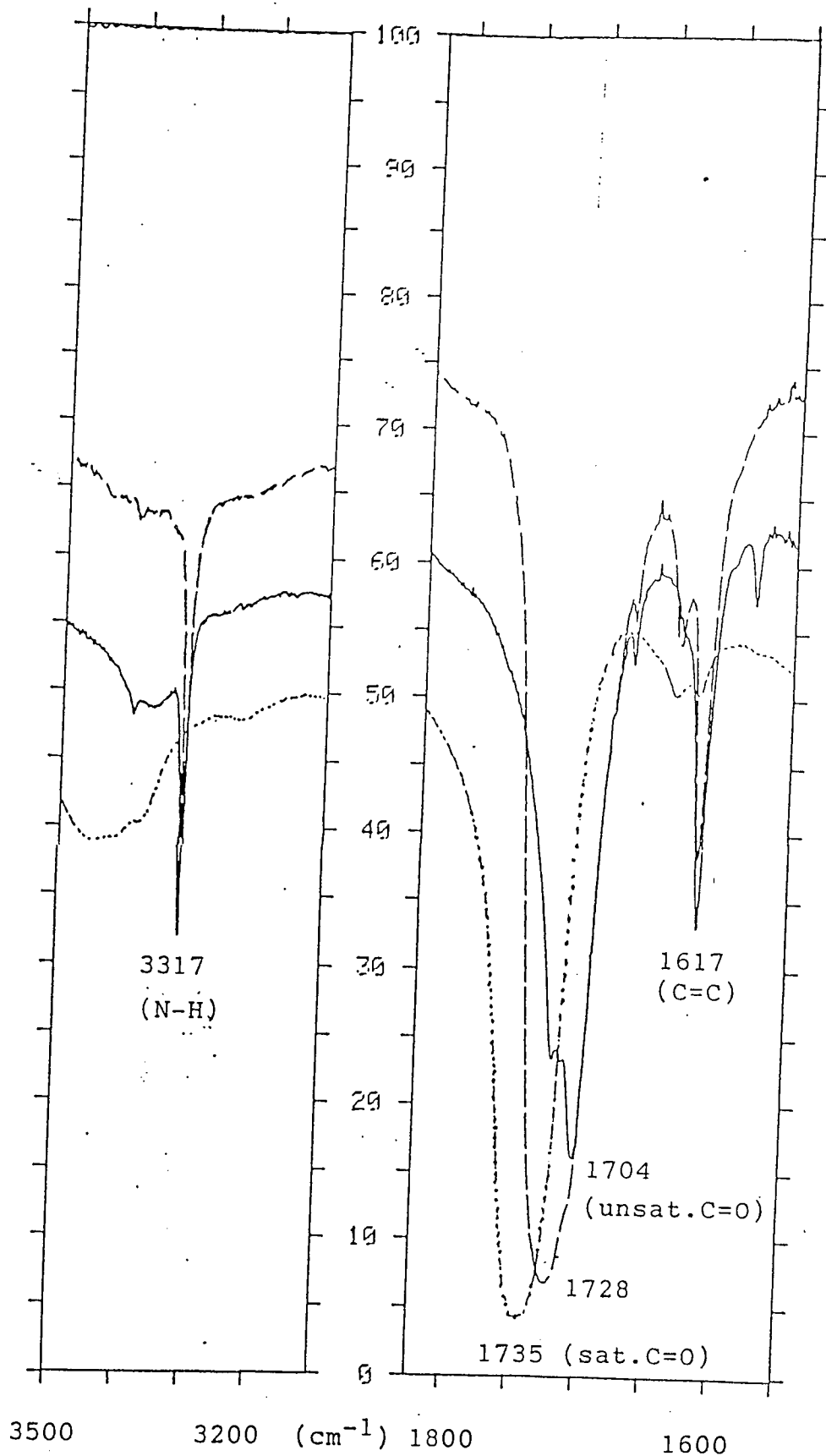


Figure 4.9 FTIR spectra (KBr-disc), window region 3500 - 3100 cm^{-1} and 1825 - 1550 cm^{-1} , of fresh AOTP (—), Residue E, i.e. acetone-water extract of polymerised AOTP in decalin (- - - -), Residue F, i.e. extracted decalin solution of polymerised AOTP (· · · ·), see Scheme 4.2 for the polymerisation procedure

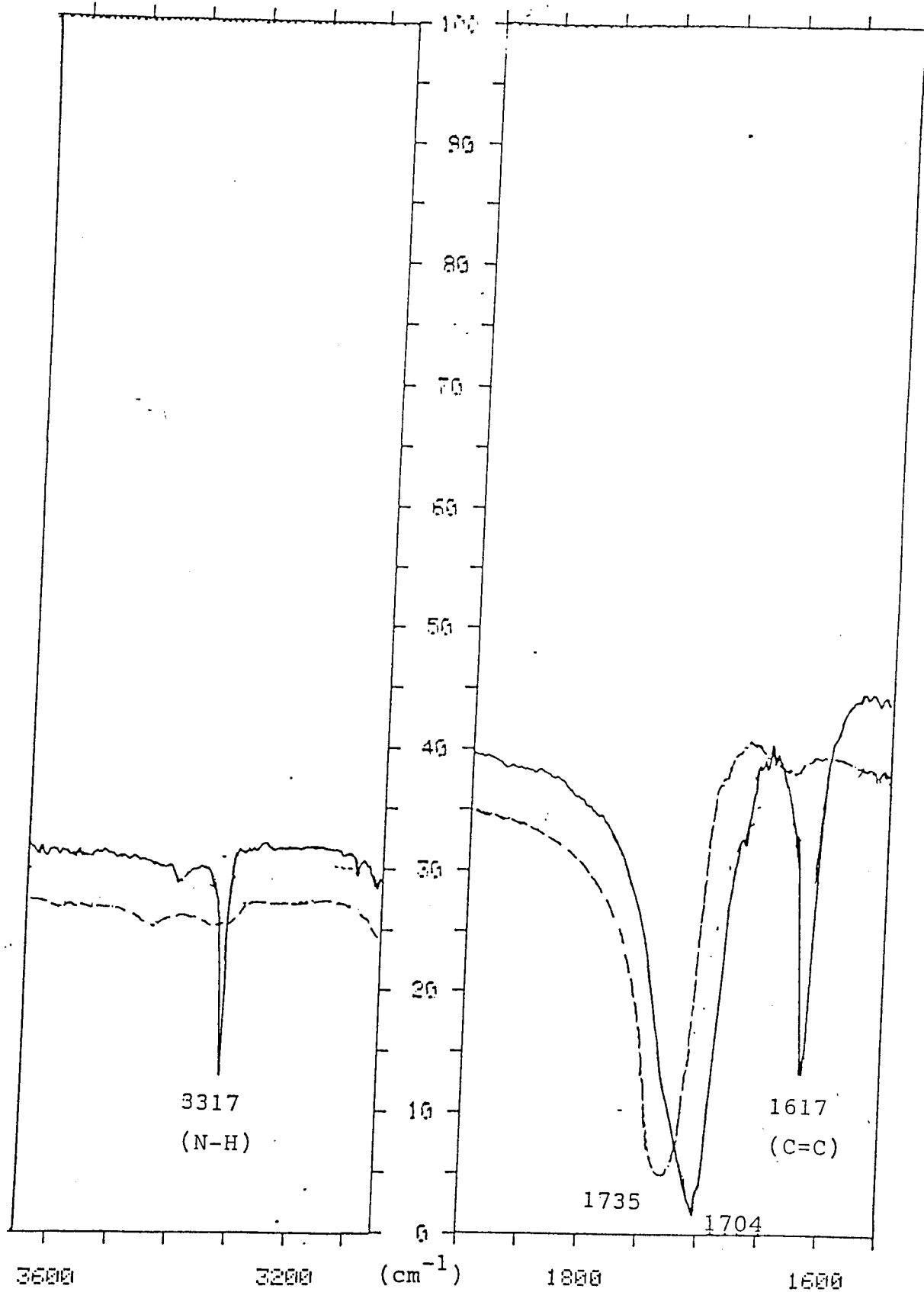


Figure 4.10 Fraction of FTIR spectra (KBr-disc, window regions 3650 - 3050 cm⁻¹ and 1900 - 1550 cm⁻¹) of polymerised AOTP without decalin at 180°C, for 30 minutes under Argon gas in the presence of DCP 0.005 molar ratio (-----), compared to that of fresh AOTP (———)

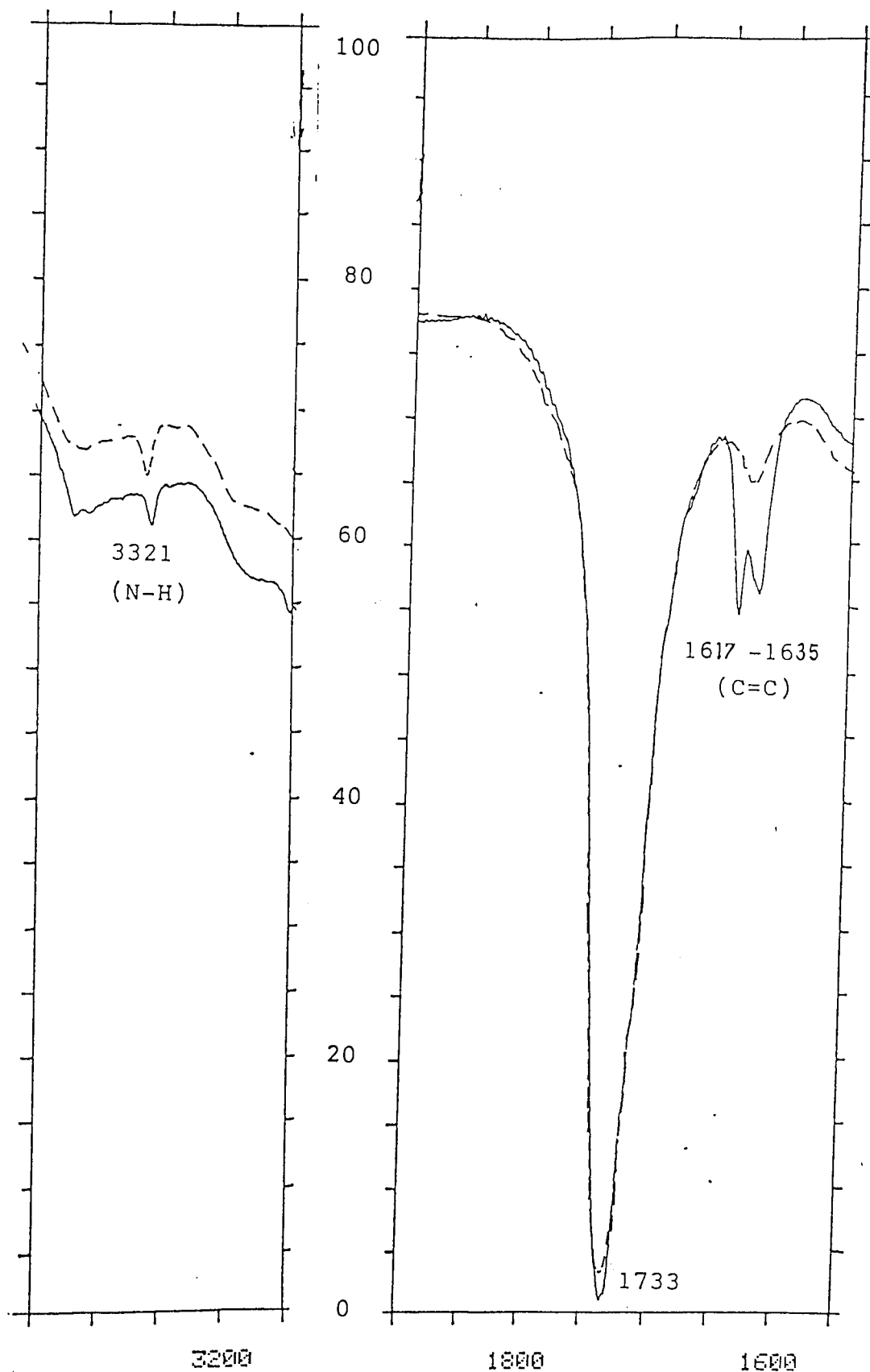


Figure 4.11 Fraction of FTIR spectra (in nujol, window regions 3600 - 3000 cm^{-1} and 1900 - 1500 cm^{-1}) of polymerised EHA with Tinuvin 770 (2:1 molar ratio) without decalin at 180°C, for 30 minutes under Argon gas in the presence of DCP 0.005 molar ratio to total reagent (-----), compared to that of unpolymerised EHA+Tinuvin 770 (—)

4.2.2.2 Proton NMR measurements

Polymerised AOTP without decalin, and evaporated polymerised AOTP in decalin (Residue F, see Scheme 4.2), were identified using Proton NMR spectroscopy in CDCl_3 (see Figures 4.12.a and 4.12.b, compared to that of fresh AOTP, see Figure 2.5). The proton NMR spectra of fresh AOTP (Figure 2.5) clearly indicated characteristic peaks of the acrylic protons ($\text{CH}_2=\text{CH}-$) at proton chemical shifts (ppm) : $\delta = 6.38$ and 6.33 (doublet), $\delta = 6.11$ to 6.02 (quartet), and $\delta = 5.79$ and 5.75 (doublet). Unfortunately, there was no sign of secondary amine proton ($>\text{N}-\text{H}$) peak in that spectra, presumably due to broadening of the peak, like ordinary amine proton, or possible overlapping with C_4 -proton of the piperidine ring ($-\text{O}-\text{CH}<$) at $\delta = 5.15$ to 5.27 (nine splits). The proton unsaturation ($\text{CH}_2=\text{CH}-$) peaks are not shown in the proton NMR spectra of both polymerised AOTP without and with decalin (Figures 4.12.a and 4.12.b). Again, this is due to the complete polymerisation of AOTP through the acrylate group. Moreover, proton NMR spectra of evaporated polymerised AOTP in decalin (Figure 4.12.b) exhibited NMR bands in the region : $\delta = 0.8 - 1.6$ ppm, which are due to methylene groups ($-\text{CH}_2-$) of the remaining unevaporated or grafted decalin.

Two new broad singlet peaks, maximum at $\delta = 1.54$ and 2.25 ppm (with intensity ratio about 5 : 4), were observed from Proton NMR spectra of polymerised AOTP without decalin (see Figure 4.12.a), which may be due to formation of saturated acrylic [$-\text{CH}_2-\text{CH}(\text{CO})-$] through polymerisation, δ of $-\text{CH}_2-$ = 1.54 ppm and δ of $-\text{CH}(\text{CO})-$ = 2.25 ppm. One of these peaks ($\delta = 2.25$ ppm) is also shown in the proton NMR spectra of polymerised AOTP in decalin (Figure 4.12.b), whereas the other one is covered by absorption bands due to decalin. However, the peak intensity of the $-\text{CH}(\text{CO})-$ group ($\delta = 2.25$ ppm) is too high as the intensity ratio of the saturated acrylic protons should be 2 to 1. Therefore, there is also evidence of possible reaction of $>\text{N}-\text{H}$ group of AOTP to form other groups during polymerisation which possess absorption bands in the region overlapped to that of the saturated acrylate [$-\text{CH}(\text{CO})-$, $\delta = 2.25$ ppm], which may be due to $>\text{CH}-\text{N}<$ or $-\text{CH}_2-\text{N}<$ ($\delta = 2.1 - 2.5$ ppm).

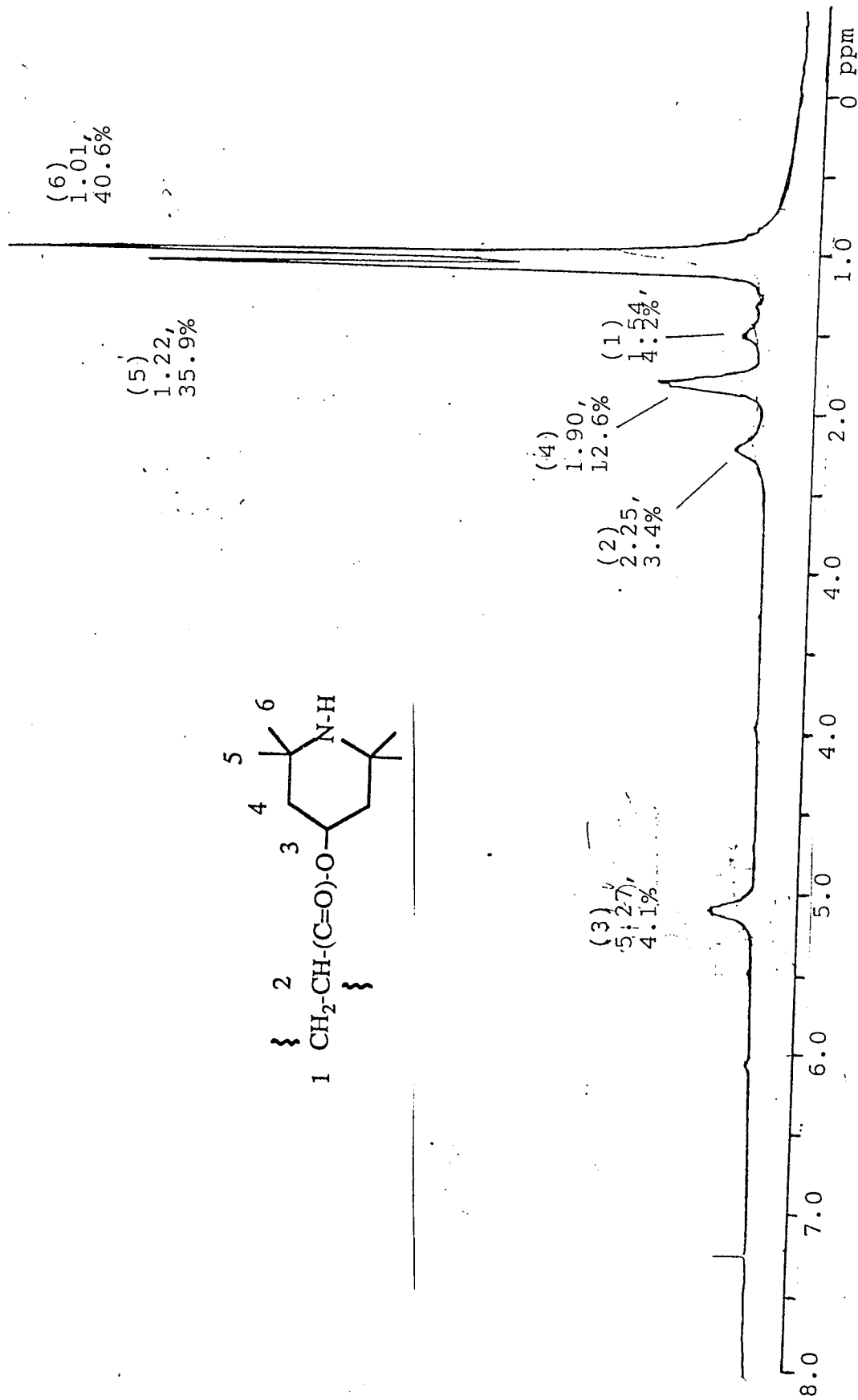


Figure 4.12.a Proton NMR spectra (in CDCl_3) of polymerised AOTP without decalin at 180°C in the presence of DCP 0.005 molar ratio under Argon atmosphere

For peak numbers, see Figure 4.11.a

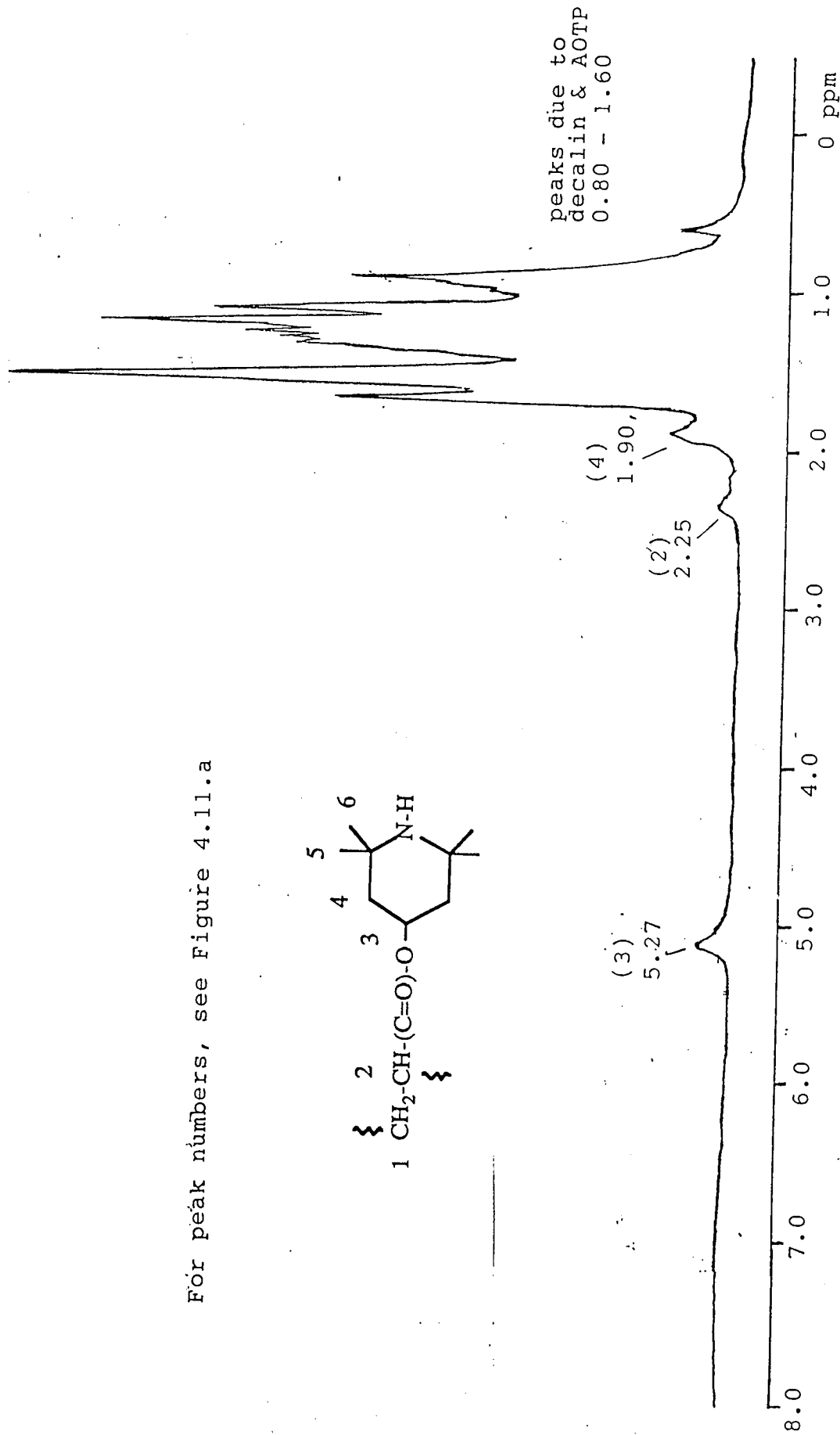
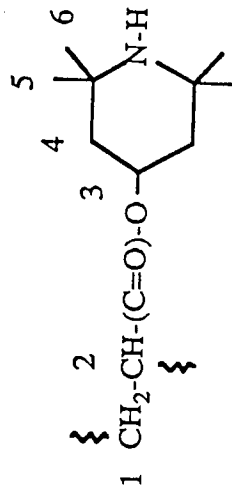


Figure 4.12.b Proton NMR spectra (in CDCl₃) of evaporated polymerised AOTP in decalin at 180°C in the presence of DCP 0.005 molar ratio under Argon atmosphere (Residue F in Scheme 4.2)

Proton NMR spectra of reagents and products of the second control experiment without decalin carried out under similar condition as in Scheme 4.2, i.e. those of fresh EHA (ethylhexylacrylate), fresh Tinuvin 770, polymerised EHA with Tinuvin 770 and polymerised EHA without Tinuvin 770, are shown in Figures 4.13.a to 4.13.d. The NMR spectra also exhibited virtual disappearance of unsaturation peaks of EHA ($\delta = 5.50 - 6.24$ ppm) after polymerisation with or without Tinuvin 770 (Figures 4.13.c and 4.13.d). This proves that the polymerisation of EHA in the presence of DCP 0.005 molar ratio to total reagent is evident under such condition, although the appearance of two new peaks due to saturated acrylate (as shown at $\delta = 1.54$ and 2.25 ppm in Figure 4.12.b) in the case of polymerised EHA with Tinuvin (Figure 4.13.c) is only exhibited by peak broadening as the new peaks may overlap with the existing methylene peaks due to Tinuvin 770 and ethylhexyl group of EHA as also shown in Figures 4.13.a and 4.13.b. In addition, both new saturated acrylate peaks are apparently shown in the proton NMR spectra of polymerised EHA without Tinuvin 770 (Figure 4.13.d), but at slightly different chemical shifts ($\delta = 1.84$ and 2.27 ppm). It is not clear, however, whether there is any evidence of involvement of >N-H group of Tinuvin 770 in the polymerisation of EHA and Tinuvin 770 because the >N-H peaks cannot be seen even before reaction. The chemistry of AOTP polymerisation in decalin substrate will be further investigated using Carbon-13 NMR spectroscopy in the following section.

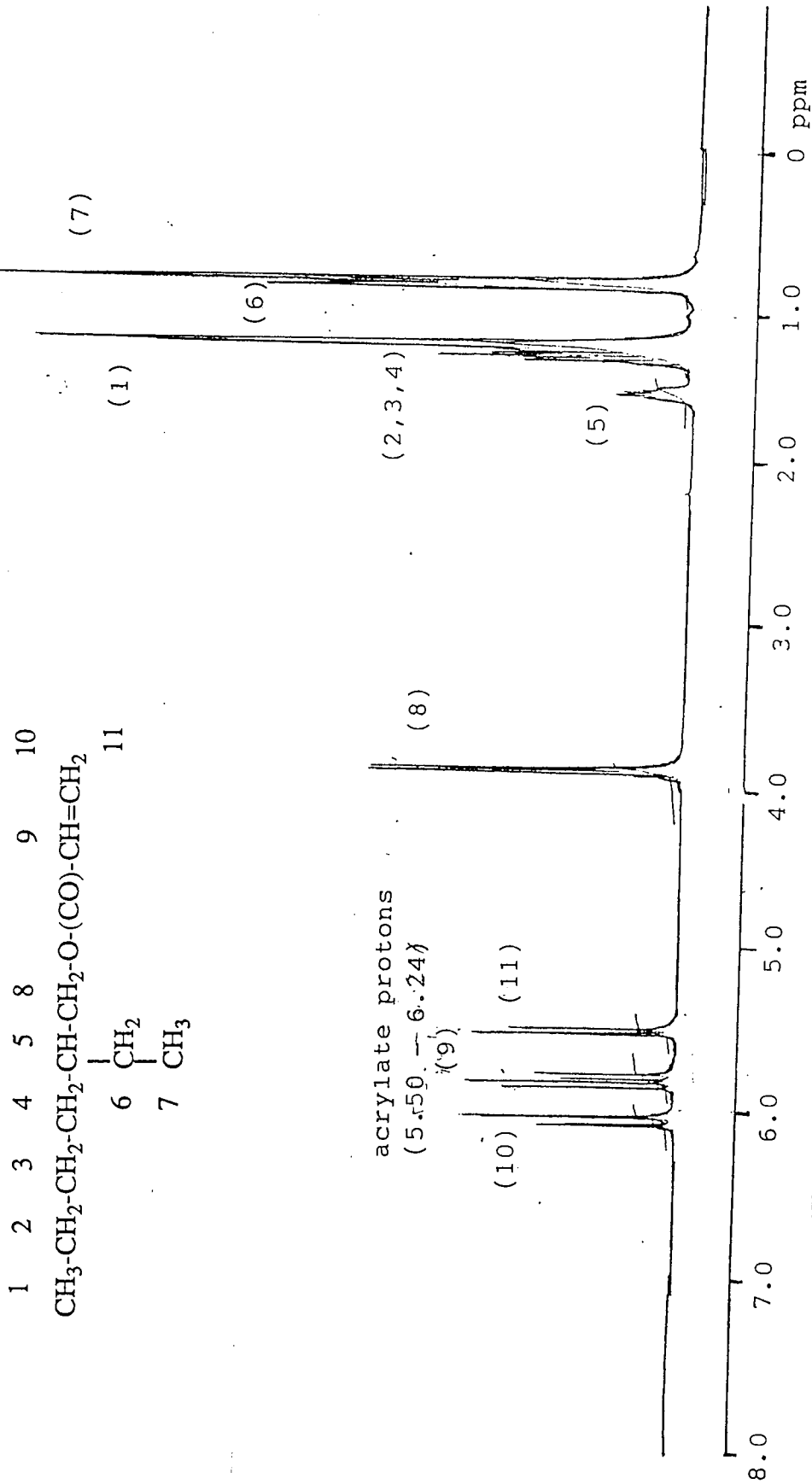


Figure 4.13.a Proton NMR spectra (in CDCl₃) of fresh EHA (2-ethylhexylacrylate)

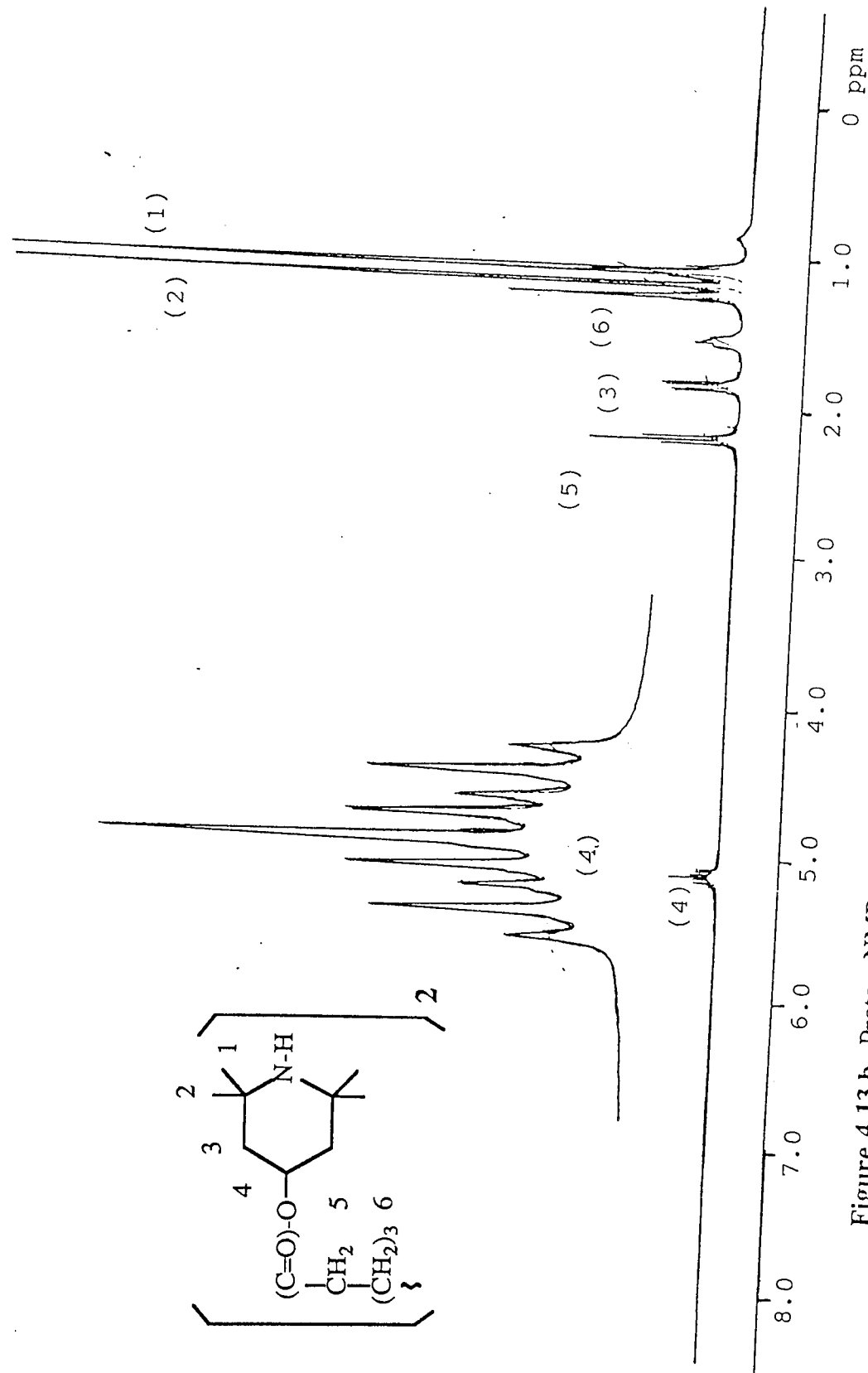
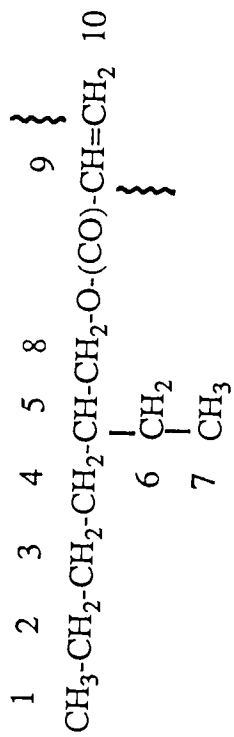


Figure 4.13.b Proton NMR spectra (in CDCl_3) of fresh Tinuvin 770 [bis-(2,2,6,6-tetramethyl-4-piperidiny) sebacate]



T: peaks due to Tinuvin-770
(unchanged)

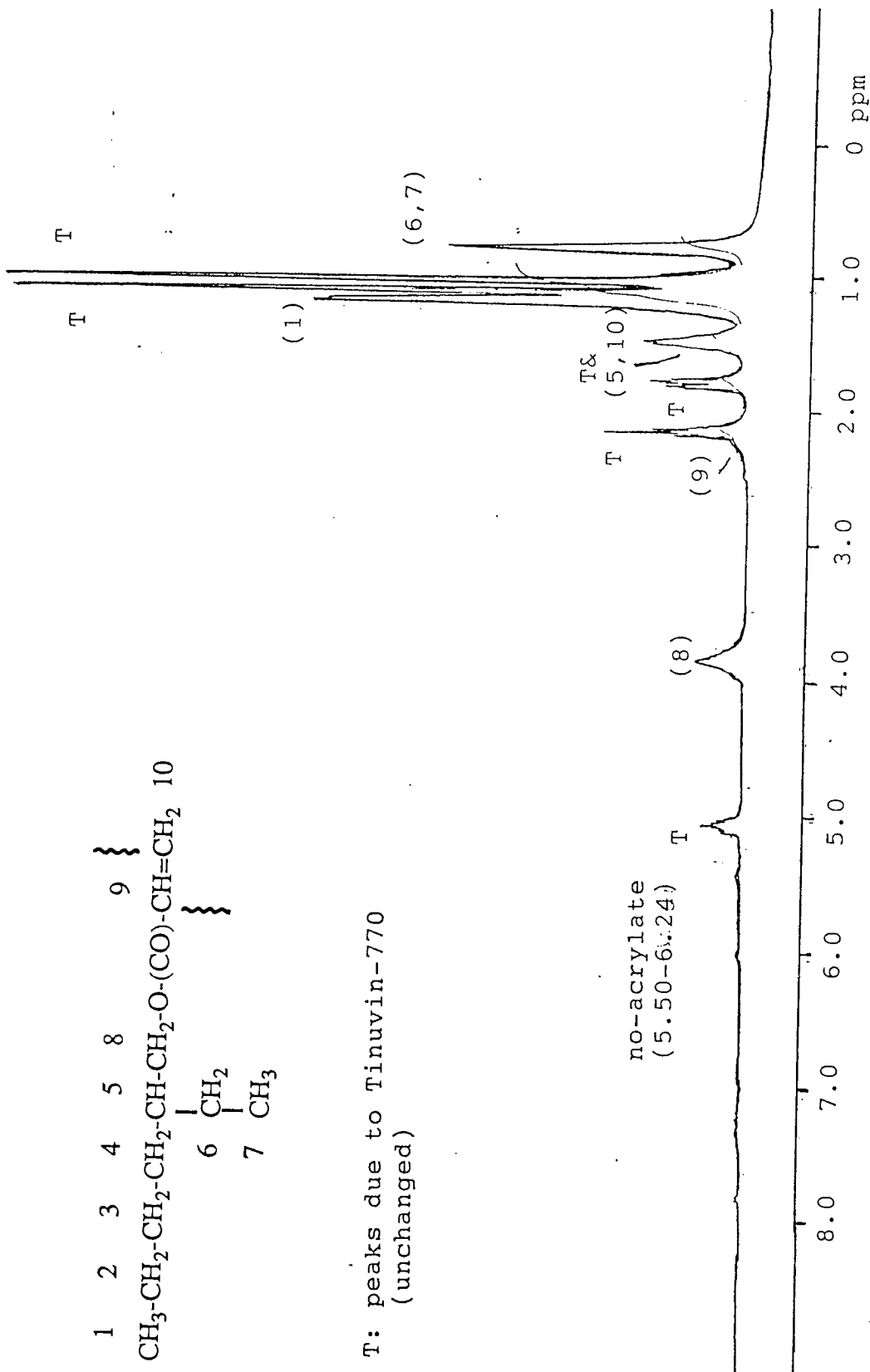


Figure 4.13.c Proton NMR spectra (in CDCl_3) of polymerised EHA with Tinuvin 770 without decalin at 180°C in the presence of DCP 0.005 molar ratio under Argon atmosphere

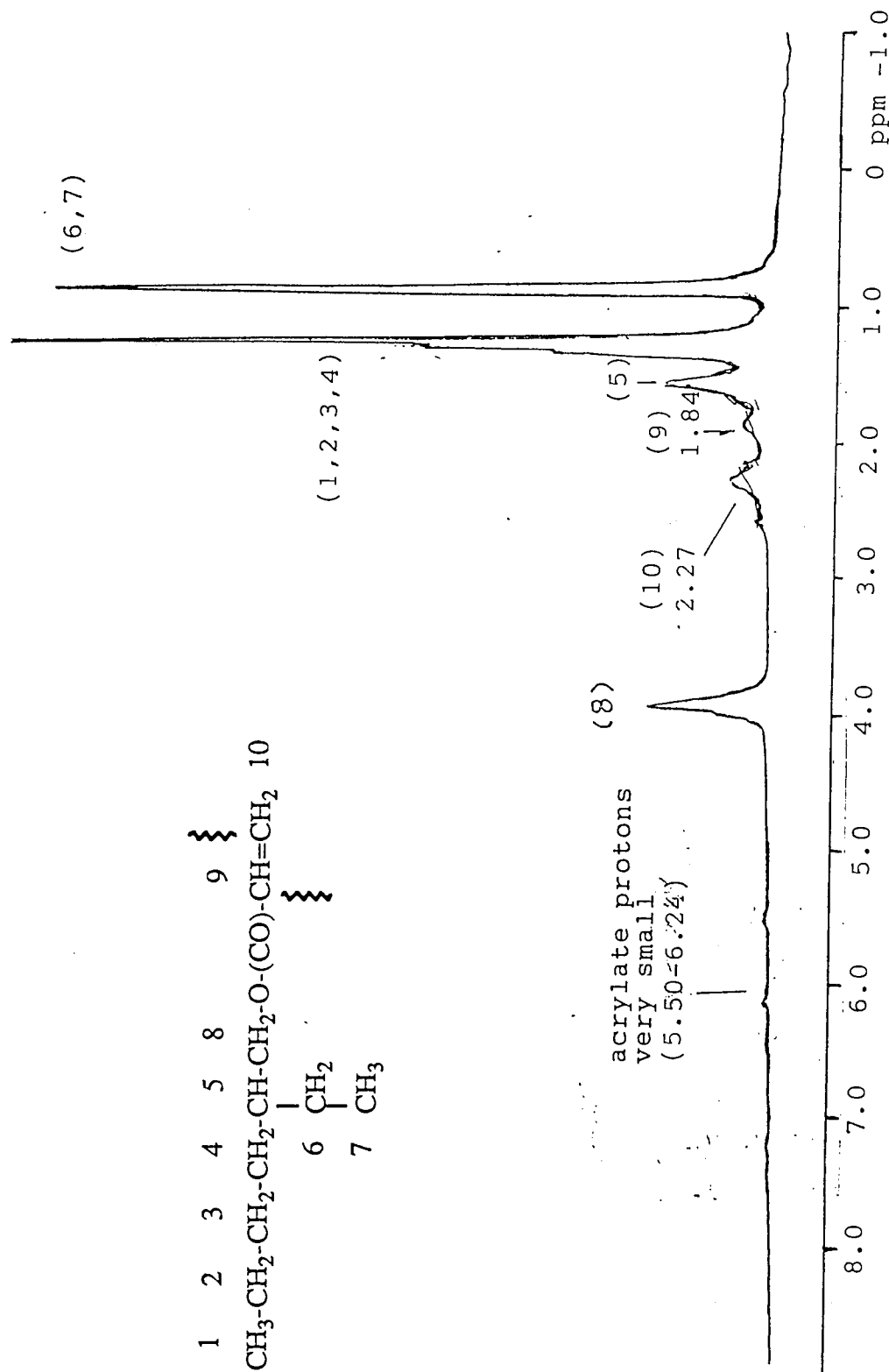


Figure 4.13.d Proton NMR spectra (in CDCl₃) of polymerised EHA without decalin at 180°C in the presence of DCP 0.005 molar ratio under Argon atmosphere

4.2.2.3 Carbon-13 NMR measurements

Carbon-13 NMR spectra of polymerised AOTP without and with decalin (Figures 4.14.a and 4.14.b, see Scheme 4.2 for the polymerisation procedure, see also that of fresh AOTP, Figure 2.6, for comparison) were recorded using a BRUKER High Resolution NMR Spectrometer, which enables us to distinguish each particular carbon peak. Based on the difference of spin coupling constant, the NMR spectrometer plots Carbon-13 NMR spectra in such a way that methyl ($-\text{CH}_3$) and tertiary ($>\text{CH}-$) carbon peaks appear as positive (+) values, whereas methylene ($-\text{CH}_2-$) and quaternary ($>\text{C}<$) carbon atoms exhibit negative (-) values.

Carbon-13 NMR spectra of fresh AOTP (Figure 2.6) clearly exhibits particular peaks of interest at various carbon chemical shifts (δ , ppm) : carbonyl ($\text{C}=\text{O}$) at 165.1 (-), $\text{CH}_2=$ at 129.7 (-), $=\text{CH}-$ at 128.5 (+), $-\text{O}-\text{CH}<$ at 67.3 (+), $>\text{C}<$ at 51.2 (-), $-\text{CH}_2-$ at 43.6 (-), and two $-\text{CH}_3$ peaks at 34.5 (+) and 28.7 (+). After 30 minutes polymerisation without decalin in the presence of DCP 0.005 molar ratio at 180°C (Figure 4.14.a), both unsaturation peaks, $\text{CH}_2=$ at 129.7 (-), $=\text{CH}-$ at 128.5 (+), almost completely disappeared, a trace of these peaks indicates the remaining unreacted AOTP.

As a result of the acrylate polymerisation, $-\text{CH}_2-$, $\delta = 49.0$ (-), and $-\text{CH}(\text{CO})-$ peaks, $\delta = 41.2$ (+), of the polymer backbone (saturated acrylate) were formed. When compared to that of fresh decalin (Figure 4.14.b), Carbon-13 NMR spectra (Figure 4.14.c) of evaporated polymerised AOTP in decalin (Residue F) showed trace of decalin peaks at $\delta = 36.0$ (+), 33.9 (-) and 26.5 (-), in spite of after exhaustive vacuum evaporation of the sample (see Scheme 4.2 for the procedure). The decalin peaks, therefore, may be due to either the grafted decalin onto polymerised AOTP or the remaining unevaporated high boiling point decalin.

Interestingly, Carbon-13 NMR spectra of both polymerised AOTP without and with decalin (Figures 4.14.a and 4.14.c) exhibited a multiplet peaks at $\delta = 67.3 - 67.2$ (+) ppm, whereas spectrum of fresh AOTP (Figure 2.6) shows only a singlet peak at

that area $\delta = 67.3 (+)$ ppm, which indicates that the singlet peak at $\delta = 67.3 (+)$ ppm is due to C4-atom of the piperidine ring (-O-CH<). Additional multiplet peaks in this area shown in the spectra of polymerised AOTP without and with decalin (Figures 4.14.a and 4.14.c), therefore, may be due to formation of other -CH- groups (positive intensity), presumably such as >N-CH<, δ (ppm) = 47 - 65 (+) or >N-O-CH<, δ (ppm) = 50 - 75 (+). In addition, the NMR spectra of polymerised AOTP without decalin (Figures 4.14.a) shows higher intensity of peak at $\delta = 51.2 (-)$ ppm (relative to total intensity = 22.5%) when compared to that for fresh AOTP (relative to total intensity = 6.9%, see Figure 2.6). This peak increase was also observed in the NMR spectra of polymerised AOTP with decalin (relative to total intensity = 18.7%, see Figure 4.14.c), which may be associated with formation of other -CH₂- groups, possibly from the reaction of >N-H and CH₂=CH- groups to form >N-CH₂- [$\delta = 40 - 60$ ppm (-)].

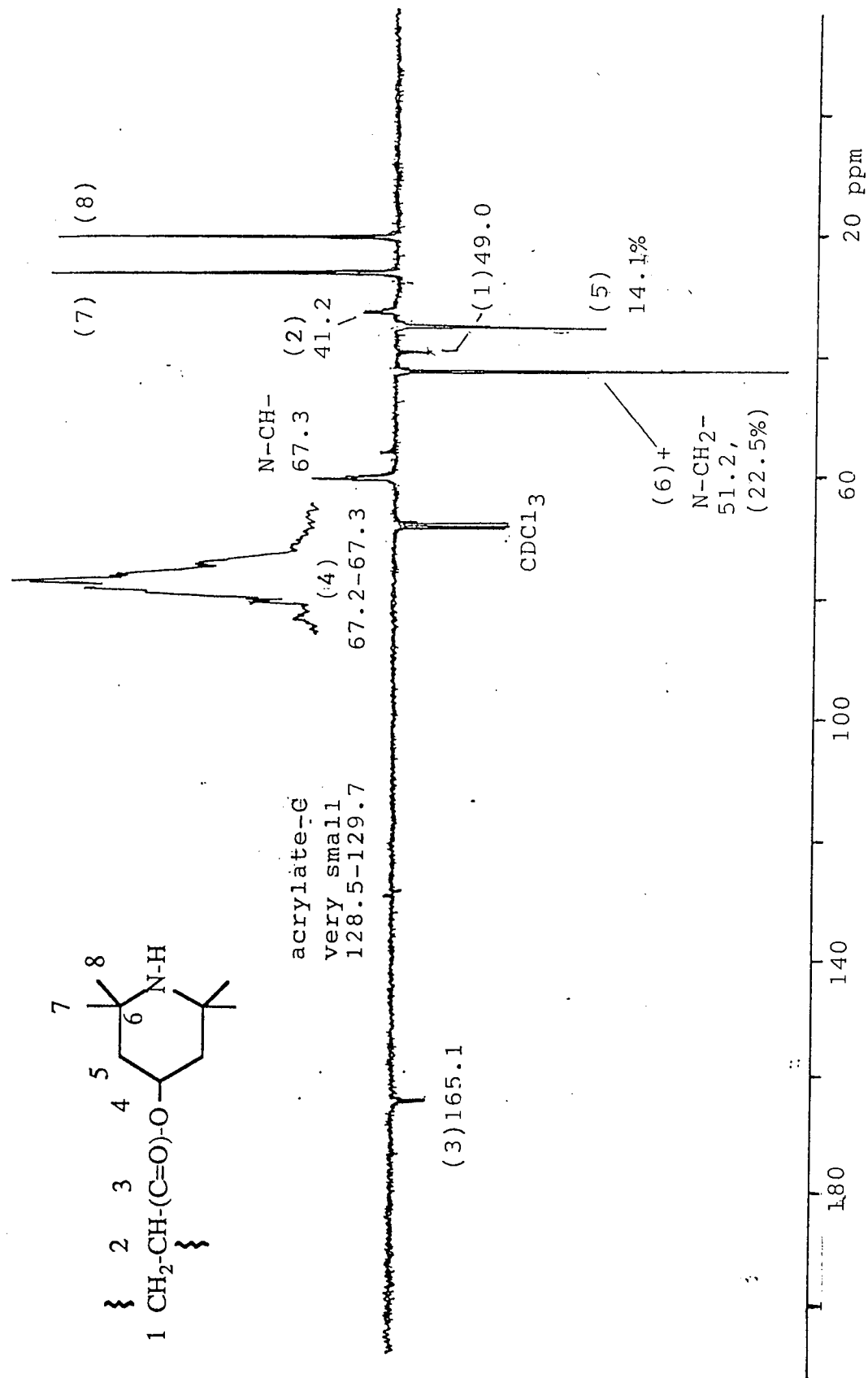


Figure 4.14.a Carbon-13 NMR spectra (in CDCl₃) of polymerised AOTP without decalin at 180°C in the presence of DCP 0.005 molar ratio under Argon atmosphere

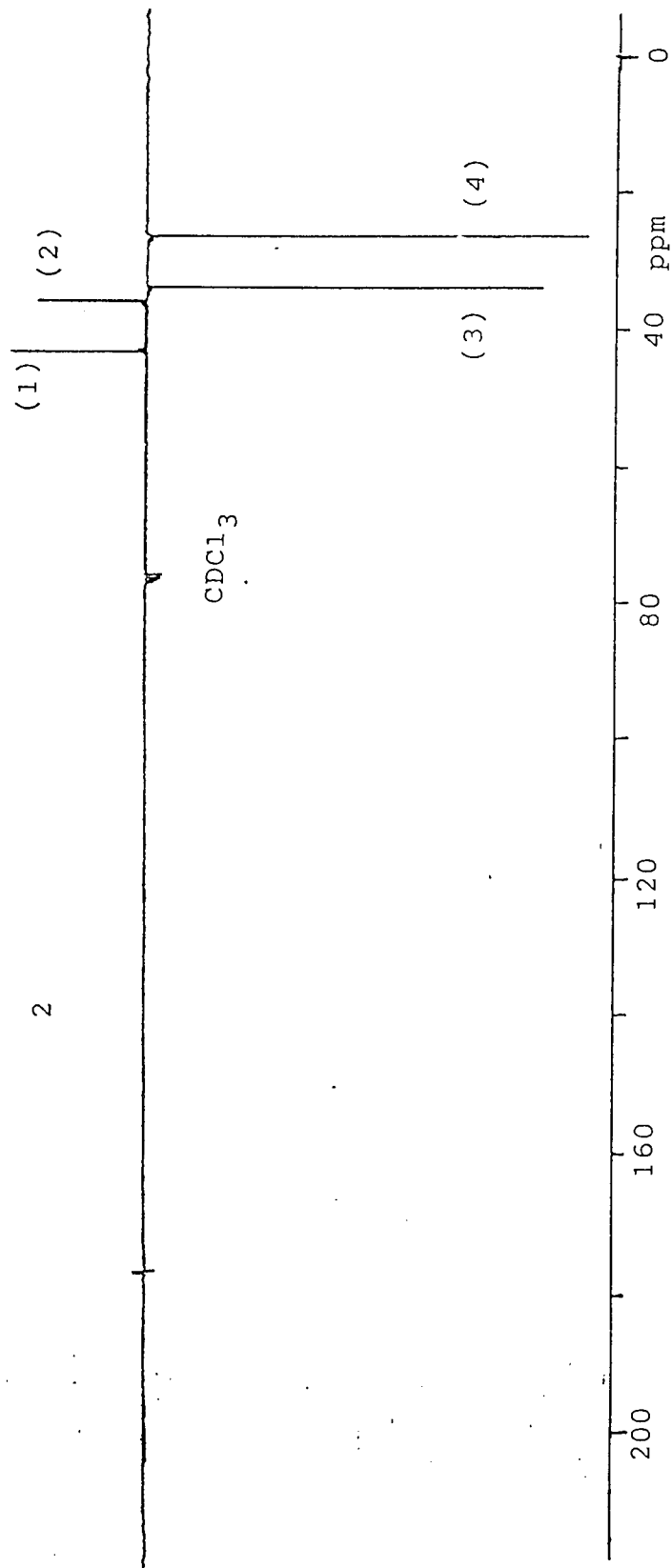
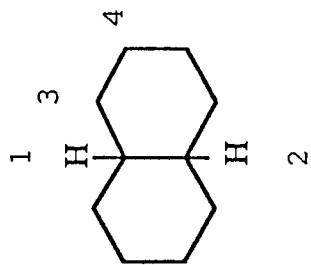


Figure 4.14.b Carbon-13 NMR spectra (in CDCl₃) of fresh decalin

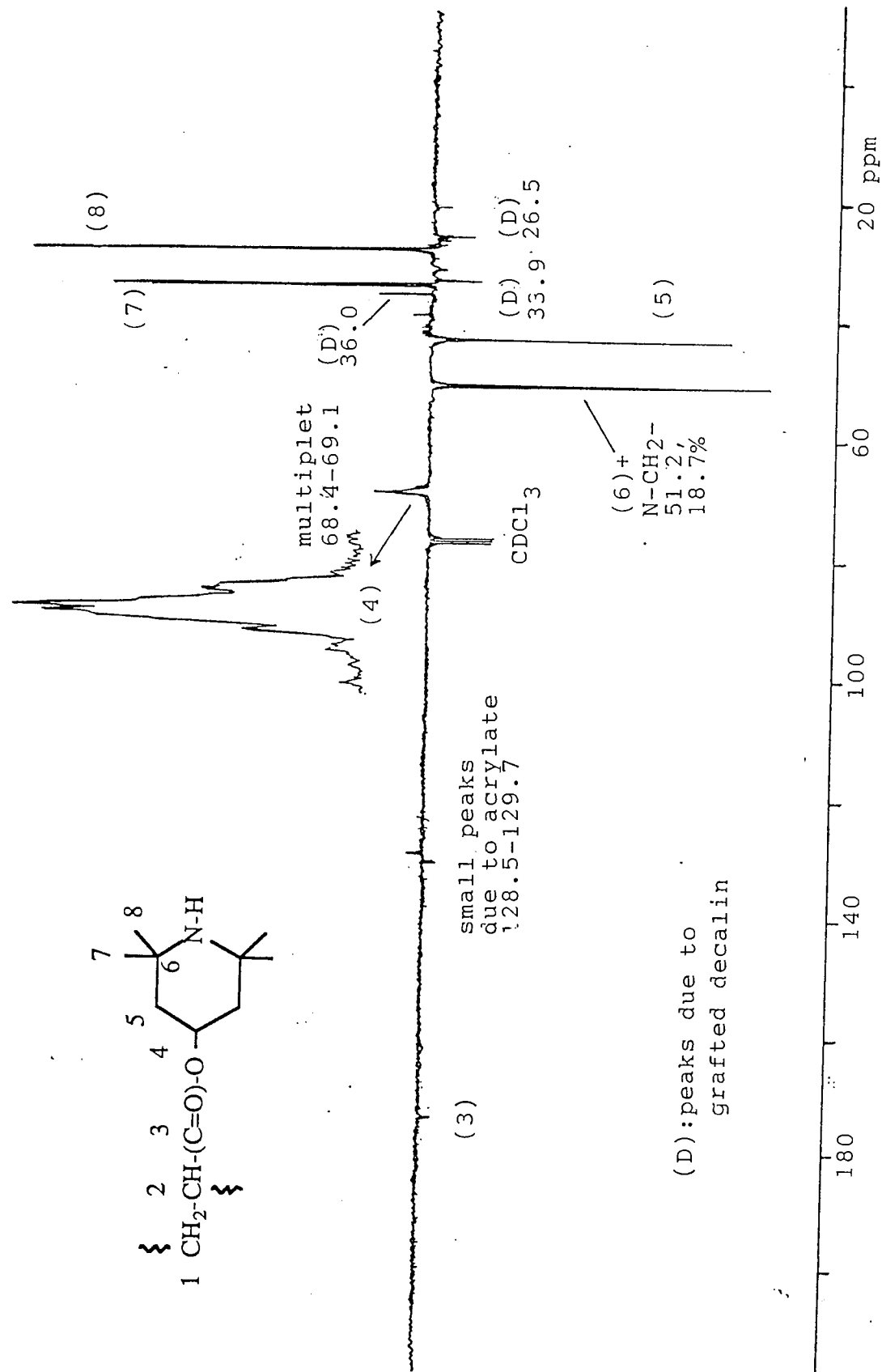


Figure 4.14.c Carbon-13 NMR spectra (in CDCl₃) of polymerised AOTP in decalin at 180°C in the presence of DCP 0.005 molar ratio under Argon atmosphere

In the control experiment, when EHA was polymerised with Tinuvin 770 in the presence of DCP 0.005 molar ratio to total mol of reagent's functionals under similar conditions mentioned in Scheme 4.2 (the Carbon-13 NMR spectra are shown in Figures 4.15.a - 4.15.d), it was also clear that no peaks from the acrylic group as exhibited by spectra of fresh EHA (in Figure 4.15.a at $\delta = 126.7$ [+] and 128.1 [-] ppm) were observed (see Figure 4.15.d). Again, this indicates that the entire double bond has been saturated during the polymerisation.

Formation of new saturated acrylic [-CH₂-CH(CO)-] peaks is also evident in this control experiment, i.e. that of -CH(CO)- group at $\delta = 41.1$ ppm (+), see Figures 4.15.c and 4.15.d, and virtually that of -CH₂- group of saturated acrylate (broad) at $\delta = 35.0 - 35.5$ pm (-) as shown in the spectra of polymerised EHA without Tinuvin 770 (Figure 4.14.c). It is also shown in the spectra of polymerised EHA with Tinuvin 770 (Figure 4.15.d) that all peaks due to polymerised EHA appear thicker, whereas those due to Tinuvin 770 appear as normal thin peaks. The peak thickening is a characteristic of increase in the viscosity of the compound as a result of polymerisation of the EHA without involvement of the Tinuvin 770. In addition, it is also observed that there is no formation of multiplet peaks in the region of δ (+) = $67.3 - 67.2$ ppm due to new -CH- group nor peak increase, at δ (-) = $40 - 60$ ppm, which was associated with the formation of other -CH₂-N< group. Therefore, it seems likely that in the control experiment when the EHA was polymerised with Tinuvin 770, there was no evidence of "inter-molecular interaction" between >N-H group of the Tinuvin 770 with the acrylate group of the EHA.

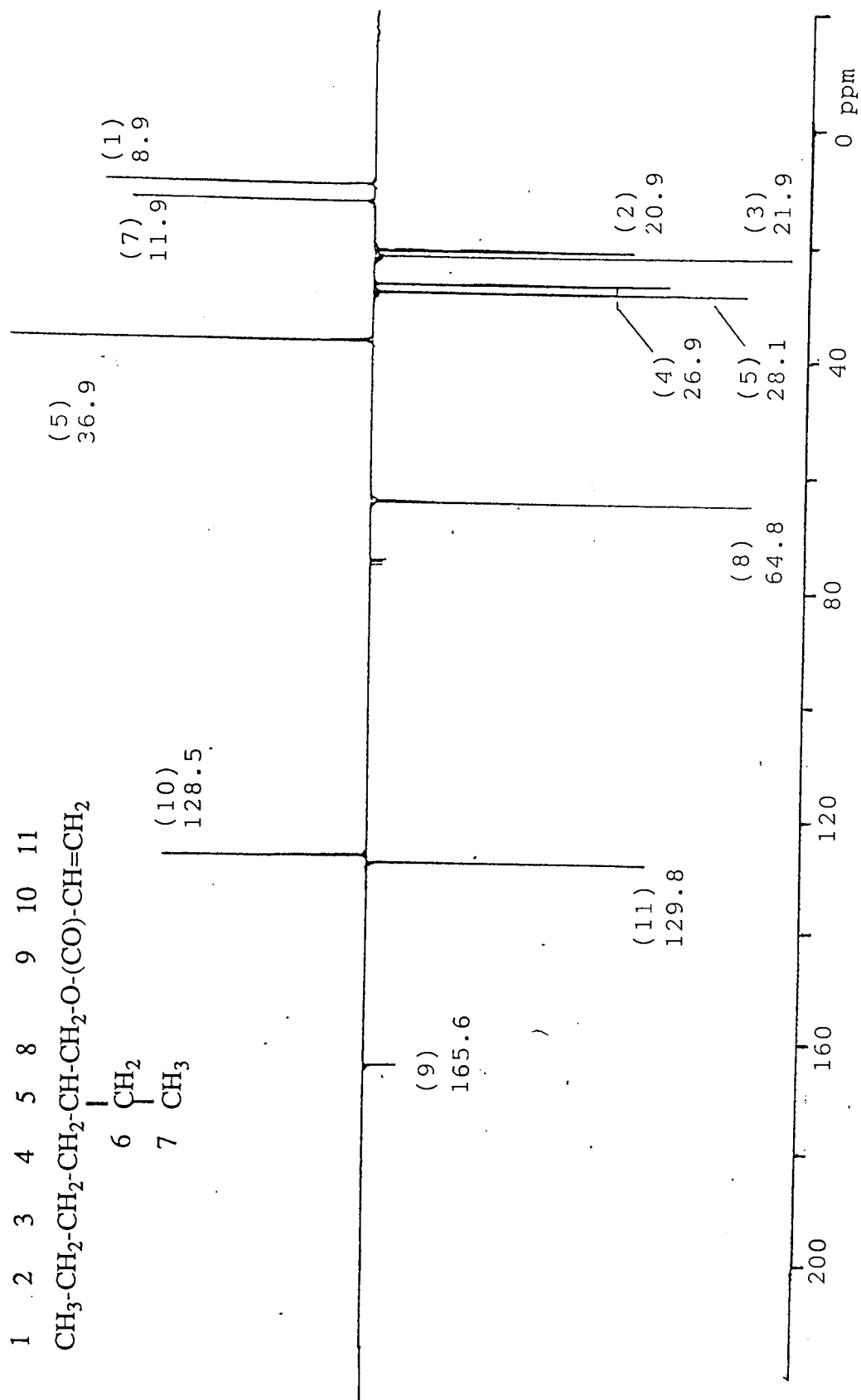


Figure 4.15.a Carbon-13 NMR spectra (in CDCl₃) of fresh EHA (2-ethylhexylacrylate)

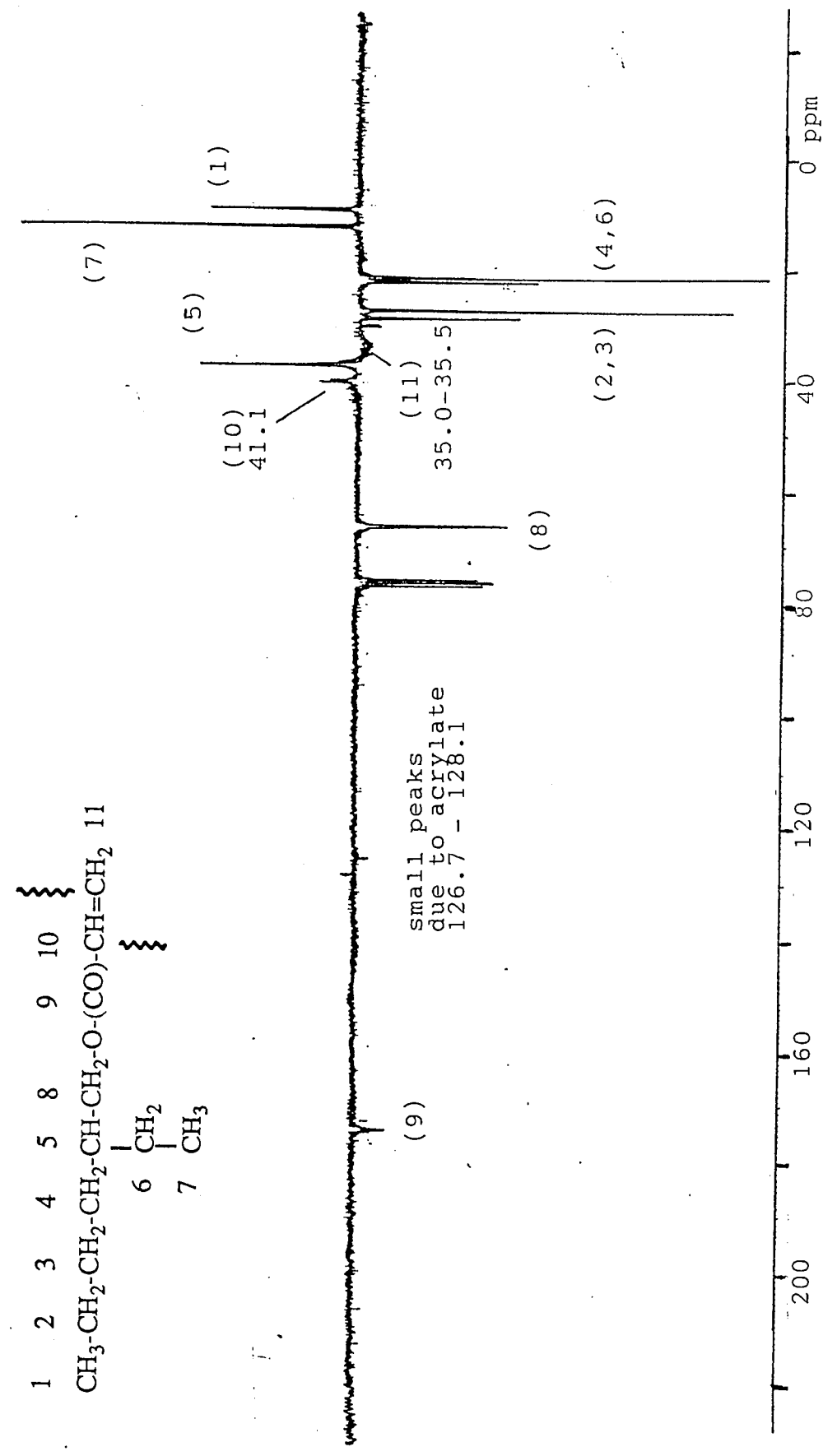


Figure 4.15.c Carbon-13 NMR spectra (in CDCl₃) of polymerised EHA without Tinuvin 770 at 180°C in the presence of DCP 0.005 molar ratio under Argon atmosphere

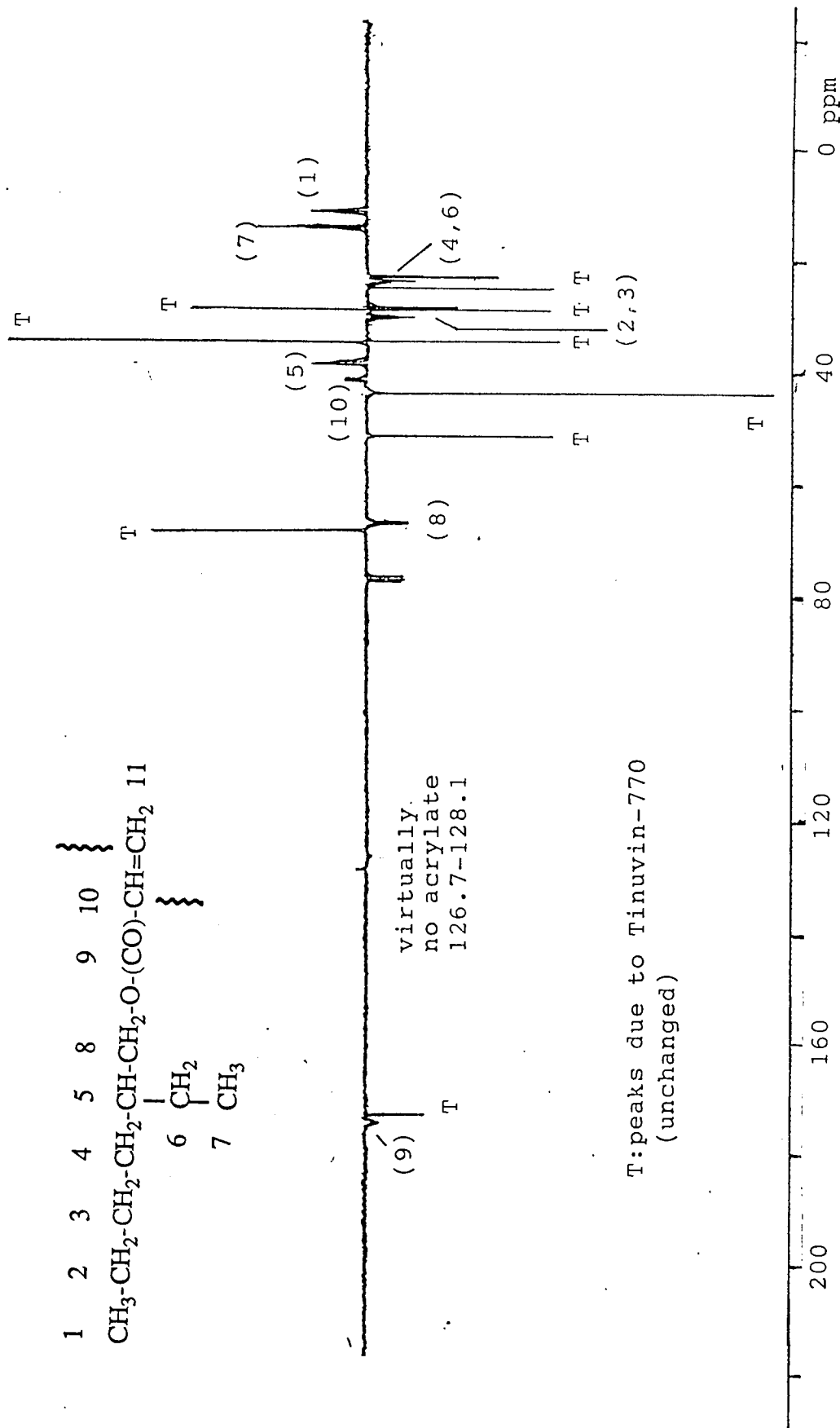


Figure 4.15.d Carbon-13 NMR spectra (in CDCl₃) of polymerised EHA with Tinuvin 770 without decalin at 180°C in the presence of DCP 0.005 molar ratio to total reagent under Argon atmosphere

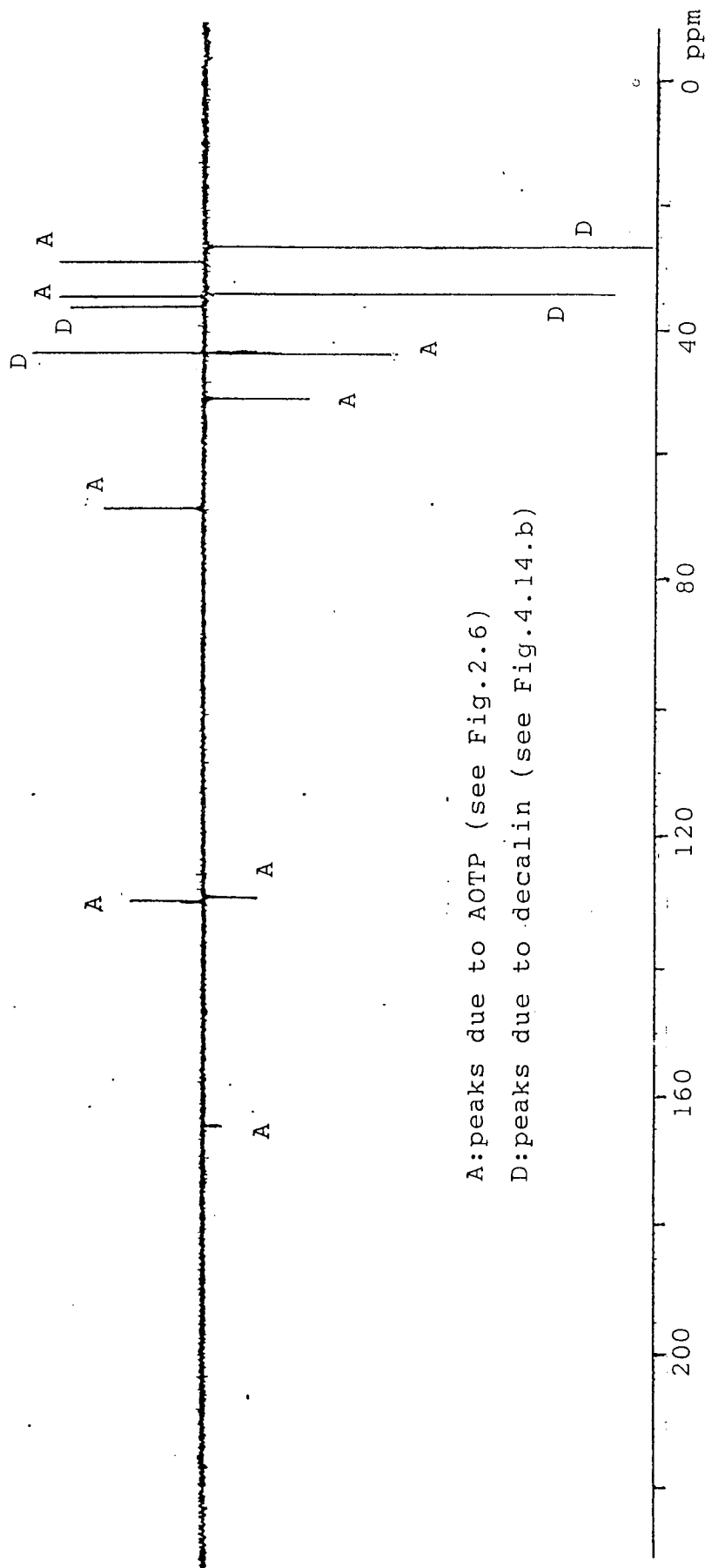
4.2.2.4 "Insitu" polymerisation of AOTP in NMR sample area

C^{13} NMR investigation has also been carried out "in-situ" in the sampling cavity of an NMR machine. Solution of 10% AOTP and DCP (0.005 molar ratio) in decalin (cis and trans) in the presence of small amount of deuterated-decalin was placed in NMR sample tube at 297°K and its C^{13} NMR spectra was recorded (Figure 4.16.a). The sample tube was removed and the temperature of the sample cavity of the NMR machine was increased to 373°K (for safety reasons the measurement was not carried out above that temperature). The sample tube was then inserted back in the sample cavity and the C^{13} NMR spectra were recorded again after 30 and 120 minutes (Figures 4.16.b and 4.16.c).

Carbon-13 NMR spectra of the AOTP solution in decalin (Figure 4.16.a) shows all similar peaks to those of its corresponding spectrum of fresh AOTP in Figure 2.6, with addition of decalin peaks at $\delta = 26.5$ [-CH₂- (-)], 33.9 [-CH₂- (-)], 36.0 [cis >CH- (+)] and 43.9 [trans >CH- (+)] ppm. When the decalin solution was heated up to 373°K, both -CH₂- peaks of the decalin split to four peaks at δ (ppm) = 24.1 (-), 26.45 (-), 31.1 (-) and 33.9 (-). This peak splitting also occurs when fresh decalin was heated and recorded at a similar temperature (Figure 4.16.d), which is due to reversible chain rotation of both decalin rings at high temperature, since when the decalin was cooled down and recorded at room temperature the four peaks became two peaks again, similar to that in Figure 4.16.a.

After 30 minutes heating at 373°K, trace of both unsaturation peaks of AOTP at δ (ppm) = 129.7 (-) and 128.5 (+) still appeared in this spectrum (Figure 4.16.b). Further reaction after 120 minutes (Figure 4.16.c) gives a similar spectrum to that of 30 minutes polymerisation (Figure 4.16.b), except that both unsaturation peaks of unreacted AOTP have completely disappeared. Like Spectrum of polymerised AOTP without decalin (Figure 4.14.b), Spectrum of in-situ polymerised AOTP in decalin for 30 and 120 minutes (Figures 4.16.b and 4.16.c) also show multiplet peaks at δ (ppm) = 67.2 - 67.3 (+). On the other hand, one of the >CH- peak due to decalin at δ (ppm) =

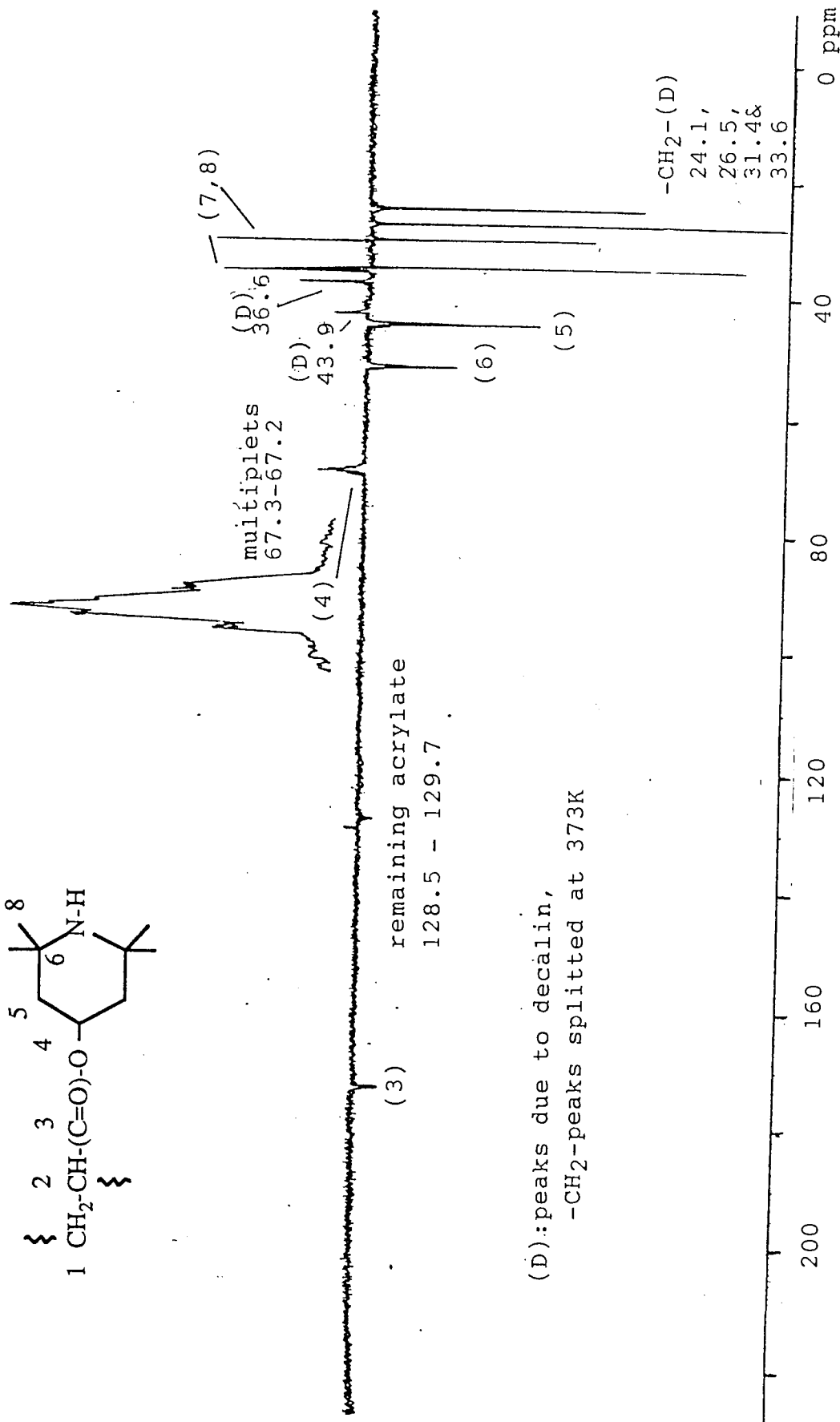
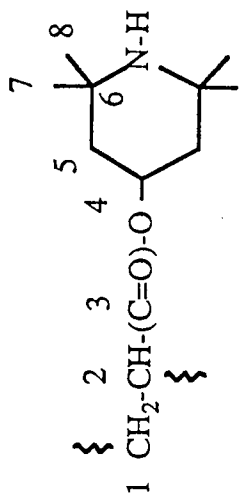
43.9 (+), which is recognised as that of trans >CH- (the more susceptible to radical attack than the cis), decreased sharply. This indicates that the decalin substrate also involves in the polymerisation reaction with the acrylate through hydrogen elimination from the >CH- group, which in turn may form grafting structures onto the polymerised AOTP backbone.



A: peaks due to AOTP (see Fig. 2.6)

D: peaks due to decalin (see Fig. 4.14.b)

Figure 4.16.a ^{13}C NMR-spectra of 10% AOTP solution in decalin at 296°K in the presence of DCP 0.005 molar ratio and small amount of deuterated decalin



(D): peaks due to decalin,
 -CH₂-peaks splitted at 373K

Figure 4.16.b ¹³C NMR-spectra of 10% AOTP solution in decalin at 373°K for 30 minutes in the presence of DCP 0.005 molar ratio and small amount of deuterated decalin

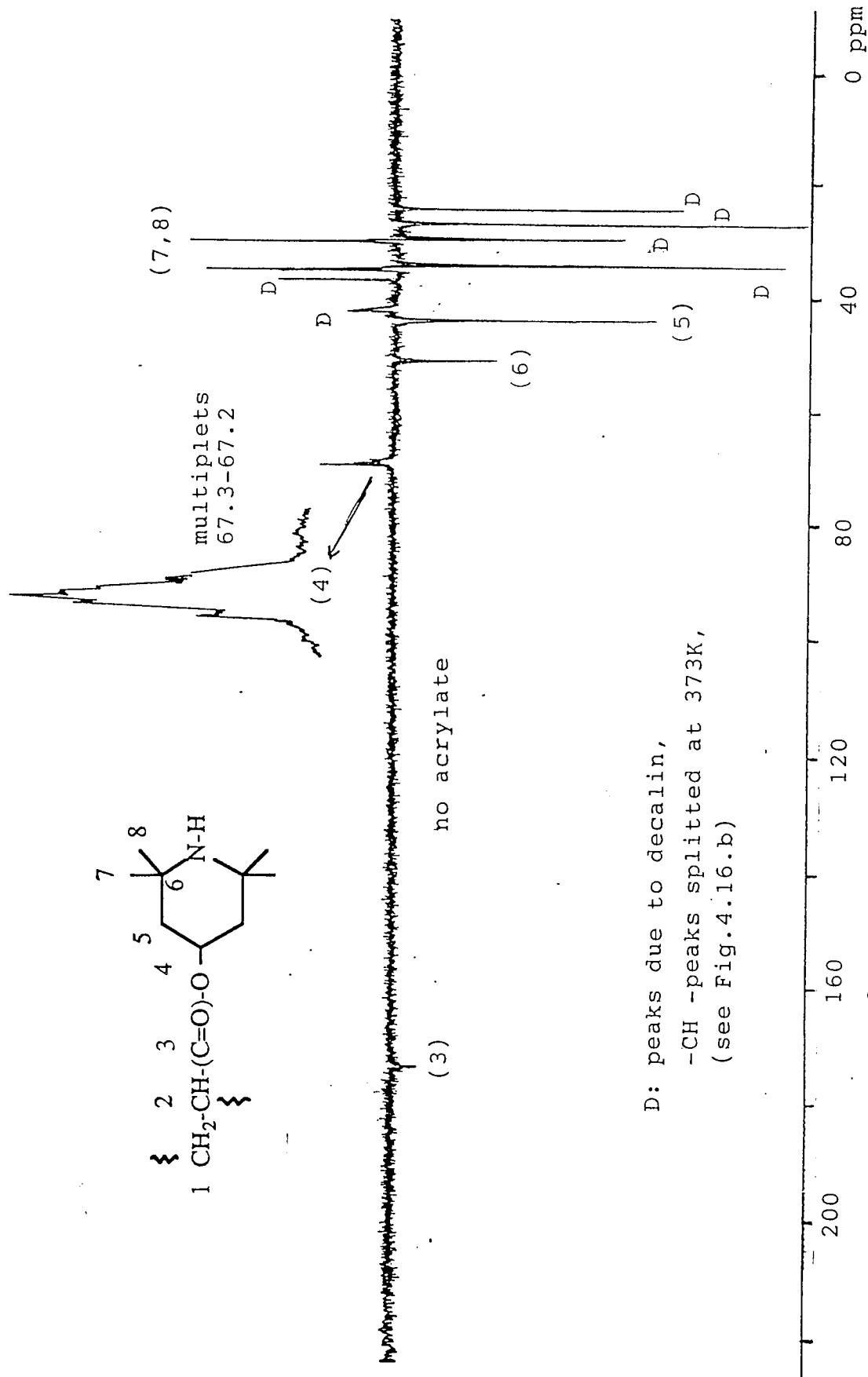


Figure 4.16.c ¹³C NMR-spectra of 10% AOTP solution in decalin at 373°K for 120 minutes in the presence of DCP 0.005 molar ratio and small amount of deuterated decalin

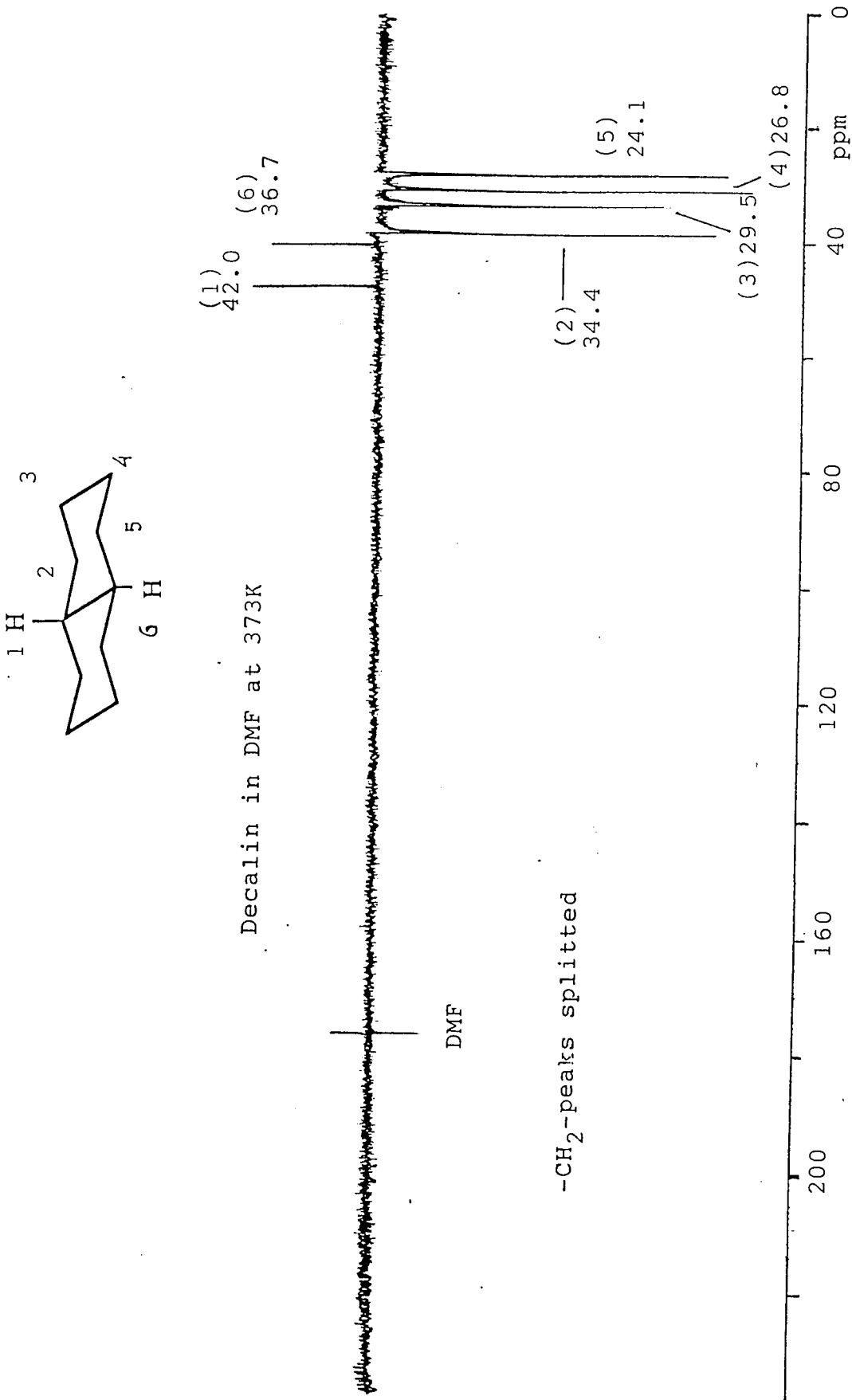


Figure 4.16.d ¹³C NMR-spectra of fresh decalin at 373°K for 30 minutes in the presence of small amount of deuterated decalin

4.2.2.5 Polymerisation of AOTP in isooctane

Further polymerisation of AOTP has also been carried out in a lower boiling point solvent, such as isooctane (bp 110°C). Although the polymerisation was only possible at reaction temperature below the boiling point, it was found from the NMR-measurement (Section 4.2.2.2), that even at 100°C the polymerisation of AOTP had been taken place after 30 minutes. The advantage of a polymerisation study in this system is that the solvent can be easily evaporated to give unevaporated polymer residue. Any remaining unevaporated solvent is expected to be due to grafting of the solvent molecule onto the polymerised AOTP.

Around 2 gram of the correct amount of AOTP, TMPTA and their mixture (TMPTA/AOTP, weight ratio = 2 : 8) were separately polymerised in 5 ml of isooctane at 110°C (reflux) for 30 minutes in the presence of DCP 0.005 molar ratio, under Argon atmosphere. The reaction products were vacuum evaporated quantitatively at room temperature for constant weight. Increase in weight of the residues were measured gravimetrically.

Results shown in Table 4.5, indicate that when AOTP alone was polymerised in isooctane under the above conditions, the polymer residue after exhaustive evaporation exhibits weight increase of around 18.2%. This weight increase is associated with attachment of the hydrocarbon molecules onto the polymerised AOTP. However, when TMPTA was polymerised in isooctane at the same condition, within seconds the reaction mixture solidified and precipitated out from the solution. The polymerised product was found to give no weight increase from the original weight of the monomer. In this case, the solvent molecule may not be able to compete with TMPTA monomer to participate in the polymerisation due to high reaction rate of TMPTA homopolymerisation. On the other hand, when AOTP was polymerised in the presence of TMPTA (weight ratio to AOTP = 2 : 8), the TMPTA-AOTP copolymerisation product exhibited around 5.3% weight increase, which indicates that in this system, there is a possibility of solvent grafting onto the TMPTA/AOTP copolymer.

Table 4.5 Weight increase of exhaustively evaporated polymerised AOTP, AOTP/TMPTA (weight ratio = 8 : 2) and TMPTA alone in isooctane in the presence of DCP 0.005 molar ratio at 110°C under Argon atmosphere.

Additives	% increase of weight
AOTP only	18.2
TMPTA/AOTP (2:8)	5.3
TMPTA only	--

4.3 DISCUSSIONS

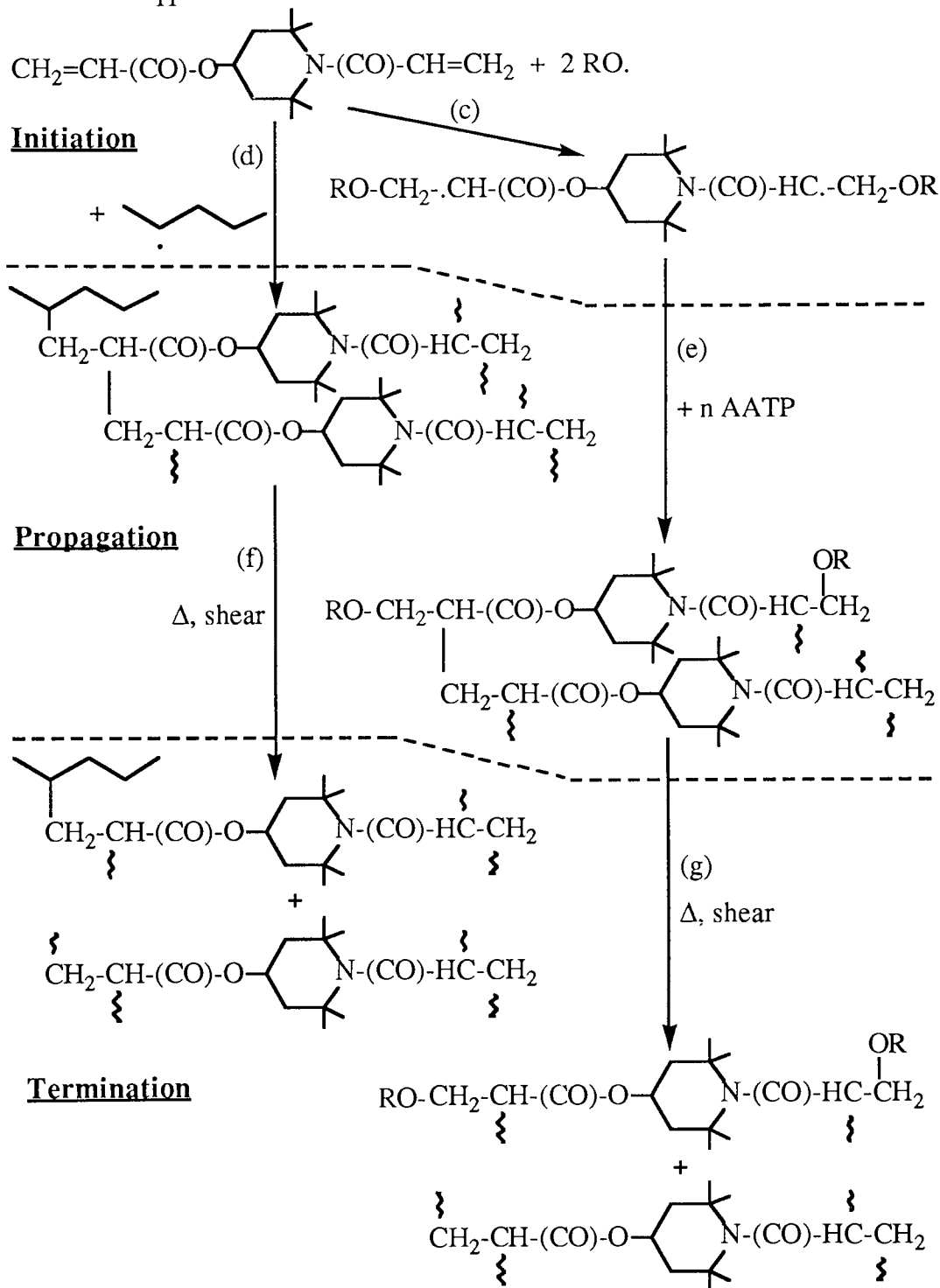
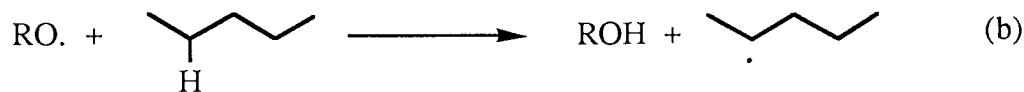
4.3.1 Reactive processing mechanism of AATP and AOTP in polymer melts

Like other polyenes monomers, when AATP (a bisacrylic nitroxyl precursor) is reactively processed in polypropylene melts, several competitive chemical processes may take place. For example, linear homopolymerisation of the more reactive acrylic group may take place leaving the second pendant acrylic group unreacted. Further linear homopolymerisation may be followed by intra- and inter-crosslinking reactions by the pendant groups, in addition to grafting of the antioxidant monomer onto the polymer backbone. The first process preferably takes place at the very beginning of processing, in which the rate constant ratio of linear homopolymerisation relative to the crosslinking reaction by the acrylic pendant group is high⁽⁵⁸⁾.

The ratio of rate constant of acrylic ester against acrylic amide groups found in the literature⁽⁹⁹⁾ at 180°C is about 1.3. Therefore the extent of the crosslinking of AATP during reactive processing may take place in the early conversion, which results in low possibility of linear homopolymerisation of the AATP. This prediction is in agreement with the experimental results that even after only 3 minutes processing (Table 4.3) there was no sign of the formation of linear (DCM extractable) AATP homopolymer (almost 100% is unextractable). In addition, from the FTIR spectra of the AATP masterbatch processed at 3 minutes in the presence of peroxide (Figure 4.3) the unsaturation peak (at 1608 cm⁻¹) had diminished, indicating that the entire acrylic group has been polymerised or crosslinked. Almost the entire AATP in the masterbatch (out of 20% of total AATP in the original masterbatch) had been crosslinked and grafted in the gel, as the gel contained around 19.7% AATP and 7.3% polymer matrix (total gel = 27%)

As the processing continued to 10 minutes, the percentage of insoluble gel in the AATP masterbatch decreased considerably. This indicates that the crosslinked

insoluble residue formed at 3 minute processing, might break down due to heat and shear to form smaller fraction and become distributed along with the polymer matrix (the small fraction of crosslinked AATP become soluble in xylene). The fact that polymerised AATP is insoluble in DCM and even after 10 minutes processing the binding efficiency of AATP is 100%, suggests that the bound-AATP consists of the small fraction (xylene soluble) of crosslinked AATP in addition to the grafted antioxidant onto the polypropylene backbone. The mechanism of AATP binding in polypropylene melts, therefore, may be visualised as shown in Scheme 4.3.



Scheme 4.3 Suggested mechanism of reactive processing of AATP in polypropylene in the presence of DCP 0.005 molar ratio, processed at 180°C for 10 minutes under closed mixing conditions

In contrast, when masterbatches containing 10 and 20% of AOTP (a monoacrylic secondary amine) were reactively processed, there was no high torque maximum. Further reactive processing of AOTP masterbatches at different times (2.5, 5 and 10 minutes) did not show any gel content, i.e. the entire masterbatches were soluble during Soxhlet extraction in xylene, which indicates that the AOTP (monoacrylic derivative) does not undergo crosslinking. Ten minutes reactive processing of this antioxidant gave very low absorption of unsaturation at 1617 cm^{-1} in the FTIR spectra, see Figure 4.4. However, this antioxidant exhibited low binding efficiency (50%), in spite of the fact that almost the entire acrylic group has been polymerised. FTIR spectra of DCM extract of AOTP masterbatch, on the other hand, showed trace of unsaturation peak (around 10% of the original peak). The fact that the AOTP homopolymer (polymerised with and without liquid hydrocarbon) is DCM soluble (extractable), suggesting that the bound AOTP (50%) may contain only the grafted-AOTP onto the polymer. Therefore, during 10 minutes reactive processing of AOTP in polymer melts the following chemical reactions may take place.

1. Reversible linear homopolymerisation of the AOTP to produce extractable polymerised AOTP (~ 40%) and unreacted AOTP (~ 10%)
2. Grafting of AOTP growing homopolymer onto the polymer (PP) backbone (~ 50%).

Measurement of molecular weight distribution of AATP and AOTP masterbatches processed for 10 minutes at 180°C under closed mixing conditions, gave average molecular weights (M_n and M_w) in between those of unprocessed polypropylene and processed polypropylene with DCP. Processing of polypropylene in the presence of peroxide but in the absence of antioxidant, leads to chain scission⁽⁵⁾. In the presence of AATP or AOTP the extent of the chain scission may be reduced or inhibited, due to consumption of the peroxide by the antioxidant.

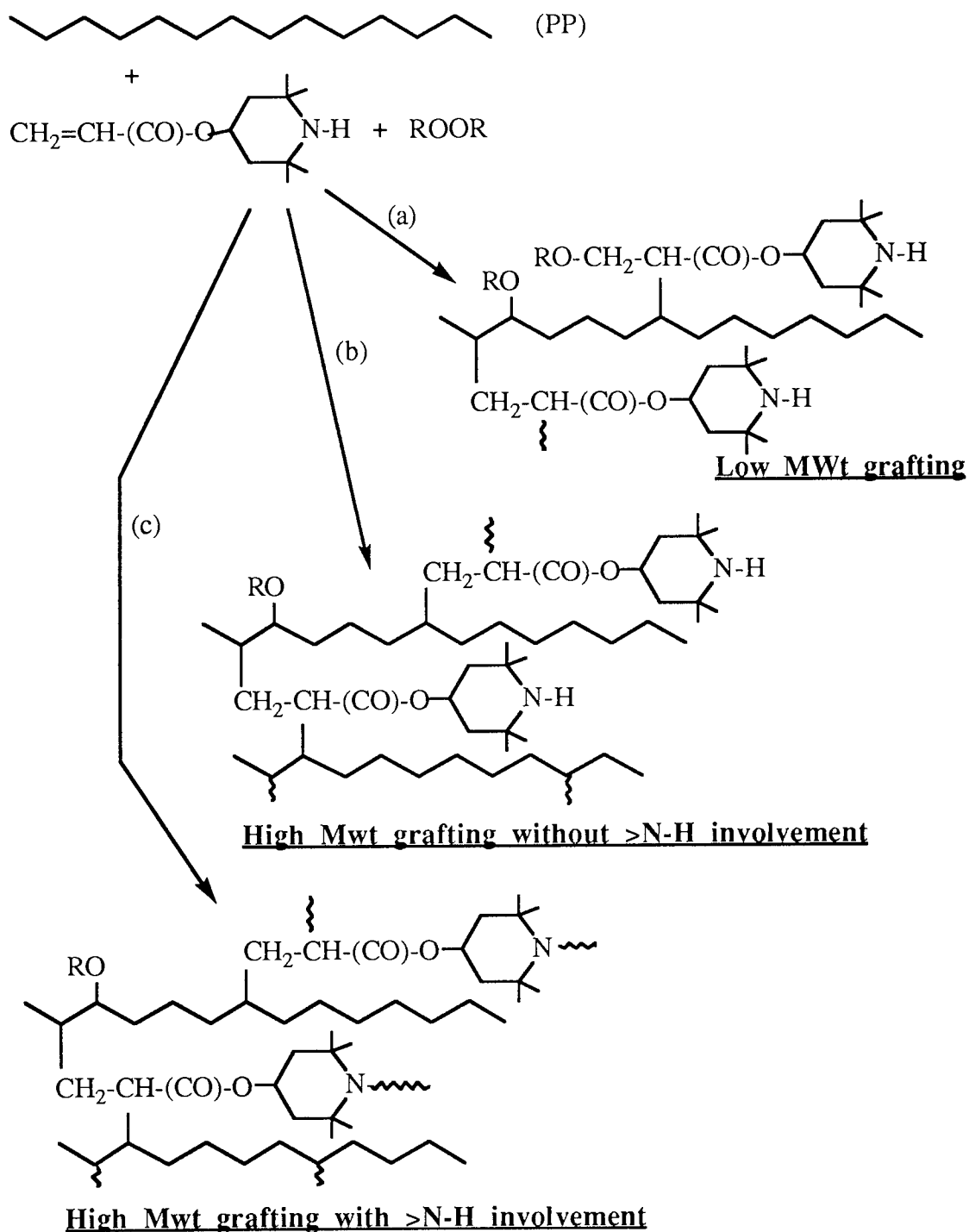
Surprisingly, molecular weight distribution (MWD) data of AOTP masterbatches showed high molecular weight (M_w) peaks, which exhibit M_n around 50 - 200 times higher than those of the corresponding low M_w peaks. These M_n

values of the high MWt component might not be realistic, because the MWt calibration using Mark-Houwink equation, $[\text{intrinsic viscosity}] = K' M^a$, is valid only for linear polymers. However, the deviation of the MWt calibration itself indicated the present of "non-linear" polymer in the system (i.e. grafted or crosslinked polymer).

It is expected from monomers containing one acrylate group, like AOTP, to generate linear homopolymer during polymerisation (112). The question is, *how does AOTP propagate a grafted or crosslinked structure during reactive processing?* It is likely, therefore, that there may be another reactive group in the antioxidant which also produces radical and functions as another active centre for polymerisation. This will be discussed in the next section (Section 4.3.2). In contrast, masterbatches containing 10 and 20% of AATP (bisacrylic) did not exhibit a high MWt peak. This is in agreement with the evidence that AATP formed highly crosslinked residue, which is even insoluble in the polymer solvent (m-dichlorobenzene), and thus is excluded from the GPC analysis.

The low MWt component of AOTP masterbatch was soluble in toluene, although exhaustive Soxhlet extraction in toluene did not remove completely the low MWt component from the masterbatch. The residue, which was xylene soluble (Xylene-extract, see Section 4.2.1.2), contained both low and high MWt components, whereas the toluene extract (Toluene-extract) exhibited only a small amounts of the high MWt component (see Table 4.4 and Figure 4.7). It was found that the content of AOTP bound in the toluene extract is higher than that in the fresh AOTP masterbatch, whereas the xylene extract contained less AOTP bound than the fresh masterbatch. Therefore, the nature of bound AOTP in the masterbatch may be as follows,

1. The majority of bound AOTP is present in the toluene extract, which contains the lower MWt component, in the form of grafted-AOTP onto polymer backbone.
2. The rest of the bound AOTP is in the "crosslinked" but xylene soluble structure represented in the higher MWt component (probably with more than one polymer backbone), see Scheme 4.4.



Scheme 4.4 Suggested mechanism of formation of high MWt fraction without and with involvement of >N-H group in masterbatch containing AOTP

4.3.2 Mechanism of AOTP polymerisation in solution

Decalin (decahydronaphthalene, b.p. 190°C) contains two tertiary hydrogen atoms similar to that of polypropylene, which are susceptible to hydrogen elimination to form radicals (4,113). Model reactions of reactive processing of antioxidant in polypropylene can be adequately carried out in this hydrocarbon at a similar standard processing temperature (180°C).

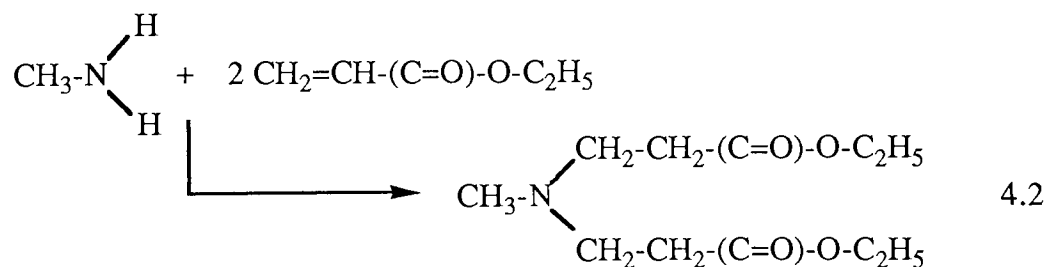
Infrared absorption band (stretching) of an >N-H group of a primary and secondary amines appear in the range of 3500 - 3200 cm^{-1} . In a condensed phase (liquid film and KBr disc) the bands are less intense and shifted toward a lower wave length(114), whereas in dilute solution free >N-H band clearly appears near 3500 cm^{-1} . In solid polymer, the >N-H absorption can still be identified as shown by Grassie and Zulfiqar(115). They studied thermal degradation of polyurethane and observed the disappearance of the >N-H band at 3330 cm^{-1} , due to formation of isocyanate monomer. The peak at 3317 cm^{-1} in the FTIR spectra of AOTP and its disappearance when the AOTP was polymerised with and without decalin, therefore, was due to >N-H group of the AOTP monomer, which underwent "interaction" during polymerisation. However, when a nitroxyl precursor containing 2 secondary amines but without acrylic group (Tinuvin 770) was polymerised without and with double-molar of 2-ethylhexylacrylate (EHA) at similar conditions, the peak at 3321 cm^{-1} due to the >N-H group of the Tinuvin 770 remains unchanged even after deliberate polymerisation of the EHA. This suggests that there was no "inter-molecular interaction" between the >N-H group of Tinuvin 770 with the EHA.

Using proton NMR analysis the >N-H peak of the AOTP even before polymerisation could not be observed. This may be due to that the N-atom of the secondary amine, which possesses electric quadrupole, interacts with both the electric and magnetic fields of the hydrogen atom(93). Consequently, the life time of the excited state hydrogen is short, which in turn gives rise to low intensity and broad absorption lines in the NMR spectra. Nevertheless, the proton NMR analysis (see

Figure 4.12.a), clearly observed disappearance of acrylic ($\text{CH}_2=\text{CH}-$) peaks ($\delta = 6.2 - 5.5$ ppm), due to the complete polymerisation of the group. On the other hand, the spectra of polymerised AOTP, both without and with decalin, showed formation of new peaks, especially at $\delta = 2.3$ ppm. Elucidation of this peak may indicate the formation of new $-\text{CH}_2-$ group possibly $>\text{N}-\text{CH}_2-$ ($\delta = 2.1 - 2.5$ ppm) as ordinary $-\text{CH}_2-$ group of saturated acrylate appears in the region of $\delta = 1 - 2$ ppm⁽⁹³⁾.

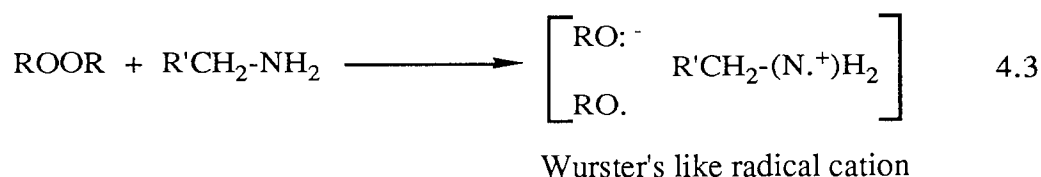
Complete polymerisation of AOTP upon heating in the presence of DCP 0.005 molar ratio at 180°C for 30 minutes, also could be shown by Carbon-13 NMR analysis of the polymerised product, see Figure 4.14.a, which shows that the unsaturation peaks of AOTP at $\delta_{\text{C}} = 129.7$ (-) and 128.5 (+) ppm disappeared after polymerisation. As a result, three new peaks at $\delta = 41.2$ (+) ppm, 49.0 (-) ppm and 63.5 (+) ppm appeared as well as multiplicity of peak at $\delta = 67.3 - 67.2$ (+) ppm. The first two peaks possibly due to $-\text{CH}(\text{CO})-$ and $-\text{CH}_2-$ groups of saturated acrylate, which formed during polymerisation, whereas the rest may be due to formation of an $>\text{N}-\text{CH}<$ group. In addition, Carbon-13 NMR spectra of polymerised AOTP even the one without decalin showed higher intensity of the $>\text{C}<$ (quaternary Carbon) peak at $\delta = 51.4$ ppm (-), see Figures 4.14.a and 4.14.c. This may be attributed to the formation of the $>\text{N}-\text{CH}_2-$ group, $\delta = 40 - 60$ (-) ppm⁽⁹⁴⁾, since the possibility of formation of the $>\text{C}<$ group from the interaction with decalin had been excluded.

It has been reported⁽¹¹⁶⁾ that primary and secondary amines react readily with styrene upon standing overnight at room temperature. Mozingo and Mc.Cracken⁽¹¹⁷⁾ observed a nucleophilic disubstitution between methyl amine and ethyl acrylate.



Moreover, amine compounds have been reported to interfere in radical polymerisation of vinyl monomers. Bevington⁽¹¹⁸⁾ showed retardation by diphenylpicrylhydrazyl in the polymerisation of styrene initiated by azoisobutyronitrile as radical generator. The

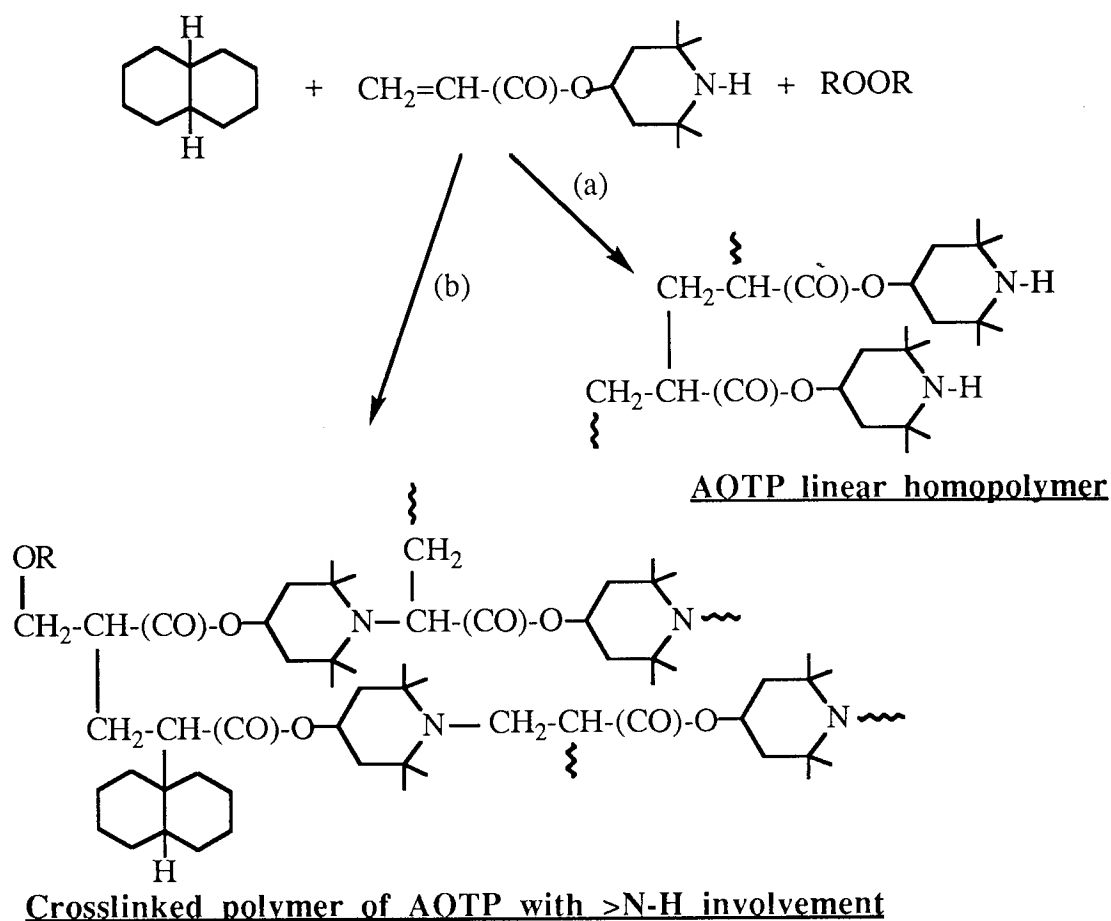
picrylhydrazyl was postulated to react with styrene growing polymer to produce styrene monomer again. Yates and Ihrig⁽¹¹⁹⁾ reported the effect of various aromatic amines in the inhibition of oxidation and polymerisation of methyl methacrylate. The mechanism by which the amines involved in the inhibition was similar to those of phenolic compounds. Beside interaction with monomer, the amines may also react with peroxy radical of the initiator to form unreactive products. Reaction of some aliphatic amines (primary, secondary and tertiary) with tert.butylhydroperoxide has been studied by De La Mare⁽¹²⁰⁾. It was suggested that in the reaction a "Wurster's like" radical cation was formed as intermediate, which can further interact with either peroxide or monomer molecules.



The structure of the radical involved in the inhibition reaction has been investigated by Coppinger and Swallen⁽¹²¹⁾ using ESR spectroscopy. They observed an amine oxide free radical. From the above discussions the possibility of an >N-H group involvement in the polymerisation of AOTP may be through the following reactions,

1. Nucleophilic substitution of the >N-H to the acrylic group, as has been proposed by Mozingo et al.
2. Reaction of the >N-H group with peroxide as radical generator either by hydrogen elimination or via formation of a Wurster's like radical cation.
3. Inhibition of acrylic polymerisation by the amine via reaction of the radical cation with acrylic monomer, this will be discussed in Section 5.3.1.

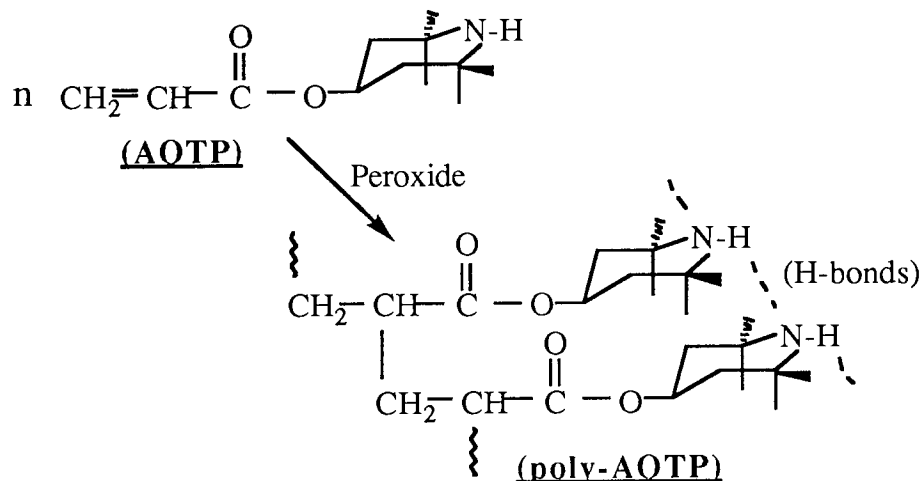
Therefore, the structure of polymerised AOTP in decalin in the presence of DCP 0.005 molar ratio, may be suggested as shown in Scheme 4.5, although the fact that there was no external-interaction between >N-H of Tinuvin 770 with EHA during polymerisation is still a mystery to be solved.



Scheme 4.5 Suggested chemical structure of polymerised AOTP in decalin in the presence of DCP 0.005 molar ratio at 180°C for 30 minutes under Argon atmosphere

It should be borne in mind that there is no evidence that >N-H group of AOTP reacts entirely with the acrylate group, as this interaction also in competition with the main homopolymerisation of the acrylate. On the other hand, it was shown in the FTIR spectra of polymerised AOTP with and without decalin (Figures 4.9 and 4.10) that the entire >N-H absorption diminished to zero. Therefore, there may be another possibility which causes the disappearance of >N-H peak at 3317 cm^{-1} in the FTIR spectra of polymerised AOTP, i.e. when the AOTP was polymerised the hindered piperidine groups became very close to each other and crowded (one hindered piperidine group per unit of acrylate). This may create a conformational strain in the hindered piperidine ring and formation of hydrogen bonds among the >N-H groups, which in turn dissipates the vibration energy of the >N-H bond, i.e. broadening of the >N-H

absorption band⁽¹²²⁾, see Scheme 4.6 for the possibility of "physico-chemical interaction" between the >N-H groups. This is in agreement with the fact that no >N-H peak disappearance of Tinuvin 770 when polymerised with EHA. In this case the Tinuvin 770 molecules are still freely mobile since they do not chemically attach onto the polymerised EHA.



Scheme 4.6 Possibility of "physico-chemical interaction" between the adjacent >N-H groups in polymerised AOTP, which cause dissipation of vibration energy of the >N-H bond and give rise to the disappearance of the >N-H peak in the FTIR spectra of the polymerised AOTP

Polymerised AOTP was found to interact with isooctane during polymerisation in the presence of DCP 0.005 molar ratio. When the AOTP was polymerised in iso-octane at similar conditions but in the presence of TMPTA (ratio = 2/8 to the AOTP), the amount of iso-octane grafted on to the polymerised product was lower, in spite of the fact that during reactive processing of AOTP with TMPTA (ratio = 2/8 to the AOTP), the binding efficiency was higher than that for without TMPTA. The amount of isooctane attached was even undetectable when the TMPTA was polymerised alone in the solvent at similar condition. It is likely, therefore, that the presence of coagent (TMPTA) during reactive processing may improve the binding efficiency of the AOTP both by formation of coagent-antioxidant copolymer, which is unextractable, in addition to grafting of the copolymer onto the polymer backbone.

CHAPTER 5

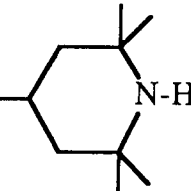
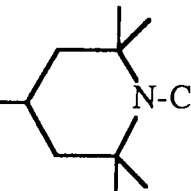
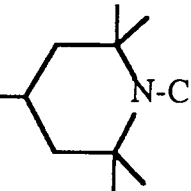
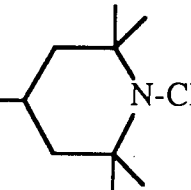
REACTIVE PROCESSING AND STABILISING ACTIVITY OF N-ALKYLATED ACRYLIC AND METHACRYLIC DERIVATIVES OF STABLE NITROXYL RADICAL PRECURSORS

5.1 OBJECTS AND METHODOLOGY

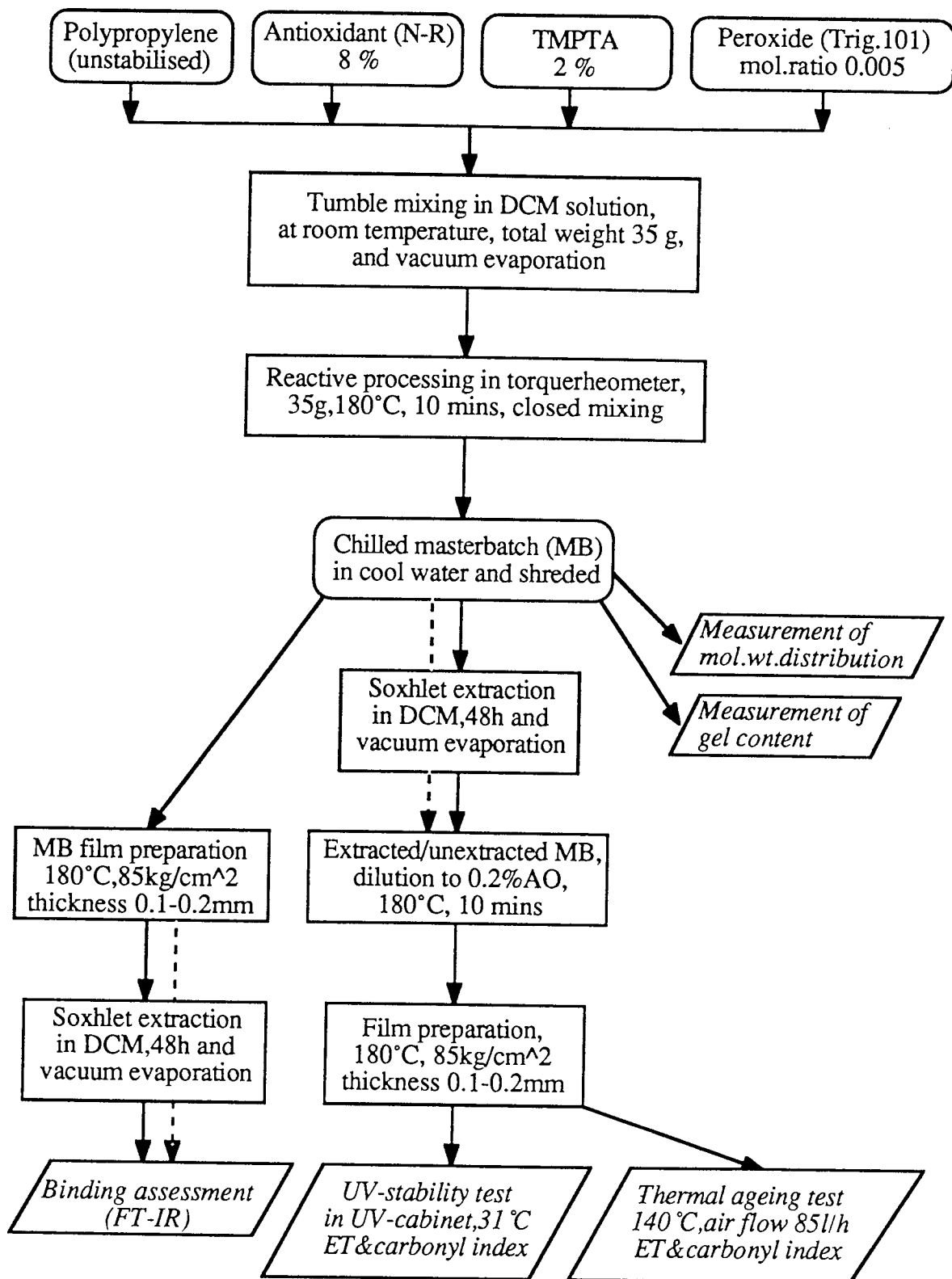
From results discussed in Chapters 3 and 4, it was shown that the photo-stabilising activity of 4-acryloyloxy 2,2,6,6-tetramethyl piperidine (AOTP) decreased when it was attached to the PP backbone via reactive processing. It is well known that the hindered amine group of the nitroxyl precursors is the active side which plays the main role in the stabilisation action^(43,44). Structural changes on the hindered amine side of such molecules during reactive processing may interfere with nitroxyl radical generation, which in turn can affect the stabilisation activity of such antioxidants. One of the reasons of the decrease in the stabilising activity of bound AOTP may be due to side reaction on the secondary amine group (>N-H) which is susceptible to radical attack during processing.

The objects of the work in the first part of this chapter is intended to investigate the effect of various >N-alkyl groups on the reactive processing and stabilising activity of N-alkylated derivatives of acrylic nitroxyl precursors, shown in Table 5.1, which were synthesised using the procedures mentioned in Section 2.2 (Chapter 2). Various N-alkyl groups have been selected in the synthesis, such as N-methyl (>N-CH₃), N-ethyl (>N-CH₂-CH₃) and N-benzyl (>N-CH₂-C₆H₅).

Table 5.1 Various N-alkylated nitroxyl precursors containing acrylic group

Structure number	Chemical structure, name and molecular weight (MWt)	Abbreviation
VIII	$\text{CH}_2=\text{CH}-(\text{C}=\text{O})-\text{O}$ -  4-acryloyloxy 2,2,6,6-tetramethyl piperidine (MWt=211)	AOTP
XI	$\text{CH}_2=\text{CH}-(\text{C}=\text{O})-\text{O}$ -  4-acryloyloxy 1,2,2,6,6-pentamethyl piperidine (MWt=225)	AOPP
XII	$\text{CH}_2=\text{CH}-(\text{C}=\text{O})-\text{O}$ -  1-ethyl 4-acryloyloxy 2,2,6,6-tetramethyl piperidine (MWt=239)	EATP
XIII	$\text{CH}_2=\text{CH}-(\text{C}=\text{O})-\text{O}$ -  1-benzyl 4-acryloyloxy 2,2,6,6-tetramethyl piperidine (MWt=301)	BATP

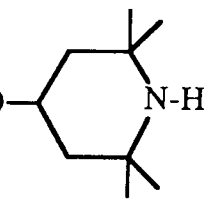
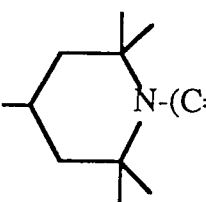
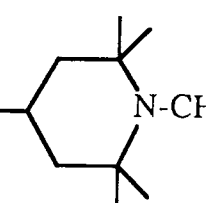
The above N-alkylated nitroxyl-precursors were then reactively processed separately at the best conditions optimised for secondary amine nitroxyl precursor (AOTP) discussed in Section 3.2.4, i.e. with TMPTA as coagent (ratio = 2:8) in 10% masterbatches at 180°C for 10 minutes in closed mixing conditions, but in the presence of Trigonox-101 0.005 molar ratio as radical initiator. Detail of the procedure is shown in Scheme 5.1.



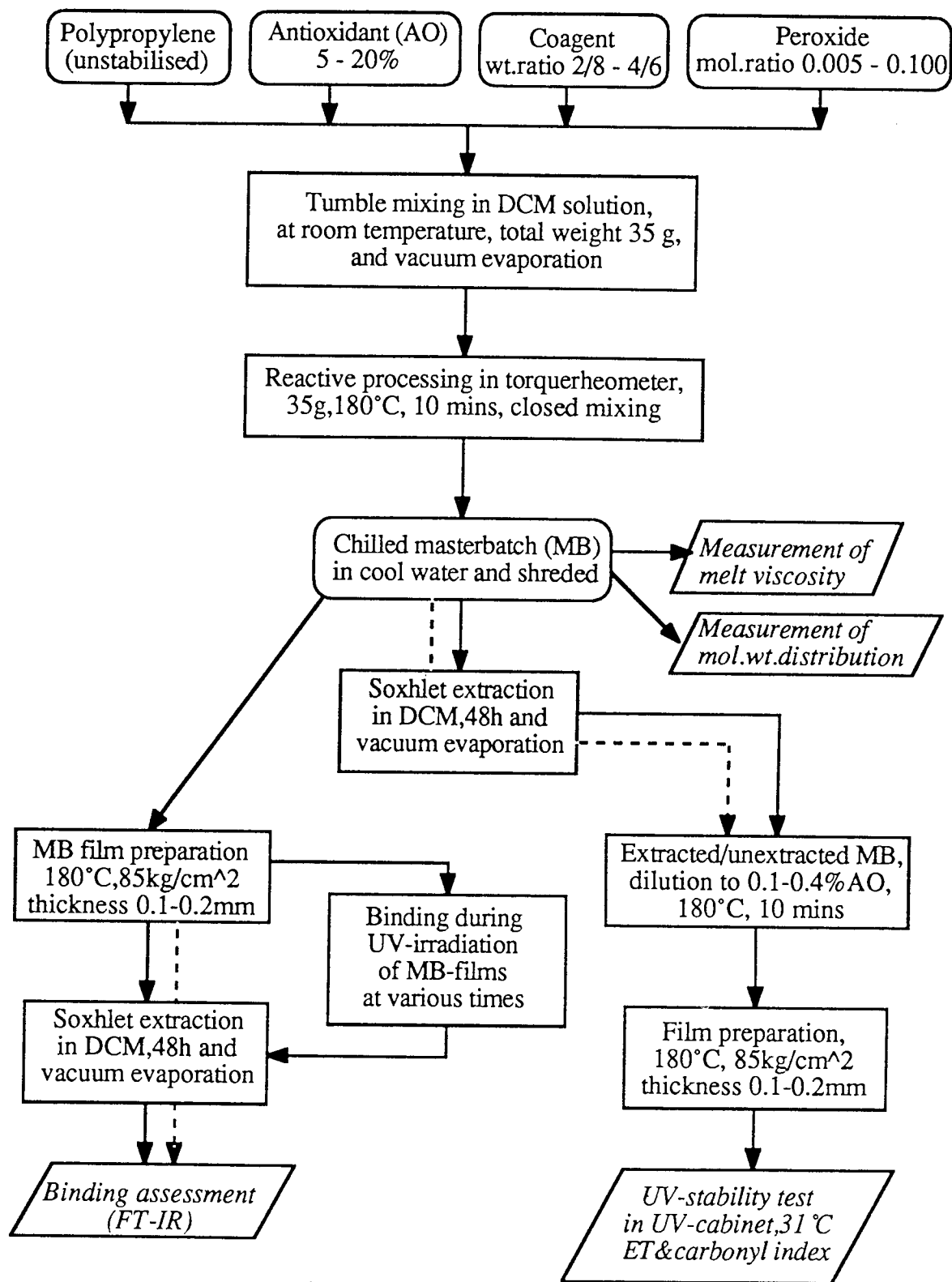
Scheme 5.1 Reactive processing and stability tests of masterbatches containing >N-alkylated acrylic nitroxyl precursors, processed with TMPTA (weight ratio = 2:8) in the presence of Trigonox 101 0.005 molar ratio at 180°C for 10 minutes under closed mixing conditions

The second part of this chapter deals with nitroxyl precursors containing bis and monomethacrylic group(s), see Table 5.2. Analogy of their binding and stabilising behaviours with their corresponding bis and monoacrylic derivatives discussed in Chapters 3 and 4, was investigated. The MOTP and MMTP were synthesis from the preparative procedure mentioned in Section 2.2, whereas the MOPP was supplied by Ancomer Ltd. and used directly without further purification.

Table 5.2 Various nitroxyl precursors containing methacrylic group(s)

Structure number	Chemical structure, name and molecular weight (MWt)	Abreviation
XIV	$\text{CH}_2=\text{C}(\text{CH}_3)-(\text{C}=\text{O})-\text{O}$  4-methacryloyloxy 2,2,6,6-tetramethyl piperidine (MWt=225)	MOTP
XV	$\text{CH}_2=\text{C}(\text{CH}_3)-(\text{C}=\text{O})-\text{O}$  1-methacryloyl 4-methacryloyloxy 2,2,6,6-tetramethyl piperidine (MWt=293)	MMTP
XX	$\text{CH}_2=\text{C}(\text{CH}_3)-(\text{C}=\text{O})-\text{O}$  4-methacryloyloxy 1,2,2,6,6-pentamethyl piperidine (MWt=239)	MOPP

The above antioxidants were processed in PP at various concentration without and with different coagents in the presence of DCP at various molar ratio at 180°C for 10 minutes under closed mixing conditions, see Scheme 5.2 for the general procedure.

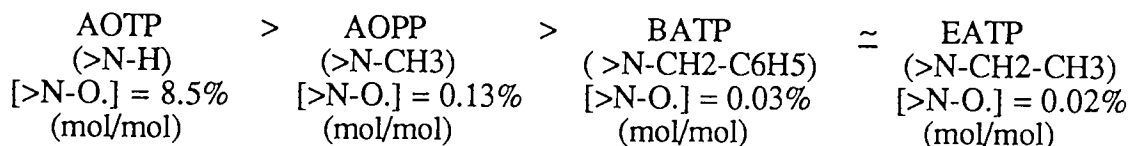


Scheme 5.2 A schematic diagram of reactive processing procedure and photostabilisation test of methacrylic-containing nitroxyl precursors in polypropylene

5.2 RESULTS

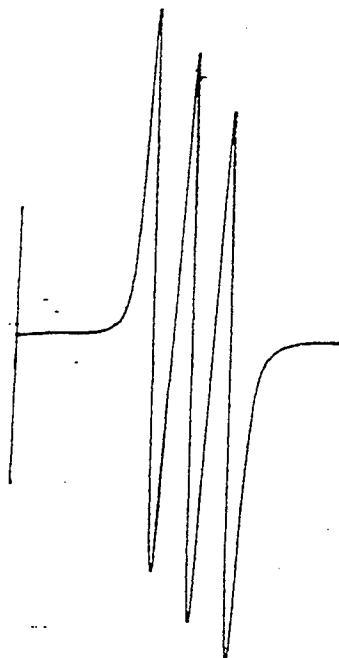
5.2.1 Reactive processing of N-alkylated nitroxyl precursors containing acrylic group in conjunction with TMPTA as coagent

For preliminary investigation, 0.25 ml of benzene solutions, each containing 2.5×10^{-5} mol of AOTP and different N-alkylated nitroxyl precursors (AOPP, EATP and BATP) were added separately to an equimolar of m-chloroperbenzoic acid in 0.25 ml of benzene solution at room temperature in an ESR sample tube. The nitroxyl radical formation was then measured "in situ" after 10 minutes reaction, under air atmosphere, in the presence of internal reference solution containing 2×10^{-6} mol of CuSO_4 using ESR spectroscopy, see Figure 5.1, see Figure 4.8 for the ESR spectra of reference solution. It was found that the percentage of nitroxyl conversion, i.e. molar ratio of nitroxyl radical formed from the corresponding antioxidant is in the order of :

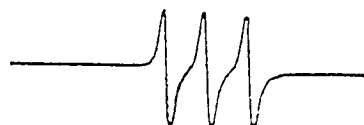


This suggests that the >N-R groups are less susceptible to nitroxyl formation during the oxidation than the >N-H group.

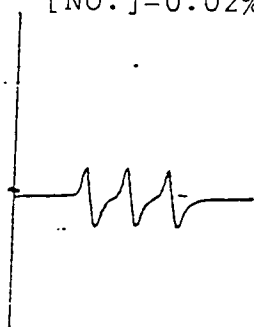
(A) AOTP+oCPBA
 amplification=1x1
 [NO.]=8.5%



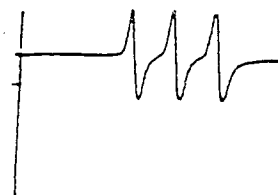
(B) AOPP+oCPBA
 amplification=2x10
 [NO.]=0.13%



(C) EATP+oCPBA
 amplification=2x10
 [NO.]=0.02%



(D) BATP+oCPBA
 amplification=2x10
 [NO.]=0.03%



Note:

oCPBA : o-chloroperbenzoic acid

Figure 5.1 ESR spectra of various benzene solutions each containing 2.5×10^{-5} mol of secondary and tertiary amine nitroxyl precursors, i.e. (A) AOTP amplification 1×1 , (B) AOPP amplification 2×10 , (C) EATP amplification 2×10 and (D) BATP amplification 2×10 , after 10 minutes oxidation with equimolar of m-chloroperbenzoic acid at room temperature, the nitroxyl radical concentration was calculated using reference solution containing 2×10^{-6} mol of CuSO_4 (see Figure 4.8 for the ESR spectra, amplification 1×100)

Reactive processing of masterbatches containing 10% of N-alkylated nitroxyl precursors and TMPTA (weight ratio 2:8) in the presence of Trigonox 101 0.005 molar ratio was carried out using the procedure in Scheme 5.1. Similar to AOTP, the N-alkylated analogous did not give any torque maximum during reactive processing of these derivatives, indicating no crosslinking reaction during processing. To study the effect of the different N-alkyl groups on the MWt, the masterbatches were further analysed using GPC, and their molecular weight distribution (MWD) curves were compared to that of masterbatch containing AOTP in combination with TMPTA in Figure 5.2. It was shown that all masterbatches containing N-alkylated nitroxyl precursors also exhibit high molecular weight peak similar to that of the analogous samples containing AOTP.

When the percentage of these high-MWt components were calculated from the peak area ratio, however, the values were found to be between 5 - 6 %, which is lower than that produced from AOTP masterbatch (see Table 5.2). In addition, when the high MWt peaks were calibrated separately, they gave number average molecular weight (M_n) around $670 - 760 \times 10^4$. These values are also lower than that of high-MWt component of AOTP masterbatch ($M_n = 1155 \times 10^4$). This indicates that the N-alkyl groups on the amide side have reduced formation of high-MWt component in masterbatches containing N-alkylated nitroxyl precursors.

Results of the binding efficiency (calculated after subtraction of absorbance due to TMPTA) was shown in Table 5.2 and Figure 5.3, which indicates that there were no significant differences on of N-alkylated derivatives (AOPP, EATP and BATP) when compared to that of AOTP, processed with the same amount of TMPTA at similar conditions, see also Tables 3.7 and 3.11.

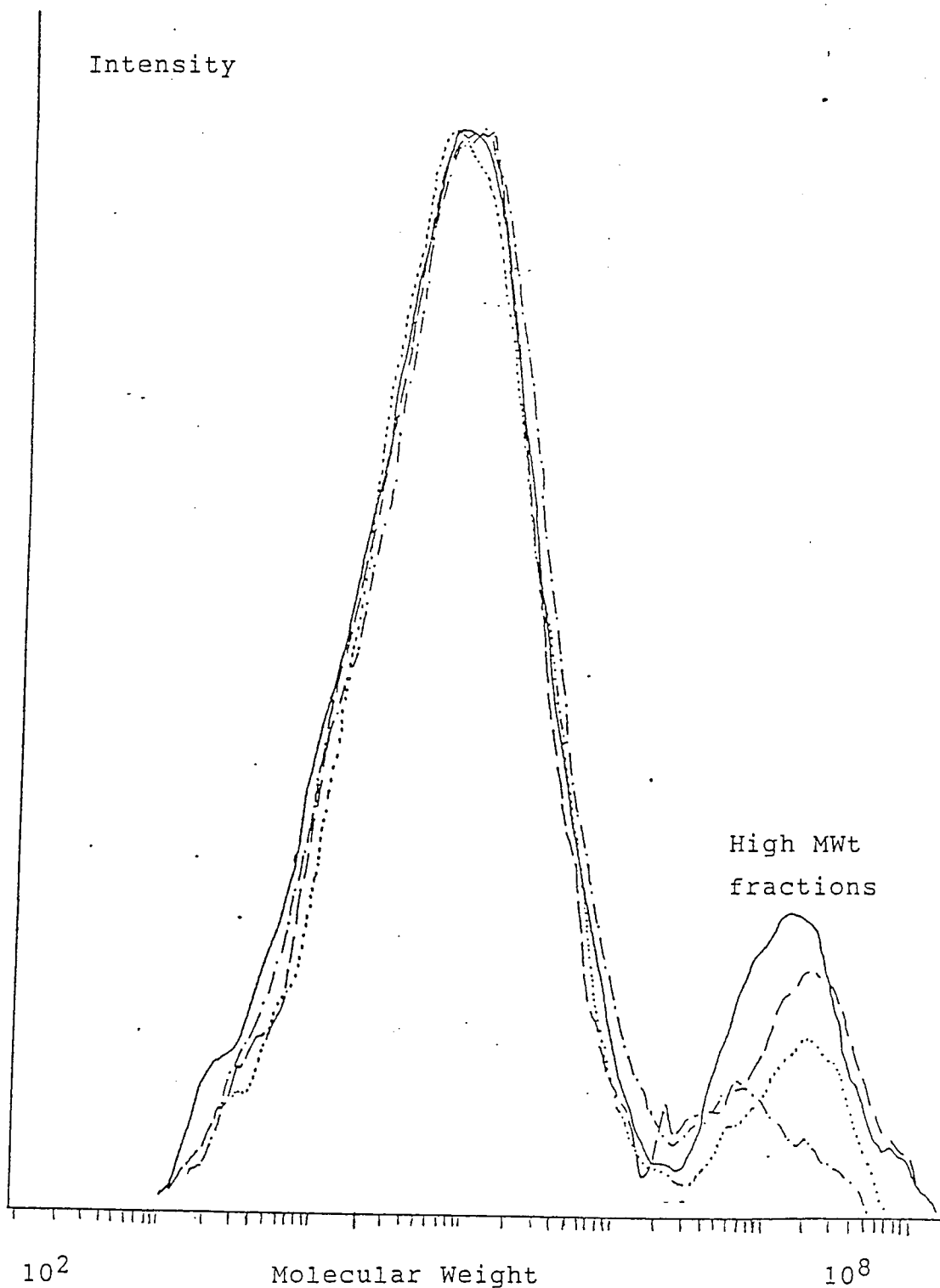


Figure 5.2 Molecular weight distribution (MWD) curves of masterbatches containing 10% of various N-alkylated nitroxyl precursors and TMPTA (weight ratio 2:8), containing : TMPTA/AOPP (-----), TMPTA/EATP (- · - · -) and TMPTA/BATP (· · · · ·), processed in the presence of Trigonox 101 0.005 molar ratio as in Scheme 5.1, compared to that containing AOTP and TMPTA processed at similar conditions (———)

Table 5.2 Binding and MW-distribution data of masterbatches containing N-alkylated acrylic nitroxyl precursors, processed with TMPTA (weight ratio 2:8) and Trigonox 101 (molar ratio=0.005) at standard processing conditions (Scheme 5.1)

Masterbatches contg. 10% of:	Binding (%)	Mn (10^4) of.		% of High-MWt Component
		Low MWt	High MWt	
TMPTA/AOTP(2:8)	80	2.63	1155	9.8
TMPTA/AOPP(2:8)	82	2.96	757	6.0
TMPTA/EATP(2:8)	82	3.11	675	5.1
TMPTA/BATP(2:8)	83	3.05	728	5.3
PP, unprocessed	--	3.28	---	--
PP + Peroxide	--	1.95	---	--

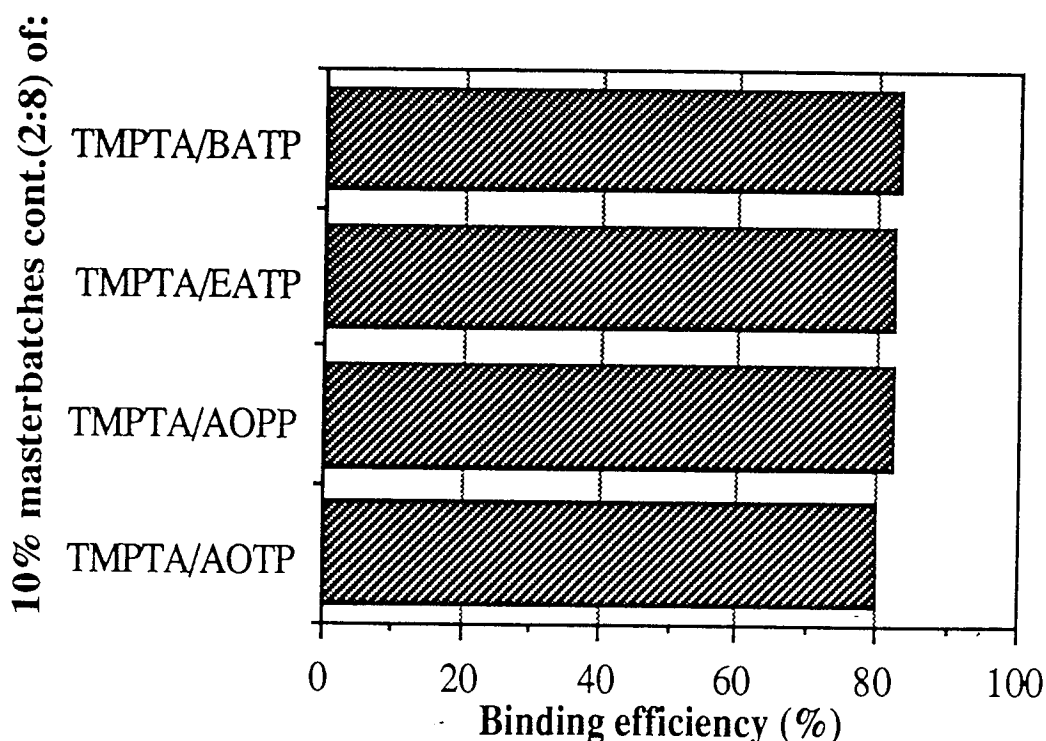


Figure 5.3 Binding efficiency of various N-alkylated nitroxyl precursor processed as 10% masterbatches at standard conditions with TMPTA ratio 2:8

The reaction mechanism by which the high MWt component may be formed in reactively processed of N-alkylated nitroxyl precursors was further studied by

polymerisation of the antioxidant monomer. AOPP (N-methyl derivative) was polymerised at 180°C for 30 minutes under Argon gas without liquid hydrocarbon, in the presence of Trigonox-101, 0.005 molar ratio. The product was analysed by FTIR and Proton as well as Carbon-13 NMR spectroscopy, see Figure 5.4 for FTIR spectra and Figures 5.5 and 5.6 for Proton and Carbon-13 NMR spectra, respectively. From the FTIR spectra (Figure 5.4), polymerised AOPP in the presence of peroxide showed total polymerisation (i.e. its unsaturation peak diminished completely). The polymerised gelly like product was found to be soluble in DCM but only partially soluble in hexane.

Proton NMR measurement of the polymerised AOPP with Trigonox-101 also supported the FTIR evidence, where the proton NMR spectra (see Figure 5.5) showed complete disappearance of the double bond in the region of $\delta = 5.50 - 6.06$ ppm formerly shown in that of fresh AOPP (Figure 2.14). NMR spectra of Figure 5.5, also indicates that the peak due to $>N-CH_3$ which appear multiplet at δ about 1.95 ppm in Figure 2.14 (fresh AOPP) is shown as singlet peak at $\delta = 2.11$ ppm. Broad peaks due to saturated acrylate at $\delta = 1.45$ and 2.18 as well as another broad peak at $\delta = 2.95$ also appear. The latter is a characteristic of proton with Carbon atom attached to a Nitrogen, which may be due to formation of $>N-CH<$ or $>N-CH_2-$ groups.

Spectra from Carbon-13 NMR measurement of the polymerised AOPP clearly showed the disappearance of double bond peaks at $\delta = 128.5 (+)$ and $129.7 (-)$ ppm, see Figure 5.6, and compared to that of fresh AOTP, Figure 2.15, which gave rise to the appearance of new peaks due to saturated acrylate after polymerisation at $\delta = 45.8 (-)$ and $34.7 (+)$ ppm. Whilst peak due to $>N-CH_3$ at $\delta = 34.3 (+)$ ppm (Figure 2.15) shifted towards a lower chemical shift at $\delta = 27.9 (+)$ ppm (see Figure 5.6), which indicates changes in the chemical environment of the group. New peaks also appear in the spectra of Figure 5.6, especially at $\delta = 67.7 (+)$ and $55.2 (-)$ ppm [close to peak due to $>C<$ at the piperidine ring at $\delta = 54.7 (-)$ ppm]. The former may be attributed as the formation of $>N-CH<$, whereas the latter may be due to $>N-CH_2-$ group, which also formed during polymerisation.

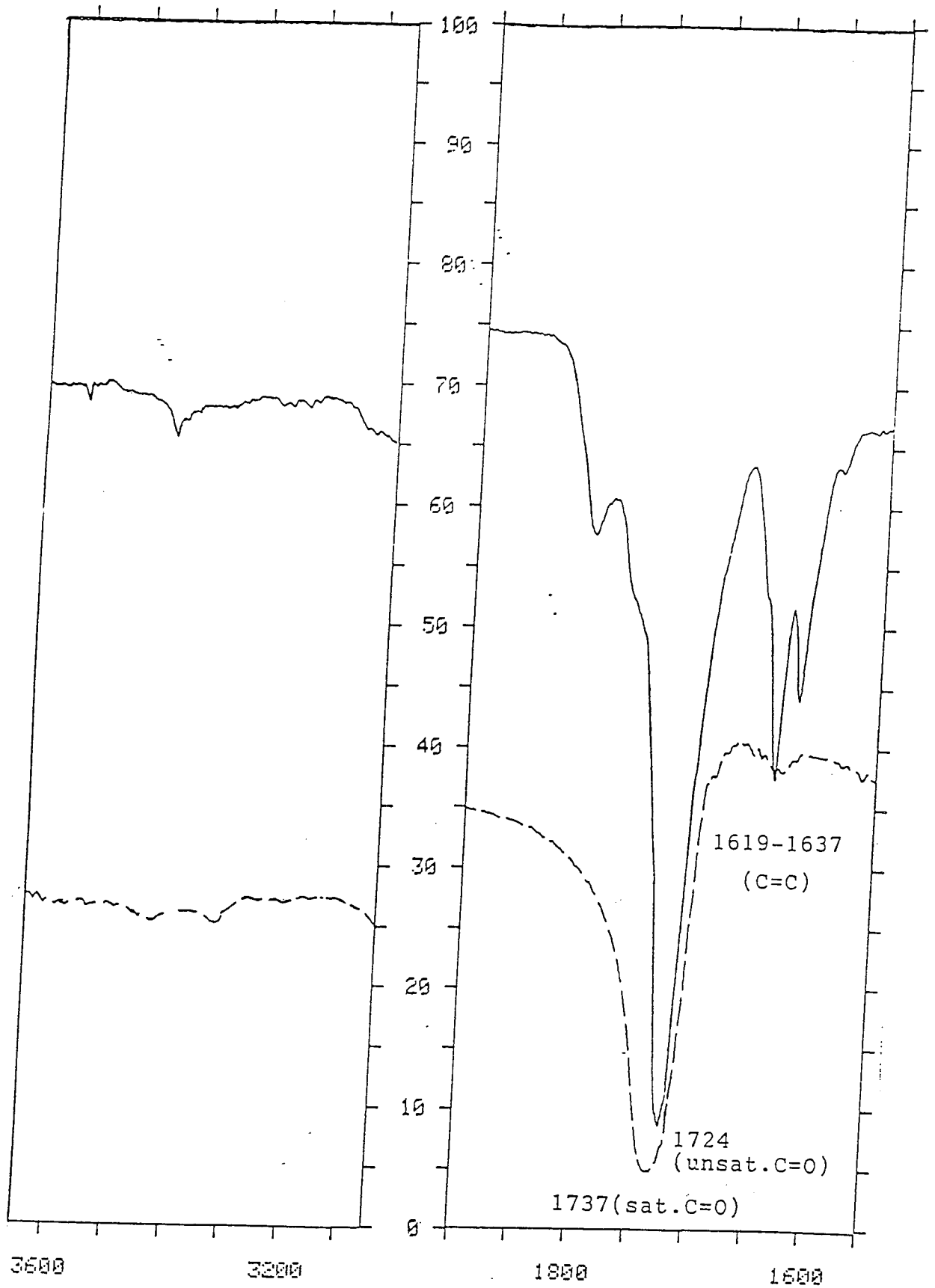


Figure 5.4 Fraction of FTIR spectra in KBr disc (3650 - 3050 cm^{-1} and 1900 - 1550 cm^{-1}) of fresh AOPP (—) and heated with peroxide (----)

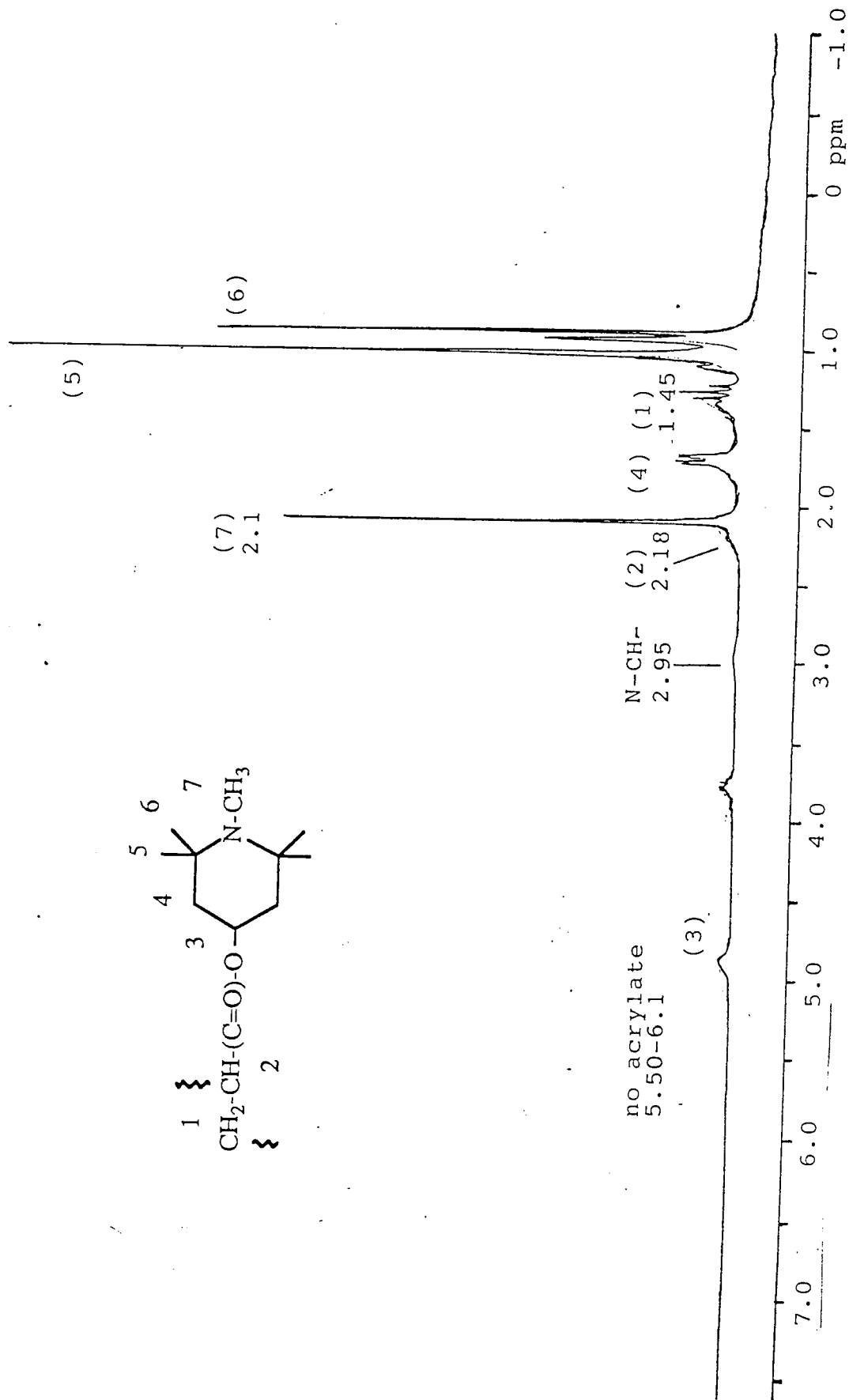


Figure 5.5 Proton NMR spectra (in CDCl_3) of polymerised AOPP (N-methyl derivative) in the presence of Trigonox-101 0.005 molar ratio at 180°C for 30 minutes under Argon gas

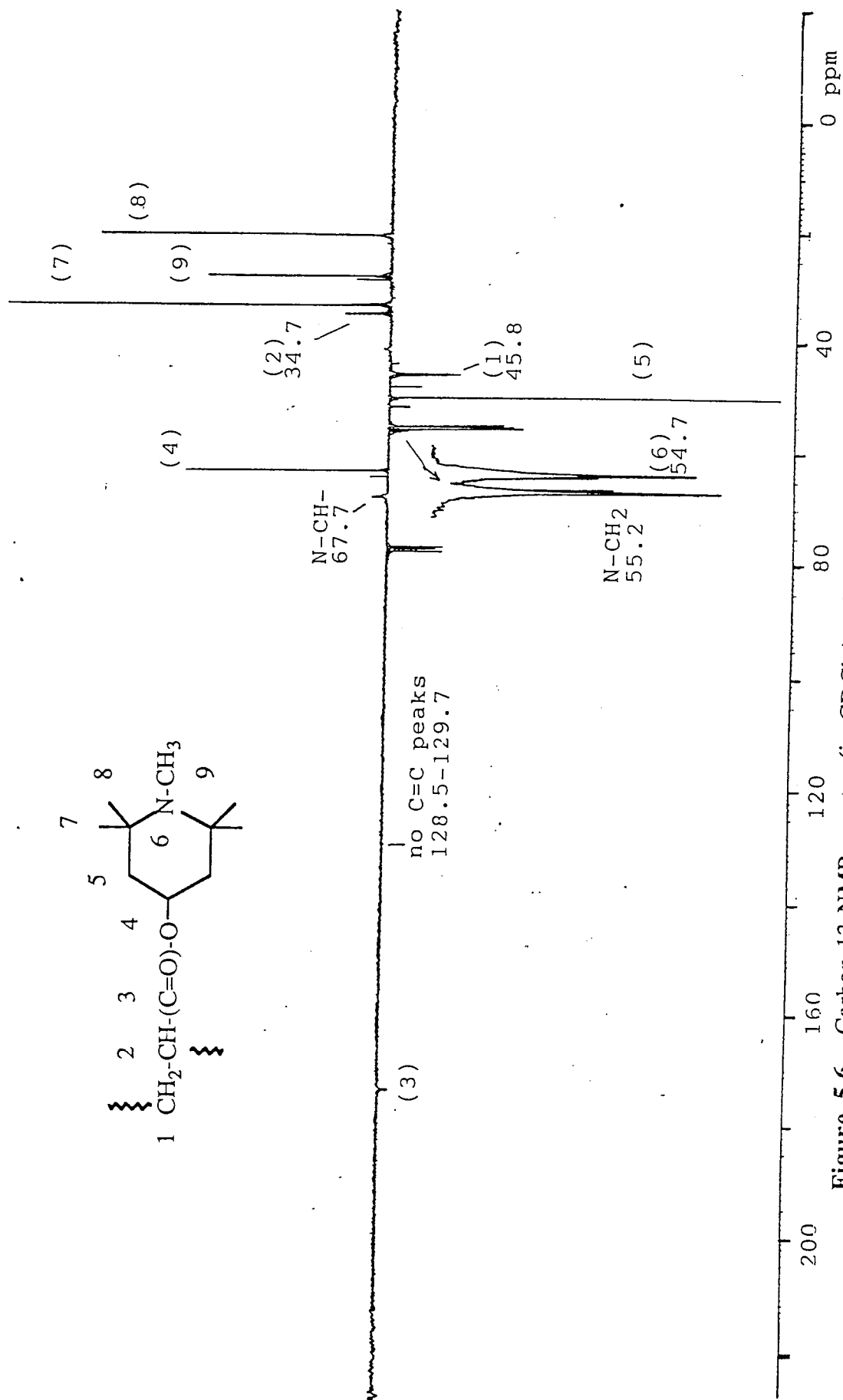
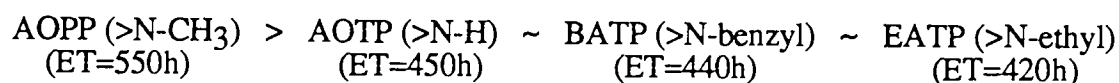


Figure 5.6 Carbon-13 NMR spectra (in CDCl₃) polymerised AOPP (N-methyl derivative) without liquid hydrocarbon in the presence of Trigonox-101 0.005 molar ratio at 180°C for 30 minutes under Argon gas

5.2.2 Photo and thermal stabilising activity of N-alkylated nitroxyl precursors

Results of reactive processing of N-alkylated derivatives of nitroxyl precursors (processed with TMPTA) described in the previous section suggest somewhat similar reaction(s) in the melt to that of the corresponding reactively processed AOTP masterbatch. The stabilising activity (uv-irradiation and thermal ageing), was therefore, examined and compared with that of the corresponding AOTP.

Reactively processed masterbatches containing combination of various N-alkylated nitroxyl precursors with TMPTA were diluted down to 0.2% antioxidant after and before exhaustive Soxhlet extraction in DCM, with and without addition of 0.2% HOBP. The extracted as well as unextracted diluted masterbatch (d-MB) films were then uv-irradiated for photostabilisation test. It was found (Table 5.3, Figures 5.7 and 5.8) that the photostabilising activity of various bound extracted N-alkylated nitroxyl precursors (B,E) are in the order of :



Like that of bound-extracted-AOTP, photostabilising activity of bound extracted N-alkylated nitroxyl precursors (ET = 420 - 550 h) also show considerable decrease when compared to those of their corresponding unbound antioxidants (ET = 1370 - 1610 h). However, when these bound antioxidants were used in conjunction with only 0.2% HOBP, their high stabilising activity were recovered (ET up to 2520 - 2950 h), see Table 5.3 and Figures 5.9 and 5.10. AOPP (>N-CH₃) showed the best stabilising activity among the N-alkylated derivatives under all conditions used.

Table 5.3 Extent of binding of different reactively processed masterbatches containing 10% combination of N-alkylated derivatives and TMPTA (ratio 2:8) in the presence of Trigonox 101 (molar ratio=0.005), and embrittlement times (ET, h) of diluted masterbatch films containing 0.2% of bound and extracted (B,E) antioxidants, Unbound (Ub) antioxidants, diluted from 10% masterbatches processed without peroxide, bound and unextracted (B,Ue) antioxidants without and with addition of 0.2% HOBP

Concentrates- containing 10% of:	Binding (%)	ET (h) of d-MB films containing 0.2% AO			
		(B,E) (0.2%)	(Ub) (0.2%)	(B,Ue) (0.2%)	(B,Ue+HOBP) (0.2% + 0.2%)
PP,processed	--	70	90	90	730
TMPTA/AOTP(2:8)	80	450	1500	660	2720
TMPTA/AOPP(2:8)	82	550	1610	780	2950
TMPTA/EATP(2:8)	82	420	1370	590	2520
TMPTA/BATP(2:8)	83	440	1540	620	2710
HOBP alone	--	70	730	--	--

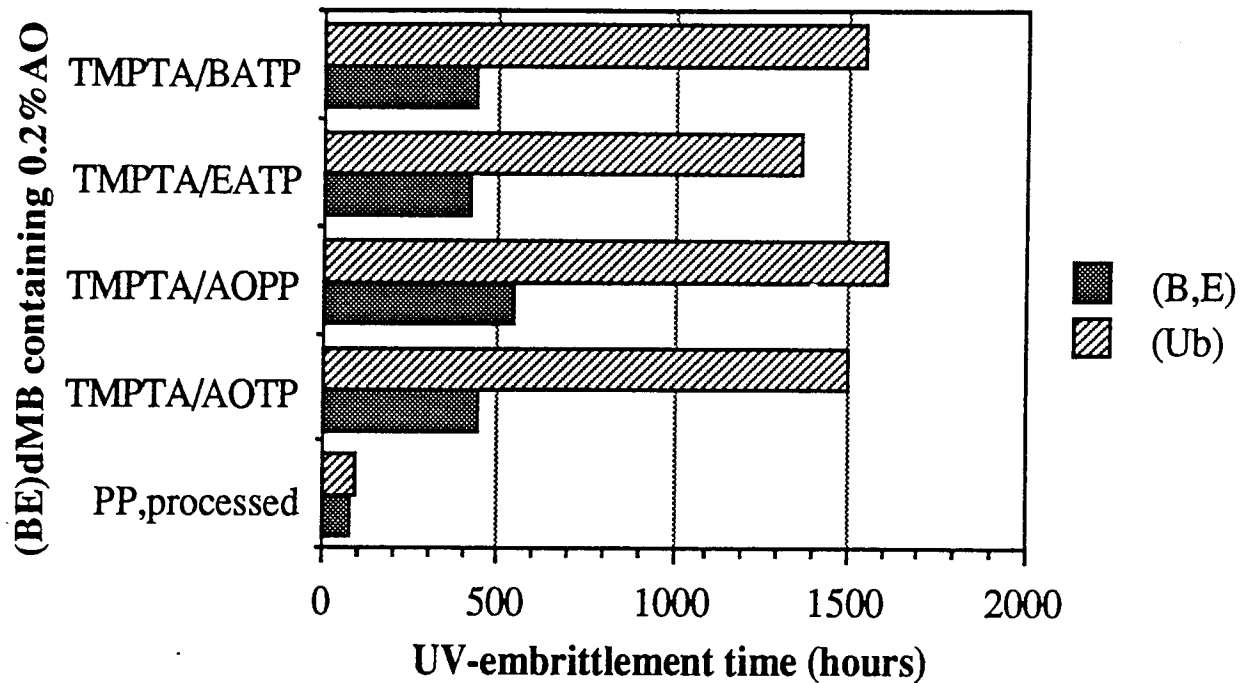


Figure 5.7 Embrittlement time of d-MB films containing 0.2% of various bound extracted (B,E) N-alkylated nitroxyl precursors, processed in combination with TMPTA (weight ratio 2:8), compared to those of PP films containing the corresponding unbound (Ub) antioxidant, diluted from 10% masterbatch without peroxide

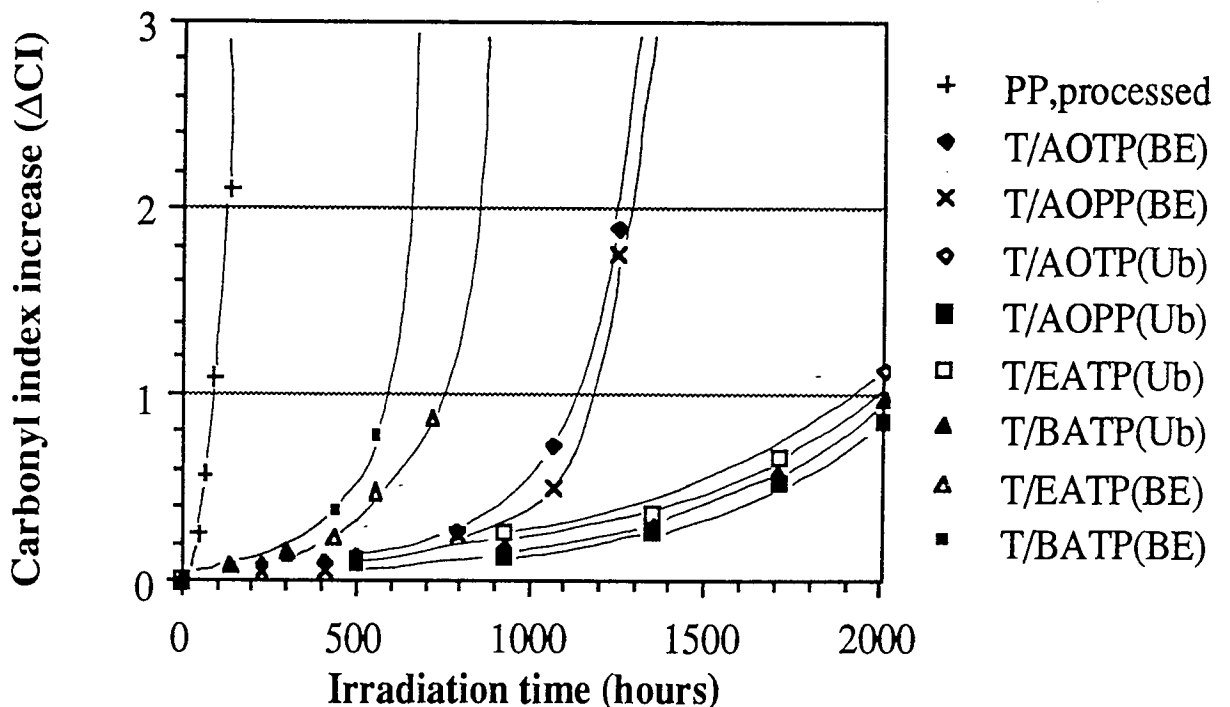


Figure 5.8 Carbonyl index increase (ΔCI) during uv-irradiation of d-MB films containing 0.2% of various bound extracted and unextracted N-alkylated nitroxyl precursors, processed with TMPTA ratio 2:8

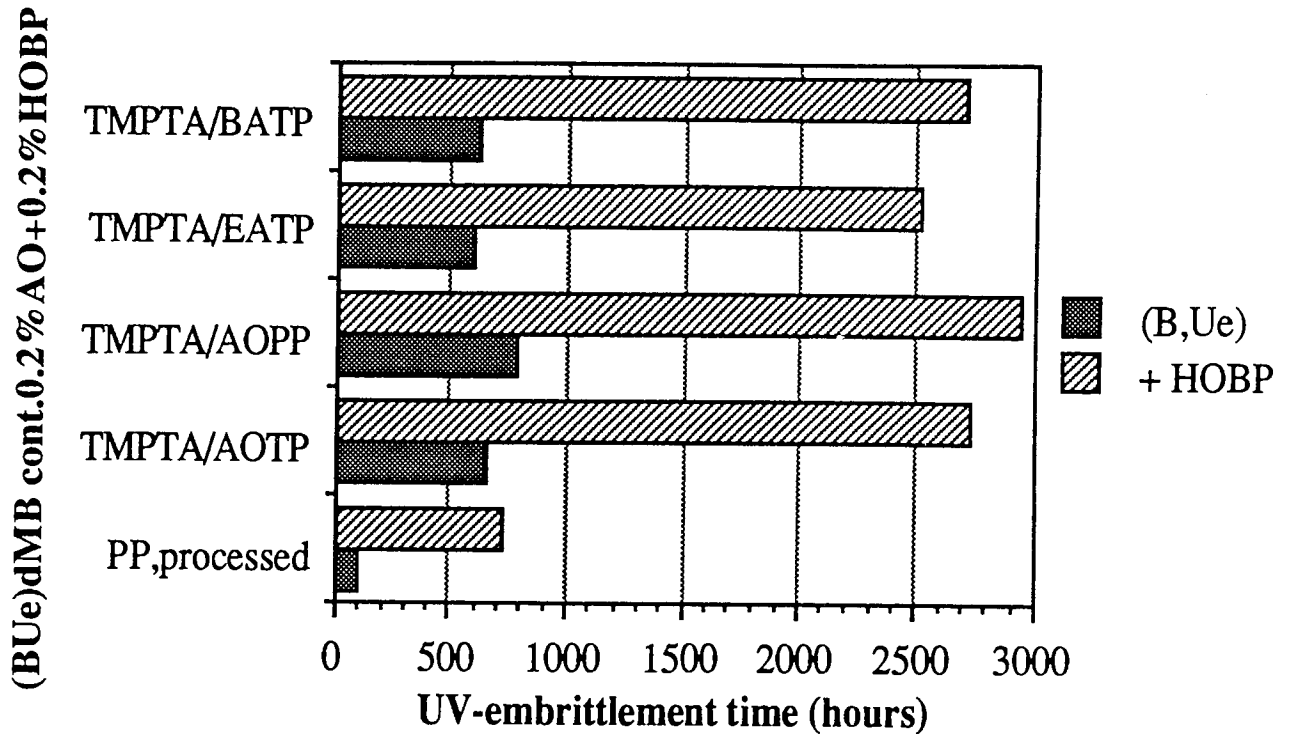


Figure 5.9 UV-embrittlement time of d-MB films containing 0.2% of various N-alkylated nitroxyl precursors, processed with TMPTA ratio 2:8 (B,Ue), with and without addition of 0.2% HOBP

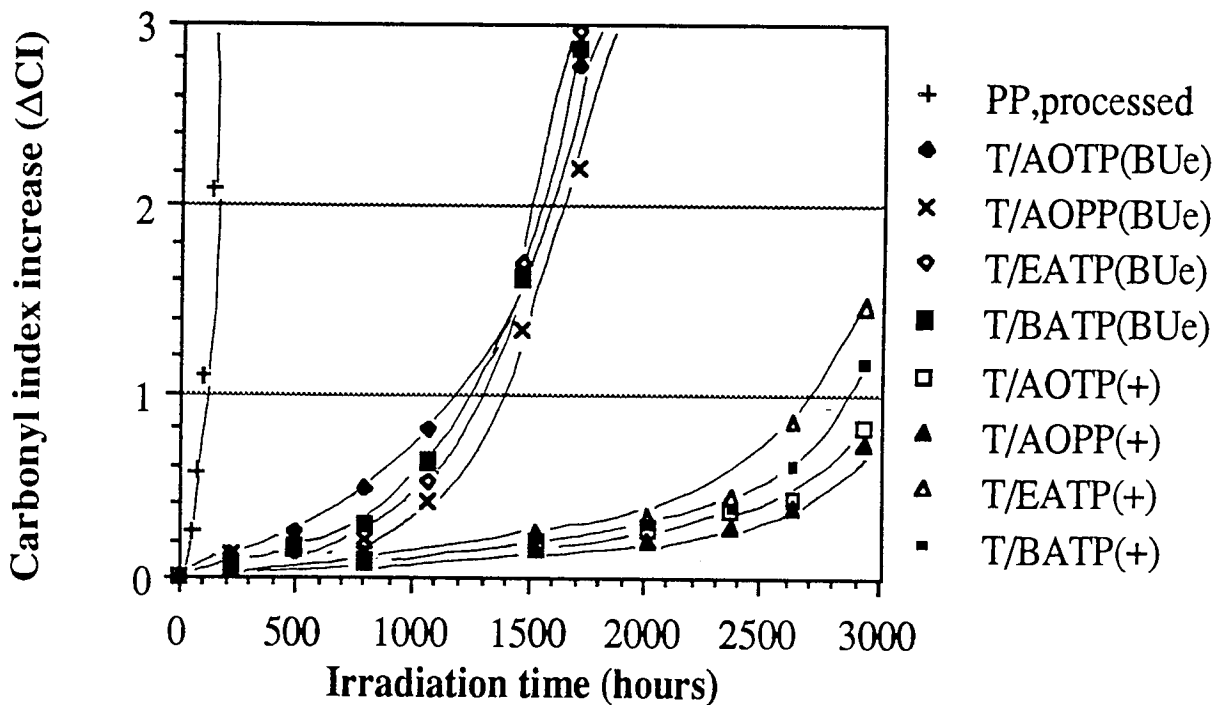


Figure 5.10 Carbonyl index increase (ΔCI) during uv-irradiation of d-MB films containing 0.2%(B,Ue) of various N-alkylated nitroxyl precursors, processed with TMPTA ratio 2:8, with addition of 0.2% HOBP

Diluted masterbatch (d-MB) films containing 0.2% of these bound N-alkylated nitroxyl precursors were also tested without extraction for thermal stability in a thermal oven at 140°C and air flow 85 l/h, (see Table 5.4 and Figures 5.11 and 5.12).

Table 5.4 Thermal ageing of diluted masterbatch films (dMB) containing 0.2% of various bound and unextracted (B,Ue) N-alkylated acrylic nitroxyl precursors with TMPTA (weight ratio = 2:8), at 140°C, air flow 85 l/h

diluted masterbatch-films containing 0.2% of,	Thermal-embrittlement Time (hours)
PP unprocessed	2
Tinuvin 770	15
Irganox 1076	275
TMPTA/AOTP(B,Ue)	120
TMPTA/AOPP(B,Ue)	145
TMPTA/EATP(B,Ue)	100
TMPTA/BATP(B,Ue)	110

Interestingly, when the N-alkylated derivatives were bound, processed with TMPTA and unextracted (B,Ue), their thermal stabilising activity are comparable to that of the corresponding (B,Ue) AOTP. It was shown that AOPP (>N-Me) exhibits better thermal stabilising activity among other N-alkylated derivatives and AOTP.

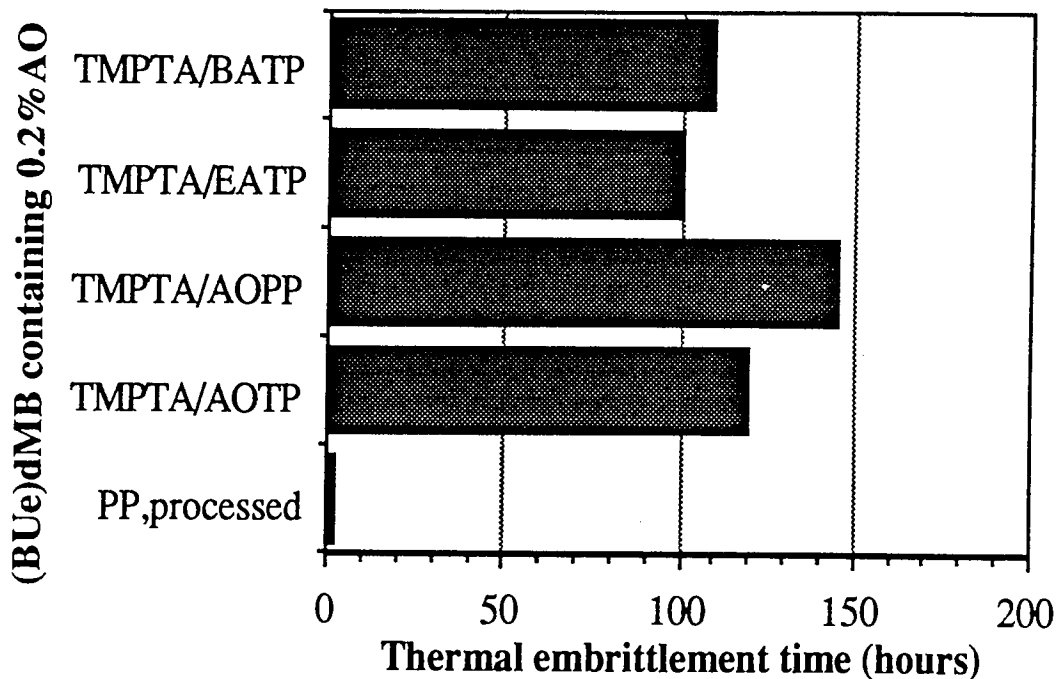


Figure 5.11 Thermal-embrittlement time of d-MB films containing 0.2%(B,Ue) of various N-alkylated nitroxyl precursors, processed with TMPTA ratio=2:8

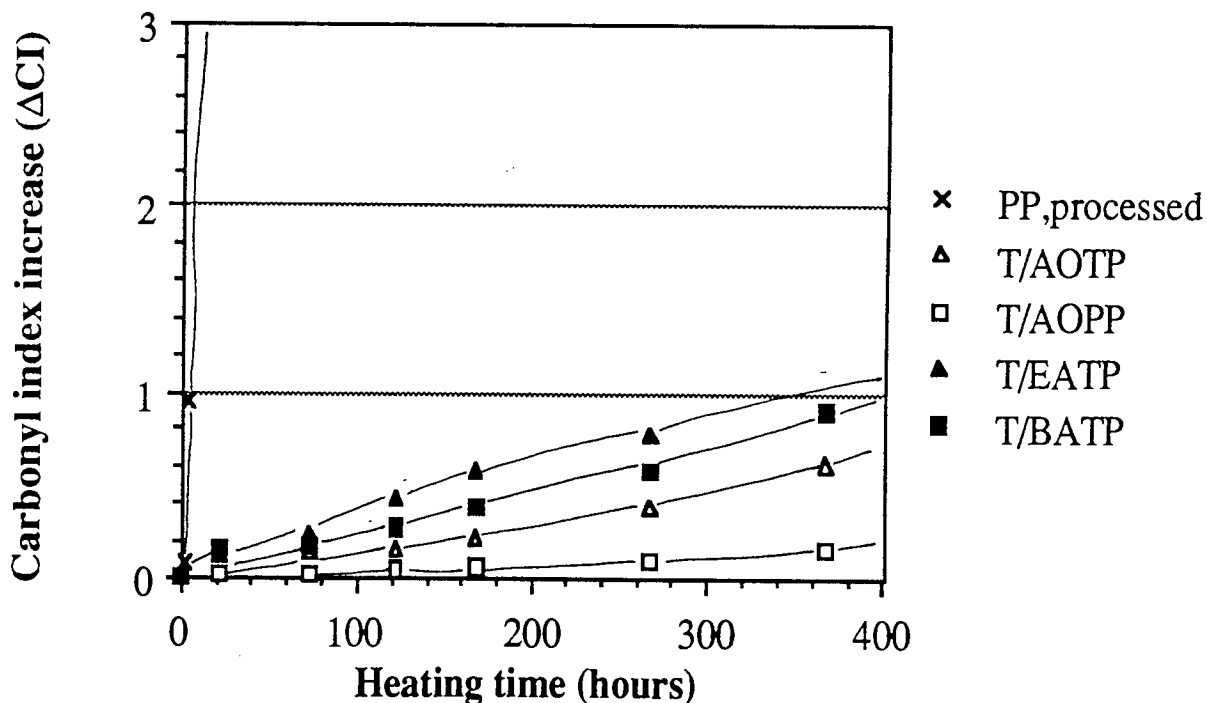


Figure 5.12 Carbonyl index increase during thermal ageing of d-MB films containing 0.2% of various (B,Ue) N-alkylated nitroxyl precursors, processed with TMPTA ratio 2:8

5.2.5 Reactive processing of nitroxyl precursors containing methacrylic group(s)

Results of binding efficiency of different methacrylic-containing nitroxyl precursors (see Table 5.2 for the chemical structure) processed in polypropylene at various concentration in the presence of DCP 0.010 molar ratio using the procedure described in Scheme 5.2, are shown in Table 5.6 and Figure 5.13.

Table 5.6 Effect of antioxidant concentration on the binding efficiency of methacrylic nitroxyl precursors, processed at standard conditions in the presence of DCP 0.010 molar ratio

Antioxidant-concentration (%)	Binding (%) of masterbatches containing		
	MMTP	MOTP	MOPP
5	10	8	8
10	15	10	15
15	20	15	15
20	22	15	15

It was found that all methacrylic nitroxyl-precursors exhibit low binding efficiency (less than 22%) at various antioxidant concentration from 5 - 20%. Their torque records also do not indicate formation of any crosslinking reaction.

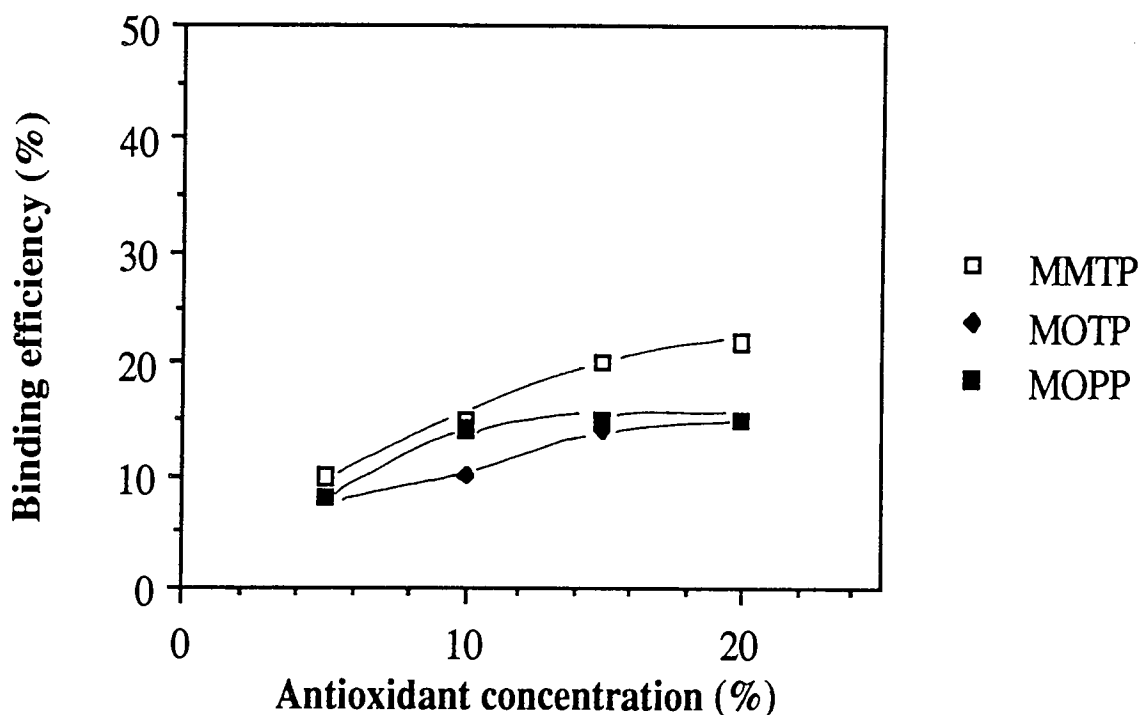


Figure 5.13 Binding efficiency of methacrylic nitroxyl precursors masterbatches at various antioxidant concentration, processed at standard conditions, in the presence of DCP 0.010 molar ratio

Further optimisation of the binding efficiency was then carried out by varying the peroxide (DCP) concentration. 10% of various methacrylic nitroxyl-precursors in polypropylene were again reactively processed using various peroxide concentrations. The binding efficiency (after exhaustive Soxhlet extraction in DCM) and melt flow index (using small die, $\varnothing = 0.1181$ cm) were measured.

As shown in Table 5.7 and Figures 5.14 and 5.15, binding efficiency of methacrylic(s) nitroxyl precursors in 10% masterbatches cannot be achieved to more than 20%, even in the presence of high DCP content (up to 0.080 molar ratio). On the other hand, high DCP content increases MFI values from 0.7 to 10.1 g/10minutes, which indicates some extent of masterbatch degradation. When the peroxide effect was compared to that observed for the analogous samples containing various acrylic nitroxyl precursors (MFI increase 0.6-16.5 to 0.9-73.9 g/10min, see Table 3.3 Chapter 3) it was demonstrated that much lower MFI increase was observed for the methacrylate derivatives.

Table 5.7 Effect of peroxide (DCP) contents on the binding of methacrylic nitroxyl precursors processed at standard conditions. *MFI was measured using small die ($\varnothing = 0.1181$ cm)

Masterbatches- containing 10% of,	DCP contents (molar ratio)	Binding (%)	MFI *(g/10minutes)
MMTP	0.000	0	0.7
	0.005	15	1.4
	0.010	15	2.2
	0.038	20	2.9
	0.080	20	6.7
MOTP	0.000	0	0.8
	0.005	8	1.4
	0.010	10	2.5
	0.036	10	3.8
	0.090	15	11.3
MOPP	0.000	0	0.8
	0.005	15	1.6
	0.010	15	2.7
	0.050	15	4.4
	0.080	17	10.1

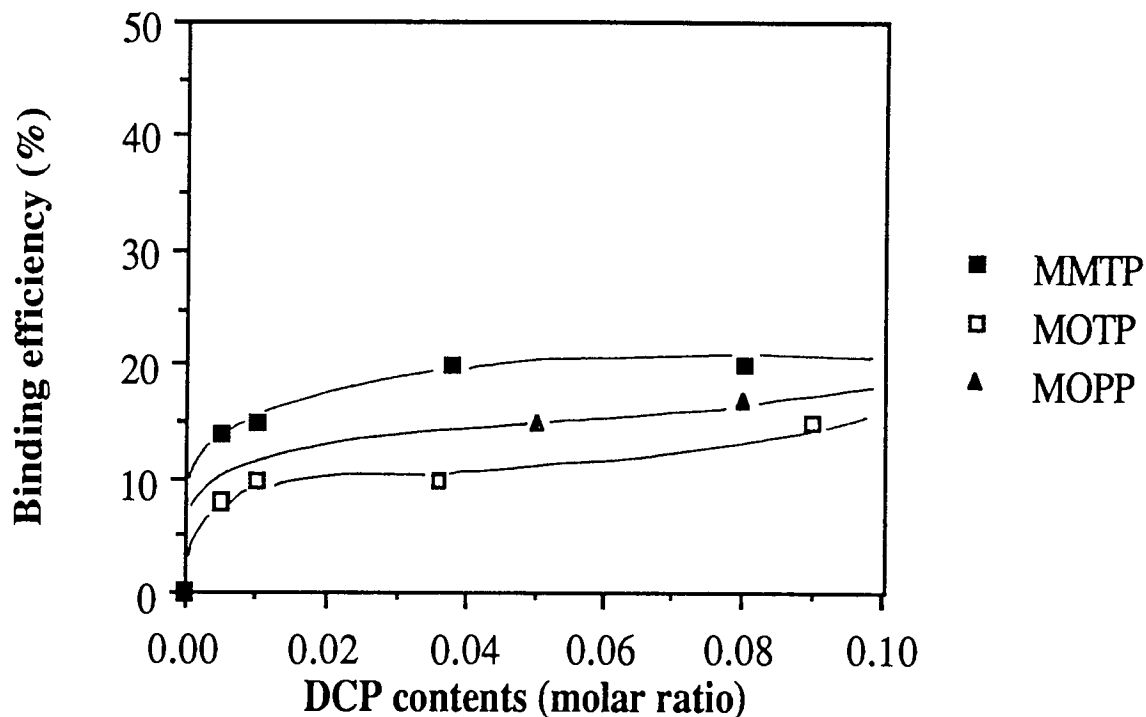


Figure 5.14 Effect of peroxide (DCP) contents on the binding efficiency of various methacrylic nitroxyl precursors

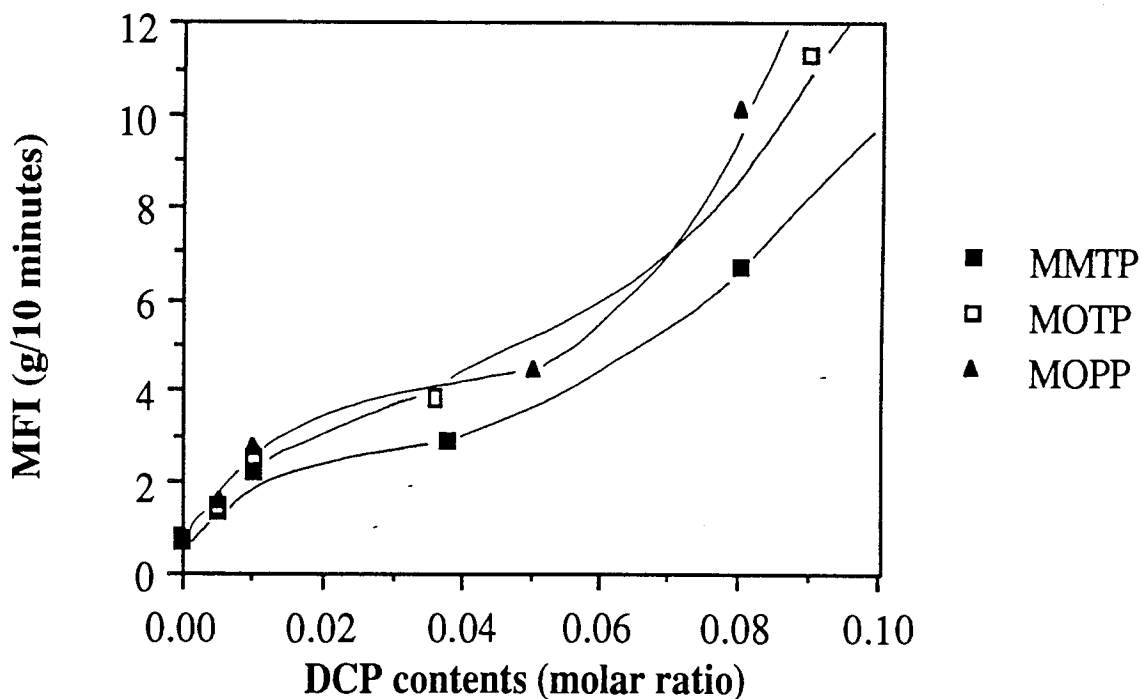


Figure 5.15 Effect of peroxide content on the MFI of masterbatches containing various methacrylic nitroxyl precursors

Photostability of PP-films containing 0.2% of unbound (Ub) methacrylic nitroxyl precursors (diluted from the corresponding 10% masterbatches processed without peroxide), was compared with that of diluted masterbatches containing 0.2% antioxidant (some antioxidants become bound), processed with DCP 0.005 molar ratio but are unextracted (B,Ue), as shown in Table 5.8.

Table 5.8 Binding of methacrylic nitroxyl precursors processed with DCP (molar ratio=0.005). and uv-embrittlement time of unextracted diluted masterbatch films containing 0.2% of the antioxidants (B,Ue), compared to that of PP films containing 0.2% of the corresponding unbound (Ub) antioxidants, diluted from 10% masterbatches processed without peroxide

Masterbatches containing 10% of,	Binding (%)	UV-ET(h) of d-MB films	
		(0.2%, B, Ue)	(0.2%,Ub)
PP,processed	--	70	70
MMTP	15	140	750
MOTP	8	680	1620
MOPP	15	820	1550

Table 5.8 and Figures 5.16 and 5.17, show that bound and unextracted (B,Ue) antioxidants exhibit lower photostabilising effectiveness than the corresponding unbound (Ub) analogous. Furthermore, when the methacrylic group is present on the amide side, such as the case with the bis-methacrylic (MMTP), even poorer stabilising activity was exhibited. It seems that radical scavenging effect of the N-methacrylic group is antagonistic with stabilising activity of the amide group of MMTP. Poor compatibility of bis-methacrylic (MMTP) in polypropylene may also contribute to the low stabilising activity.

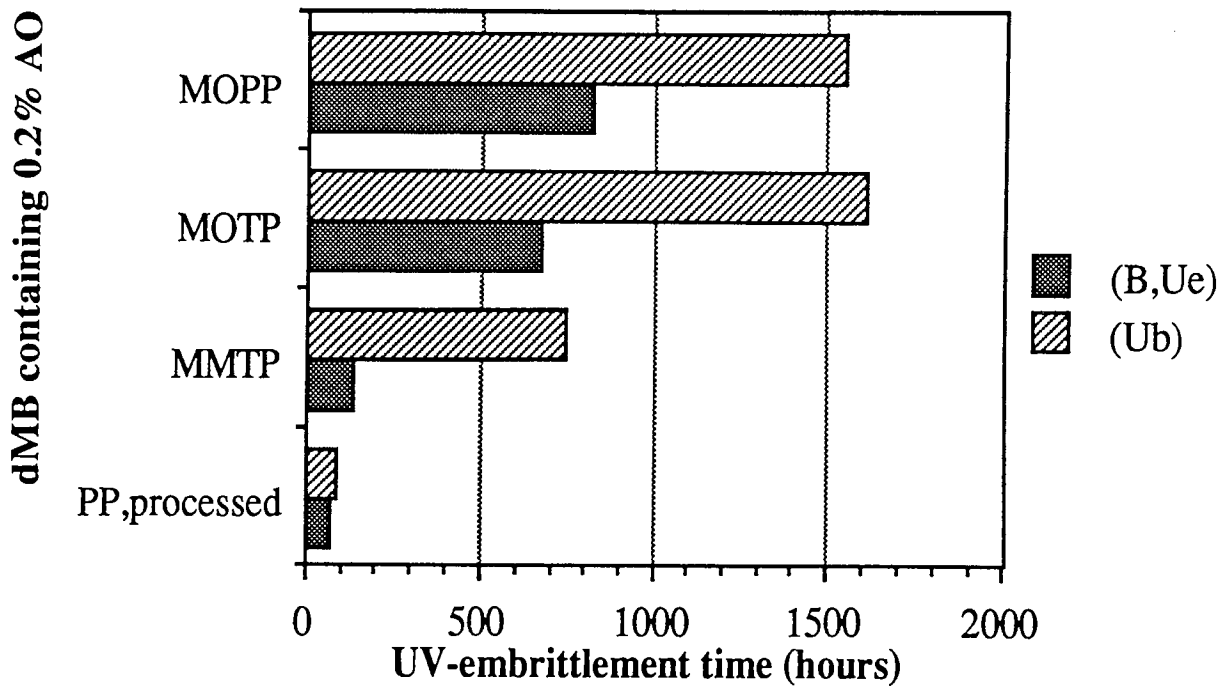


Figure 5.16 UV-embrittlement time of d-MB films containing 0.2% of various bound unextracted (B,Ue) and unbound (Ub) methacrylic nitroxyl precursors

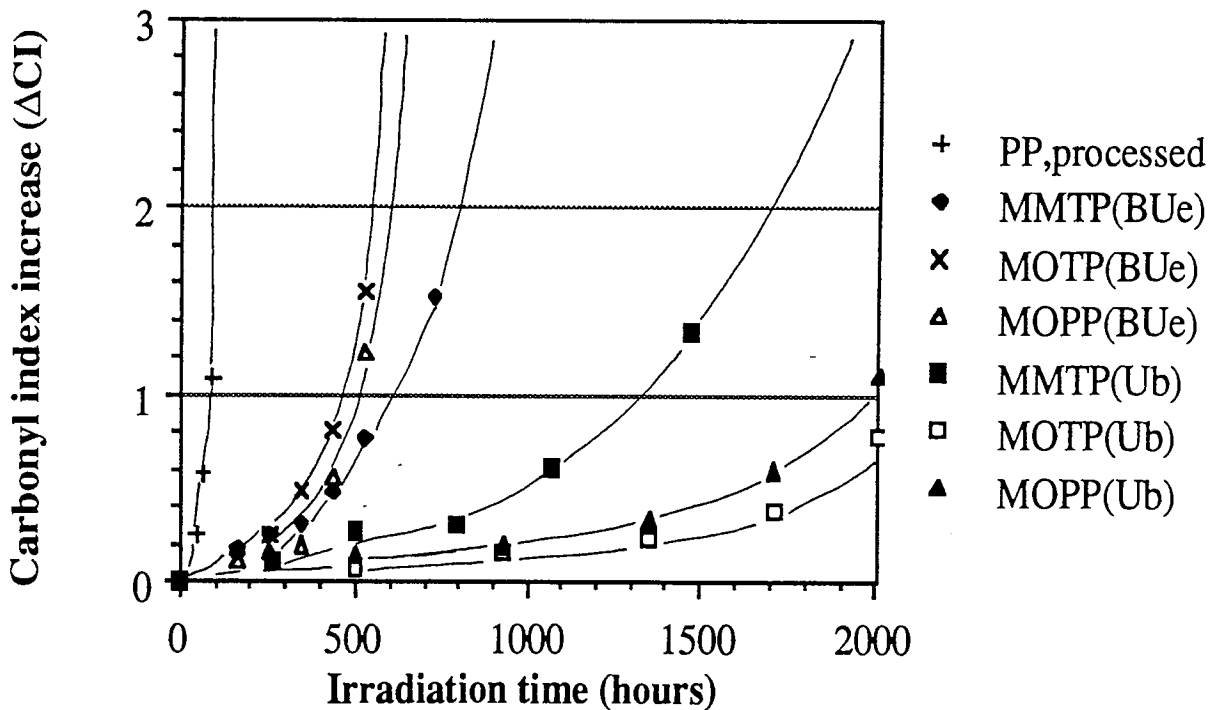


Figure 5.17 Carbonyl index increase during uv-irradiation of d-MB films containing 0.2% (B,Ue) and (Ub) of various methacrylic nitroxyl precursors

5.2.4 Extended binding of MOTP and MOPP using various coagents

It was shown in the previous chapter that the binding efficiency of AOTP (a mono acrylic nitroxyl precursors) can be improved considerably when reactively processed in the presence of TMPTA (ratio 2:8). The binding efficiency of the monomethacrylic nitroxyl precursors, MOTP and MOPP, was, therefore, examined in the presence of multifunctional coagents, such as AATP, TMPTA, HDA, TMPTM and BGDM, coagent ratio 2:8 (see Table 3.6 for chemical structure of the coagents); DCP was used as radical generator at molar ratio of 0.005. The amount of antioxidants in the polymer samples was measured using FTIR spectroscopy and calculated after subtraction of absorbance due to the coagents, before and after exhaustive Soxhlet extraction in DCM.

Table 5.9 Binding of 10% MOTP and MOPP masterbatches containing various coagents (ratio 2:8), *the amount of antioxidants retained was calculated after subtraction of FTIR absorbance due to the coagents

Masterbatches	Binding (%)*
AATP/MOTP(2:8)	35
TMPTA/MOTP(2:8)	45
HDA/MOTP(2:8)	40
TMPTM/MOTP(2:8)	25
BGDM/MOTP(2:8)	17
TMPTA/MOPP(2:8)	62
MOTP alone	8
MOPP alone	15

As shown in Table 5.9 and Figure 5.18, using TMPTA as coagent binding of MOTP and MOPP can be extended from 8 to 45% and 15 to 62%, respectively. The

presence of methacrylics coagents (TMPTM and BGDM), however, does not improve binding of MOTP considerably (binding efficiency less than 25%). This may be due to the fact that the methacrylics coagent may easily depolymerise during processing at 180°C.

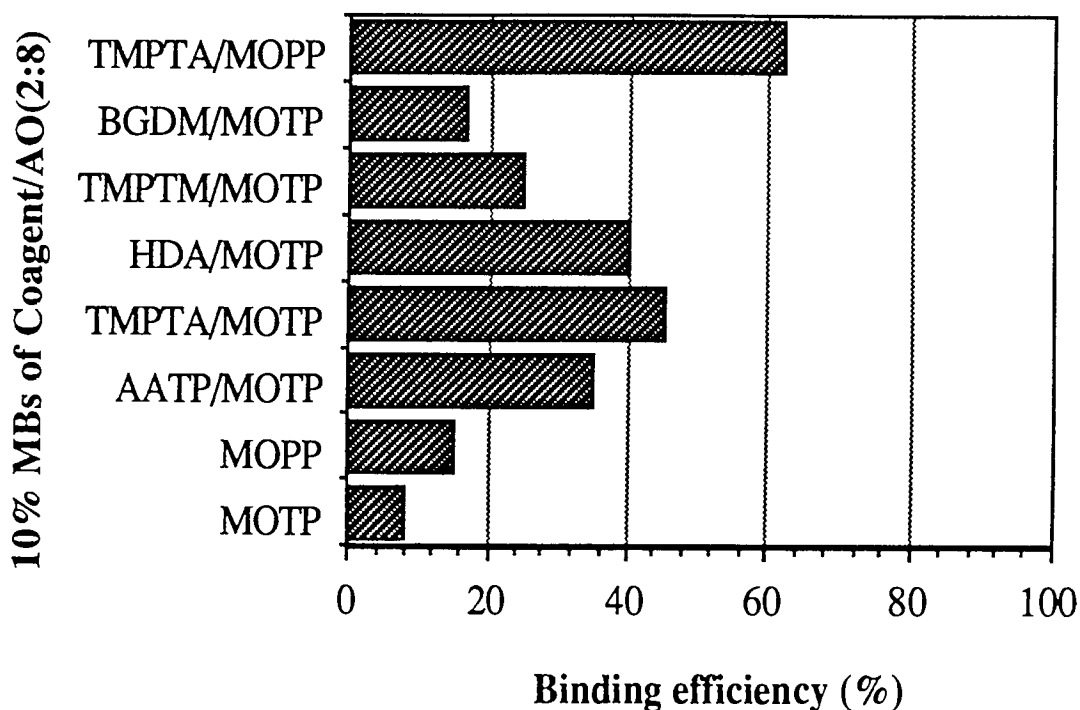


Figure 5.18 Binding efficiency of MOTP and MOPP in 10% masterbatches, processed with various coagent (ratio 2:8)

When MOTP was reactively processed with various weight ratios of TMPTA in the presence of DCP 0.005 molar ratio, Table 5.10 and Figure 5.19, the binding efficiency can be extended up to 85% using TMPTA ratio of 4:6 to MOTP. However, as TMPTA concentration increases, the masterbatches show a sign of crosslinking, which is indicated by the decrease of their MFI (from 0.80 - 0.30 g/10minutes).

Table 5.10 Binding and MFI of masterbatches containing 10% MOTP, TMPTA (at various ratios) and DCP 0.005 molar ratio

Coagent ratio	Binding (%)	MFI (g/10min)
0 : 10	10	0.70
1 : 9	15	0.50
2 : 8	45	0.50
3 : 7	70	0.40
4 : 6	85	0.30
PP, unprocessed	--	0.40
PP + DCP	--	4.10

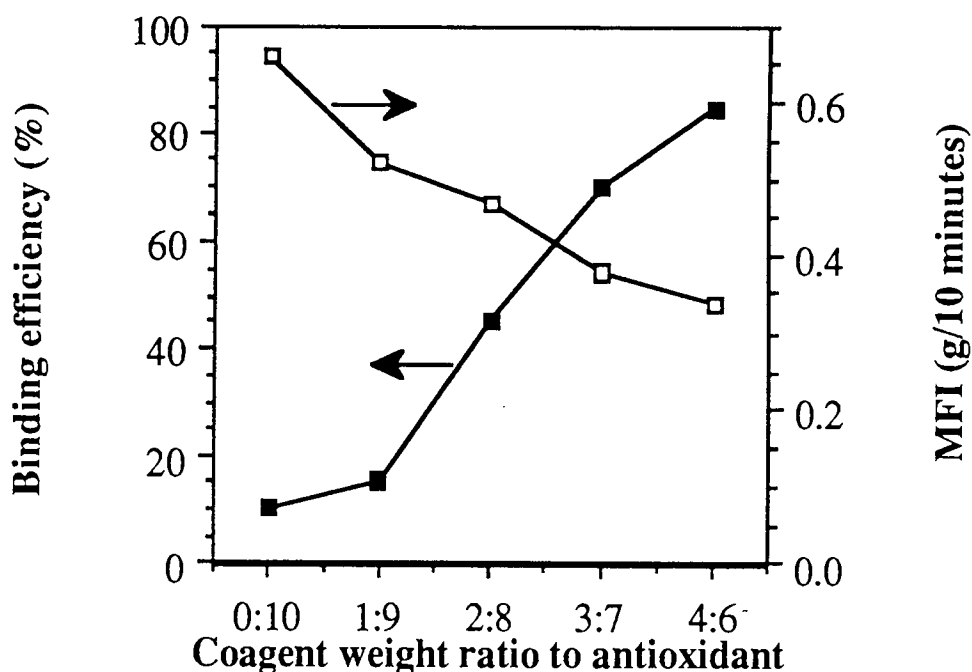


Figure 5.19 Effect of coagent ratio (TMPTA) on the binding efficiency and MFI of MOTP in 10% masterbatches

To optimise the binding of MOTP using TMPTA coagent, the peroxide (DCP) content in the masterbatches was also varied. Masterbatches containing 10% of MOTP and TMPTA ratio 2:8 were prepared in the presence of various DCP content. Table

5.11 and Figure 5.20 show clearly that increase in the DCP content (up to 0.01 molar ratio) may also increase the binding efficiency of MOTP, after which further increase in peroxide concentration has no effect on the binding efficiency.

Table 5.11 Binding and MFI of masterbatches containing 10% MOTP and TMPTA (ratio=2:8), in the presence of various DCP contents

DCP molar ratio	Binding (%)	MFI (g/10min)
0.000	28	0.40
0.005	45	0.45
0.010	50	0.70
0.020	50	1.30
0.050	53	4.20

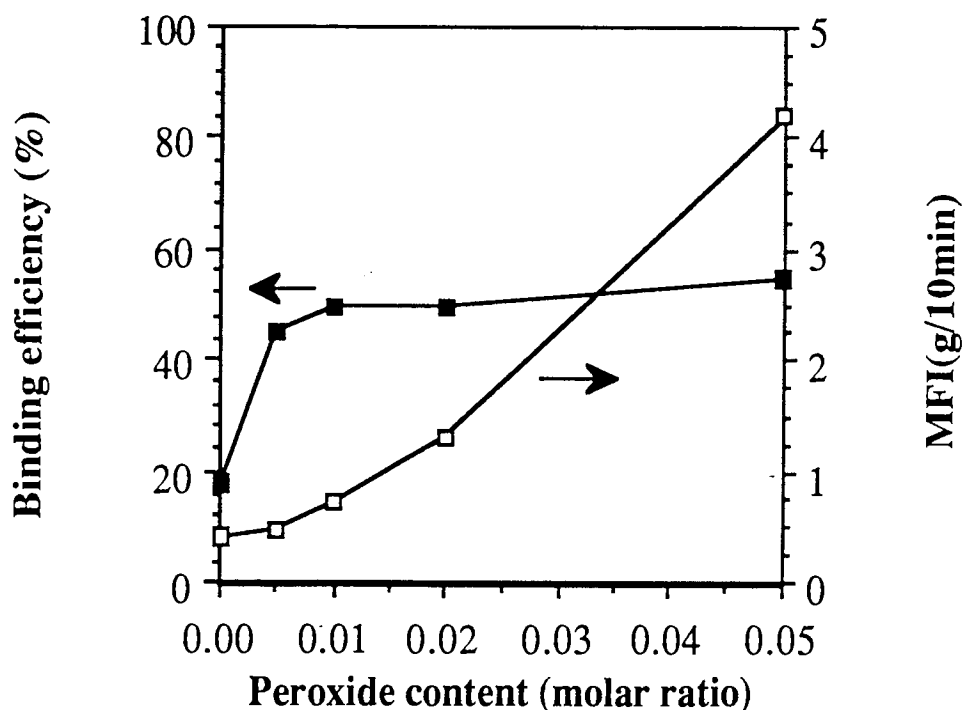


Figure 5.20 Effect of peroxide (DCP) content on binding efficiency and MFI of masterbatches containing 10% MOTP, processed with TMPTA, ratio 2:8, at standard conditions

MFI results of these masterbatches, however, suggest that degradation of the polymer increase steadily with increasing peroxide concentration. Optimum binding of MOTP processed as 10% masterbatch with TMPTA was chosen using coagent ratio 2:8 in the presence of DCP 0.005 molar ratio

To investigate the nature of the binding process of methacrylic nitroxyl precursors, MOTP was polymerised without liquid hydrocarbon at 180°C under argon gas in the presence of DCP 0.005 molar ratio, for 30 minutes using similar procedure for AOTP polymerisation described in Scheme 4.2. Analysis of the white solid polymerised product using FTIR spectroscopy (in KBr-disc, see Figure 5.21.a) showed that the unsaturation peak at 1635 cm^{-1} , as well as >N-H peak at 3317 cm^{-1} are almost unchanged. However, when compared to that of fresh MOTP, the decrease of the unsaturation peak (calculated from the unsaturation area index to the corresponding carbonyl peak) indicates about 50% of saturation reaction of the methacrylic group.

The polymerised MOTP was also analysed using Proton NMR spectroscopy in CDCl_3 . Compared to that of fresh MOTP (Figure 2.23) the Proton NMR spectra of polymerised MOTP (Figure 5.21.b) also showed decrease of intensity of peaks due to methacrylate protons, i.e. at $\delta = 5.50$ (singlet) and 6.04 (singlet) ppm, from intensity = 5.1 - 5.4% before to 2.4 - 2.5% after polymerisation (about 50% decrease). This evidence is also supported by the formation of broad peak (Figure 5.21.b) at $\delta = 4.90$ ppm (intensity = 2.7%), which is attributed to be due to shifting of chemical shift of C4-proton of the piperidine ring (-O-CH<) formerly at $\delta = 5.17 - 5.27$ ppm (intensity = 5.3%, Figure 2.23) as a result of polymerisation.

When compared to that of fresh MOTP (Figure 2.24), Carbon-13 NMR spectroscopy (CDCl_3) of polymerised MOTP (Figure 5.21.c) showed four new peaks as a result of the polymerisation. The first two peaks at $\delta = 34.8$ (+) and 43.3 (-) ppm may be attributed as those of saturated acrylate, whereas the last two peaks at $\delta = 45.2$ (-) and 69.8 (+) ppm may be due to formation of other methylene (-) and tertiary carbon (+), such as -CH₂-N< and >CH-N< groups.

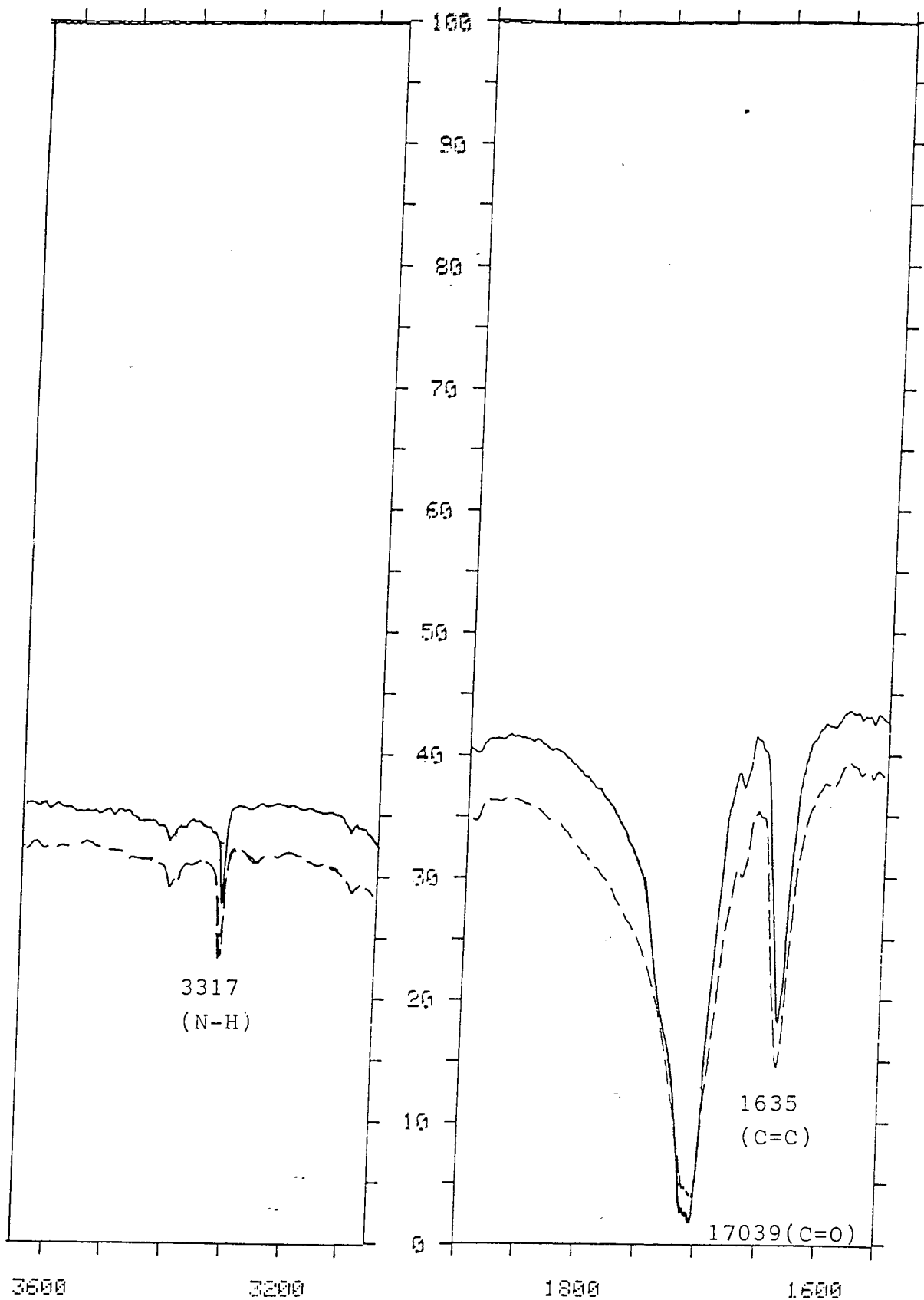


Figure 5.21.a Fraction of FTIR spectra in KBr disc (3500 - 3200 cm⁻¹ and 1850 - 1550 cm⁻¹) of polymerised MOTP (—) compared to that of fresh MOTP (-----)

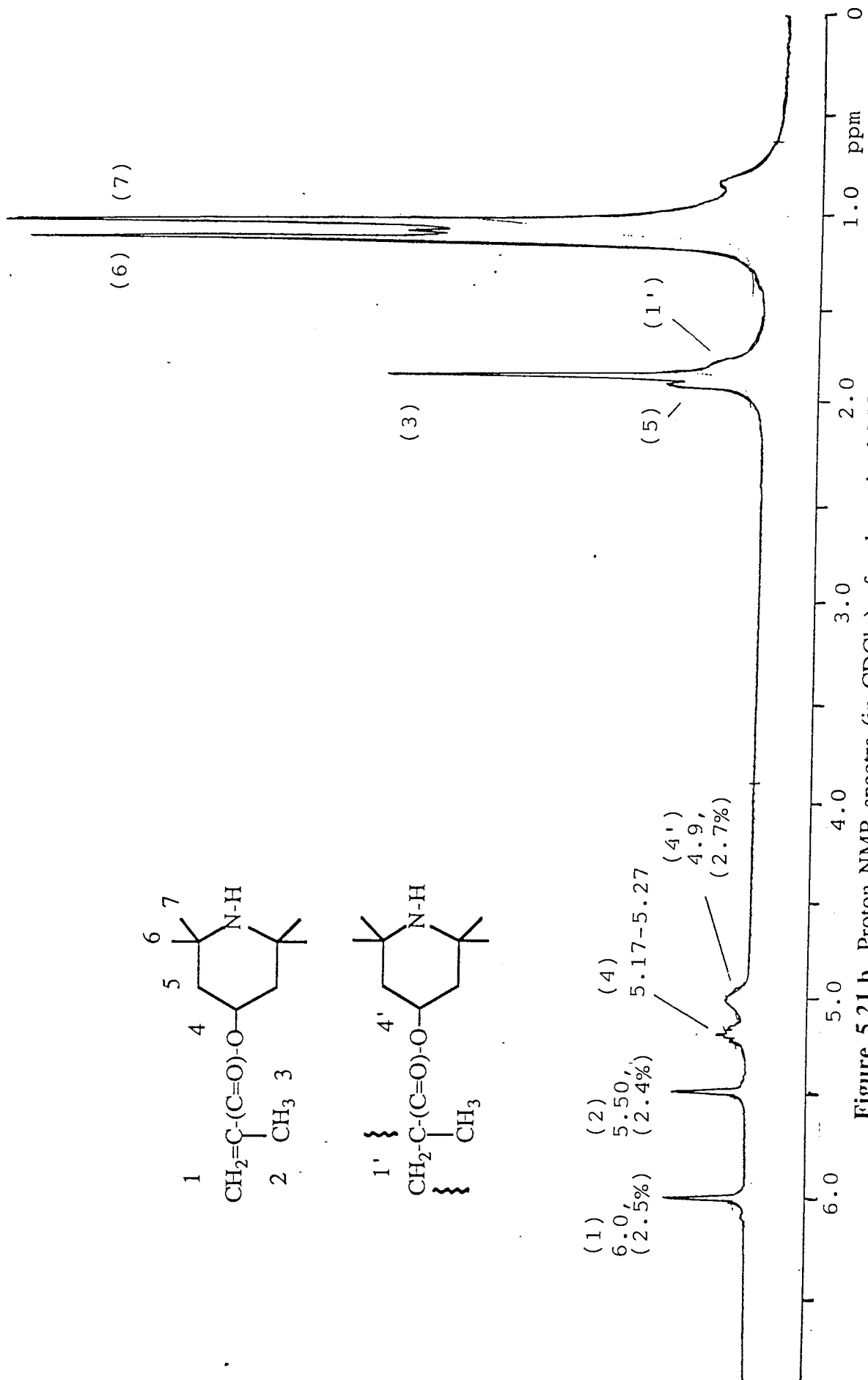


Figure 5.21.b Proton NMR spectra (in CDCl_3) of polymerised MOTP without liquid hydrocarbon in the presence of DCP 0.005 molar ratio, at 180°C for 30 minutes under Argon gas

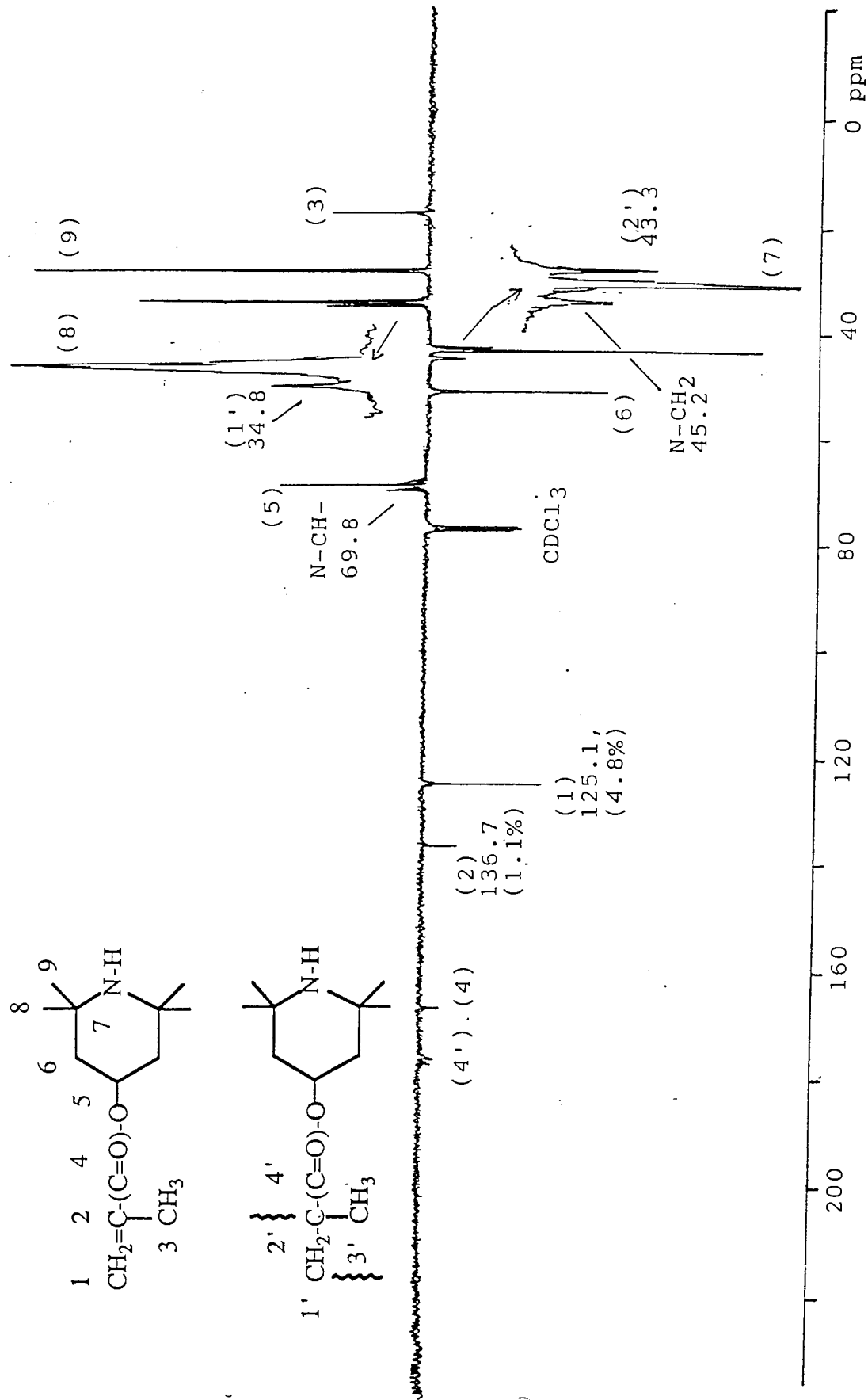


Figure 5.21.c Carbon-13 NMR spectra (in CDCl₃) of polymerised MOTP without liquid hydrocarbon in the presence of DCP 0.005 molar ratio, at 180°C for 30 minutes under Argon gas

Materbatches containing methacrylic nitroxyl precursors (MOTP and MOPP) processed without and with TMPTA were then analysed by GPC for molecular weight distribution (MWD) data. It was found that none of these masterbatches exhibited a high MWt-peak, see Table 5.12 and Figure 5.22, inspite of the fact that the NMR analysis of the polymerised MOTP exhibited involvement of the >N-H group.

Table 5.12 Molecular weight distribution (MWD) data of masterbatches containing MOTP and MOPP processed without and with TMPTA as 10% masterbatches

Masterbatches contg.10% of,	Binding (%)	Mn (10 ⁴) of the masterbatches
MOTP	8	3.06
TMPTA/MOTP(2:8)	45	3.24
TMPTA/MOPP(2:8)	62	2.71
PP,unprocessed	--	3.28
PP,rctv.proc'd	--	1.95

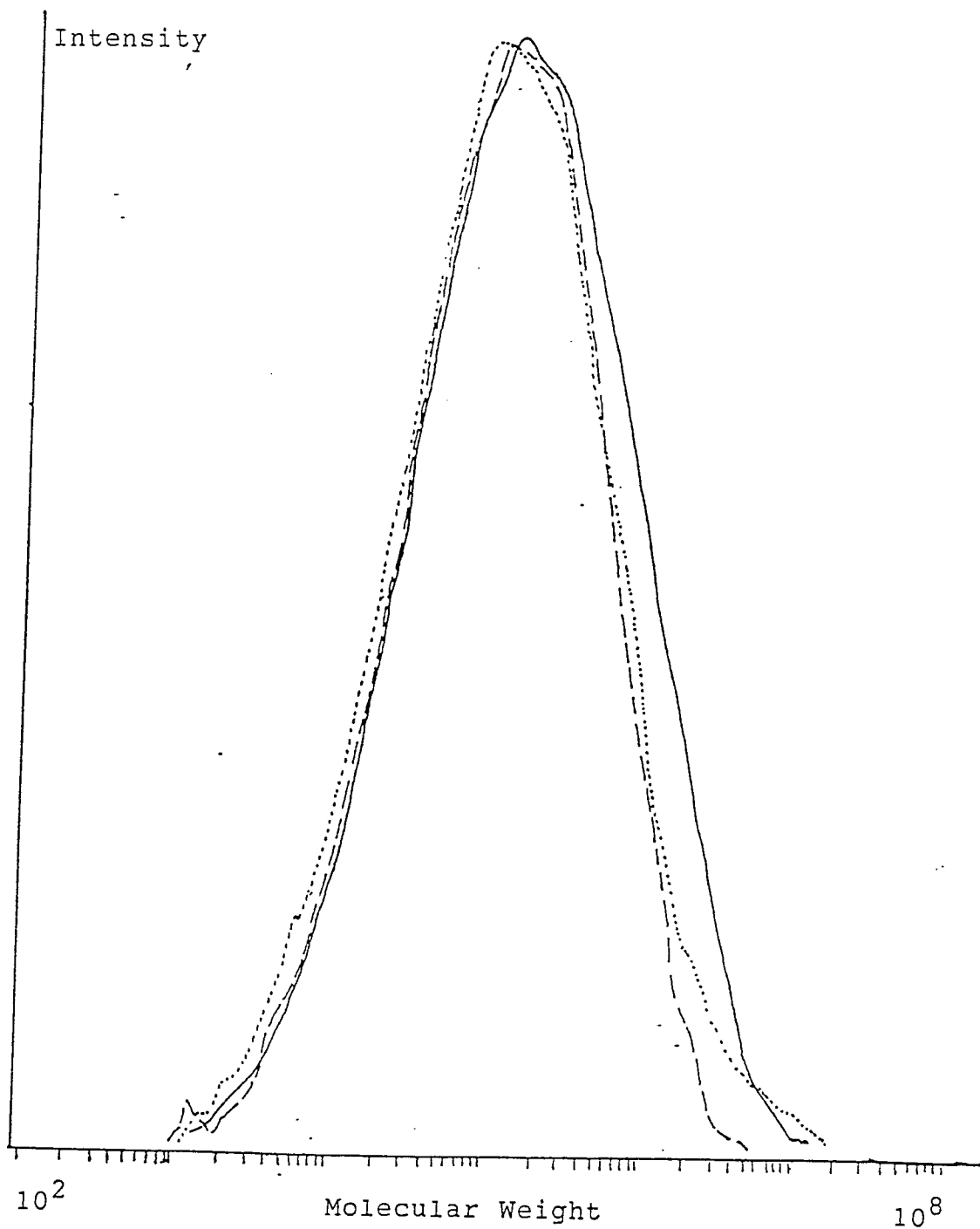


Figure 5.22 Molecular weight distribution (MWD) curves of masterbatches containing 10% of MOTP (-----) and MOPP (.....), processed with TMPTA (weight ratio = 2:8), compared to that of fresh PP (—)

5.2.5 Photostabilising activity of extended-bound methacrylic nitroxyl precursors

Masterbatches containing 10% of MOTP (methacrylic, >N-H) and MOPP (methacrylic, >N-CH₃) processed with various coagents (weight ratio of coagent to antioxidant = 2:8) in the presence of DCP 0.005 molar ratio, were diluted down to 0.2% antioxidant, without extraction (B,Ue), for photostabilisation test. Results are shown in Table 5.13 and Figures 5.23 and 5.24.

Table 5.13 Photo-embrittlement time of unextracted diluted masterbatch films containing 0.2% of bound methacrylic antioxidant (B,Ue), processed with various coagent (ratio 2:8)

Masterbatches	Binding (%)	ET (h) of d-MB films (B,Ue)
PP,processed	--	70
TMPTA/AOTP(2:8)	80	660
AATP/MOTP(2:8)	35	800
TMPTA/MOTP(2:8)	45	710
HDA/MOTP(2:8)	41	850
TMPTM/MOTP(2:8)	25	570
BGDM/MOTP(2:8)	17	550
TMPTA/MOPP(2:8)	62	850

The methacrylate analogous of AOTP (i.e. MOTP and MOPP) gave a little longer embrittlement time than AOTP (see Table 5.13). This is in agreement with the result recorded in Section 5.2.3, Table 5.8, that the stabilising activity of methacrylic nitroxyl precursors is higher than their corresponding acrylic derivatives. However, when MOTP was processed with methacrylic coagent (TMPTM and BGDM), the d-MB films degraded faster (ET=570 - 550 h) than that containing AOTP, processed under similar conditions and in the presence of same coagent

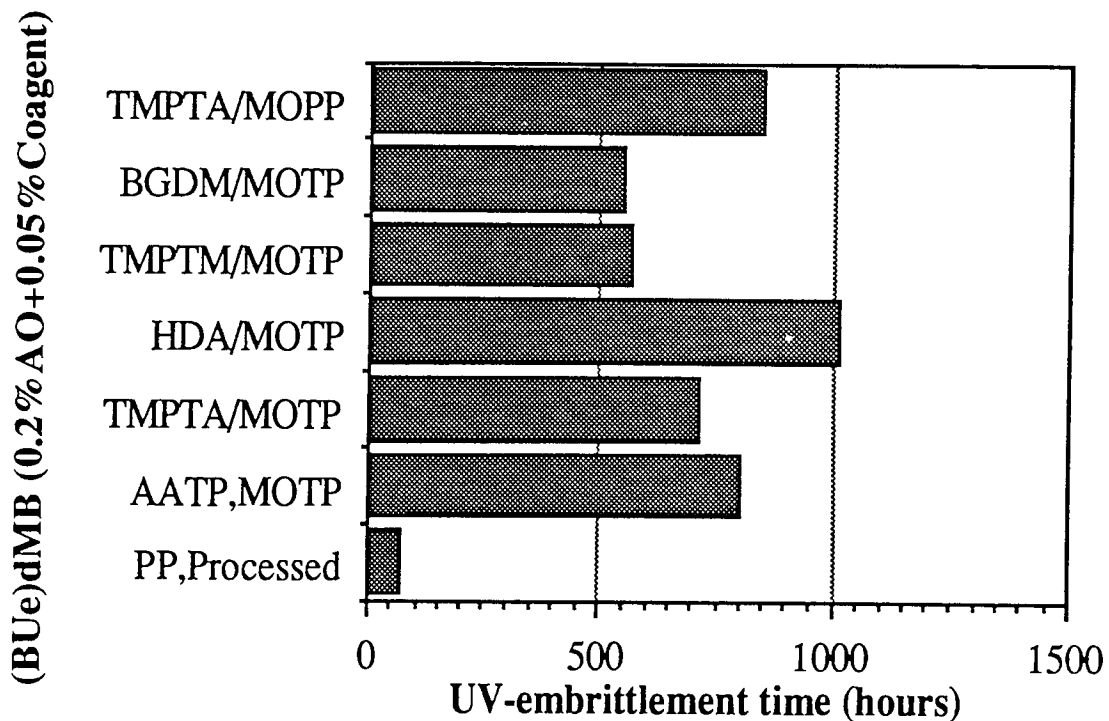


Figure 3.23 UV-embrittlement time of d-MB films containing MOTP and MOPP processed with various coagents (ratio 2:8)

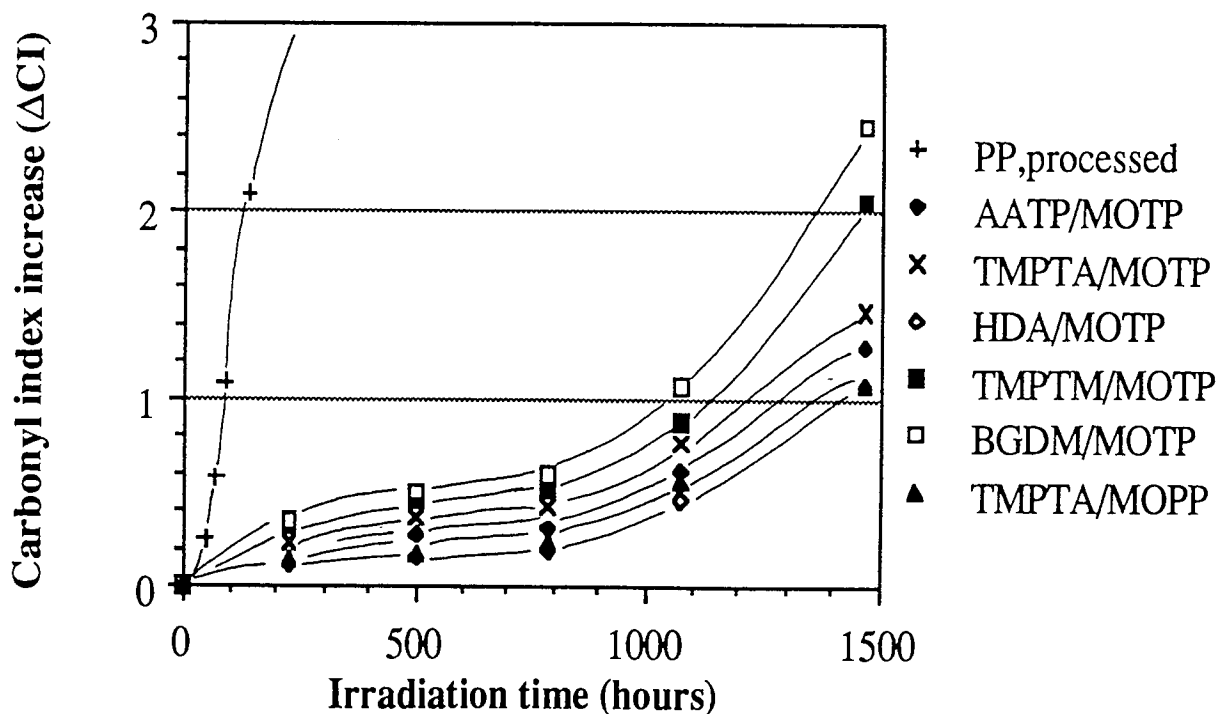


Figure 5.24 Carbonyl index increase during uv-irradiation of d-MB films containing 0.2% (B,Ue) MOTP and MOPP processed with various coagents ratio 2:8

To recover the high photostabilising activity of fresh MOTP and MOPP, a UV-absorber, HOBP at concentration of 0.2% was added into various diluted masterbatches containing 0.2% MOTP and MOPP. The photostabilising activity of the diluted masterbatch films was compared with their corresponding films but containing no HOBP.

Table 5.14 Photostability of 0.2% unextracted diluted masterbatch PP films containing MOTP and MOPP, 10% masterbatch processed with DCP 0.005 molar ratio at 180°C for 10 minutes diluted to 0.2%, with addition of 0.2% HOBP, B is bound, Ue is unextracted

d-MB films containing :	UV-embrittlement Time (hours)
MOTP(Ub) + HOBP	2550
MOPP(Ub) + HOBP	3200
TMPTA/MOTP(2:8)(Ub) + HOBP	2920
TMPTA/MOPP(2:8)(Ub) + HOBP	3210
MOTP(B,Ue)	680
MOPP(B,Ue)	820
TMPTA/MOTP(2:8)(B,Ue)	570
TMPTA/MOPP(2:8)(B,Ue)	850
HOBP	730

Results shown in Table 5.14 and Figures 5.25 and 5.26 indicate that methacrylic nitroxyl-precursors offer higher synergistic stabilising activity with HOBP when compared to the corresponding synergistic mixtures of HOBP with the acrylic nitroxyl-precursors, see Tables 3.11 (Chapter 3) and 5.3 (Chapter 5).

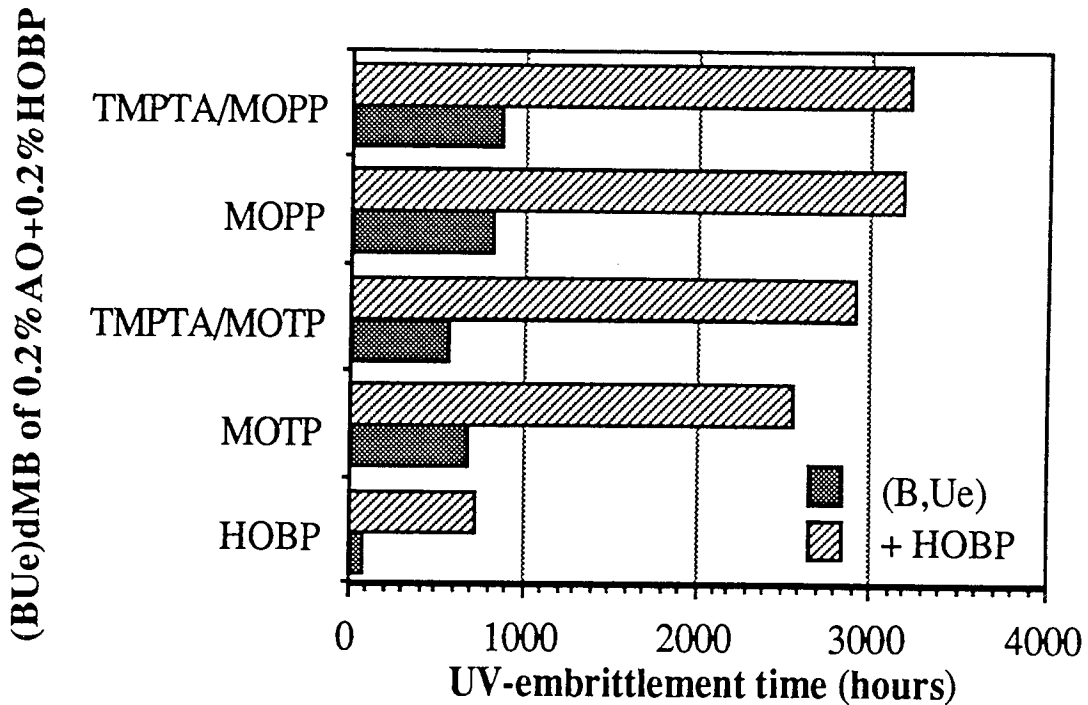


Figure 5.25 UV-embrittlement time of d-MB films containing unextracted 0.2% MOTP and MOPP, processed with TMPTA (ratio 2:8), with addition of 0.2% HOBP

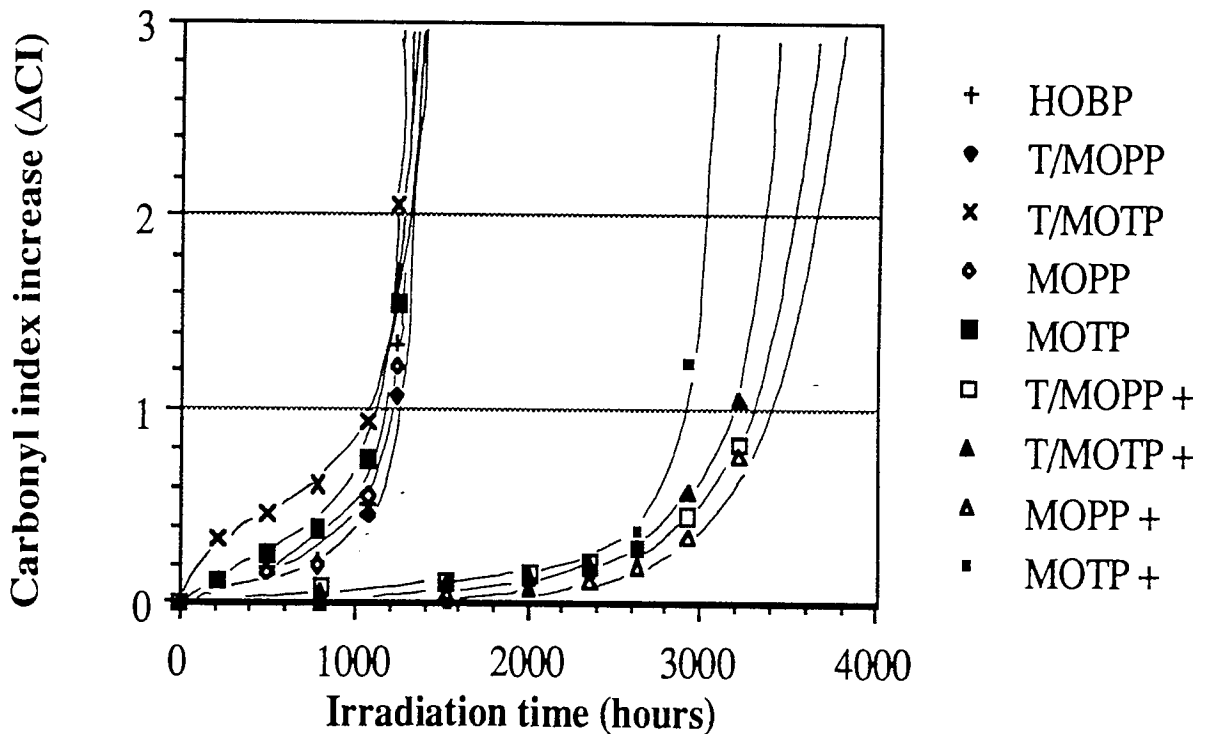


Figure 5.26 Carbonyl index increase during uv-irradiation of d-MB films containing 0.2%(B,Ue) MOTP and MOPP, processed with TMPTA ratio 2:8, diluted with addition of 0.2% HOBP

5.2.6 Binding of Masterbatches During UV-Irradiation

Possibility of photo-grafting of acrylic and methacrylic nitroxyl precursors during UV-irradiation was also investigated. Masterbatch films containing 10% of various antioxidants were UV-irradiated at room temperature, without extraction. After several hours the films were exhaustively extracted in DCM, and the binding efficiency of the antioxidants was measured using FTIR spectroscopy. Table 5.15 and Figure 5.27 show that there is no significant changes in the binding efficiency of masterbatches containing AOTP after uv-irradiation.

Table 5.15 Changes in binding of masterbatches containing AOTP and MOTP after various time of UV-irradiation at room temperature.

Masterbatch (10%,T.101)	Binding (%) before irradiation	Binding (%) after uv-irradiation for			
		145h	260h	430h	650h
AOTP	50	48	48	46	45
MOTP	8	4	2	2	2
AATP/AOTP(2:8)	70	71	71	70	70
TMPTA/AOTP(2:8)	80	78	78	76	76
AATP/MOTP(2:8)	35	31	28	25	23
TMPTA/MOTP(2:8)	45	41	38	34	31

Masterbatches containing methacrylic nitroxyl precursors (MOTP and MOPP), however, show decrease in binding (from 45 - 31% and 62 - 42%) after 650 h uv-irradiation. This is presumably due to depolymerisation of the bound methacrylate antioxidant during uv-irradiation, like ordinary methacrylate polymer.

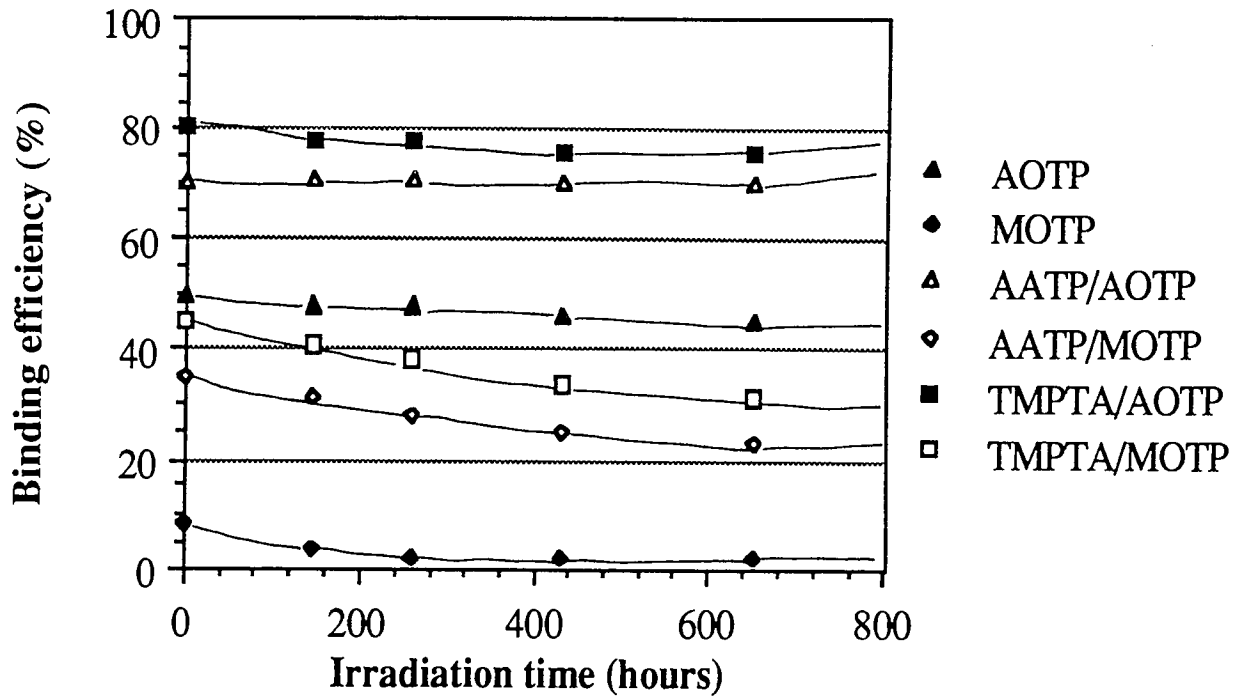
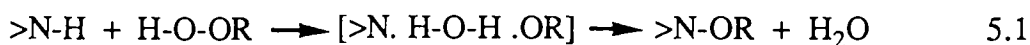


Figure 5.27 Changes in binding efficiency of masterbatch-films containing 10% of various acrylic and methacrylic nitroxyl precursors

5.3 DISCUSSION

5.3.1 Reactive processing and stabilising activity of N-alkylated acrylic nitroxyl precursors

Preliminary test for nitroxyl (>N-O.) concentration showed that the percentage of nitroxyl conversion from the N-alkylated (>N-R) derivatives after oxidation with m-chloroperbenzoic acid at room temperature is lower than that from AOTP (>N-H). Gueskens and Nedelkos⁽¹²³⁾ reported that an N-methyl derivative of hindered amine (Tinuvin 292, bis-[1,2,2,6,6-pentamethyl 4-piperidiny] sebacate) produced only around 1/30 the amount of nitroxyl radical when compared to the corresponding >N-H derivative (Tinuvin 770, bis-[2,2,6,6-tetramethyl 4-piperidiny] sebacate) after exposure to gamma radiation in cyclohexane solution. It was suggested that this may be due to reaction of hydroperoxide (H-O-OR) formed during photo-reaction with secondary amine (>N-H) through the following reaction,



Whilst, formation of nitroxyl radical from the N-alkylated amine (>N-R) may only be possible through reaction with the more reactive peroxy radicals (ROO.).

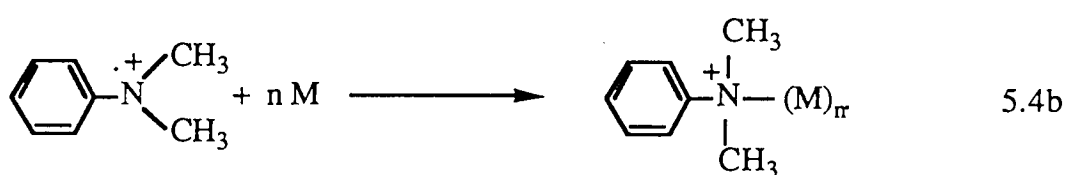
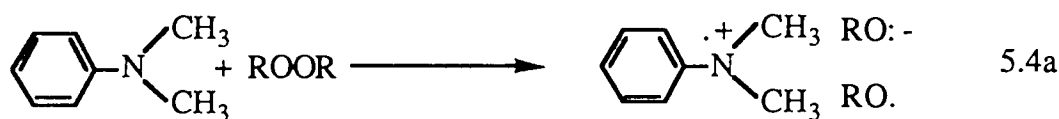


This is in agreement with the preliminary test for the nitroxyl formation from the N-alkylated nitroxyl precursors compared to that from the >N-H analogue.

Reactive processing of AOTP (acrylic >N-H) has been reported in the previous chapter to generate side reaction because of the susceptibility of the secondary amine (>N-H) group to radical attack during processing, which in turn can lead to grafting or branching, which is responsible for the formation of high MWt product. Surprisingly, masterbatches containing N-alkylated nitroxyl precursors also exhibited the high MWt component, although to a lower extent than that of the AOTP masterbatch. Formation

of the high-MWt component in AOTP masterbatch has been suggested, in previous chapters, to be due to formation of radicals (i.e. >N. or >N-O.) from the secondary amine (>N-H) group⁽⁴⁸⁾, which was then readily grafted with other growing polymer in the system. If this is the case, then the formation of the high MWt in the case of reactively processed N-alkylated nitroxyl precursors is peculiar, since these N-alkylated analogues do not possess labile (>N-H) hydrogen.

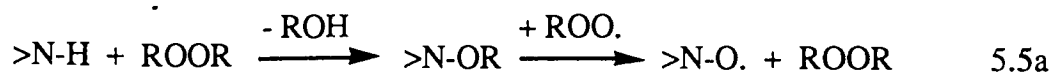
It is well known that several radical vinyl polymerisations are inhibited by amines and related compounds. Even tertiary amines (dimethyl aniline, N,N,N',N'-tetramethyl p-phenylenediamine) may function as inhibitor by scavenging the radical initiator as in the stabilisation of oxidation⁽¹²⁴⁻¹²⁷⁾. Therefore, the effectiveness of a vinyl polymerisation inhibitor is closely related to its oxidation retardation (antioxidant) activity⁽¹²⁸⁾. Horner and coworkers⁽¹²⁹⁾ suggested that during vinyl polymerisation by a peroxide (ROOR) in the presence of dimethyl aniline, the tertiary amine may propagate the polymerisation of the vinyl monomer, via an intermediate radical cation (XVI) in the following reactions (Reactions 5.4.a and 5.4.b).



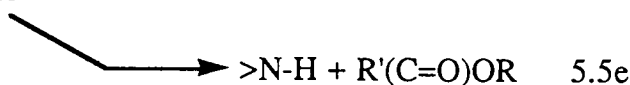
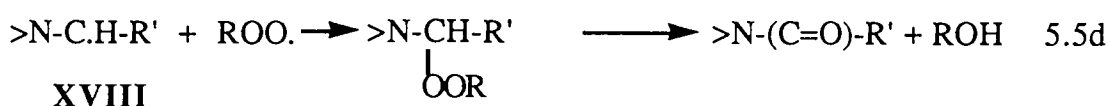
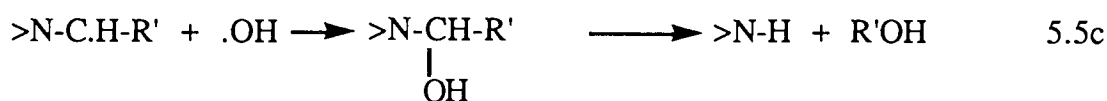
(XVI)

Moreover, Imoto et al.⁽¹³⁰⁾ proposed an alternative mechanism of vinyl polymerisation in which the process is instituted by a radical formed through the interaction of dimethylaniline with the peroxide. Finally Horner⁽¹³¹⁾ and Kurumada et al.⁽⁵⁴⁾ suggested the reaction of tertiary amines with peroxide via formation of a Wurster's like cation radical.

Secondary amine.

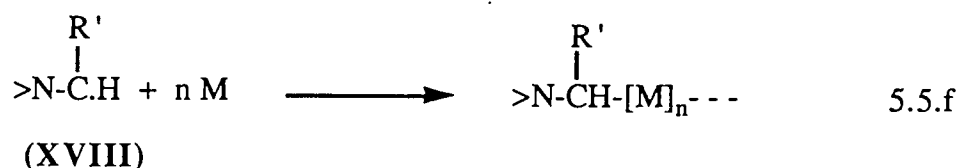


Tertiary amine,



Therefore, formation of high MWt product by N-alkylated nitroxyl precursors during reactive processing may occur via the following ways,

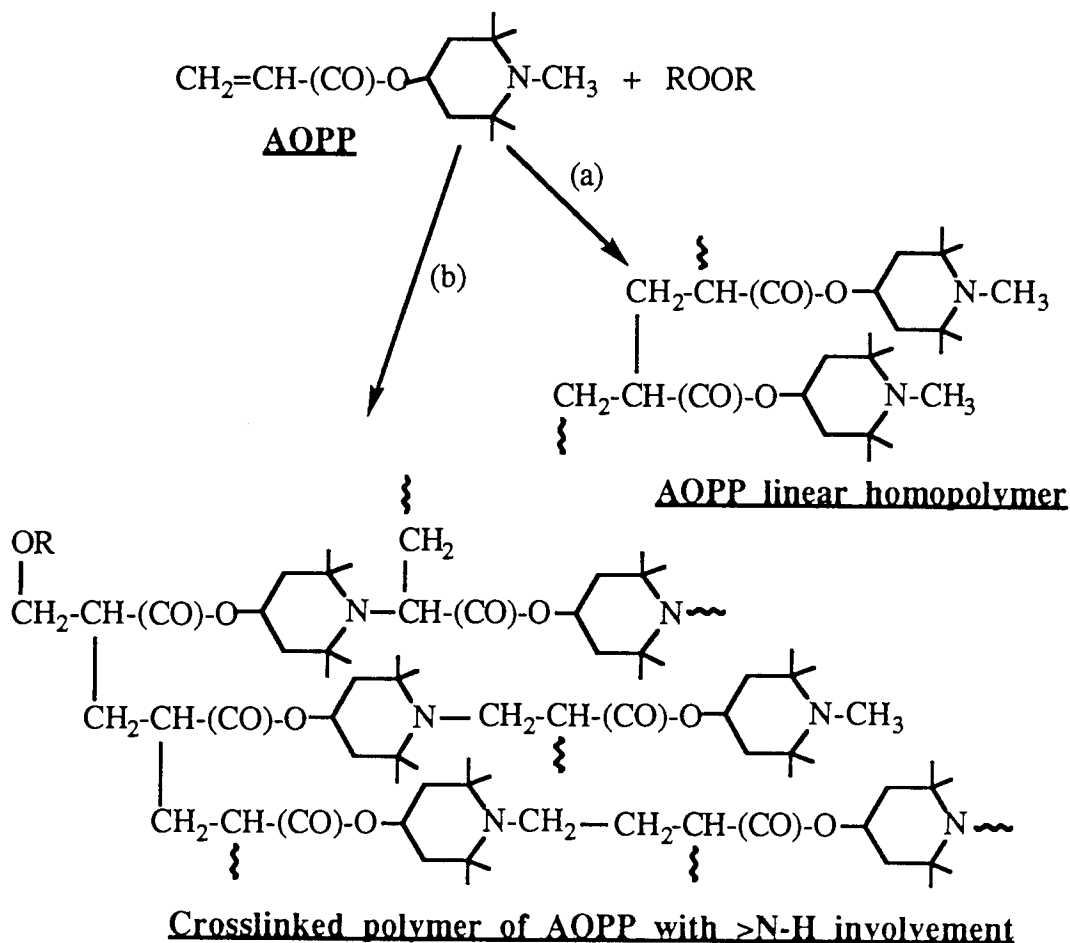
1. Direct reaction of amine radical ($>N-C.H-R'$, XVIII) with monomer molecules as described in reactions 5.4.a & 5.4.b.



2. Reaction of tertiary amine with peroxide to form the corresponding secondary amine ($>N-H$), see reactions 5.5b - 5.5e, which in turn may form the high MWt product through a mechanism like that of AOTP.

The above discussion is in agreement with results showed from polymerisation experiment of the $>N$ -Methyl derivative (AOPP). Carbon-13 NMR analysis of polymerised N-methylated derivative (AOPP) also exhibited shifting of the $>N-CH_3$ peak at $\delta = 34.3$ (+) ppm (Figure 2.15) towards a lower chemical shift at $\delta = 27.9$ (+) ppm (see Figure 5.6), which indicates changes in the chemical environment of the group. Both Proton and Carbon-13 NMR spectra of the polymerised AOPP exhibited an indication of formation of $>N-CH<$ and $>N-CH_2-$ groups during the polymerisation. The former may be formed via reaction of intermediate radical (XVIII), whereas the later may be attributed as a result of reaction of the acrylate group (as in the case of AOTP polymerisation) with the secondary amine ($>N-H$)

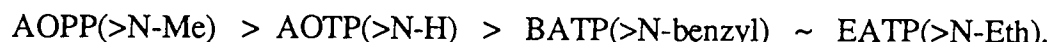
which is also formed during the reaction of the >N-R with peroxide. Therefore, the structure of polymerised N-methylated nitroxyl precursor (AOPP) may be visualised as shown in Scheme 5.3.



Scheme 5.3 Proposed structure of polymerised AOPP in the presence of Trigonox-101 0.005 molar ratio at 180°C for 30 minutes, which indicates involvement of the >N-CH₃ group

When compared to those of the corresponding unbound antioxidants, the uv-stabilising activity of bound N-alkylated nitroxyl precursors is lower. The N-alkylated group transformation during reactive processing as visualised in Scheme 5.3 may also be responsible for the decrease of the stabilising activity, since it has been reported⁽⁸²⁾ that a nitroxyl precursor, which crosslinked through its both ester and amide sides (crosslinked AATP), forms less nitroxyl radicals after oxidation compared to the fresh AATP.

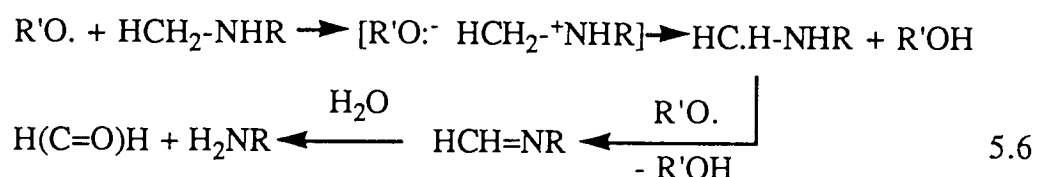
Stabilising activity of bound but unextracted (B.Ue) N-alkylated nitroxyl precursors in PP was found to be in the order of,



This order is not directly related to the ability of these N-alkylated derivatives to form nitroxyl radical (resulted from oxidation with m-chloroperbenzoic acid) in the preliminary test, which are in the order of,



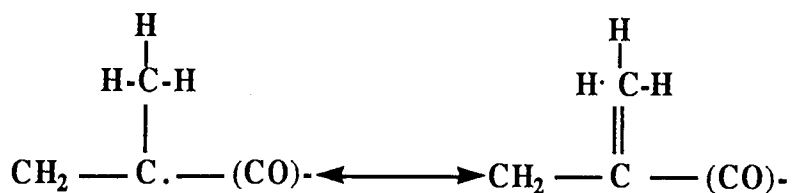
Nevertheless, it has been mentioned above by Horner⁽¹³¹⁾ and Kurumada⁽⁴⁸⁾ that N-alkylated nitroxyl precursors are readily dealkylated in the presence of hydroperoxide or peroxy radicals (ROOH or ROO.) to form the parent secondary amine (>N-H). This was reported to be an additional stage in the stabilisation action of the N-alkylated derivatives. Urry and Juveland⁽¹³²⁾ reported that hydrogen donation of aliphatic amine having α -hydrogen (R-CH₂-NHR') to an alkoxy radical is suggested to occur via an electron exchange, instead of direct hydrogen abstraction from the secondary amine.



The above evidence is also supported by the fact that N-H bond dissociation energy of amines is around 100 - 104 kcals/mol, whereas the energy of C-H bond of α -hydrogen to nitrogen is less than 89 - 94 kcals/mol⁽¹²⁰⁾. Therefore, two factors may determine the stabilising activity of N-alkylated nitroxyl precursors, firstly, the ease of nitroxyl radical formation from the derivatives and secondly the reactivity of the α -hydrogen to nitrogen atom in donating hydrogen to hydroperoxide or peroxy radicals formed in the early stage of the stabilisation action. The reactivity of α -hydrogen atoms of N-methylated nitroxyl precursors (AOPP and MOPP) is reportedly higher than those of the corresponding >N-Ethyl and >N-Benzyl derivatives⁽⁴⁷⁾ which may be due to hyperconjugation of the methylene radical [$>\text{N-(C.)H}_2$] within the methylene group.

5.3.2 Reactive processing of methacrylic(s) nitroxyl precursors

Methacrylic group is reportedly to be more susceptible to radical attack than the corresponding acrylic^(27,99), which is due in part, to the stabilisation of methacrylic radical by hyperconjugation within the methyl group.



5.7

He and Hu⁽¹⁴³⁾ had successfully photo-grafted a methacrylic nitroxyl precursor (4-methacryloyloxy 2,2,6,6-tetramethyl piperidine = MOTP) on to polypropylene

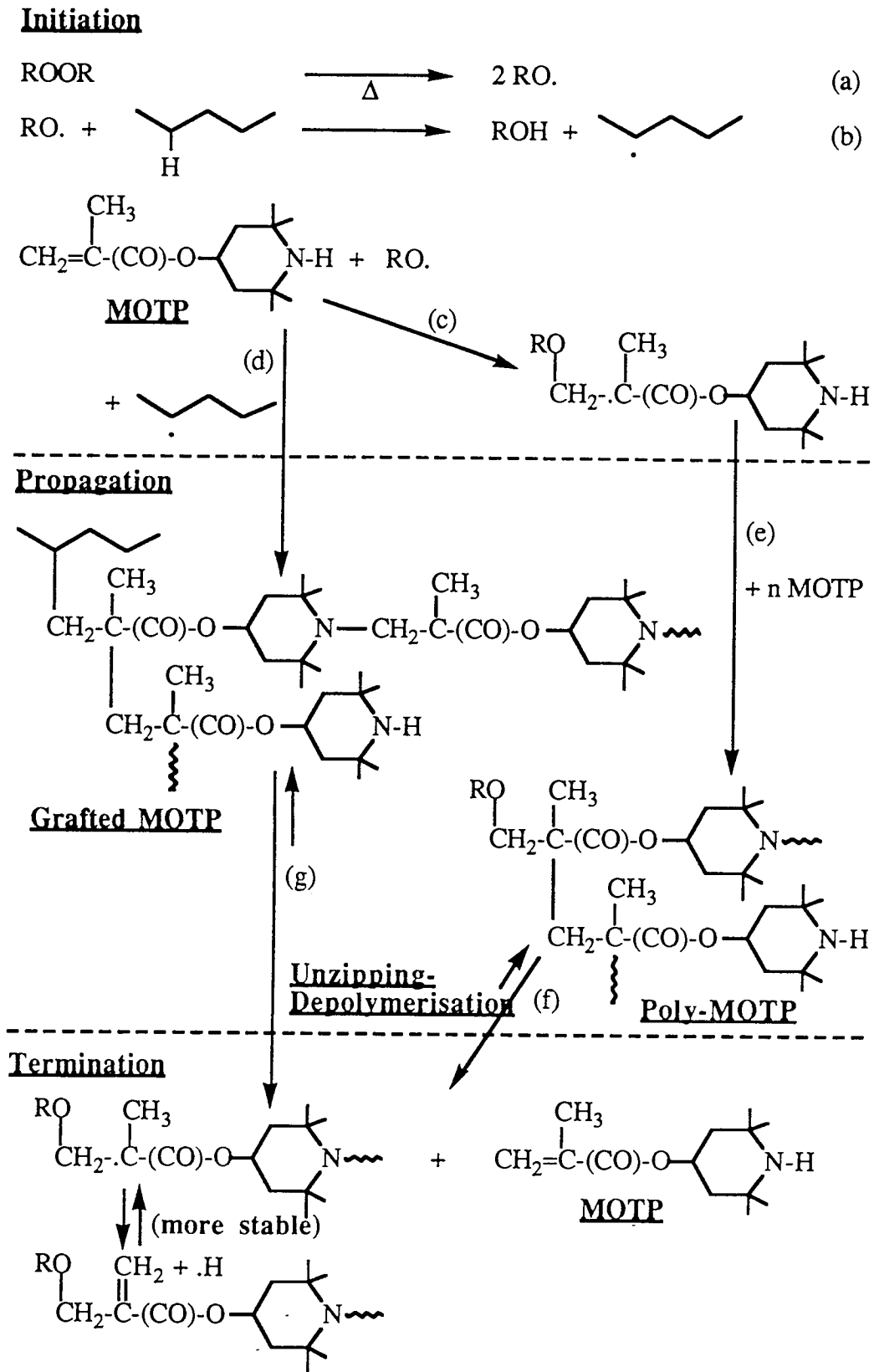
predicted, therefore, that the methacrylic nitroxyl precursors might bind in polymer melts to a higher extent than the corresponding acrylic derivatives.

When a methacrylic antioxidant monomer is reactively processed in polymer melts both homopolymerisation and grafting reaction take place. On the other hand, both the methacrylic graft and homopolymers may also depolymerise to form the corresponding monomers, especially at high temperature⁽¹³⁴⁾. Grassie and Scott⁽²⁷⁾ suggested that depolymerisation of polymethylmethacrylate (PMMA) at high temperature is initiated by radical formation through chain scission of the polymer backbone. This is then followed by "unzipping" reaction of these radicals to form the original monomer. Evaporation of low MWt monomers at high temperature increases the rate of the depolymerisation up to 100% conversion at 300-400°C. This explanation is in agreement with the results of low binding efficiency (less than 20%) of various methacrylic nitroxyl precursors (MOTP, MOPP and MMTP) in PP.

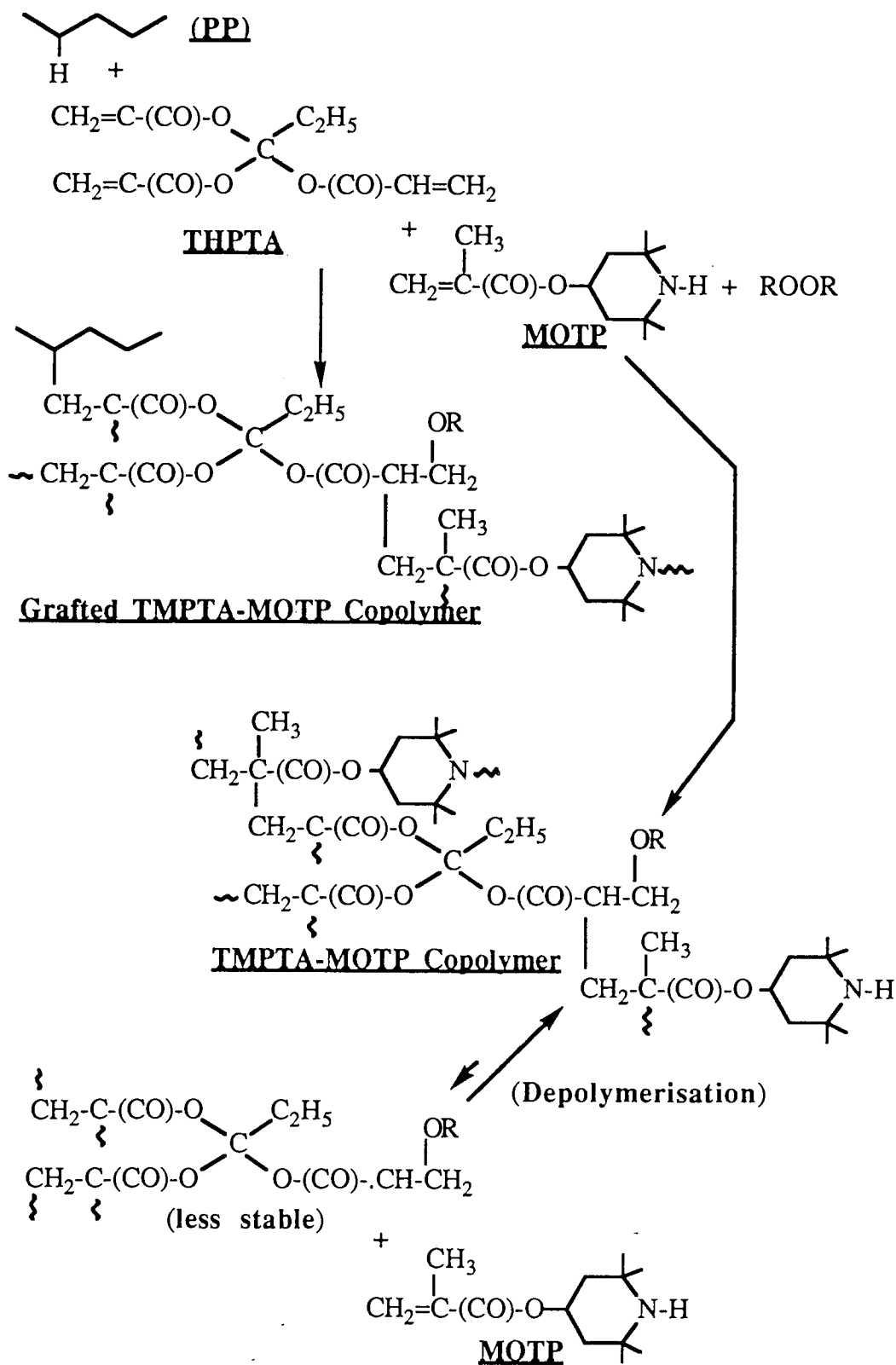
Results from solubility test in DCM suggests that, the nature of bound methacrylic nitroxyl precursors is most probably in the form of grafted moiety onto the polymer backbone and not as the homopolymerised antioxidants; since even the

polymerised bismethacrylic (poly-MMTP) was found to be soluble in DCM. FTIR spectra analysis of polymerised monomethacrylic nitroxyl precursor (MOTP) showed the remaining unsaturation peak at 1635 cm^{-1} , exhibiting about 50% polymerisation of the methacrylic group. Surprisingly, the polymerised MOTP also underwent crosslinking reaction through the secondary amine (>N-H) group, which was shown, especially, from the Carbon-13 NMR spectra of the polymerised MOTP. Appearance of new peaks at $\delta = 45.2$ (-) and 69.8 (+) ppm is evident, which may be due to formation of other methylene (-) and tertiary carbon (+) attached to nitrogen, such as $-\text{CH}_2-\text{N}<$ and $>\text{CH}-\text{N}<$ groups. Nevertheless, the "crosslinking" reaction did not form high MWt products in the masterbatch, since the efficiency of grafting of the MOTP onto the PP backbone is low. Possible mechanism of reactive processing of MOTP in polymer melts, which involves a reversible (polymerisation - depolymerisation) propagation, can be proposed as shown in Scheme 5.4.

Unlike the methacrylates, acrylate polymers do not depolymerise at 180°C , only 10 - 20% conversion of the depolymerisation has been reported⁽¹³⁵⁾ at $290 - 310^\circ\text{C}$. In fact, acrylate monomers have been used in the polymer industry to stabilise depolymerisation of PMMA during processing⁽²⁷⁾. In the presence of acrylate monomer, the depolymerisation can be inhibited from the early stage of the unzipping process, i.e. when methacrylic radicals are formed from chain scission during processing, the acrylate monomers deactivate the radicals and unzipping reaction does not proceed. Similarly, the methacrylic nitroxyl precursors (MOTP and MOPP) when reactively processed in the presence of acrylic coagents (AATP, HDA and TMPTA) may follow the above mechanism as well as form the unextractable copolymers with the coagents, which in turn give rise to the increase in binding efficiency, see Scheme 5.5 for the proposed reaction. Methacrylic coagents (BGDM and TMPTM) do not possess that function, and hence did not improve the binding efficiency of the methacrylic antioxidants.



Scheme 5.4 Proposed mechanism of processing reaction of MOTP in PP in the presence of DCP 0.005 molar ratio at 180°C for 10 minutes, binding efficiency < 10% due to unzipping depolymerisation



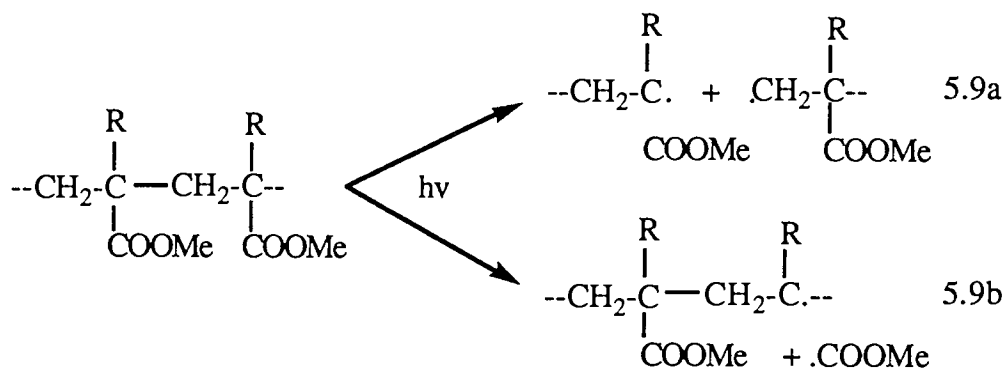
Scheme 5.5 Proposed improved binding reaction of MOTP in PP processed with TMPTA (weight ratio 2:8) at 180°C for 10 minutes in the presence of DCP 0.005 molar ratio, binding efficiency > 60% as a result of copolymerisation/grafting of PP-TMPTA-MOTP and inhibited depolymerisation of MOTP by the TMPTA

5.3.3 Stabilising activity of methacrylic(s) nitroxyl precursors

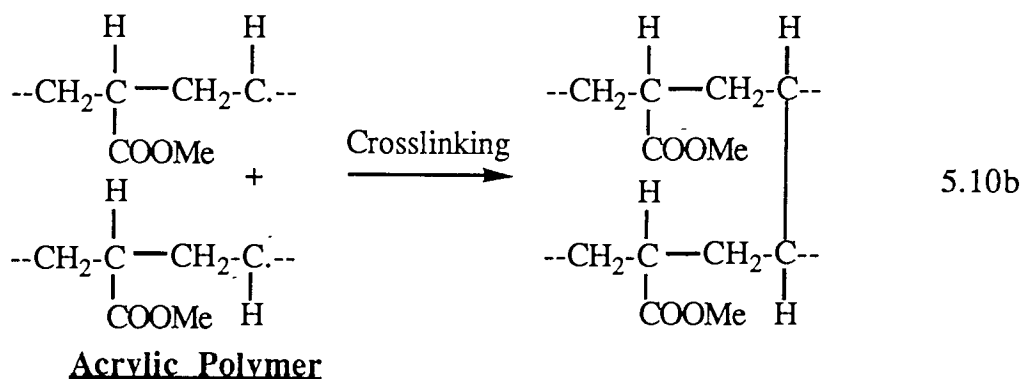
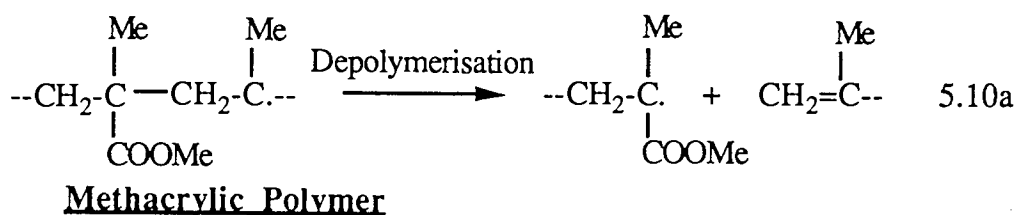
Stabilising activity of nitroxyl precursors as well as other antioxidants containing acrylic or methacrylic or other polymerisable groups have been reported^(84,136). It was found that the stabilising activity against thermal and UV-irradiation of the antioxidant monomers were always higher than those of their homopolymers⁽⁸²⁾. One of the reasons for this, in the case of nitroxyl precursors, is due to the fact that the polymerisable groups may function as photosensitiser and this will lower the activation energy for nitroxyl formation. On the other hand, Yachigo and his coworkers⁽¹³⁷⁾ at Sumitomo Chemical Co. Ltd., demonstrated that a phenolic stabiliser containing methacrylic group (Sumiliser GM) exhibited higher stabilising activity than the corresponding analogue without methacrylic group. The action of the stabiliser was confirmed based on the ability of the methacrylic group to trap radical generated by azobisisobutyronitrile (AIBN). Higher stabilising activity of methacrylic nitroxyl precursors (MOTP and MOPP) compared to those of the corresponding acrylic derivatives (AOTP and AOPP) at every conditions even when they are used in synergistic combination with HOBP, may be due to the above evidence. Nitroxyl precursor containing bismethacrylic (ester and amide) groups (MMTP) does not seem to show high stabilising activity. The reason for this is not clear, and further work is needed to investigate the effect of N-methacrylic group on the stabilising activity of MMTP and related compounds. Nevertheless, bismethacrylic additives were reported to be less compatible with polypropylene than the monomethacrylate derivatives^(84,85), which may be one of the reasons for the low stabilising activity of MMTP when compared to that of MOTP and MOPP.

Involvement of methacrylic group in the stabilisation mechanism of methacrylic nitroxyl precursors was supported by the fact that under uv-irradiation binding efficiency of methacrylic nitroxyl precursors did decrease slightly, see Table 5.15, whereas, masterbatch films containing acrylic analogues did not show considerable decrease in the binding efficiency after uv-irradiation. UV-irradiation may also

photoinitiate homopolymerisation and grafting of polymerisable antioxidant, in the presence of a photosensitiser (64,133,137). It was reported(138) that the methacrylates predominately underwent chain scission leading to depolymerisation, whereas the acrylates predominately experienced crosslinking. Apparently, the uv-irradiation may bring about similar primary effect to both the acrylates and the methacrylates, i.e. formation of acrylate or methacrylate radicals mainly through homolytic chain scission and photolitic at ester side.



Furthermore, chain scission of the methacrylate and crosslinking of the acrylate radicals may take place via the following reactions,



It is, therefore, suggested that masterbatch films containing 10% of methacrylic nitroxyl precursors (MOTP and MOPP) processed with acrylate coagent (TMPTA, ratio 2 : 8) may undergo depolymerisation during uv-irradiation at 30°C by the above

mechanism. Moreover, the depolymerised methacrylate groups of the antioxidant may function as radical scavenger, which inturn improve stabilising activity of the antioxidant. This may be the reason why bound methacrylate nitroxyl precursors exhibit better stabilising activity than their corresponding acrylate derivatives.

CHAPTER 6

CONCLUSIONS AND RECOMMENDATIONS FOR FURTHER WORKS

6.1 CONCLUSIONS

These following conclusions can be drawn from the results discussed in Chapters 3 to 5 :

1. In the reactive processing procedures of various acrylic nitroxyl precursors in polypropylene it was found that the binding level of derivatives containing monoacrylic group, such as AOTP, MyATP and AMyTP can only be achieved upto 50%. Increase in antioxidant's concentration (from 5 - 15%) improved the binding efficiency slightly, but almost levels off when the concentration reaching 20%. Further increase in concentration of antioxidants in the polymer leads to incompatibility of the antioxidant and causing bad mixing.

At higher peroxide content (upto 0.08 molar ratio of the peroxide to antioxidant) the binding efficiency increases considerably. However, higher concentration of peroxide also initiate severe melt-degradation of the polymer, which is indicated by immense increase in melt flow index of the polymer products. Optimum binding of acrylic nitroxyl precursors in polypropylene with good compatibility and minimum melt degradation effect was therefore achieved in 10% masterbatches using peroxide molar ratio of 0.005 - 0.010.

Nitroxyl precursor containing acrylic amide group (AMyTP) showed lower binding efficiency than that of containing monoacrylic ester (MyATP), which is presumably due to lower reactivity of the acrylic amide compared to the acrylic ester groups. When both the acrylic ester and acrylic amide groups are present in the same molecule such as the case with AATP, however, the binding

efficiency increased by more than double. This result can be explained by the fact that the reaction probability of polymerisable group is increased by N^2 , where N is number of the polymerisable groups per antioxidant molecule. Formation of unextractable (insoluble) crosslinked homopolymer of the bisacrylics also contributes to the high binding efficiency.

2. To extend maximum binding level of AOTP, various binding coagents containing bis- and tris-acrylates, such as AATP, HDA and TMPTA, as well as bis- and tris-methacrylates, e.g. BGDM and TMPTM, were used. After variation of coagent weight ratio to antioxidant and peroxide content, it was found that the binding level of AOTP can be improved up to 80%, using TMPTA as coagent at weight ratio 2 : 8, in the presence of peroxide 0.005 molar ratio. However, it was found that a complete efficiency of the binding reaction (i.e. 100% binding) of monoacrylic nitroxyl precursors using reactive processing was not possible (even in the presence of coagent) due to the inevitable formation of extractable (soluble) homopolymerised antioxidant. Higher coagent ratio increased the binding level, but was not used as it propagated crosslinked homopolymerisation of the coagent. Binding of AOTP using methacrylate coagents also showed an increase in the binding efficiency, despite the fact that methacrylate may be depolymerised again during in service and uv-irradiation.
3. Photo stabilising activity of bound nitroxyl precursors was found to be lower than that of their corresponding unbound analogous. This is presumably due to inhibition of nitroxyl radical formation from the bound antioxidant, as reactive processing of antioxidant may propagate homopolymerisation to form grafted and crosslinked structures. However, when the bound AOTP, processed with and without TMPTA, was used in conjunction with small amount of a

uv-screen (HOBP), the excellent uv-stabilising activity of the antioxidant can be fully recovered. On the other hand, when the HOBP was deliberately extracted from the polymer film after short interval of uv irradiation, it was found that the unextractable bound AOTP can no longer protect further degradation of the polymer. This fact suggested that in the presence of the uv-screen formation of alkyl radical (R.) may still in the level below scavenging capacity of the bound nitroxyl radical.

Thermal stabilising activity of bound AOTP (at 140°C with air flow 85 l/hour), processed with and without TMPTA, was shown to be better than that of unbound AOTP. This is attributed to evaporation of the unbound AOTP. Substantivity of the antioxidant becomes more important when the polymer is used at high temperature as a high surface-weight ratio material, such as fibre or film.

4. Investigation of reactive processing mechanisms of acrylic nitroxyl precursors in polypropylene was carried out using both physical and spectroscopic methods. From the torque records during reactive processing, masterbatches containing 20% bis-acrylic (AATP) exhibited crosslinking after 3 minutes processing. After exhaustive soxhlet extraction in xylene it was found that the insoluble crosslinked product formed was of the order of 28% in masterbatch containing 20% AATP. The xylene-soluble fraction of this masterbatch, on the other hand, contained very low concentration of AATP (0.5%). As the reactive processing was continued to 10 minutes, the insoluble crosslinked product decreased to 3.2%, whereas the AATP concentration in the soluble fraction increased up to 19.2%. This indicates that, even at the beginning of reactive processing, the AATP has crosslinked to form insoluble fraction, which contains high concentration of AATP. After 10 minutes processing the majority of the crosslinked AATP seems to breakdown and goes into the soluble fraction

of the masterbatch (soluble in hot xylene), but still is unextractable in DCM (physico-chemically bound).

Masterbatches containing monoacrylic derivative (AOTP), on the other hand, did not show high crosslinking during reactive processing. This antioxidant exhibits low binding efficiency (50%), despite almost entire AOTP had been polymerised during processing (total disappearance of double bond). The homopolymerised as well as unreacted AOTP in the masterbatch were fully extractable in the extracting solvent (unbound).

Molecular weight distribution data of masterbatch containing AATP showed slight decrease when compared to that of fresh polypropylene, indicating that the insoluble crosslinked high molecular weight fraction in the masterbatch had broken down at the end of processing. The latter was excluded from the molecular weight distribution measurement due to its insolubility. Interestingly, molecular weight distribution data of masterbatch containing AOTP showed additional peak in the high molecular weight region, with M_n around 50 - 200 times higher than their corresponding low MWt component. The high MWt component, which is still soluble in both xylene and o-dichlorobenzene, is presumably due to the possibility that AOTP molecules may be grafted on more than one repeat units per polymer backbone and both ends of the AOTP chains may bind to the polymer backbone. Attempted isolation of the high MWt component in the masterbatch from the low MWt component, after exhaustive soxhlet extraction in toluene, does not separate the low MWt component completely.

5. FTIR analysis of polymerised AOTP (polymerisation in decalin solution at 180°C for 30 minutes) showed disappearance of secondary amine (>N-H) peak at 3317 cm^{-1} . The polymerised solution did not exhibit nitroxyl radical peaks (ESR analysis), and even trace of nitroxyl peaks which were present in fresh

AOTP solution have disappeared after polymerisation. This suggests that during polymerisation (or reactive processing) instead of generating nitroxyl radical ($>N-O\cdot$) the $>N-H$ group of AOTP must have experienced chemical/physical transformations

Analysis of the polymerised AOTP by means of proton NMR spectroscopy does not show any secondary amine proton ($>N-H$) peak in the spectrum of both fresh and polymerised AOTP. The $>N-H$ proton peak may overlap with the C_4 ($-O-CH<$) proton of piperidine ring at δ (ppm) = 5.27 - 5.15 (multiplet). The spectra showed disappearance of all unsaturated ($CH_2=CH-$) peaks after 30 minutes polymerisation. In addition the spectra of polymerised AOTP also indicated formation of $-CH_2-$ bond at $\delta = 2.3$ ppm, i.e. formation of saturated $-CH_2-$ from acrylic group ($CH_2=CH-$), due to polymerisation. C^{13} NMR spectra of the polymerised AOTP showed complete disappearance of unsaturation peaks $CH_2=$ at δ (ppm) = 129.73 (-) and $=CH-$ at δ (ppm) = 128.51 (+), when compared to that of fresh AOTP. The spectra also exhibited trace of remaining decalin, which is possibly due to grafted decalin onto AOTP polymer.

In-situ C^{13} NMR investigation of polymerisation of AOTP in decalin at $100^\circ C$ (in the NMR machine) gave similar evidence. In addition, after polymerisation even at 30 minutes, one of the $>CH-$ peak of the decalin δ (ppm) = 43.88 (+), decreased sharply. This peak is recognised as that of trans $>CH-$ which is more susceptible to hydrogen elimination than the cis. Therefore, the peroxide used in the polymerisation may also attack the trans $>CH-$ of the decalin solvent, which then may be grafted onto the AOTP polymer.

From the reaction of Tinuvin 770 and ethyl hexylacrylate at similar condition, however, the $>N-H$ peak in the FTIR-spectra of the polymerised product was still apparent. Proton and Carbon-13 NMR spectra of polymerised AOTP and that of Tinuvin 770/ethyl hexylacrylate system did not show any indication of

reaction between >N-H and acrylate group to form >N-CH₂- (δ -Proton ~ 3 ppm, δ -Carbon-13 ~ 50 ppm). This suggests that the disappearance of >N-H peak in the FTIR spectra of polymerised AOTP may be partly due to changes in the hydrogen or Van der Waals bond environments after polymerisation. In fresh AOTP the hindered piperidine group can be freely mobile, whereas in polymerised AOTP the groups are closed each other, which resulted in conformational strain and inhibition of >N-H bond vibration. This then may lead to peak broadening of the >N-H absorption in the FTIR spectra.

6. From molecular weight distribution (MWD) curves of masterbatches containing 10% of various N-alkylated nitroxyl precursors (Figure 5.2.2. and Table 5.2.2.), it was found that the N-alkylated nitroxyl precursors still generate high MW product during reactive processing, although to a lower extent (5 - 6%) compared to that of AOTP masterbatch (9.8%). This supports conclusion-4, that the formation of high MWt component may be due to the presence of acrylic group in the system, which acts as interlinking agent to join a number of polymer molecules together.
7. When these reactively processed (bound) N-alkylated nitroxyl precursors were used as photoantioxidant in PP-films, their photostabilising activity, like that of bound AOTP, was lower than their corresponding unbound antioxidants. The photostabilising activity of various bound N-alkylated nitroxyl precursors was shown to be in the following order.

AOPP(>N-Me) > AOTP(>N-H) > BATP(>N-benzyl) ~ EATP(>N-Et).

Two factors may determine the order of the stabilising activity, firstly, susceptibility of the derivatives to nitroxyl formation and secondly, reactivity and number of α -H to N of the N-alkyl groups. The stabilising activity order is

also repeated when the N-alkylated nitroxyl precursors were used as thermal stabiliser. However, the thermal stabilising activity of unbound N-alkylated nitroxyl precursors was lower than those of their corresponding bound antioxidants, due to low substantivity of the unbound antioxidants at high temperature. The excellent photoantioxidant activity of bound N-alkylated nitroxyl precursors can also be recovered when used in conjunction with 0.2% HOBP in PP-films (ET upto 2520 - 2950h).

8. Compared to acrylic group, methacrylic analogous are known to be more reactive towards radical polymerisation due to stabilisation of the methacrylic radical by hyperconjugation of methyl group. It was found (section 5.4.), however, that nitroxyl precursors containing bis- and mono-methacrylic group(s) (i.e. MMTP, MOTP and MOPP) exhibited low binding efficiency (less than 25%) when processed at standard condition without coagent. This is associated to the ease of methacrylic group to trap and to deactivate peroxide radicals necessary for propagation of grafting reaction. This is supported by the fact that methacrylic(s) containing masterbatches showed relatively low MFI (maximum at 6.70 - 11.32 g/10minutes at DCP content 0.080 - 0.090 m.r.) when compared to those of their corresponding acrylic(s)-containing masterbatches, discussed in Chapter 4, (MFI maximum = 16.52 - 73.90 g/10minutes at DCP content 0.080 - 0.100 m.r.).
9. Photostabilising activity of mono-methacrylate nitroxyl precursors (MOTP and MOPP) was slightly better than their corresponding monoacrylates (AOTP and AOPP), under all condition, i.e. bound, unbound and in conjunction with HOBP. Using TMPTA as coagent (ratio 2:8), binding efficiency of mono-methacrylate nitroxyl precursors (MOTP and MOPP) can be extended from 10 - 45% and 14 - 62%, respectively. Photostability of their unextracted

diluted masterbatch films containing 0.2% of the bound antioxidants (ETs=800h and 850h, respectively) was slightly better than those containing 0.2% of the corresponding bound(unextracted) acrylate derivatives (AOTP , ET=660h, and AOPP, ET=780h). Methacrylate nitroxyl precursors (MOTP and MOPP) processed with and without TMPTA coagent, showed excellent synergistic stabilising activity with 0.2% HOBP in PP-films (ET upto 2910 - 3210 h). The methacrylate group in the nitroxyl precursors may function as another radical trap, which supplementary increases stabilising activity of amide group of the derivatives.

10. Masterbatch films containing acrylate nitroxyl precursors processed with coagent (AATP or TMPTA) did not exhibit changes in the binding efficiency during 650 hours uv-irradiation. Whereas the ones processed without coagent showed slight decrease in the binding around 10 - 20% of the original binding before irradiation, see Table 5.7.1. UV-irradiation of masterbatch films may initiate photografting of the remaining unreacted polymerisable antioxidant. On the other hand, this treatment may also generate depolymerisation of bound antioxidant and evaporation of the depolymerised product and other low molecular weight additives due to high surface-weight ratio of the films and air flow in the uv-cabinet.

6.2 RECOMMENDATIONS FOR FURTHER WORKS

1. The main objective of reactive processing of a modifier with polymer in the presence of a peroxide is, firstly to create polymer radicals from the reaction of polymer and peroxide under the influence of shear and heat. Secondly, the polymer radicals are expected to function as "active centres" for the grafting reaction of the modifier molecules along the polymer backbone. However, reactive processing of polymer systems in an internal mixer, such as a torquerheometer, is similar to a batch reaction in which the polymer, modifiers and peroxide are mixed together from the beginning to the end of the processing. This operation inevitably allows various "undesired" side-reactions to occur, e.g. melt degradation (chain scission or cross-linking) of the polymer and homopolymerisation of the modifiers. Consequently, the efficiency of "desired" reaction, i.e. grafting of modifier molecules onto polymer backbone is relatively low due to competition with the undesired reactions.

To improve the efficiency of a grafting reaction one should allow the first step of the reactive processing to take place effectively, i.e. formation of sufficient polymer radicals as active centres and consumption of the entire peroxide content, before adding the modifier monomer(s) into the reaction system. In addition, the modifier should be added in such a way so that it can quickly disperse in the reaction system to avoid accumulation, which leads to homopolymerisation. The latter was observed when the modifier (liquid) was injected into polymer melt (in the presence of peroxide) and processed in torquerheometer after various times, in which aggregates of the homopolymer were found incompatible with the polymer after processing. On the other hand, when the injection was carried out slowly to enhance dispersion, the modifier concentration in the processed polymer became lower than the originally added due to evaporation .

Therefore, a better design of processing operation is necessary to achieve this objective. A continuous processing machine with many inlets at different positions and possibility of residence time variations, such as a Twin Screw Extruder, but with low capacity of the processing chamber to allow variations in composition can be suggested to carry out this effective reactive processing operation.

2. Efficiency of grafting reaction, structure of the antioxidant-grafted polymer and whether the bound antioxidants are fully grafted or homopolymerised and become unextractable (physically bound), have not been fully understood. Estimation of the grafting efficiency, so far is limited only in the systems where the homopolymerised antioxidant is soluble (extractable from the polymer matrix). To further investigate this, high sensitive analytical techniques, such as solid state NMR for polymer, which can identify the change of chain sequence of polymer backbone and distinguish various configurations of carbon atoms in the polymer, are necessary to analyse the polymer product.
3. Reactive processing of various antioxidants containing polymerisable group(s), such as hindered phenols, benzophenones, as well as non-antioxidant compound(s) containing acrylic or vinyl group(s) in saturated/unsaturated polymers may be carried out to establish the general mechanism of the reactive processing in the presence of peroxide. This work may also be used to estimate the degree of involvement of the stabilising-active group of the antioxidants in the reactive processing. Such active groups, e.g. hindered amines, are strong radical scavengers which may inhibit the extent of the reactive processing by trapping radicals necessary for the grafting reaction and consuming some of the peroxide used.

4. Factors which contribute to reduction of stabilising activity of bound antioxidant are still not clear and further work is necessary to understand this. It is understandable that during reactive processing some of the polymer has been degraded under the influence of shear, heat and the peroxide, which indicates that the antioxidant might have been consumed and decomposed during processing. Physical aspects, such as reduced mobility, homogeneity and configurational changes of the bound antioxidants may also contribute to the decrease of the stabilising activity. These have to be further investigated.
5. Disappearance of >N-H peak (of especially AOTP) after processing have also to be studied, whether this is due to physical or chemical transformation. This can be investigated by unbounding the antioxidant (e.g. by hydrolysis) and analyse and characterise the hydrolysed antioxidant using general analytical techniques.
6. The fate of antioxidant(s) during reactive processing in polymer melt can also be studied using a numeric simulation method based on general mechanism of polymerisation reaction and the rate constant(s) of every possible reaction takes place during reactive processing. The basic idea of this study, known as "Monte Carlo Method", is to calculate the probability of all reactions involved in a competitive mechanism from the experimental rate constants available in the literature. Product of the reaction, then, can be simulated using random numbers (generated from a computer) and the reaction probability, which determine the direction of the reaction to form the product.
From the proposed reactive processing mechanism and the occurrence probabilities of reactions involved the Monte Carlo Method is able to predict the chain length as well as to display the sequence of units of every antioxidant(s)-polymer molecules produced after the simulation of the reactive processing. The characteristic of the polymer product, e.g. chemical structure,

% of grafting, crosslinking, homopolymerisation, etc, then can be estimated from the structure of molecules predicted in the simulation. A Monte-Carlo simulation (e.g. in the prediction of polydispersity of homopolymer) has been proved to be statistically reliable when the number of simulated molecules is > 500.

REFERENCES

1. Seymour R.B., *History of polyolefins*, Chapter 1, R.B. Seymour and T. Cheng (Eds.), D. Reindell Publ.Co., 1986.
2. Billingham.N.C., Calvert.P.D., *in Degradation and Stabilisation of Polyolefins*, Chapter-1, N.S.Allen (Ed.), App. Sci. Publ. Ltd., London, 1983.
3. Grassie.N., Scott.G., *Polymer Degradation and Stabilisation*, Chapter-1, Cambridge University Press., London, 1985.
4. Scott G., *Atmospheric Oxidation and Antioxidants*, Chapter-1, Elsevier Publishing Company, Amsterdam, 1965.
5. Chakraborty.K.B., Scott.G., *Eur. Polym. J.*, **13**, 731 (1977).
6. Gol'dberg V.M. and Zaikov G.E., *Polym. Deg. & Stab.*, **19**, 221 (1987).
7. Basedow A.M., Ebert K.H., Hunger H., *Macromol. Chem.*, **180**, 411 (1979).
8. Wall L.A., Flynn J.H., *Rubber Chem. Technol.*, **35**, 1157 (1962).
9. Tsuchiya Y. Sumi K., *J. Poly. Sci.*, A-7, 1599 (1969).
10. Kiran E., Gillham J.K., *J. Appl. Polym. Sci.*, **20**, 2045 (1976).
11. Stivala S.S., Kimura J., Gabbay S.M., *Thermal degradation and oxidative process, in Degradation and Stabilisation of Polyolefins*, N.S.Allen (Ed.), App. Sci. Publ. Ltd., London, 1983.
12. Iring M., Zsuza L.H., Keller T., Tudos F., Fuzes L., Somay G., and Bodor G., *J. Polym. Sci., Polym. Symp.*, **57**, 55 (1977).
13. Reich L., Stivala S.S., *Autoxidation of hydrocarbons and polyolefins*, Marcel Dekker, New York, 1969.
14. Grassie.N., Scott.G., *Polymer Degradation and Stabilisation*, Chapter-3, Cambridge University Press., London, 1985.
15. Vink.P., *in Degradation and Stabilisation of Polyolefins*, Chapter-5, N.S.Allen (Ed.), App. Sci. Publ. Ltd., London, 1983.
16. Bolland.J.L., Gee.G., *Trans. Faraday. Soc.*, **42**, (1946).

17. *Ibid* (16), **44**, 669 (1948).
18. Bateman L., *Quart. Rev.*, **8**, 147 (1954).
19. Scott.G., *Chem. Ind.*, **7**, 271 (1963).
20. Hawkins.W.L., *Polym. Eng. & Sci.*, **5**, 196 (1965).
21. Chakraborty.K.B., Scott.G., *Polymer*, **18**, 98-99 (1977).
22. Carlsson.D.J., Wiles.D.M., *Macromolecules*, **2**, 257 (1969).
23. Amin.M.U., Scott.G., and Tillekeratne.L.M.K., *Eur. Polym. J.*, **11**, 85 (1975).
24. Ginhac J.M., Gardette J.L., Arnaud R., and Lemaire J., *Macromol. Chem.*, **182**, 1017 (1981).
25. Chew C.H., Gan L.M., and Scott G., *Eur. Polym. J.*, **13**, 361 (1977).
26. Carlsson.D.J., Wiles.D.M., *Macromolecules*, **2**, 257 (1969).
27. Scott.G., in *Developments in Polymer Stabilisation-4*, Chapter-1, G. Scott (ed.), App. Sci. Publ. Ltd., London, 1981.
28. Allen.N.S., in *Developments in Polymer Photochemistry-2*, Chapter-7, App. Sci. Publ. Ltd., London, 1982.
29. Grassie.N., Scott.G., *Polymer Degradation and Stabilisation*, Chapter 5, Cambridge University Press., London, 1985.
30. Al-Malaika.S.,Scott.G., in *Degradation and Stabilisation of Polyolefins*, Chapter-7, N.S.Allen (Ed.), App. Sci. Publ. Ltd., London, 1983.
31. Toda.T., Kurumada.T., Murayama.K., *A.C.S. Symposium-280 Am. Chem. Soc.*, Chapter-3, P.P.Klemchuk (Ed.), A.C.S., Washinton, 1985.
32. Ivanov V.B., Shlyapintokh V.YA., *Synergism in the photostabilisation of polymers*, in *Developments in Polymer Stabilisation-8*, G. Scott (ed.), App. Sci. Publ. Ltd., London, 1987.
33. Chakraborty.K.B., Scott.G., *Eur. Polym. J.*, **13**, 1007 (1977).
34. Scott G., Yusoff M.F., *Polym. Deg. & Stab.*, **2**, 309 (1980).
35. Ranaweera R.P., Scott G., *Eur. Polym. J.*, **12**, 591 (1974).
36. Chakraborty.K.B., Scott.G., *Polym. Deg. & Stab.*, **1**, 37 (1979).

37. Lozovskaya E.L., Ivanov V.B., Shlyapintokh V.YA., *Vysokomol. Soed.*, **A-27**, 1589 (1985).
38. Allen N.S., Homer J., Mc.Kellar J.F., *J. Appl. Polym. Sci.*, **22**, 611 (1978).
39. *Brit. Patent*, **1,296,245**, Aug. 1970.
40. *U.S. Patent*, **3,542,729**, Nov. 1970.
41. *U.S. Patent*, **3,684,765**, Aug. 1972.
42. Hodgeman.D.K.C., in *Developments in Polymer Degradation-4, Chapter-6*, N.Grassie (Ed.), App. Sci. Publ. Ltd., London, 1982.
43. Rozantsev.E.G., *Free Nitroxyl Radicals*, Chapter-1, Plenum Press, N.Y., 1970.
44. Shlyapintokh.V.YA., Ivanov.V.B., in *Developments in Polymer Stabilisation-5, Chapter-3*, G.Scott (Ed.), App. Sci. Publ. Ltd., London, 1983.
45. Rogers.M., *J. Chem. Soc.*, 2784 (1956).
46. Johnson.D., Rogers.M., Trappe.G., *J. Chem. Soc.*, 1093 (1956).
47. Kurumada.T., Ohsawa.H., Fujita.T., Toda.T, *J. Polym. Sci., Polym. Chem. Ed.*, **22**, 1984, 277-281.
48. Grassie.N., Scott.G., *Polymer Degradation and Stabilisation*, Chapter 5, Cambridge University Press., London, 1985.
49. Carlson.D.J., Chan.K.H., Wiles.D.M., *J. Polym. Sci., Polym. Lett. Ed.*, **19**, 1981, 549-554.
50. Carlson.D.J., Jensen.J.P.T., Wiles.D.M., *Makromol. Chem. Suppl.*, **8**, 79-88 (1984).
51. Bagheri.R., Chakraborty.K.B., Scott.G., *Polym. Degrad. Stab.*, **4**, 1-16 (1982).
52. Al-Malaika.S., Omikorede.E.O., Scott.G., *Polym. Commun.*, **27**, 173 (1986).
53. Kurumada.T., Ohsawa.H., Oda.O., Fujita.T., Toda.T., Yoshioka.T., *J. Polym. Sci., Polym. Chem. Ed.*, **23**, 1477 (1985).
54. *Ibid.* , **23** , 2747 (1985).

55. Carlson.D.J., Wiles.D.M., *Polym. Degrad. Stab.*, **6** , 1 (1984).
56. Billingham.N.C., Calvert.P.D., in *Developments in Polymer Stabilisation-3*, Chapter-5, G.Scott (Ed.), App. Sci. Publ. Ltd., London, 1980.
57. Luston.J., in *Developments in polymer Stabilisation-2*, Chapter-5, G.Scott (Ed.), App. Sci. Publ. Ltd., London, 1980.
58. Flory P., *Principles of Polymer Chemistry*, Chapter 12, Cornell, New York, 1953.
59. Roe R.J., Bair H.F., and Gieniewski C., *J. Polym. Sci.*, **18**, 843 (1974).
60. Luston J., Manasek Z., and Kosik M., *J. App. Polym. Sci.*, **21**, 915 (1977).
61. Scmitt R.G., Hirt R.G., *J. Polym. Sci.*, **45**, 35 (1960).
62. Plant M.A., Scott G., *Eur. Polym. J.*, **7**, 1173 (1971).
63. Kumins C.A., Kwei T.K., in *Diffusion in Polymers*, J. Crank & G.S. Park (Eds.), Academic Press, London, 1968, p 107.
64. Munteanu.D., *Polyolefins Stabilisation by Grafting* , in *Developments in Polymer Stabilisation-8*, G.Scot (Ed.), App. Sci. Publ. Ltd., London, 1987.
65. Tucker.R.J., Susi.P.V., *A.C.S. Symposium-280*, Chapter-11, P.P.Klemchuk (Ed.), A.C.S., Washinton, 1985.
66. Scott.G., *A.C.S. Symposium-280*, Chapter-14, P.P.Klemchuk (Ed.), A.C.S., Washinton, 1985.
67. Sjothun I.J., and Allinger G., in *Vulcanisation of elastomers*, G Allinger and I.J. Sjothun (Eds.), Reinhold, New York, 1964, p.1.
68. Miles G.W., *U.S. Patent* , **733,729** (1903).
69. Flory P., *J. Am. Chem. Soc.*, **59**, 241 (1937).
70. Houtz R., and Adkins J., *J. Am. Chem. Soc.*, **55**, 1609 (1933).
71. Greber G., *Macromol. Chem.*, **101**, 104 (1967).
72. Casale A., and Porter R.S., *Polymer stress reactions*, Academic Press, London, 1978-79.
73. Scott.G., in *Developments in Polymer Stabilisation-4*, Chapter-6, G.Scott (Ed.), App. Sci. Publ. Ltd., London, 1981.

- 74 Al-Malaika S., Goonetilleka M.D.R.J, Scott G., *Polymer Degradation and Stability*, **32**(2), 231 (1991).
- 75 Cain M.E., Knight G.T., Lewis P.M., and Saville B., *Rubb. J.*, **150**(2), 204 (1968).
- 76 Cain M.E., Gazeley K.F., Gelling I.R., and Lewis P.M., *Rubb. Chem. Tech.*, **45**, 204 (1972).
- 77 Pradellok W., Gupta A., Vogl O., *J. Polym. Sci., Polym. Chem. Ed.*, **19**, 3307 (1981).
- 78 Sumida Y., Vogl O., *Polym. J. (Japan)*, **13**, 521 (1981).
- 79 Cooray B.B., and Scott G., *Eur. Polym. J.*, **16**, 1145 (1980).
- 80 Cooray B.B., and Scott G., *Eur. Polym. J.*, **17**, 379 (1981).
- 81 Scott G., Setoudeh E., *Polym. Deg.&Stab.*, **5**, 1 (1983).
- 82 Al-Malaika S., Ibrahim A.Q., Rao M.J., Scott G., *Mechanisms of antioxidant action. Photoantioxidant activity of polymer bound hindered amines. Part II Bis-acrylates*, *J. Appl. Polym. Sci.*, Inpress.
- 83 Kurosaki.T., Lee.K.W., Okawara.M., *J. Polym. Sci., Polym. Chem. Ed.*, **10**, 3295 (1972).
- 84 Chmela.S., Hrdlovic.P., Manasek.Z., *Polym. Degrad. Stab.*, **11**, 233 (1985).
- 85 Chmela.S., Hrdlovic.P., *Polym. Degrad. Stab.*, **11**, 339 (1985).
- 86 Miyazawa.T., Endo.T., Okawara.M., *J. Polym. Sci., Polym. Chem. Ed.*, **23**, 1527 (1985).
- 87 Coker M.R.S., *Ph.D. Thesis* , Aston University, 1986.
- 88 Cooley J.W., and Tukey J.W., *Math. Comput.*, **19**, 297 (1965).
- 89 Wexler A.S., *Spectrochim. Acta.*, **21**, 1725 (1965).
- 90 Zakrzewski L., Henniker J.C., *unpublished report.*, (from ref. 93).
- 91 Kremmer T., *Methods and techniques in gel chromatography*, T. Kremmer and L Boross (Eds.), John Wiley & Sons, New York, 1979.
- 92 Tager A., *Physical chemistry of polymers*, Chapter 18, MIR publishers, Moscow, 1972.

93. Kemp W., *Organic spectroscopy, NMR spectroscopy*, The Macmillan Press Ltd., London, 1975.
94. Johnson L.T., Jankowski W.C., *Carbon-13 NMR spectra*, Wiley, New York, 1972.
95. Blumenfeld L.A., Voevodski V.V., Semenov A.G., *Electron spin resonance in chemistry*, Chapter 7, Adam Hilger Ltd., London, 1973.
96. Bevington J.C., *Radical polymerisation*, Chapter 4, Academic Press, London, 1961.
97. Simha R., Bransen H., *J. Chem. Phys.*, **12**, 253 (1944).
98. Izu M., O'Driscoll K.F., *Polym. J.*, **1**, 27 (1970)
99. Young L.J., *Copolymerisation reactivity ratios in Polymer handbook.*, Chapter II-5, Brandrup J., Immergut E.H., (Eds.), John Wiley & Sons, New York, 1975.
100. Al-Malaika S., Rao M.J., Scott G., *unpublished work*.
101. Al-Malaika S., Ibrahim A.Q., Scott G., *Polym. Deg. & Stab.*, **22**, 233 (1988)
102. Al-Malaika S., Ibrahim A.Q., Scott G., *Brit.U.K. Pat. Appl.*, **G B 2,202,226**, March 1987.
103. Allen N.S., Gardette J.L., Lemaire J., *Polym. Deg. & Stab.*, **8**, 133 (1984).
104. Allen N.S., Kotecha J.L., *Polym. Deg. & Stab.*, **11**, 181 (1985)
105. Sharma Y.N., Naqv M.K., Gawand P.S., Bhardwa I.S., *J. App. Polym. Sci.*, **27**, 2605 (1982).
106. Chirinos-Padron A.J., Suarez F.A., Berroteran H., *Polym. Deg. & Stab.*, **14**, 295 (1986).
107. Allen N.S., Parkinson A., Gardette J.L., Lemaire J., *Polym. Deg. & Stab.*, **5**, 135 (1983).
108. Vink P., *In Developments in polymer stabilisation-3.*, Chapter 4, Scott G., (Ed.), Applied Sci. Publishers, London, 117 (1980).
109. Chakraborty K.B., Scott G., *Eur. Polym. J.*, **15**, 35 (1979).
110. Carlsson D.J., Wiles D.M., *Advan. Polym. Sci.*, **7**, 70 (1970).

111. Scott G., *Stable radicals as catalytic antioxidants in polymers in Developments in polymer stabilisation-7*, Scott G., (Ed.), Appl. Sci. Publishers, London, 89 (1984).
112. Odian G., *Principles of polymerisation*, Chapter 3, 2nd ed., John Wiley & Sons, New York (1981).
113. Holinquist H.E., Rothrock H.S., Theobald C.W., Englund B.E., *J. Am. Chem. Soc.*, **78**, 5339 (1956).
114. Reff. (93), Chapter 2, 38 - 64.
115. Grassie N., Zulfiqar M., *in Developments in polymer stabilisation-1*, Chapter 6, Scott G. (Ed.), Appl. Sci. Publishers, London (1979).
116. Dale W.J., Buell G., *J. Org. Chem.*, **21**, 45 (1956).
117. Mozingo R., McCracken J.H., *Org. Synthesis -III*, 258 (1955).
118. Bevington J.C., *J. Chem. Soc.*, 1127 (1956).
119. Yates W.R., Ihrig J.L., *J. Am. Chem. Soc.*, **87**(4), 710 (1965).
120. De La Mare H., *J. Org. Chem.*, **25**, 2114 (1960).
121. Coppinger G.M., Swalen J.D., *J. Am. Chem. Soc.*, **83**, 4900 (1961).
122. Henniker J.C., *Infrared spectrometry of industrial polymer, principles of molecular spectrometry*, Academic Press, London, 1967.
123. Geusken G., Nedelkos G., *Polym. Deg. & Stab.*, **19**, 365 (1987).
124. Boozer C.E., Hammond G.S., *J. Am. Chem. Soc.*, **76**, 3861 (1954).
125. Hammond G.S., Boozer C.E., Hamilton C.E., Sen J.N., *J. Am. Chem. Soc.*, **77**, 3238 (1954).
126. Pederson C.J., *Ind. Eng. Chem.*, **48**(10), 1181 (1956).
127. Adamic K., Ingold K.U., *Can. J. Chem.*, **47**, 295 (1969).
128. Reff. (4), Chapter 4, p.166.
129. Horner L., Schwenk E., *Ann.*, **566**, 69 (1950).
130. Imoto M., Otsu T., Kimura K., *J. Poly. Sci.*, **15**, 475 & 485 (1955).
131. Horner L., *J. Polym. Sci.*, **18**, 438 (1955).
132. Urray W.H., Juveland O.O., *J. Am. Chem. Soc.*, **80**, 3233 (1958).

133. He M., Hu X., *Polym. Deg. & Stab.*, **18**, 321 (1987).
134. Cameron G.G., Kane D.R., *Makromol. Chem.*, **115**, 268 (1968).
135. *Ibid* (156), **109**, 194 (1967).
136. Vogl O., Albertson A.C., Janovic Z., *A.C.S. Symposium-280*, Chapter 15, Klemchuk P.P. (Ed.), A.C.S. Washinton 1985.
137. Yachigo S., *PDDG-Meeting*, Aston University, Sept. 1987.
138. *Reff.* (14), Chapter 14, pp. 72-77.